BRAINSTEM PLASTICITY IN VESTIBULAR MOTION-PROCESSING SENSORIMOTOR NETWORKS

Clayton Jackson Gordy

Graduate School of
Systemic Neurosciences

LMU Munich

Dissertation der Graduate School of Systemic Neurosciences
der Ludwig-Maximilians-Universität München

September, 2022

Supervisor
Prof. Dr. Hans Straka
Faculty of Biology
Ludwig-Maximilians-Universität München

First Reviewer: Prof. Dr. Hans Straka
Second Reviewer: Prof. Dr. Anja Horn-Bochtler

Date of Submission: September 29, 2022
Date of Defense: December 20, 2022

To my parents Craig and Kandi, and also to my aunt Jodi who asked me long ago for a book dedication, and finally to my Grandmother Phyllis, to whom my passion for reading is owed.

ACKNOWLEDGMENTS

What an adventure this has been. This dissertation exists only because of countless people, and although I will fail in doing so, I will try to thank them all the best I can.

First off, a most significant thank you is owed to my advisor Prof. Dr. Hans Straka. Hans, I am not sure what made you decide to open your lab to an unknown American, but I am glad you did. I truly appreciate you allowing me to conduct my doctoral work under your supervision. You have always allowed me the creative freedom to do as I wished and for that I am grateful. Our countless discussions, scientific musings, and heated debates are things I will reflect fondly on and carry forward. I have learned a lot from you (including how to properly chill red wine) and am privileged to count myself among those who can refer to you as their Doktorvater. Due to your teachings, and much like some species of changelings, I find myself different from when I arrived.

My profound thanks are due to all the members of the Straka lab, both past and current, for surely my time in Munich would not be as it was without you all. In particular, tremendous thanks and gratitude are owed to Patty and Michi. I am incredibly grateful for your support both in and outside of the lab. Much of my German bureaucratic adventures would be null without your help Michi, and I have often enjoyed our disagreements on coding (#annotations are nice, right?) and owe a large portion my coding knowledge to your efforts. Patty, you continue to inspire me in many ways, and I owe much of my ability to think critically to you, for truly if one can hold their own against your extensive questions (“What? Who? When?”) then science is easy by comparison.

Significant gratitude is due to Ms. Verena Winkler of the RTG who helped in no small part with my arrival, settling, and acclimation in Germany. I am very grateful for your efforts and kindness. To the GSN Team, this program is excellent and lives up to its reputation and I thank you all for your continual help. I would also like to thank my thesis advisory committee members Prof. Dr. Anja Horn-Bochtler, Prof. Dr. Jovica Ninkovic and Prof. Dr. Bernd Fritzsch for their scientific advice and guidance over the last years.

To Dr. Bernd Fritzsch and Dr. Karen Thompson, my erstwhile and original mentors, my academic beginning is due entirely to you. Bernd, thank you for introducing me to the world of science. Karen, your meritorious and laudable tutelage is very appreciated. Pretty good word usage for a “hard worker”, right?

Penultimately, I wish to thank my friends and family. In particular: To Jess, who is there for me every single day, though it feels weird to offer you a compliment, without you this would never

have been possible. You are an inspiration. Chris, words fail me, but know I am eternally grateful for you. You have made my time here most meaningful. It's a good thing you survived that fall on the Alps. Robert, I always look forward to our scientific and general life discussions. And now to all my family members, for which there are countless of them, thank you for your words of encouragement and support over the years. Specifically, to Ali, my sister: you're up next kid. Finally, to my parents, Craig and Kandi, above all your support means more than I can express. Thank you for teaching me to follow my passion. Dad, this one is for you.

ABSTRACT

Sensory detection of self-motion provides information on movement and orientation in space. Vertebrates detect these features in part through dedicated vestibular sensory endorgans in the inner ear. Vestibular signaling during self-motion drives motor commands which permit the eyes to remain stable while moving. Maintaining this stability allows a continual preservation of visual acuity on the retina while moving in three-dimensional space. Such signaling is stereotyped in its computational processing and occurs through evolutionary conserved brainstem circuits. These brainstem gaze-stabilizing circuits, however, are not always perfectly suited to respond with immediate perfection to all manner of possible stimuli complexities. Counteracting this rigidity is the intrinsic ability to be plastic and reorganize along many systemic levels. The balance between keeping essential processing measures while also maintaining a degree of flexibility is still incompletely understood, particularly with respect to scopes of permissive extents and corresponding mechanisms of reorganization. In this dissertation I expand upon these biological considerations through a series of experimental manipulations which challenge vestibular processing in *Xenopus laevis.* Leveraging these induced manipulations, I examine a range of anatomical, electrophysiological, and behavioral consequences of three specific atypical sensory conditions. In the first study of this work, I profiled the extent to which gaze-stabilizing reflexes can develop following embryonic removal of one inner ear, thus challenging traditional circuit connectivity and processing of bilateral input. In the second study, embryonic transplantation of the inner ear anlage generated animals with an additional ear on their trunk, a condition which assessed processing measures following introduction of extra input from an atypical origin. The final study of this work used pharmacological aided inactivation of phasic vestibular pathways to investigate possible sensorimotor consequences of an impairment in high frequency self-motion detection. The collective findings of this dissertation reveal a considerable extent of plasticity in vestibular networks. Despite the sensory challenges presented, these results report a common ability to transform self-motion input into appropriate extraocular motor commands. This ability is inferred to be the result of reorganization at multiple sites which aimed at homogenizing central activity levels and/or establishing dynamic processing ranges. These findings add to the current scope of knowledge on the permissive extents of the vestibular system to be plastic in the face of sensory influences.

TABLE OF CONTENTS

LIST OF FIGURES

LIST OF TABLES

LIST OF ABBREVIATIONS

AMPA	α-amino-3-hydroxy-5-methyl-4-isoxazolepropionic acid
AOS	accessory optic system
Atoh1	atonal homolog 1
BMP	bone morphogenetic protein
Ca^{2+}	calcium ion
CNS	central nervous system
DTN	dorsal terminal nucleus
EOM	extraocular muscle
FGF	fibroblast growth factor
GABA	γ-aminobutyric acid
K^{+}	potassium ion
LTN	lateral terminal nucleus
MTN	medial terminal nucleus
nBOR	nucleus of the basal optic root
NLM	nucleus lentiformis mesencephali
NMDA	N-methyl-D-aspartate
NOT	nucleus of the optic tract
NT	neural tube
OKR	optokinetic reflex
PCP	planar cell polarity
PNS	peripheral nervous system
RGC(s)	retinal ganglion cell(s)
Shh	sonic hedgehog

VOR	vestibular-ocular reflex
4-AP	4-Aminopyridine

CHAPTER I:

INTRODUCTION

Detection of the external world is accomplished through the physiological efforts of sensory systems. In vertebrate species, following signal transduction from sensory organs and transmission into the central nervous system (CNS), sensory modalities become represented as neuronal computations within dedicated circuits. These computational transformations, combined with the ability to detect simplistic or increasingly complex characteristics of an environment, allow organisms to behaviorally respond to dynamic changes relative to themselves and their environment (Burgess and Granato, 2007). Such responsive actions constitute aspects of the full behavioral repertoire of an organism and originate from coordinated motor commands. The general ability to integrate sensory inputs to produce relevant motor outputs is termed sensorimotor processing and has historically been studied among the major sensory modalities, such as vision, hearing, olfaction, taste, and touch (Linford et al., 2011). Beyond these traditional senses, a variety of others exist and despite varying levels of ubiquity across vertebrates (Hodos and Butler, 1997; Gracheva et al., 2010; Crampton, 2019), all nonetheless contribute to sensorimotor environmental interactions. Inarguably, one of the most universal and evolutionary conserved modalities is the ability to detect changes in position and motion in space (Markl, 1974; Straka et al., 2014). In vertebrates, this detection ability is afforded through dedicated vestibular sensory endorgans in the inner ear (Beisel et al., 2005). Sensory information of linear and angular accelerations resulting from changes in position enable the vestibular system to contribute to neuronal computations associated with self-motion. The ability to detect and interpret self-motion dynamics is a fundamental feature of all vertebrates and it permits a spectrum of behaviors (Goldberg and Cullen, 2011). Most notable of these behaviors are stabilizing-reflexes which operate to ensure proper balance, posture, and visual acuity by generating motor commands which compensate for head/body deviations (Raymond and Lisberger, 1996; Bagnall and Schoppik, 2018). All vertebrates which locomote and change position in space rely on these reflexes to cope with the simultaneous detrimental effects of the latter deviations, which impact subsequent sensorimotor processing and behavioral interactions.

Vestibular evoked gaze-stabilizing reflexes are of particular importance as they aid in correcting retinal image slip, a physical consequence of body/head motion which causes loss of visual acuity on the retina (Glasauer and Straka, 2022). Stabilization of gaze in such a manner is executed with relatively little delay (Collewijn and Smeets, 2000), and without such temporally appropriate corrective measures visual perception is challenged as the eyes are unable to maintain a position

where the visual scene remains fixed on the retina. Sensorimotor transformations that execute these vestibular driven gaze-stabilizing reflexes are processed through neural circuits in the brainstem. Afferent sensory neurons from inner ear endorgans relay self-motion information into hindbrain vestibular targets, which in turn project and signal to brainstem motor centers that drive extraocular muscles for subsequent yoking of the eye. This synaptic arrangement is conserved across all vertebrates with few deviations (Fritzsch, 1998; Straka et al., 2014; see below for exceptions), suggesting that gaze-stabilization from these sensorimotor networks has consistently provided a beneficial behavioral substrate under evolutionary pressure (Fritzsch, 1998). Despite the conserved and seemingly hard-wired nature of vestibular gaze-stabilizing reflexes, a considerable spectrum of functional plasticity exists (Miles and Lisberger, 1981; Hirata and Highstein, 2002; Paterson et al., 2005). Such adaptability manifests intrinsically as changes in vestibular circuits themselves and their synaptic elements (Boyden et al., 2004; Paterson et al., 2005) and occurs either in isolation or with assistance from other brain networks that participate in self-motion processing, such as visual-motion and proprioceptive signaling (Zennou-Azogui et al., 1994; Sadeghi et al., 2012) which converge with vestibular signals (Angelaki and Cullen, 2008). As with all forms of plasticity in the CNS and peripheral nervous system (PNS), maintaining a dynamic range of adaptability beyond developmentally defined functionality provides considerable benefits when continuously responding to complex environments with varying demands (Pascual-Leone et al., 2005). However, holistic understanding of plasticity in vestibular gaze-stabilizing circuits, and by extension the vestibular system as a whole, is a sizable task which requires experimentation across many disciplines and profiling on systematic scales. Efforts to examine the permissive scopes and corresponding magnitudes of vestibular plasticity have traditionally leveraged induced or innate deviations in processing abilities. Such disruptions range from e.g., developmental modifications (Lilian et al., 2019), induced damage (Dutia, 2010), or motor learning paradigms (Boyden et al., 2004) and are followed by experimental profiling of functional and anatomical consequences. Owing to the complexity and distribution of these centers, no single experimental manipulation aimed at creating deviations of this nature can comprehensively assess all features of vestibular plasticity. Nonetheless, stepwise exploration can assist in navigating neural plasticity spectra and broaden our scientific understanding of how flexible the vestibular system is.

In this thesis, I explore plasticity in vestibular gaze-stabilizing reflexes through a series of manipulations in the model system *Xenopus laevis* which aimed at inducing targeted changes in processing ability along vestibular pathways. In the following chapters, I will introduce three independent experimental manipulations which provoked changes in vestibular sensory detection and/or processing in central vestibular targets. The first two manipulations, corresponding to chapters II (Gordy and Straka, 2022) and III (Gordy et al., 2018), initiated changes during embryonic

development which challenged ontogenetic formation of peripheral sensory detection through either a decrease or increase in inner ear endorgans, respectively. Chapter IV (I Gusti Bagus et al., 2019) explores the effects of a selective, and acute, pharmacological targeting of functionally mature peripheral sensory neurons and central brainstem targets. Subsequent behavioral and physiological consequences of these experimental deviations are presented and used to approximate degrees of permissible plasticity in gaze-stabilizing vestibular reflexes. In the final chapter of this thesis, I discuss the implications of these findings and their contributions to the current and future field of vestibular research.

Peripheral detection of self-motion

Sensory encoding of self-motion is a necessity for any organism that moves in three-dimensional space (Walls, 1962; Land, 1999). In a general sense, detection of any external stimulus is typically isolated to a select number of sensory organs. Precepts are often even restricted to one organ, such as detection of light, which derives in vertebrates from the retina and is unable to be encoded elsewhere such as for example, through somatosensory touch receptors (Delhaye et al., 2018). Self-motion detection is of a noteworthy complexity by comparison, where multiple sensory systems are recruited, either passively or actively, to extract features of bodily movement in space (Tanahashi et al., 2015; Chagnaud et al., 2017; Cullen and Zobeiri, 2021). Such recruitment is due to the dynamic and complex nature of motion as a stimulus that influences a wide range of sense organs and their subsequent processing during body movement. Auditory information is a substantial contributor to self-motion percepts (Tanahashi et al., 2015). Likewise, proprioceptive signaling gives feedback approximations of positional changes, which is a useful method of self-motion estimation (Cullen and Zobeiri, 2021). While a similar argument can likely be made for a range of sensory systems (e.g., the amphibian and teleost lateral line systems; Chagnaud et al., 2017; see below) and thus offer interesting philosophical considerations from an evolutionary perspective, the primary contributors to self-motion detection are the visual and vestibular systems (Dichgans and Brandt, 1978). These systems, which are evolutionarily tied very closely (Straka et al., 2014), operate synergistically to contribute toward central percepts of self-motion. Research on the vestibular system therefore benefits from considerations into synergistic visual contributions. The following pages will discuss both systems in detail. Emphasis will first be made toward their peripheral sensor organs and cell types followed by representative central targets and circuits involved in one avenue of self-motion processing, specifically the stabilization of gaze.

Vestibular sense organs in the inner ear

Vestibular processing of motion stimuli in vertebrates initiates in dedicated bilateral inner ear vestibular endorgans. Such endorgans exist in conserved and highly stereotyped spatial arrangements within an anatomically complex network of ducts and pouches (Torres and Giráldez, 1998). These ducts/pouches, which are collectively termed the membranous labyrinth of the inner ear, are structurally supported by enclosure within a rigid cartilaginous (e.g., in larval *Xenopus*) or bony (e.g., in adult mouse) structure of matching anatomical dimension (Quick and Serrano, 2005; Ekdale, 2013; Pfaff et al., 2019). The neurosensory components within individual endorgans are mechanosensory hair cells and afferent neurons (Lewis and Li, 1975; Fekete and Campero, 2007; Fritzsch and Straka, 2014). Irrespective of individual endorgan structural or positional arrangements, which imparts specific functional consequences during motion vector detection (see below), hair cells and afferent fibers are the dedicated effectors for sensory transduction and transmission into central brainstem targets, respectively. Cells of the former type are organized into distinct epithelial patches that are flanked by supporting cells (Wan et al., 2013). Hair cells within these patches have their apical sides embedded in endorgan-specific gelatinous structures and are bathed in a potassium ion (K^+) rich endolymph fluid. A characteristic feature of these cells, from which their name derives, is a collection of stereocilia bundles along their endolymph-projecting apical side (Lewis and Li, 1975; Hudspeth, 1997) organized in a staircase fashion of increasing height. In vestibular hair cells, an anatomically distinct terminal cilia termed the kinocilium is present. Additionally, hair cell stereocilia are mechanically linked along the tips, a feature which when combined with their stepwise arrangement enables their function as a sensor for the shearing forces originating from acceleration dynamics during positional changes of the head/body (Hudspeth, 1997). Displacement of the stereocilia, for example during head rotation or head tilts, initiates either an increase or reduction of K^+ conductance into hair cells though mechanically gated ion channels (Hudspeth, 1989; Zdebik et al., 2009). Thus, depending on the direction and degree of mechanical displacement, graded depolarization or hyperpolarization of the hair cell occurs. Evoked fluctuations in K^+ conductance and subsequent changes in depolarization influence downstream signaling mechanisms within hair cells, such as e.g., activation of voltage-sensitive calcium (Ca^{2+}) channels, which ultimately culminates in dynamic modulations of glutamate release onto innervating sensory neurons (Jones et al., 2008). Such changes in hair cell synaptic release modulate around a spontaneous homeostatic level (Goldberg, 2000; Jones et al., 2008), which in turn is reflected in deviations of spontaneous firing rates of afferent fibers. Spontaneous firing rates in afferent vestibular fibers range from small values as in e.g., *Xenopus laevis*

which operate around 0.1 to 14 Hz (Gensberger et al., 2016), to average rates which can occur well above 100 Hz in birds (Anastasio et al., 1985) and primates (Goldberg, 2000) or intermediate levels as in the gerbil (Dickman et al., 1991). Thus, vestibular afferent fibers universally exhibit a consistent and sustained tonic baseline spontaneous firing rate which can increase or decrease depending on upstream hair cell activity. Afferent vestibular neurons are anatomically of the bipolar type (Maklad and Fritzsch, 2003). Peripheral dendrites of these sensory neurons synapse on all hair cells within vestibular endorgans, and their central projecting axons terminate in stereotyped hindbrain target regions. The collective population of cell bodies for vestibular afferents, alternatively known as Scarpa's ganglion (Curthoys, 1981; Horn, 2020), are located adjacent to sensory neurons which relay auditory information such as from e.g., the cochlea in mammals or lagena/saccule in amphibians (see below, Fritzsch et al., 2002; Koundakjian et al., 2007). The primary function of vestibular afferent fibers is to conduct sensory input into the brain. However, these afferent fibers on their own lack any internal physiological indication for which dimensional plane a motion is occurring in. To circumvent such a deficiency, which in the null condition would render the inner ear as being a simple on/off detector for bodily movement in space, afferent fibers are physiologically labeled by their peripheral endorgan targets (Kuruvilla et al., 1985; Beraneck and Lambert, 2020). In addition, specific morphophysiological characteristics can be used to distinguish afferent fibers for certain features of information they process. However, this is limited to frequency characteristics and continues to lack specificity of peripheral sensory origin (Eatock and Songer, 2011). In addition to afferent sensory fibers, cholinergic efferent neurons (Fritzsch and Elliott, 2017a) are also connected to vestibular endorgans. The axons of these fibers project from their cell body origin in the brainstem and innervate hair cells and afferent fibers directly (Hellmann and Fritzsch, 1996; Mathews et al., 2017). Vestibular efferent neurons are believed to serve a modulatory role in influencing peripheral sensitivity, however a spectrum of specific functionalities is described for them (Mathews et al., 2017).

As mentioned above, the inner ear is not merely a simplistic on/off detector for body motion in space. Rather, it faithfully encodes various features of motion parameters. Positional and structural features of specific endorgans enable them to achieve such detailed encoding. Vestibular endorgans can thus be roughly divided into two categories: those which encode linear accelerations and those which encode rotational accelerations (Angelaki and Cullen, 2008; Glasauer and Knorr, 2020). Linear accelerations, such as during translational movements or positional alterations within the earth's gravitational field, are detected by otolith endorgans. Within these organs are clusters of hair cells which are termed maculae that are embedded into a gelatinous matrix that is covered by collections of calcium crystals, typically termed otoconia or otoliths (Popper et al., 2005). Inertial displacement of these crystal masses, for example during a forward linear motion or head tilt, induces positional

changes in hair cell bundles which in turn influence synaptic release onto afferent dendrites. All vertebrates possess at least two otolith endorgans, the utricle and the saccule. Further otolith endorgans exist in certain species, such as the lagena in all non-therian mammals (Branoner et al., 2016), the macula neglecta in coelacanths, reptiles, and sharks (Brichta and Goldberg, 1998), the amphibian papilla in urodeles and anurans (Fritzsch et al., 2002), and the basilar papilla in amphibians, birds, and reptiles (Fritzsch et al., 2013). Though beyond the scope of this dissertation, it is important to note that certain otolith endorgans are not specific to detecting self-motion alone. Specific endorgans in aquatic organisms such as e.g., the amphibian and basilar papillae as well as the saccule, are known to detect auditory stimuli from the environment mediated by sound wave propagation in aqueous environmental mediums, though this is likely a possibility to some degree for all otoliths (Ross and Smith, 1980; Fritzsch and Straka, 2014). The utricle is mostly horizontally positioned while the saccule and lagena are vertically orientated, though the utricle and saccule exhibit slight deviations from perfect horizontal or vertical positioning. Hair cells within utricular and saccular maculae are arranged non-uniformly with respect to the polarity of their stereocilia bundles, and group instead into roughly two oppositely orientated clusters which span a 360° directional range (Ono et al., 2020). These roughly dichotomously orientated clusters localize discretely on individual maculae between a central line of polarity reversal called the striola (Li et al., 2008; Ono et al., 2020). The relative orientations of the two macular endorgans and their corresponding hair cell polarities ensure a range of sensitivity across a complete three-dimensional space for linear accelerations. Otolith organ-mediated inertial sensitivity, however, is unable to detect fast angular accelerations in space and thus alone would be unable to provide the CNS with information about rotational movements. Such an ability derives exclusively from the semi-circular canal system.

Semi-circular canals are the anatomical structures which permit the detection of rotational movements in space. Jawed vertebrates possess three such canals which consist respectively of a singular canal which is situated in the horizontal plane, as well as two additional in a non-overlapping arrangement in the vertical plane (Groves and Fekete, 2012). The latter two canals are positioned ~45° either antero- or postero-laterally with respect to the midline of the head (Simpson and Graf, 1981). Nomenclature for the three semi-circular canals is apt and conforms to their geometric organization: horizontal canal(s), anterior canal(s), and posterior canal(s). Each canal is filled entirely with endolymph fluid and swells at one terminal end in a structure called an ampulla. The canals themselves lack any neurosensory components which are instead housed in individual ampullae (Chang et al., 2004). Located in each ampullar structure are canal cristae, which consist of hair cells and supporting cells that are embedded in a gelatinous matrix called the cupula that spans the ampullar pouch (Chang et al., 2004). Unlike macular endorgans, where force bearing otoconia deflect their underlying matrix,

canal hair cell activity is influenced instead by deflections of the cupula from inertial lagging of endolymph fluid through the canals during head/body rotation (Hullar, 2006). Deflections of the cupula are bidirectional depending on the direction of head rotation. However, the excitatory sensitivity of a single semi-circular canal endorgan is for one direction only. Indeed, cristae hair cells exhibit a uniform polarity and are therefore all simultaneously either activated or deactivated depending on deflection of the cupula (Deans, 2021). This polarity homogeneity presents with physiological consequences such that sensory input from a singular canal report solely on rotational movements from one dimensional plane and sensory neurons are therefore excited from only one rotational direction (Blanks et al., 1975). Combined with the unique orthogonal distribution of the three canals, the inner ear is thus able to profile rotational accelerations faithfully in three-dimensional space.

Linear and angular acceleration signaling enable vertebrates to perceive all manner of active and passively generated movements. However, it is critical to note that vertebrates are bilaterians and thus naturally develop with two inner ears. As a result, vestibular endorgans exist as bilateral pairs across the midline of the head. Furthermore, bilateral pairs are arranged in a mirror-symmetry to each other (Curthoys, 2020; Deans, 2021). Coupled with individual intra-endorgan directional sensitivities (see above), bilateral pairs work in synergy to encode motion vectors. This is particularly evident for the semi-circular canals where bilateral pairs are excited by opposite directional motions in the same dimensional plane. Alternating rotations in the horizontal plane, for example, will drive excitatory responses in hair cells for one canal or the other, but in mutual exclusivity. Accordingly, rotation in the off-direction will elicit a decrease in endorgan activity on one side while the activity on the contralateral side is simultaneously increased. Bilateral otolith maculae follow a synergistic functionality for populations of hair cells with similar polarity. Tilts which activate hair cell populations of one polarity type in the left inner ear will also activate a corresponding population on the other bilateral side, albeit these populations will exist on different sides of their respective striola macular reversal lines, which differ between specific macular endorgans (Curthoys, 2020). As further discussed in chapter II of this dissertation, the mirror-symmetry of inner ears therefore ensures that individual endorgans on both bilateral sides are unique in their sensory capacity. Since the discharge rates of associated afferent fibers are causally linked to upstream hair cells, such functional dynamics are maintained during neuronal transmission into the hindbrain. Indeed, fluctuation of afferent resting activity above and below homeostatic rates is a key feature of vestibular sensory processing (Kim and Curthoys, 2004; Gensberger et al., 2016). These combined features contribute to a hallmark characteristic of functionality in the vestibular periphery referred to as “push-pull” functionality, which assists in strengthening and amplifying sensory detection (Platt and Straka, 2020).

Dynamic transformations of vestibular signaling

Head/body movements of vertebrates span a considerable spectrum of accelerations and resultant frequency profiles (Carriot et al., 2017; Wang et al., 2021). Beyond simple computations of directionality, vestibular endorgans can extract features from such complex movements which assist in discriminating frequency spectra during self-motion. Sensory resolution of this manner is afforded by a diversity of hair cells and afferent neurons with distinctive morphophysiological properties (Eatock and Songer, 2011). Hair cells, which universally maintain their role as sensors of mechanosensory stimuli, have a heterogeneity in morphophysiological traits that is observable at the level of stereocilia bundles, cell body morphology, and afferent terminal innervation (Goldberg, 2000; Eatock and Songer, 2011). Differences in the latter two features enable a classification of vestibular hair cells into two varieties: type I and type II. Type I hair cells are bulbous, flask shaped, and innervated by afferent terminals of the calyx type, while type II hair cells are more slender, columnar in shape, and innervated in a bouton-like fashion (Lewis and Li, 1975; Gopen et al., 2003; Burns and Stone, 2017). Type I and type II can be further differentiated based on stereocilia features such as e.g., bundle height, stereocilia quantity, and structure of terminal edge cilia, which are known to differently influence electrophysiological properties of sensory transduction (Spoon et al., 2011; Eatock and Songer, 2011). Type I hair cells in turtles, for example, have been shown to have more stereocilia than type II, a feature which contributes to higher degrees of current flow in the former (Moravec and Peterson, 2004). Differences in bundle morphologies are not exclusive to type I or type II designations however, particularly given that anamniotes possess only type II (Lewis and Li, 1975; Straka et al., 2009) and yet maintain several different types of hair cell bundles as e.g., shown in the bullfrog (Lewis and Li, 1975). These variations in response characteristics assign individual hair cells to a functional dichotomy of being selective filters for the processing of either low frequency (e.g., slow head tilts) versus higher frequency (e.g., fast head rotations or translations) movements (Beraneck and Straka, 2011).

Sensory afferent fibers present with similar features that permit the continued disassociation of low versus high frequency movement processing. As mentioned above, type I hair cells in amniotes are innervated in a calyx fashion. In line with the properties of these hair cells that enable their selectivity for high frequency motions, terminal calyces contribute to fast conduction of synaptic signaling (Schneggenburger et al., 1999). However, it is of worth to note that not all afferents correspond to simple calyx or bouton terminals, as some afferents are dimorphic and indeed innervate

with both terminal types (Goldberg, 2000; Eatock and Songer, 2011). Therefore, afferents are better classified according to their response timing and dynamics. Tonic afferents are so termed due to their regularity in spontaneous response timing and maintained spike rates during continued stimulation. In contrast, phasic afferents exhibit irregular firing rates at rest and upon stimulation undergo a burst of activity followed by fast spike attenuation (Blanks and Precht, 1976; Lasker et al., 2008; Kalluri et al. 2010). Tonic fibers thus are more suitable for encoding e.g., head tilts or slow translations, whereas phasic fibers are ideal for higher frequency head/body movements. In regard to endorgan distribution, tonic fibers mostly innervate extra-striolar regions in macular endorgans and peripheral regions of canal cristae, while phasic fibers mostly target areas around the striola and central cristae regions, respectively (Lysakowski and Goldberg, 2004; Eatock et al., 2008; Eatock and Songer, 2011). Generation of these distinct response characteristics is attributed to multiple mechanisms, such as e.g., anatomical characteristics based on zonal location in endorgan sensory epithelia from frequency tuned hair cells, biophysical hair cell-afferent synaptic mechanisms, and intrinsic modulation of spike regularity through specific sets of ion channels (Eatock et al., 2008; Straka et al., 2009; Kalluri et al., 2010; Contini et al., 2022). In the case of the latter, a few notable contributors have been reported, such as γ-aminobutyric acid (GABA) mediated activation of metabotropic GABA-B receptors (Holstein et al., 2004). Vestibular afferents are excited by hair-cell derived glutamate through α-amino-3-hydroxy-5-methyl-4-isoxazolepropionic acid (AMPA) and N-methyl-D-aspartate (NMDA) receptors (Niedzielski and Wenthold, 1995), which drive depolarizations and subsequent action potential generation. In contrast, phasic neurons are unique in their inhibition by GABA release which permit K^+ mediated hyperpolarization of the cell, leading to spike attenuation. Such K^+ conductance is known to be mediated by low-voltage gated potassium channels of the Shaker related Kv1 family (Kalluri et al., 2010). In fact, selective use of the chemical 4-Aminopyridine (4-AP), which blocks Kv1 channels, has been shown to convert response dynamics of phasic neurons into those expected in tonic fibers (Kalluri et al., 2010). More passive features, such as cell body and neurite size also contribute to the generation of phasic responses simply by conduction velocity alone, which is proportional to diameter. In the case of phasic fibers, their size has been demonstrated to be larger than their tonic counterparts (Honrubia et al., 1989; Goldberg, 2000).

Encoding the diverse features of self-motion which span variable frequency domains is a task well suited to the dynamic properties of frequency-tuned vestibular neurosensory cells. This discriminatory transmission ability has also been shown to be present in hindbrain vestibular targets in *Ranid* frogs (Beraneck et al., 2007; Pfanzelt et al., 2008; Straka et al., 2009) as well as downstream motor effectors for gaze-stabilization in larval *Xenopus* (Dietrich et al., 2017) to assist in faithful vestibular sensorimotor processing. In the case of motor commands, frequency tuned pathways are

present in the morphophysiological properties of motoneurons themselves (Dietrich et al., 2017). The ability to process differential frequency characteristics simultaneously through neurosensory and central pathways is referred to as parallel-processing and constitutes a general principle for vestibular sensorimotor transformations (Straka et al., 2004; Beraneck and Lambert, 2020). In addition, from a perspective of neural plasticity where flexibility in the face of environmental demands is paramount, parallel channels offer a provocative site of modulatory ability to assist in adaptive responses. In summary, vestibular endorgans in the inner ear are optimal peripheral sensors for detecting changes in body position and motion in space.

Visual input during self-motion: optic flow from the retina

Self-motion results in dynamic shifts of head/body position. As mentioned previously, a result of this movement is that the eyes of an organism accompany the head/body during its three-dimensional displacement and thus are simultaneously moved with it. During conjoint displacement with the head/body, the area of the visual periphery that the eyes view changes accordingly. Such changes of the visual scene are used to estimate self-motion (Lappe et al., 1999). The neurosensory cells of the eyes include light sensitive photoreceptors and their associated sensory afferents, the retinal ganglion cells (RGCs; Kim et al., 2021). These cells localize in the retina, a highly organized laminar structure within the complex architecture of the eye along with other supporting cells such as bipolar, horizontal, and amacrine cells (Kha et al., 2019). Visual detection of the world is accomplished by coordinated efforts of the cell types within the retina, but the effectors for sensory transduction and transmission into the brain are photoreceptors and RGCs, respectively. Sensory input to the eyes is topographic, with characteristics of the peripheral visual scene being represented in spatial correspondence on the retina (Cline and Constantine-Paton, 1989; Cang et a., 2018). In the case of self-motion mentioned above, the entire visual scene is shifted concomitantly with movement of the head/body. This generates a full-field panoramic shift of the visual scene that is classically referred to as optic flow and is used as an estimate of bodily motion in space (Angelaki, 2014; Matsuda and Kubo, 2021). Indeed, visual motion alone can be convincing enough to cause perceptions of apparent self-motion despite being physically stationary (Dichgans and Brandt, 1978; McAssey et al., 2020). Optic flow signaling originates from changes in light detected by photoreceptors, however, single photoreceptors alone are argued to be incapable of motion processing (Borst, 2007). Instead, motion percepts are attributed to the signaling efforts of direction sensitive populations of RGCs (Barlow and Hill, 1963; Matsuda and Kubo, 2021) which process and relay this information into stereotyped second

order targets in the brainstem where computations continue (e.g., Nikolaou et al., 2012; see below). In addition, contributions from other retinal cell types through specific synaptic connectivities influence the processing of visual motion stimuli (Briggman et al., 2011).

Optic flow contributes to a variety of environmentally relevant visuomotor behaviors such as navigation, heading, collision avoidance, and distance approximations (Lappe, 1999; Bhagavatula et al., 2011; Helmer et al., 2017). Furthermore, such visual input assists in stabilization of the body (Kist and Portugues, 2019), the head (Wagner et al., 2022), and the eyes (Masseck and Hoffmann, 2009a) with respect to the visual world. In visually guided vertebrates, and indeed many invertebrates (Helmer et al., 2017; Busch et al., 2018), all head/body motion in space will coactivate visual-mediated panoramic optic flow. Therefore, visual information is recruited by the CNS to aid in interpreting and responding to self-motion.

Multi-modal convergence of self-motion information

Beyond vestibular and visual input, sensory information from other environmental modalities contribute to self-motion processing. For example, proprioceptive input from muscle spindles (Cullen and Zobeiri, 2021) is a prominent contributor to motion precepts given that it provides real time feedback on how the body is physically positioned. Additionally, non-vestibular mechanosensory gated modalities are also recruited to extract features of head/body movements, such as auditory information (Tanahashi et al., 2015) as well as the lateral line system of teleosts and amphibians (Chagnaud et al., 2017). In addition, olfaction helps with gaze-stabilizing movements as demonstrated in the fruit fly (Chow et al., 2011). Combined with concomitant visuo-vestibular signaling and given the wealth of additional input afforded by these other sensory systems, encoding of self-motion is thus rarely accomplished by a singular modality.

Within the CNS, visual, vestibular, and proprioceptive information converges extensively along vestibular network pathways, starting at the vestibular nuclei and ranging to even the telencephalon (Angelaki and Cullen, 2008; Fritzsch et al., 2022). For example, cells within the vestibular nuclei have been shown to be responsive to visual input alone, as well as during vestibular stimulation (Waespe and Henn, 1977). One benefit of such combinations is likely in the reduction of sensory ambiguities. Optic flow for example is not a perfect solution for determination of body movement. Indeed, it is only an approximation generated by motion of the visual scene relative to the organism and is thus sensitive to objects which independently move in the environment (Sasaki et al., 2017). Cooperative processing between vestibular and visual input has been demonstrated to help reduce such ambiguity

in the rhesus monkey through converging inputs (Sasaki et al., 2017). Auditory information is also known to resolve sensory differences in a similar manner. Echolocating bats have demonstrated the ability to integrate visual and auditory stimuli to good effect (Kugler et al., 2019) despite the low reliance on vision by these nocturnal animals (Kugler et al., 2016), which was argued to help resolve extrinsic and intrinsic ambiguities (Kugler et al., 2019). Auditory cues are apparently rather effective in their recruitment for self-motion percepts. Human subjects reported experiencing illusions of self-motion from auditory stimuli alone, which was strengthened considerably when combined with visual input (Keshavarz et al., 2014), a sign that convergent processing is robust in these modalities. Behavioral consequences of vestibular impairments have even been shown to be ameliorated due to contributions from other modalities (Darlington and Smith, 2000). Even olfaction, as demonstrated in the fruit fly, is integrated extensively with visual and mechanosensory input and helps gaze-stabilization (Sherman and Dickinson, 2003; Chow et al., 2011). Proprioceptive signaling is another noteworthy example in its beneficial interactions with the vestibular system which aids in the disassociation of active and passive movements (Cullen and Zobeiri, 2021). The former movements are generated by the organism directly (e.g., running, swimming, flying) while the latter are the result of extrinsically driven displacements of the body (e.g., wind buffering midflight, unexpected falls, or bodily displacements by water). Specific cellular targets in the vestibular nucleus exhibited prominent activity profiles during passive movements but were suppressed during actively generated motion (Roy and Cullen, 2001). Importantly, proprioceptive feedback during motion was critically important in such modulatory ability (Brooks and Cullen, 2014), further highlighting the necessary contributions of the latter modality for self-motion computations. A distinguishing note here is that vestibular nuclei target neurons which show this effect appear to be specific to those which project to the spinal cord or to the thalamus. In contrast, ocular motor projecting neurons use an alternate strategy which aims at suppression of gaze-stabilizing commands during voluntary shifts of the eye (Cullen and Zobeiri, 2021). Therefore, it seems that proprioceptive feedback is relevant for ensuring physiologically appropriate behaviors resulting from self-motion.

Though this section seeks to provide select examples of the importance of multi-sensory integration, it should be noted that non-sensory predictive motor signaling also operates in the computational processing of self-motion (Straka et al., 2018). Duplication of motor signaling is often relayed in the CNS and derives from either higher order centers in the form of corollary discharge pathways or from motor execution circuits as efference copies (Straka et al., 2018). In the above example of active/passive discrimination, the ability to gate central vestibular activity is believed to be due to a proprioceptive comparison to internal efference copies (Brooks and Cullen, 2014). Predictive motor signaling also seems to be instrumental in modulating activity of efferent

motoneurons which regulate inner ear sensory transduction (Chagnaud et al., 2015) as well as during suppression of vestibular evoked gaze-stabilization during undulatory swimming in larval *Xenopus* tadpoles and lamprey (Lambert et al., 2012; Wibble et al., 2022).

Neuronal circuit control of gaze-stabilization

Gaze-stabilization is an important sensorimotor transformation for moving vertebrates. As mentioned previously, dynamic changes in position displace the entire body, which includes the eyes. Motion-induced displacement of the eyes is rather detrimental for maintenance of visual acuity, as unexpected or continual optic flow is often not beneficial for an organism when visually interacting in their environment (Land, 1999; Angelaki and Hess, 2005). A method of counteracting this diminution of visual acuity is through short latency neuronal reflexes which derive from vestibular and visual inputs (see above). These reflexes transduce, transmit, and finally transform motion sensory information into motor commands which execute corrective adjustments of the eyes to keep the visual scene stable (Schweigart et al., 1997; Straka et al., 2014). Stabilizing movements of the eyes serve to negate bodily-induced displacements and thus maintain visual acuity during motion. Given that vestibular and visual information is processed through different peripheral sensory organs, a conceptual separation of these modalities into discrete pathways has led to a classification of a distinctive vestibular-ocular reflex (VOR) and optokinetic reflex (OKR). Though this thesis is focused on plasticity in the VOR, the synergistic co-activation of these two reflexes (França de Barros et al., 2020), and their extensive central convergence (Angelaki and Cullen, 2008), necessitates the discussion of both. The following sections will introduce and describe these reflexes.

Extraocular muscles and their cranial motoneurons

The common effector targets of motor commands for both the VOR and OKR are the extraocular muscles (EOM). Jawed vertebrates possess six primary EOMs, organized locally into antagonistic pairs. Two oblique muscles; superior and inferior, and four recti muscles; superior, inferior, lateral, and medial which are arranged around the eye (Fritzsch et al., 1990; Spencer and Porter, 2006). The collective contraction dynamics of all six extraocular muscles allow precise movements of the eyes, which are generally separated into two categories: movements that shift the eyes or that stabilize them (Horn and Straka, 2021). The latter is of interest in the work presented

here, however the former warrant a special notice given their prominence in a variety of species with a fovea or similar structures in the eye which permit high resolution detection (Land, 2015). Irrespective of movement type however, eye motion is accomplished through signaling from dedicated extraocular motor nerves (Spencer and Porter, 2006).

The innervation of the extraocular muscles is rather conserved throughout evolution with just few exceptions. Innervating the superior and inferior recti (SR, IR), as well as the medial rectus (MR) and inferior oblique (IO) muscles are branches of the oculomotor cranial nerve (III^{th}). The abducens cranial nerve (VI^{th}) innervates the lateral rectus muscle (LR), while the trochlear nerve (IV^{th}) connects its axons with the superior oblique muscle (SO; Büttner-Ennever, 1992; Horn, 2020). This innervation organization principle is lateralized in jawed vertebrates, with the corresponding nuclei (nIII, nVI, and nIV, respectively) of these nerves being located on the ipsilateral side to their target muscles (Büttner-Ennever, 1992; Horn, 2020). However, an exception to this arrangement is in the case of the axonal branches of the III^{th} and IV^{th} nerve which innervate the contralateral SR and SO muscles respectively, following either cell migration or axonal crossing of the midline during development (Gilland and Baker, 2005; Bjorke et al., 2016). A further noticeable exception to this arrangement is in elasmobranchii such as shown in the stingray, where in addition to SO and SR contralateral innervation, the MR is innervated by axons from the contralateral nIII (Graf and Brunken, 1984; Puzdrowski and Leonard, 1994). Non-motor internuclear populations in both the nIII and nVI exist adjacent to motor clusters. These populations project, respectively, to abducens or oculomotor motor areas (Straka and Dieringer, 1991). Internuclear projections from the abducens nucleus terminate contralaterally (Baker and Highstein, 1975), whereas oculomotor axonal trajectories show mixed ipsi- and contralateral terminations (Clendaniel and Mays, 1994). Both are assist in the generation of conjugate horizontal eye motions (Baker and Highstein, 1975; Clendaniel and Mays, 1994). A critical organizational feature in all vertebrates is in the spatial positioning of respective EOMs and their pulling directions, which are generally rather aligned with the semi-circular canals of the inner ear with only slight deviations across species (Simpson and Graf, 1981). The functional importance of this will become clear in the following section.

Vestibulo-ocular reflex (VOR)

Linking vestibular endorgans to the extraocular muscles is the vestibulo-ocular reflex. Traditionally considered to be one of the most conserved of vertebrate circuits, and often referred to as a "simple reflex-arc" (Straka et al., 2014) due to its simplistic three-neuronal arrangement

(Szentágothai, 1950) and short latency processing time (Collewijn and Smeets, 2000), the VOR is afforded a prominent place in vestibular circuit research. Any meaningful neurobiological profiling of a particular circuit requires a defined behavior which approximates the functional permissivity of neuronal processing (Bagnall and Schoppik, 2018) and indeed the VOR serves a singular purpose in executing compensatory movements of the eyes to reduce retinal image slip. This relatively simple behavior is executed through just few select muscles (see above) and is largely invariant in its outcome across vertebrates (Straka and Dieringer, 2004; Straka et al., 2014), including even the lamprey, the oldest extant vertebrate (Rovainen, 1976). The conserved and simplistic VOR behavior has correspondingly conserved circuit functionalities and anatomical arrangements (Graf et al., 1997), which is not surprising given that evolutionary pressures such as natural selection act on behavior only and thus indirectly on circuits themselves (Tosches, 2017). Due to this commonality across vertebrates, understanding of the principles of vestibular processing has benefited from experimental profiling of VOR circuits in many species such as frog (Gensberger et al., 2016), fish (Graf et al., 1997; Bianco et al., 2012), cat (Zennou-Azogui et al., 1994), and monkeys (Sadeghi et al., 2007) where general conclusions find applicability in holistic understanding of the vestibular system (Straka et al., 2016).

Sensory afferents carrying input from the vestibular endorgans project into the vestibular nuclei in the hindbrain (Fritzsch et al., 2005; Soupiadou et al., 2020), where they innervate second-order vestibular neurons. While not all afferent fibers project to the vestibular nuclei, as some exhibit a direct termination in the cerebellum (Barmack et al., 1993) or abducens nucleus (Uchino et al., 1994), most afferent fibers terminate in these dedicated and stereotyped regions in the hindbrain. These regions are historically classified according to their anatomical position along the developmental rhombomeric scaffold and are termed by such an arrangement: medial vestibular nucleus (MVN), lateral vestibular nucleus (LVN), superior vestibular nucleus (SVN), and descending/inferior vestibular nucleus (DVN) (Horn, 2020). In addition, teleosts, ampibians, and birds have an additional hindbrain center which receives afferent input termed the tangential nucleus (Peusner and Morest, 1997; Bianco et al., 2012; Branoner et al., 2016). Second-order vestibular neuron populations can also be mapped according to the trajectory of their projections (Glover, 1996). A projection-based map from central hindbrain targets is argued to be a better organizational determinate given that a world-topographic map is absent for vestibular inputs (Glover, 1996; Maklad and Fritzsch, 2003; Straka and Baker, 2013). For vestibulo-ocular projections, a trajectory map is particularly useful as it reveals specific clusters of second-order targets which relay signaling events for specific eye muscles and thus dedicated VOR behaviors (Straka et al., 2014). Beyond those of the vestibular-ocular type, other second-order vestibular trajectories exist, such as projections to autonomic (Holstein et al., 2012) or thalamic centers (Wijesinghe et al., 2015) but for the purposes of this VOR-centric dissertation, will not be

discussed further. Sensory information from the inner ear is separated into linear (otolith derived) and angular (semicircular canal derived) channels and is represented centrally in partially distinct circuits which comprise the linear and angular VORs, respectively.

Angular VOR pathways relay transduced signals from the semicircular canals to ipsilateral second-order vestibular neurons. From here, a general dichotomous principle is observed in the projections of second-order targets irrespective of canal origin. Vestibular-projection neurons extend their axons either contralaterally to directly innervate and excite specific extraocular motoneuron nuclei through glutamatergic signaling (Büttner-Ennever, 1992; Graf et al., 1997) or project their axons to the extraocular motor nuclei on the ipsilateral side and drive an inhibition through GABA or glycine (Spencer et al., 1989; Büttner-Ennever, 1992; Graf et al., 1997). Excitatory and inhibitory projection neurons are spatially segregated in the hindbrain (Spencer et al., 1989). The targeting of specific motoneurons depends on the peripheral identity of the canal supplying the sensory input. For example, vestibular-projection neurons receiving same-sided afferent input from a posterior canal have contralateral axonal trajectories onto the oculomotor nucleus. From here, branches of the oculomotor nerve innervate the SO and IR muscles. Due to the crossing of the SO innervating nerve however, the innervation of this muscle is ipsilateral to the activated canal, whereas the IR is contralateral. This ensures that both eyes are yoked upwards during e.g., head rotation/tilts in frontal eyed animals (reviewed nicely in Horn, 2020). In lateral eyed animals with correspondingly shifted optic axes, such yoking is more torsional in nature (Bianco et al., 2012). At the same time, inhibitory vestibular-projection neurons innervate ipsilateral IO and SR oculomotor motoneurons. Such an inhibition ensures that antagonistically pulling muscles are not activated and thus permit correctly directed eye movements. Activity profiles for the horizontal canal follows a comparable scheme, with contralateral excitation and ipsilateral inhibition of abducens motoneurons, albeit the latter inhibition is accomplished through glycinergic signaling pathways (Spencer et al., 1989; Soupiadou et al., 2018). In addition, a synaptic intermediate is present in the horizontal angular VOR in the form of abducens internuclear neurons (Baker and Highstein, 1975; Straka and Dieringer, 1993). These glutamatergic internuclear neurons project across the midline and innervate MR motoneurons ipsilateral to the excitatory vestibular projection neurons. In doing so, the MR is driven to co-contract with the LR and ensures conjugate oppositely-directed horizontal movements of the eyes during horizontal rotation (Straka and Dieringer, 1993). These pathways are found in all jawed vertebrates, although a few notable species-specific exceptions and proposed supplementary pathways have been described, particularly with respect to auxiliary connections which serve to compensate for minor misalignments between EOMs and respective semi-circular canals (Pantle and Dieringer, 1998; Straka and Dieringer, 2004). Additionally, a considerable difference is found in elasmobranchii such as the shark, where due

to the crossing MR branches of the oculomotor nerve, conjugate eye movements are produced from direct crossed excitation of MR motoneurons and disynaptic ipsilateral abducens internuclear intermediates (Graf et al., 2002).

Linear accelerations are detected by otolith endorgans and are processed accordingly in specific VOR pathways depending on the type of motion. Comparatively however, the wealth of knowledge on angular VOR has historically surpassed its linear counterparts (Büttner-Ennever, 1999; Angelaki and Hess, 1996; Straka and Dieringer, 2004). Despite this comparative empirical lag, different linear VORs are known to be activated based on specific dimensional translations, as observed from distinct eye movement types. Forward/backward translations elicit disconjugate eye movements whereas medial/lateral translations drive conjugate motion of the eyes. A rostrally directed translation, for example, will lead to convergence of the eyes toward the midline, whereas a leftward translation causes a rightward shift of the eyes (Straka and Dieringer, 2004). Additionally, tilting of the head either along the rostral/caudal axis (pitch) or to the sides (roll) drives corresponding yoking of the eyes in the upward/downward or in the corresponding counter-torsional direction, respectively (Schoppik et al., 2017). It should be noted however, that signaling from the semi-circular canals are present during motions of the latter type and contribute to disambiguating rolls/tilts from strictly linear translations (Glasauer and Knorr, 2020). Linear VOR circuits differ from angular VOR pathways in their synaptic arrangement, at least in the connections preceding motoneuron innervation of muscles. For example, linear VOR circuits lack disynaptic ipsilateral inhibition of antagonistic motoneurons (Rohregger and Dieringer, 2002), though it maintains crossed excitatory connections as shown in frogs (Straka and Dieringer, 2004; Branoner et al., 2016), fish (Bianco et al., 2012; Schoppik et al., 2017), and cat (Baker et al., 1973). Linear VOR pathways have been described in better detail for the frog, which present with clear crossed excitatory connections combined with likely uncrossed GABA-mediated inhibitory signaling (Branoner et al., 2016; Soupiadou et al., 2018). This general arrangement seems to be consistent in anurans (Straka and Dieringer, 2004; Branoner et al., 2016) and fish (Bianco et al., 2012; Schoppik et al., 2017) and is conserved across most vertebrates (Straka and Baker, 2013). Evidence of polysynaptic circuits complicates a purely simplistic arrangement beyond anurans however, as particularly shown for the cat (Sasaki et al., 1991; Uchino et al., 1996) as well as even shorter latency monosynaptic connections (Uchino et al., 1996). Nonetheless, relatively short latency pathways from otolith input onto motoneurons continues to be a hallmark for VOR processing across vertebrates. With respect to differential contributions of otolith endorgans, the utricle is the likely common contributor to vestibulo-ocular computations across species, particularly given the lack of, or relatively weak, contributions from the saccule (Rohregger and Dieringer, 2002; Isu et al., 2000). Within individual otolith endorgans, such as the utricle, distinct populations of 360°-

arranged hair cells are recruited during different motion types (Deans, 2021), which contribute the necessary spatial segregation of peripheral input needed to link movement in space to correctly generated VOR eye movements.

Variations in circuit strategies aside, a few functional principles for VOR processing are important to note. Optimal execution of any VOR is during mid-range to higher frequency head/body movements (França de Barros et al., 2020). Indeed, in foveated organisms VOR processing is sufficient for gaze-stabilization within a bandwidth of 1 Hz to 50 Hz (Eatock and Songer, 2011). However, this bandwidth level can be lower such as shown in afoveate anurans which exhibit sensitivities below 1 Hz (Gensberger et al., 2016). Irrespective of the dynamic ranges between species, very low frequency motions are difficult to interpret by the vestibular system and instead are encoded optimally through optic flow neurosensory pathways (Masseck and Hoffmann, 2009a). Transformations of optic flow are important during vestibulo-ocular processing, as VOR pathways are open loop and receive no known self-feedback on the quality or success of the executed movement (Zhou et al., 2003). One method of closing this feedback loop is through the optokinetic reflex system (Collewijn, 1989).

Optokinetic-reflex (OKR)

Gaze-stabilization through visual pathways is accomplished by the OKR. To maintain a stable image on the retina during panoramic shifting of the visual word, the OKR elicits eye movements which follow the moving visual scene (Robinson, 1981; Matsuda and Kubo, 2021). These eye movements are therefore syndirectional with the motion vector of optic flow. Given that this reflex terminates on extraocular motoneurons, it is continuously provided with direct feedback on the efficacy of sensorimotor maintenance of visual acuity (Chen et al., 2014). OKR elicited eye motion can periodically be interrupted by stereotyped, oppositely-directed, fast jerking movements if the eyes reach the extreme ends of their motion range (Beck et al., 2004). These resetting movements, which are called fast- or quick- phases, physically ensure that the preceding following motion can be maintained (Beck et al., 2004; Gravot et al., 2017). OKR behaviors have been observed in many vertebrates and the neuronal circuity underlying these reflexes has been extensively characterized (Giolli et al., 2006; Masseck and Hoffmann, 2009a). Such behaviors and corresponding processing centers are present even in the lamprey, as remarkably demonstrated by Wibble and colleagues (2022). Axon bundles of motion sensitive RGCs target dedicated midbrain and diencephalon regions. An evolutionary conserved cluster of nuclei, referred to as the accessory optic system (AOS), receives such input. In mammals, the AOS consists of a dorsal terminal nucleus (DTN), lateral terminal nucleus (LTN), and a

medial terminal nucleus (MTN; Fredericks et al., 1988; Simpson et al., 1988a). In birds and amphibians, the AOS nuclei are referred to as the nuclei of the basal optic root (nBOR; Gruberg and Grasse, 1984; McKenna and Wallman, 1985). In addition to AOS centers, a distinct termination site exists in a diencephalic pretectal nucleus. For mammals, this consists of the nucleus of the optic tract (NOT) or the nucleus lentiformis mesencephali (NLM; McKenna and Wallman, 1985) in e.g., anurans and reptiles (Masseck and Hoffmann, 2009a). Teleost fish have a common structure termed the area pretectalis (APT) which functions analogously as an AOS and prectectal structure in the previous species (Kubo et al., 2014). AOS and pretectal nuclei have efferent axonal trajectories that terminate on extraocular nuclei directly as demonstrated in a variety of species, such as frog (Cochran et al., 1984), and pigeon (Brecha and Karton, 1979), although with only indirect polysynaptic connections in mammals (Giolli et al., 2006; Horn and Straka, 2021). The trajectories of these connections to specific extraocular motor centers correspond to the functional type of the AOS and pretectal sites. For example, the prectectal NLM is sensitive to horizontal optic flow and has ipsilateral projections to the abducens nucleus as well as likely indirect innervation of contralatetal oculomotor MR branches through abducens internuclear neurons (Holstege and Collewijn 1982; Cochran et al., 1984; Straka and Dieringer, 1991). The nBOR is sensitive for vertical visual motion and has efferent connections to relevant oculomotor and trochlear nuclei for vertical motion of the eyes (Brecha and Karten, 1980).

Synaptic relay from the AOS and pretectal centers has an additional indirect pathway to the extraocular motor nuclei which routes in sequence through the inferior olive, cerebellum, and vestibular nuclei (Horn and Straka, 2021). The OKR and VOR are therefore synergistic with each other, given that they converge on extraocular motor nuclei in the direct pathway and indirectly at the vestibular nuclei. This shared convergence, as well as a similar three-neuronal reflex arrangement in the former, highlight the cooperative nature of these circuits (Cochran et al., 1984). Indeed, APT neurons in fish and AOS cells in the rabbit have been shown to exhibit directional tuning responses which spatially align with the orientation of the semicircular canals (Simpson et al., 1988b; Masseck and Hoffmann, 2009b). This synergistic interaction is present even in the lamprey (Wibble et al., 2022), suggesting that such processing is conserved extensively.

Development of the inner ear and vestibular circuitry

The molecular identity and functional properties of neurosensory cells and neurons are defined during development. Following, circuit assembly serves to connect ensembles of neurons with each other as well as with peripheral sensory and terminal motor effectors. These ontogenetic events

establish the constraints with which the nervous system can be flexible and plastic in response to sensory conditions (Tosches, 2017; Elliott and Gordy, 2020). Understanding the events leading to the formation of mature sensorimotor circuits is thus of interest in understanding neuronal plasticity. The next sections will summarize development of the peripheral and central vestibular system with emphasis on VOR circuits.

Development of the inner ear and vestibular sensory neurons

The inner ears originate bilaterally from vertebrate otic placodes (Ohyama et al., 2007). Located dorsolateral and external to the developing neural tube (NT), the various placodes (e.g., olfactory, otic, and lateral line) arise from panplacodal ectoderm, which subdivides into discrete placodes through differential gene expression (Schlosser, 2006). The otic placode, which is specified through a series of regulated events which include fibroblast growth factor (FGF), bone morphogenetic protein (BMP), and Wnt signaling (Freter et al., 2008; Groves and Fekete, 2012), undergoes subsequent thickening and invagination to from a transitory structure called the otic cup (Torres and Giráldez, 1998). Following, the otic cup separates entirely from the surrounding placodal area and closes to form a hollow ball of cells referred to as the otic vesicle or otocyst (Elliott and Fritzsch, 2010; Fritzsch et al., 2010). The otic vesicle, and its precursor placode, are critical structures as they give rise to all neurosensory, supporting, and nonsensory cell types in the inner ear (Wu and Kelley, 2012). Patterning of the vesicle along the dorso-ventral, anterior-posterior, and medial-lateral axes is initiated by cascades of molecular and genetic events which allow the formation of the complex inner ear cytoarchitecture and its neurosensory domains (Wu and Kelley, 2012; Fekete and Wu, 2002).

Delamination and migration of neuroblasts from such neurosensory domain regions in the otic pit/otic vesicle, which is the sole provider of sensory afferents for the inner ear (Fritzsch et al., 2015), begins the development of the future statoacoustic ganglion (Fritzsch, 2003; Wanner and Miller, 2007), the identities of which are specified in part by expression of *Neurogenin 1* and *Neuronal differentiation 1* and their downstream effectors (Ma et al., 2000; Liu et al., 2000). Additionally, auditory versus vestibular neuroblasts are believed to be influenced by spatial patterning of the otocyst, given that the later exit the otic cup/otocyst more laterally than the former (Bell et al., 2008), although specific mechanisms governing acquisition of one or the other identity is still unclear (Appler and Goodrich, 2011). Notch-delta lateral inhibition assists in this process, as well as in determining the formation of prosensory cells which give rise to mechanosensory hair cells (Daudet and Lewis, 2005; Brown and Groves, 2020), which rely on *atonal homolog 1* (*Atoh1;* Bermingham et al., 1999) and other

genes (Fritzsch and Beisel, 2001). In addition to development of neurosensory cell types, the complex structural features of vestibular endorgans develop from specified regions within the otic vesicle that are dependent on prior axes patterning, such as sonic hedgehog (Shh) specification along the dorsal-ventral axis which influences endorgan formation (Bok et al., 2007). The semi-circular canals and otolith ducts form as the result of three-dimensional morphological and growth changes in the vesicle which produces chambers and channels (Groves and Fekete, 2012). For each semi-circular canal, protrusions from the vesicle extend outward and undergo a fusion to form hollow tubular structures (Haddon and Lewis, 1991; Haddon and Lewis, 1996). Formation of the otolith organs, which as mentioned previously are housed in recesses and pouches, is also due to morphological changes in the ear, and is likely the result of dynamics associated with anatomical changes of epithelial tissue (Glover, 2020). The genes and molecular pathways governing the development of the inner ear have been extensively explored, through efforts of single gene analysis as well as complex regulatory interactions between multiple genes and machinery proteins (Fritzsch and Elliott, 2017b).

Within each vestibular endorgan, the development of hair cell organization and stereocilia polarity is a critical step, particularly given the stark contrast between the 360° orientation of hair cells within macular endorgans and the uniformity observed in the canal cristae. Regulating hair cell polarities in these endorgans are planar cell polarity (PCP) genes and proteins (Deans et al., 2007; Duncan et al., 2017). Loss of these genes results in aberrant distributions of hair cell polarities in maculae/cristae with consequent behavioral phenotypes (Duncan et al., 2017). Vestibular afferent fibers, as mentioned above, derive from the otic pit/otocyst along with those which innervate auditory endorgans. Peripheral and central innervation by vestibular ganglion cells on inner ear and brainstem targets respectively is critical for vestibular processing, and the ontogenetic processes of these events will be discussed in the following section. On a comparative scale, inner ear development across vertebrates has been well described in major model systems such as in zebrafish (Haddon and Lewis, 1996; Whitfield et al., 2002), mouse (Morsli et al., 1998; Bryant et al., 2021), and even lamprey and hagfish (Higuchi et al., 2019). The African clawed frog *Xenopus laevis*, which is the model system for this dissertation, has also been explored considerably (Bever et al., 2003; Quick and Serrano, 2005) and warrants special notice here in the context of developmental timelines. In *Xenopus laevis*, the otic placode develops around embryonic stage 21, with the subsequent otocyst being fully separated around stage 28 (Schlosser and Northcutt, 2000). Otic neuroblasts have recently been shown in detail to delaminate starting at stage 26-27, a process which continues until stage 39 and includes neurite outgrowth already at stage 31-32 (Almasoudi and Schlosser, 2021). Around the time of neurite outgrowth, hair cells begin to differentiate and separate into discrete clusters (Quick and Serrano, 2005; Almasoudi and Schlosser, 2021). Subsequent morphological changes facilitate the development

of vestibular endorgans within the ear which completes around stage 47 (Quick and Serrano, 2005). Formation of the canals is initiated around stage 43 and ends at stage 47. Macular endorgans, such as the utricle and saccule, are notably compartmentalized by stage 47 as well, and by stage 50 all endorgans of the inner ear are fully formed (Bever et al., 2003; Quick and Serrano, 2005).

Development of VOR circuitry

Sensory neurons form the first component of VOR circuits and have axonal trajectories that extend into stereotyped positions within the brainstem. Direct terminations into the cerebellum and abducens nucleus exist (Barmack et al., 1993; Uchino et al., 1994), albeit at a lesser degree compared to more numerous projections onto vestibular neurons in the alar plate of the hindbrain. Within the statoacoustic ganglion, afferent cell bodies and their associated axonal fibers are arranged in a manner with respect to size (Kuruvilla et al., 1985) and are partially segregated based on peripheral endorgan (Maklad and Fritzsch, 1999; Maklad and Fritzsch, 2002). Central projections however, mostly abandon any partial segregation in favor of projecting in an overlapping fashion among the various vestibular nuclei (Kuruvilla et al., 1985; Birinyi et al., 2001) and in doing so lack an obvious topographic arrangement relative to peripheral sensor arrangements (Maklad and Fritzsch, 2003; Straka et al., 2014). These features demonstrate a developmental condition which has been proposed to represent a dynamic bandwidth for processing of VOR computations (Straka et al., 2014). However, despite this extensive overlap and thus the availability of multiple sensory inputs, most vestibular nuclei targets receive monosynaptic input from only one canal or otolith endorgan sector (Kasahara and Uchino 1974; Straka et al., 1997), while only smaller subsets receive input from two or more otolith or semi-circular canal endorgans (Straka et al., 1997). Convergence of projections in the latter condition has been shown for otolith and canal endorgans of similar directional sensitivity. For example, afferent fibers carrying utricular derived input will converge on central targets with afferents from the horizontal canal (Straka et al., 2002). This synaptic convergence is believed to represent directional tuning, a general feature which has been recently demonstrated for vestibulo-spinal projections in Zebrafish (Liu et al., 2020), and highlights the importance of activity in influencing consolidation of inputs during development. Remarkably, recent evidence in Zebrafish has demonstrated that developmental tuning is observable in the linked topography of utricular afferent cell body location in the ganglia and macular hair cell organization (Liu et al., 2022). Inferred directional sensitivity of utricular hair cells are correspondingly represented along the rostro-caudal ganglia axis, while medio-lateral organization is a function of early to later delaminating sensory neurons (Liu et al., 2022).

The molecular instructions governing the projection of afferent fibers into the hindbrain has been studied considerably in recent years, including the published work of chapter III (Gordy et al., 2018) of this dissertation. Axon navigation is the result of coordinated signaling events at the terminal growth cone, which drive movement dynamics (Russell and Bashaw, 2017). In particular, long range diffusible cues as well as short range physical cues mediate the growth of axons into brain target regions (Kolodkin and Tessier-Lavigne, 2011). Inner ear afferents can generally be traced to a singular localized area within the hindbrain dorso-ventral axis (Elliott and Fritzsch, 2018) in a function of time relative to other projecting nerves such as e.g., the lateral line or trigeminal nerve (Fritzsch et al., 2005; Zecca et al., 2015). This stereotyped spatiotemporal pattern is suggestive of specific cues which attract these fibers specifically. Projection in this manner occurs in the absence of precisely complete peripheral hair cells and/or central targets (Maricich et al., 2009; Elliott et al., 2017), indicating a possibility that such cues are intrinsic to the hindbrain region. While many diffusible and cell-surface anchored signals operate in generalized axonal pathfinding mechanisms, (Seiradake et al., 2016), only few have been demonstrated to be critical in guiding vestibular sensory fibers selectively, such as Wnt signaling through Frizzled receptors (Duncan et al., 2019; Stoner et al., 2022) as well as putative influence from Eph/Ephrin pathways (Siddiqui and Cramer, 2005). An impact from other molecular components, such as during loss of Neurod1, have been demonstrated and point to further regulatory mechanisms (Jahan et al., 2010). Additional evidence suggests that fasciculation along pioneer axons is also relevant for later forming afferents (Zecca et al., 2015). Complete understanding of the mechanistic events that drive vestibular afferent innervation, particularly with respect to auditory fiber projections, remains currently unclear (Maklad and Fritzsch, 2003; Appler and Goodrich, 2011; Elliott and Fritzsch, 2018; Stoner et al., 2022).

Development of vestibular projection neurons is the result of coordinated patterning of the hindbrain along the major anatomical axes. Differential signaling along dorso-ventral and anterior-posterior axes contribute to the determination of distinct molecular identities for vestibular populations (Pasqualetti et al., 2007), primarily driven through the presence of unique transcription factors (Storm et al., 2009; Diaz and Glover, 2022). Variance between these transcription factors and resulting cell type identities imparts differential cellular characteristics which manifest in e.g., connectivity specification in the form of axonal target trajectories (Diaz and Puelles, 2019). Along the anterior-posterior axis, such characteristics are the result of *Hox* gene transcription factors and downstream effectors (Krumlauf and Wilkinson, 2021; Tomás-Roca et al., 2016). Loss of these, such as for example in the absence of Hoxb1, results in aberrant axonal trajectory phenotypes for specific populations of vestibulo-spinal neurons (Chen et al., 2012). Dorso-ventral patterning signals, such as BMPs, Wnts, and Shh also contribute to the specification of hindbrain cell types (Hernandez-Miranda

et al., 2017), particularly of vestibular progenitor pools (Diaz and Glover, 2022). Neurogenin 1 expressing columnar lines along the dorso-ventral axis are hallmarked by their location as the site of vestibular afferent termination (Fritzsch et al., 2006). Orthogonal combination of axes signaling generate discrete populations of vestibular neurons with unique molecular signatures (Lunde et al., 2019) and resulting phenotypes, which is highly conserved across vertebrates (Straka and Baker, 2013).

Following the formation of vestibular projection neurons, axonal connections are established. As described previously, the unifying organizational principle of vestibular neurons is an arrangement according to innervation targets rather than a simple sensory topology (Glover, 1996; Maklad and Fritzsch, 2003; Straka and Baker, 2013). Vestibular-ocular and -spinal projecting neurons therefore discretely group according to their efferent connections along the hindbrain scaffold (Glover, 1996; Glover, 2000). Given the shared segmental origin for cells of similar identity and projection pattern, the processes governing the formation of connectivity are wired according to a genetically defined framework (Straka and Baker, 2013; Diaz and Glover, 2022). However, observations in the chick embryo propose that beyond these defined initial innervation patterns, instructions for synaptic specificity on specific extraocular motoneurons is influenced by signals originating from the motoneurons themselves. These signals are purported to only arrive after the motoneurons innervate their target muscles and highlights an elegant method of incorporating behaviorally relevant information to influence connectivity formation (Glover, 2003).

Development of extraocular motoneurons is a necessary step in establishing a full VOR circuit. This process is governed by differential patterning and regional specific signaling events along the anterior-posterior and dorso-ventral axes (Lance-Jones et al., 2012; Chilton and Guthrie, 2017; Glover, 2020). Such distinctive molecular specifications can be mapped according to motoneuron pool location, evident even in the oculomotor and abducens nuclei which are themselves divided into sub-nuclei (Matesz, 1990; Büttner-Ennever, 2006). These events, at least for the oculomotor nuclei, are ascribed as being a function of developmental timing and birthdate (Greaney et al., 2016; Bagnall and Schoppik, 2018). The mechanisms which govern the spatial selection of extraocular muscles have been investigated across a variety of species (Clark et al., 2013; Chilton and Guthrie, 2017). Several axonal guidance molecules play an instructive role in establishing correct synaptic specification on appropriate muscle targets (Chen et al., 2000; Chilton and Guthrie, 2017) and is anatomically described in a temporal sequence which is generally conserved with some inter-species differences (Clark et al., 2013). The importance of linking specific motor control demands to the functional and developmental properties of vestibular circuits has been demonstrated by the observation of a temporal sequence in the formation of vestibular pathways (Liu et al., 2022). Early forming pathways

and their relevant sensorimotor elements were shown to be specific to phasic relays, such as escape responses, whereas VOR transformations are established later (Liu et al., 2022). Following ontogenetic assembly of the specific elements of VOR circuits mentioned above, resultant eye movement behaviors can be executed. The developmental timeline of these behaviors in *Xenopus* again warrants a notable mention. Otolith mediated VORs can be elicited as early as stage 42 (Horn et al., 1986), a time point close to hatching, followed by angular driven VOR at stage 48 (Lambert et al., 2008). The latter behavior is delayed only due to the unsuitability in size of peripheral canals which bottleneck sensory transduction, given that relevant behaviors can be stimulated electrically prior to that stage (Lambert et al., 2008). Furthermore, the acquisition of naturalistic angular VOR processing introduces temporal tuning of otolith derived VOR, presumably at the level of the vestibular nuclei, which is resolved entirely by stage 55 (Branoner and Straka, 2015; Branoner and Straka, 2018). Thereafter *Xenopus* tadpoles exhibit fully mature and functional linear and angular VOR sensorimotor transformations.

Plasticity in the VOR and vestibular system

Neuronal circuits are highly plastic structures. A fundamental feature of the vertebrate nervous system is the ability to flexibly reorganize in response to intrinsic and extrinsic events (Tien and Kerschensteiner, 2018; Cramer et al., 2011). Such reorganization can manifest as changes across a variety of systemic levels with varying degrees of resolution, such as circuit anatomical adjustments, synaptic modifications, cellular changes, and gene expression alterations (Pascual-Leone et al., 2005). Compounding this flexibility, plasticity extents must also consider not just spatial properties but temporal characteristics as well (Hubel and Wiesel, 1970; Meredith et al., 2012), particularly given that timing is a paramount feature of any neuronal computation. The nervous system is adept at such reorganization, especially when considering the seemingly hardwired instructions during development from the genome (Pascual-Leone et al., 2005; Kolodkin and Tessier-Lavigne, 2011). However, flexibility must be maintained at a level which permits standard functional processing and therefore presents with some degree of constraint (von Bernhardi et al., 2017). Given that sensorimotor systems are the interface with the environment of an organism, understanding such extents and constraints in these systems can provide considerable knowledge into general principles of neuronal plasticity. Vestibular signaling permits reflexive behavioral adjustments (see above) and is necessary for appropriate environmental responses. Plasticity in this system should therefore be constrained by the behavioral need to achieve these reflexes while simultaneously being able to

modulate to some degree. For example, vestibulo-ocular motor circuits are highly conserved and morpho-physiologically quite stereotyped (Straka and Baker, 2013), yet are known to be modifiable (Miles and Lisberger, 1981; Hirata and Highstein, 2002; Dietrich and Straka, 2016). Three important areas in which modifiability has been explored in vestibular networks is during ontogenetic development, eco-physiological adaptive responses, and following acute injury and disease.

Developmental vestibular plasticity

The mechanisms that govern change induced reorganization are not *de novo* processes, rather, they represent neuronal mechanics which are readily used during ontogenetic development (Hensch, 2004; Tien and Kerschensteiner, 2018). In fact, plasticity-based modifications occur extensively during, and are a hallmark of, embryonic formation of neural networks and resultant behaviors (Pascual-Leone et al., 2005). This is particularly evident in sensory circuits such as in the visual and olfactory systems (Wiesel and Hubel, 1963; Wiesel and Hubel, 1965; Devaud, et al., 2001; Golovin and Broadie, 2016), largely given that patterned sensory input serves to refine central connections such as those derived from the retina (Torborg and Feller, 2005). As might be apparent from the preceding sections, this is also likely the case for the vestibular system (Straka et al., 2005). The influence of sensory input on the formation of vestibular circuits and subsequent electrophysiological and behavioral outputs is the focus of chapters II (Gordy and Straka, 2022) and III (Gordy et al., 2018) of this dissertation. Further introductory information can be found in those chapters, particularly chapter II. Here, but a few important points will be made. Refinement of central vestibular connections is speculated to occur largely from evidence of mostly monosynaptic innervation of vestibular projection neurons by only one semi-circular canal or otolith endorgan, despite the apparent availability of many inputs (Kasahara and Uchino 1974; Straka et al., 1997; Straka et al., 2014). This is proposed to be the result of either pruning or silencing of inputs during concurrent activity dynamics (reviewed in Elliott and Gordy, 2020). Similarly, convergence between canal and otolith endorgan signals on central vestibular neurons (Straka et al., 2002) are perhaps also influenced in such a manner. The recent seminal demonstration of synaptic convergence for similarly tuned afferent inputs on central targets by Liu and colleagues (2020) could potentially lend to support this claim. Activity has been shown to have some influence on afferent termination, demonstrated principally through transplantation studies (Elliott et al., 2015b). The electrophysiological properties and corresponding membrane dynamics of central vestibular neurons undergo extensive post-natal modifications (Dutia and Johnston, 1998; Murphy and du Lac, 2001) which are speculated to be

influenced in part by patterned activity levels (Straka et al., 2005). Beyond vestibular input, visual signaling appears to aid in the process of shaping synaptic plasticity in the vestibular nuclei (Grassi et al., 2004) but may not represent a general theme as functional maturation of certain firing characteristics occurs before visual activity (Murphy and du Lac, 2001). Connectivity selection by vestibular projection neurons on specific extraocular motor nuclei pools is also believed to be the result of retrograde instruction from the motoneurons themselves (Glover, 2003). Delayed input from the semi-circular canals is known to directly influence the response vectors of extraocular motoneurons (Branoner and Straka, 2015; Branoner and Straka, 2018), possibly through modifications on converging synaptic connectivities, particularly given that the utricle independently develops with a well-established 360° hair cell sensitivity arrangement which is also mostly maintained in the afferent ganglia (Liu et al., 2022). However, the full extent with which the development of vestibular circuits and behaviors are canonically influenced in some degree by patterned input remains unclear, particularly given that in some instances loss of signaling can still present with appropriate circuit development and function (Roberts et al., 2017; Bagnall and Schoppik, 2018). Nonetheless, the vestibular system is incredibly plastic in the face of atypical sensory modifications. Experiments targeted at generating non-canonical signaling levels and/or altered vestibular development in embryos, such as e.g., during embryonic ear removals, rotations, or ablations, have served to consistently highlight astonishing reorganizational extents and constraining limitations on both anatomical and functional levels during development of the vestibular circuitry (Levi-Montalcini, 1949; Peusner and Morest, 1977; Rayer et al., 1983; Fritzsch, 1990; Alagramam et al., 2005; Horn, 2014; Elliott et al., 2015a; Elliott et al., 2015b; Duncan et al., 2017; Roberts et al., 2017; Lilian et al., 2019; Ehrlich and Schoppik, 2019, Macova et al., 2019). Extensive reorganization is also present in organisms which have passed embryonic periods but nonetheless experience a considerable developmental transition. For example, the flatfish undergoes a permanent metamorphic postural rotation that brings one side into contact with the bottom of their aquatic habitat (Graf and Baker, 1985a). This is accompanied by a displacement of one eye away from the newly grounded side. Extensive central connectivity reorganization occurs during this transition which serves to link the newly aligned vestibular endorgans with spatial VOR circuits for appropriate motor transformations (Graf and Baker, 1985a; Graf and Baker, 1985b; Graf et al., 2001). In *Xenopus* tadpoles with immature and thus non-functional semi-circular canals, behavioral strategies have been shown to leverage the utricle for executing appropriate angular VOR, findings which highlight behavioral plasticity following embryogenesis (Lambert et al., 2020).

Eco-physiological plasticity: cerebellar contributions to motor learning

Mature VOR circuits are able to modify and be flexible in response to changes in naturalistic stimuli from the environment (Beraneck et al., 2008). Such stimuli can be complex, unexpected, and new to an organism. Resulting modifications should optimize and calibrate processing events to produce responses that maintain appropriate motor executions (Boyden et al., 2004; Broussard and Kassardjian, 2004). A hallmark of this VOR adaptability originates from influence by the cerebellum (Blazquez et al., 2004). Indeed, VOR-cerebellar plasticity has been a standard model for considerations into principles of general motor learning (Broussard and Kassardjian, 2004). Inhibitory efferents of Purkinje cells innervate vestibular nuclei neurons and influence the modulation of VOR response characteristics (Straka and Dieringer, 2004; Gittis and du Lac, 2006). Purkinje cell input arrives indirectly from vestibular afferent fibers (Sadeghi and Beraneck, 2020) as well as vestibular projection neurons (De Zeeuw and Yeo, 2005) by relay through granular cells and their parallel fibers (Raymond and Lisberger, 2000; De Zeeuw and Yeo, 2005; Boyden et al., 2004). An additional source of input to Purkinje cells derives from optic flow signaling from the retina which is relayed through the inferior olive by way of climbing fibers (de Lac et al., 1995). Retinal image slip is therefore integrated through these pathways (du Lac et al., 1995; Menzies et al., 2010) and provides information on the relative success of VOR evoked stabilizing eye movements. Plasticity mechanisms are believed to be localized at many sites along these circuits (Clopath et al., 2014), including the level of climbing fiber-Purkinje cell synapses (Ito, 1982) and within the vestibular nuclei themselves (Miles and Lisberger, 1981; Boyden et al., 2004), such as at the first synaptic junction of afferent fibers on vestibular neurons (McElvain et al., 2010). This variety of sites highlight a dynamic bandwidth of VOR plasticity which can selectively respond to different environmental conditions, such as adaptation resulting from visual feedback instruction (Collewijn and Grootendorst, 1979; Boyden et al., 2004; França de Barros et al., 2020) or during habituation in the case of prolonged stimulation (Collins and Updegraff, 1966; Dow and Anastasio, 1998; Gutierrez-Castellanos et al., 2013; Dietrich and Straka, 2016). At the core of this flexibility is the cerebellum and disruptions of cerebellar function present with profound effects on VOR adaptability (Robinson, 1976; Lisberger et al., 1984, McElligott et al., 1998). Despite this however, some degree of dispensability is reported in certain contexts. Following initial learning by cerebellar activity, long term storage is maintained in the vestibular nuclei and thus becomes independent of the cerebellum (Kassardjian et al., 2005; Shuto et al., 2006; Gittis and du Lac, 2006). These collective motor learning mechanisms contribute to enacting flexible sensorimotor processes needed to respond to dynamic and mutable environments.

Lesion induced adaptive plasticity

Central neuronal reorganizations are induced following lesions in the CNS or PNS (Vidal et al., 1998; Chen et al., 2010). In the vestibular system, lesions can manifest from a variety of origins, ranging from acute physical injury of vestibular structures to the effects of specific diseases (Lacour and Tighilet, 2010; Smith, 2018). Lesion evoked plasticity has been best studied following unilateral disruption of peripheral vestibular signaling in a variety of species, largely resulting in either a sudden graded or complete loss of input on one side (Dieringer and Precht, 1979; Curthoys et al., 1988; Yamanaka et al., 1995; Curthoys, 2000; Dutia, 2010). It should be noted that lesions in this manner are assumed to happen on relatively established and entrained vestibular circuits which are herein distinguished from developmental conditions where circuits have not yet fully formed. Following these lesions, behaviorally identifiable phenotypes such as impairments in positional maintenance of the body and eyes, and disruptions in gaze-stabilizing ability, are readily observed and are due to a sudden reduction of unilateral input (Smith and Curthoys, 1989; Paterson et al., 2005). In a striking representation of CNS plasticity, some of these detriments abate over time (Smith and Curthoys, 1989; Paterson et al., 2005; Dutia, 2010) while others do so to lesser extents, not at all, or differentially in certain contexts (Dutia, 2010; Dieringer, 1995; Hamann et al., 1998). Nonetheless, such abatement occurs without any regeneration of peripheral neurosensory elements (Paterson et al., 2005; Lambert and Straka, 2012).

The neuronal correlates of these recovery extents have been profiled on the anatomical, electrophysiological, and molecular level and are known to take place in the vestibular nuclei, cerebellum, and other vestibular network centers (Paterson et al., 2005; Dutia, 2010; Lambert and Straka, 2012). Additionally, a reduction in motor deficits has been shown to occur through substituting behavioral strategies (Dieringer, 1988; MacDougall and Curthoys, 2012) as well as through signaling mediated by alternate sensory systems which effectively bypass or supplement vestibular control (Lacour, 2006). These strategies make use of e.g., the visual, proprioceptive, and saccadic systems (Dieringer, 1988; Zennou-Azogui et al., 1994; Sadeghi et al., 2012). The prevailing scientific theory of these disperse processes is designated as “vestibular compensation” and describes the extent to which such processes can normalize motor detriments over time (Curthoys, 2000). Behavioral impairments are classified dichotomously between dynamic and static conditions, which respectively refer to those which occur during motion or during periods of rest (Paterson et al., 2005; Beraneck and Idoux, 2012). Static motor detriments, such as postural deviations and spontaneous nystagmus, abate considerably over relatively short time courses compared to their dynamic counterparts which

include impairments of sensorimotor transformation properties that rarely return to normal levels (Vidal et al., 1998; Paterson et al., 2005). These time course differences are proposed to reflect a spatiotemporally regulated scheme wherein more global responses, such as behavior or sensory substitution, occur earlier than local modifications in the vestibular nuclei (Beraneck and Idoux, 2012). Following, further local modifications become fixed over time and assist in the attempt to return dynamic impairments to normal levels (Beraneck and Idoux, 2012). A key feature of these compensatory mechanisms is in their equalization of activity levels between the bilateral vestibular nuclei (Beraneck et al., 2003). Unilateral loss of input imparts a sudden inequality in the resting activity levels of bilateral vestibular neurons, a feature which is augmented by a resulting imbalance in reciprocal inhibition through commissural pathways (Straka et al., 2005). Many of the plastic strategies mentioned previously serve to reduce this imbalance. Modifications of commissural activity levels can occur by regulating the sensitivity of vestibular neurons to inhibitory neurotransmitters (Vibert et al., 2000), increasing their excitability (Paterson et al., 2005), or through larger scale synaptic rearrangements (Goto et al., 2000; Goto et al., 2001). Beyond these initial responses, long term changes in the intrinsic membrane properties follow, such as e.g., in the case of phasic neurons becoming more tonic in their response properties, which serve to homogenize activity levels in the vestibular nuclei (Beraneck et al., 2003). Functional whole-brain imaging following unilateral loss revealed a disperse imbalance in activity levels in higher order centers beyond the vestibular nuclei, which re-balances over time (Zwergal et al., 2016). An important note with respect to lesion-induced plasticity is that it is not a goal-directed process (Dieringer, 1995; Dieringer, 2003; Lambert and Straka, 2012). The absence of complete deficit ameliorations as well as the maintained ability to execute motor learning despite maintained asymmetric VOR responses (Maioli and Precht, 1985) strongly support the notion that plastic responses normalize central activity levels but lack a behavioral target (Dieringer, 2003). Instead, behavioral returns result from passive neuronal reactions following sensory imbalance (Dieringer, 1995; Goto et al., 2001; Beraneck and Idoux, 2012).

Experimental Rational

The scientific goal of this dissertation is to further explore the extents and limitations of vestibular sensorimotor plasticity. The following data chapters (chapter II, Gordy and Straka, 2022; chapter III, Gordy et al., 2018; chapter IV, I Gusti Bagus et al., 2019) provide empirical evidence that expand our current understanding of adaptive reorganization responses following modulation of sensory input. As mentioned previously, the experimental aims of the following chapters use surgical

embryonic or acute pharmacological manipulations to uniquely challenge vestibular processing. In chapter II, I present the generation of a developmental model system which restricts vestibular signaling from occurring from only one side. This condition challenges the stereotyped use of bilateral sensory contributions to vestibular processing. In chapter III, I introduce another embryonic manipulation which provides additional vestibular input that originates from a non-canonical CNS entry site. This modification assesses the ability of vestibular inputs to incorporate into existing brainstem networks despite aberrant peripheral relay pathways. In chapter IV, I utilize pharmacological disruption of vestibular signaling to explore the sudden absence of phasic vestibular transmission. This latter disruption questions to which level phasic dynamic pathways can be indispensable during vestibular processing. These manipulations are all leveraged against a variety of behavioral, anatomical, and electrophysiological assessments which cooperatively report on different extents of flexibility possible in vestibular motion networks.

CHAPTER II:

DEVELOPMENTAL EYE MOTION PLASTICITY AFTER UNILATERAL EMBRYONIC EAR REMOVAL IN *XENOPUS LAEVIS*

Clayton Gordy[1, 2] and Hans Straka[1, *]

[1]Faculty of Biology, Ludwig-Maximilians-University Munich, Großhaderner Str. 2, 82152 Planegg, Germany

[2]Graduate School of Systemic Neurosciences, Ludwig-Maximilians-University Munich, Großhaderner Str. 2, 82152 Planegg, Germany

*Correspondence: straka@lmu.de (H.S.)

Contribution of authors:

C.G. and H.S. conceived the goals and aims. C.G. and H.S. designed methodological paradigms. C.G. collected data for all experiments. C.G. analyzed data for all experiments. C.G. and H.S. interpreted all data. C.G. created all the figures. C.G. wrote the original draft of the manuscript. C.G. and H.S. reviewed and edited the manuscript. Resources, supervision, project administration, and funding acquired by H.S.

My contributions to this publication in detail:

H.S. and I conceived the aims and experimental goals of this project. I designed the methodological paradigms with H.S. I performed all experiments and analyzed all data and created all the figures and supplemental material in this paper. I wrote the initial draft of this paper. H.S. and I edited all subsequent versions.

For online access, please refer to the following: https://doi.org/10.1016/j.isci.2022.105165

Developmental eye motion plasticity after unilateral embryonic ear removal in *Xenopus laevis*

Clayton Gordy, Hans Straka

PII: S2589-0042(22)01437-7

DOI: https://doi.org/10.1016/j.isci.2022.105165

Reference: ISCI 105165

To appear in: *ISCIENCE*

Received Date: 14 June 2022

Revised Date: 12 August 2022

Accepted Date: 16 September 2022

Please cite this article as: Gordy, C., Straka, H., Developmental eye motion plasticity after unilateral embryonic ear removal in *Xenopus laevis*, *ISCIENCE* (2022), doi: https://doi.org/10.1016/j.isci.2022.105165.

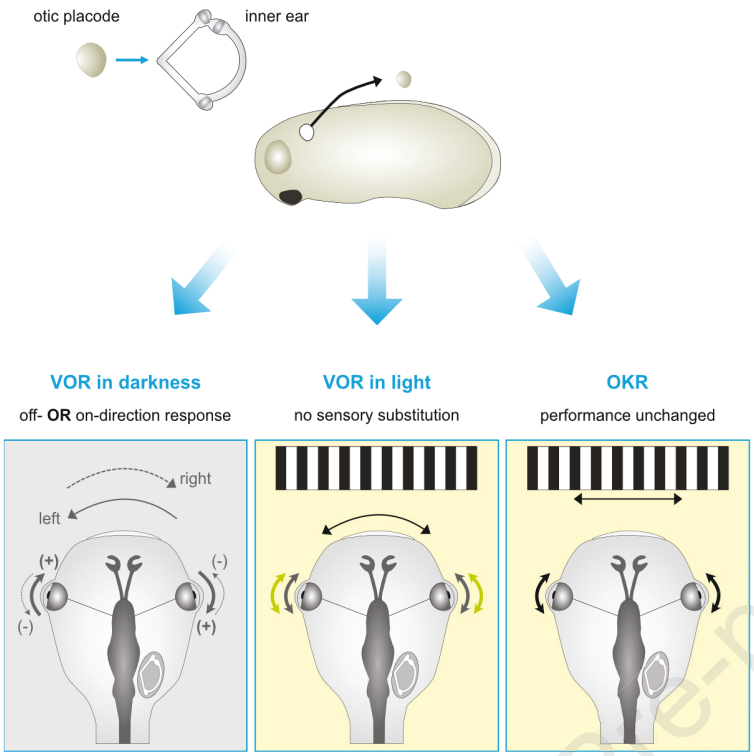

Developmental eye motion plasticity after unilateral embryonic ear removal in *Xenopus laevis*

Clayton Gordy[1, 2] and Hans Straka[1, 3 *]

[1]Faculty of Biology, Ludwig-Maximilians-University Munich, Großhaderner Str. 2, 82152 Planegg, Germany

[2]Graduate School of Systemic Neurosciences, Ludwig-Maximilians-University Munich, Großhaderner Str. 2, 82152 Planegg, Germany

[3]Lead Contact

* Correspondence: straka@lmu.de (H.S.)

Summary

Gaze stabilization relies on bilateral mirror-symmetric vestibular endorgans, central circuits, and extraocular motor effectors. Embryonic removal of one inner ear prior to the formation of these structures was used to evaluate the extent to which motor outputs in the presence of a singular inner ear can develop. Near-congenital one-eared tadpoles subjected to separate or combinatorial visuo-vestibular motion stimulation exhibited comparable eye movements, though smaller in gain to controls, whereas isolated visuo-motor responses were unaltered. Surprisingly, vestibulo-ocular reflexes were robust during off-direction motion towards the missing ear in most cases and often attenuated during on-direction motion. This bidirectional plasticity of signal encoding appears to occur at the expense of vestibular reflexes during motion in the normally preferential activation direction of the singular ear. Consequently, formation of central vestibulo-motor circuits in one-eared animals likely relies on multi-neuronal homeostatic strategies, including enhanced afferent fiber activity in the attempt to adjust bilateral sensorimotor transformations.

Introduction

Head movements are detected and mechano-electrically transduced into neuronal signals by vestibular organs in the inner ear (Angelaki and Cullen, 2008; Dieterich and Brandt, 2015). Following vectorial decomposition by semicircular canal and otolith organs, bilateral signals are reconstructed through spatially- and endorgan-specific integration in discrete central circuits and contribute to behaviors which stabilize posture and gaze during active and passive movements (Szentágothai, 1950; reviewed in Straka and Gordy, 2020). A key feature of this computation is the mirror-symmetric arrangement of sensory epithelia (Fritzsch and Straka, 2014) and the interconnection of the vestibular nuclei across the midline by commissural pathways (Markham et al., 1977; Malinvaud et al., 2010). Despite this bilaterality, such mirror-symmetry generates motion sensors and postsynaptic neuronal elements on both sides that are largely distinct from each other with respect to directional preference. This is particularly evident given that activity modulations of bilateral endorgans occur simultaneously and more importantly in mutual exclusivity with respect to their faciliatory/disfaciliatory dynamics onto central targets. Bilateral vestibular organs therefore represent complementary, though partially overlapping structures with distinct sensitivity domains rather than simple duplications with interchangeable functionality (Chagnaud et al., 2017). Thus, encoding and representation of multi-dimensional head/body movements depends on the morpho-physiological integrity of vestibular sensors within the two inner ears.

Disruption of bilateral processing, such as during an acute unilateral loss of inner ear function or inappropriate peripheral signaling, results in an impairment of self-motion encoding due to insufficient and asymmetric information from mirror-symmetrically arranged sensors. Immediate behavioral effects include dizziness, vertigo, spontaneous nystagmus, and deterioration of orientation and navigational skills (Zhao et al., 2008; see Fetter, 2016). These pathological reactions derive from excessive bilateral asymmetric activity of central vestibular circuits combined with the subsequent failure to produce adequate gaze- and posture-stabilizing neuronal commands. In addition, asymmetric neuronal activity is centrally represented as being in mismatch with other motion-related sensory signals such as visual image motion or limb/neck proprioceptive inputs (for review see e.g., Vidal et al., 1998; Curthoys, 2000; Dutia, 2010; Strupp and Brandt, 2013). However, these impairments abate,

at least partially, over time due to plasticity processes in bilateral central circuits which are distributed across various regions of the central nervous system (CNS), and occur at molecular, cellular, and anatomical levels, which collectively permit readjustments in computational strategies to alleviate the consequences of peripheral imbalance (for review see Llinás and Walton, 1979; Dieringer, 1995; Straka et al., 2005).

The remarkable plasticity of vestibular signal processing after a unilateral vestibular loss has been extensively used to study the principles of "vestibular compensation" following a variety of protocols (for review see Curthoys, 2000). These studies were usually conducted in adult or at least juvenile vertebrates with a functional vestibular sensory periphery and central pathways (Dieringer, 1995; Gordy and Straka, 2021). In this manner, unilateral impairments of inner ear function induced a loss of signal processing in already well-established, entrained, and spatio-temporally tuned circuits. Under such circumstances, vestibular lesion-induced plasticity must cope with preexisting bilateral symmetric circuits and resultant computations. In contrast, unilateral excision of the embryonic otic placode, which develops into all sensory and non-sensory tissues of the inner ear, prior to the formation of central pathways (Elliott and Fritzsch, 2010; Elliott et al., 2015a, b) might reveal plasticity processes that permit vestibular circuits to develop and function based on sensory inputs only from a single inner ear into circuits which have only ever received such unilateral input. This generates a developmental condition where relevant brainstem vestibular circuits control bilateral gaze- and posture-stabilizing motor elements from unilateral vestibular inputs alone.

Here, we demonstrate that unilateral embryonic removal of the otic placode causes one-eared tadpoles to exhibit a remarkable degree of developmental vestibular plasticity. These tadpoles develop without signs typical for a unilateral vestibular loss, such as abnormal tail deviations or uncoordinated spontaneously generated swim episodes. Gaze-stabilizing vestibulo-motor responses exhibit appropriate spatiotemporal dynamics during bidirectional motion stimulation. Behavioral analyses during unidirectional motion and electrophysiological evidence here suggest that central circuits have adapted to respond to oscillatory head motion within the singular ear, with minimal additional contributions by motion-sensitive visual pathways. Collectively these results highlight the ability of the nervous

system to develop appropriate motion direction-specific gaze-stabilizing behaviors following ontogenetic assembly of circuits in the absence of bilateral signaling.

Results

Vestibular-evoked eye movements in one-eared tadpoles

One-eared tadpoles were generated by unilateral removal of the left otic placode at embryonic stages 25-27 (Figure 1A, left; Video S1). Removal of the otic placode at these developmental stages has previously been demonstrated in *Xenopus laevis* to selectively and completely remove inner ear endorgans and corresponding neurosensory elements (Fritzsch, 1990; Elliott and Fritzsch, 2010). The absence of the entire ear and its resulting lack of peripheral sensory components was confirmed beginning at stage 46 (Figure 1A), a developmental period where the high transparency of *Xenopus* tadpoles allows direct visual assessment of the presence of inner ear structures (Figure S1A-B, F-G). As expected, stage 46 one-eared animals lacked recognizable inner ear gross-histological structures (Figure S1C, H, asterisk) as well as neurosensory elements such as hair cells and associated vestibular afferent fibers (Figure 1A, extirpated side; Figure S1D-E, I-J). Using myosin-VI and acetylated-tubulin as selective markers for hair cells and nerve fibers, respectively, a clear absence of innervated sensory epithelia on the operated side, compared to the unmanipulated side was revealed (Figure 1A, Figure S1I-J), confirming the successful and reliable embryonic removal of one ear.

Given that semicircular canals in *Xenopus laevis* tadpoles become functional at stage 48 (Lambert et al., 2008) and only elicit robust angular vestibulo-ocular reflexes (aVOR) after having reached stage 52/53, one-eared tadpoles were reared to this developmental stage (Figure 1B, Figure S1K-N). Successful rearing of surgically manipulated animals to these stages presented with high survival rates, with 100% of 115 post-surgical animals reaching stage 46, and ~85% of subsequently selected stage 46 survivors reaching stages 53-57, as quantitatively assessed from 5 independent experimental cohorts. Apart from the absence of one ear, reared tadpoles appeared indistinguishable from controls in terms of bodily development and exhibited normal spontaneous swimming behaviors. *In vitro* preparations of unmanipulated two-eared controls and one-eared tadpoles (Figure S1K-N) were used to assess the performance of gaze stabilizing vestibulo-ocular motor responses by eye motion tracking

during horizontal rotation on a motion platform in complete darkness (Figure 1B). Sinusoidal rotation of unmanipulated control tadpoles in the dark at 0.5 Hz with a peak velocity of ±31.4°/s, corresponding to positional excursions of ±10° (Figure 1C, top trace), evoked vestibular-driven compensatory eye movements in both eyes (without intermittent fast-phases) that were positional stimulus-timed and oppositely directed, features that are characteristic for the aVOR in *Xenopus* tadpoles (Figure 1C, bottom traces). Comparison between both eyes in control animals revealed a high degree of conjugate motion with correspondingly similar gain values from each eye (Figure S2A-C), features which are consistent with the expected and previously reported levels of conjugate coordination for the horizontal aVOR in larval *Xenopus* (Soupiadou et al., 2020). Therefore, the movements of both eyes were combined in each animal prior to the subsequent quantification of the performance in the different experimental groups. Across all control animals, an average over single cycles (6-40 cycles) in the dark (Figure 1D, left) exhibited a response gain (eye motion amplitude / stimulus position amplitude) of 0.24 ±0.11 (Figure 1E, left; mean ±SD, n = 13) and a considerable phase-lead *re* stimulus position of -72.46° ±23.13° (Figure 1E, right; mean ±SD, n = 13).

Despite the complete absence of inner ear endorgans on the left side, one-eared animals subjected to the same stimulation paradigm also exhibited oppositely directed eye movements indicative of a functional aVOR (Figure 1D, right). Similar to controls, robust conjugate movements of both eyes in one-eared animals were readily observed, with each eye exhibiting comparable gain values and coordinated motion (Figure S2D-F). This again allowed the motion of the two eyes to be averaged prior to further processing. Response magnitudes, obtained by averaging over multiple cycles (12-66 cycles) presented with gain values of 0.14 ±0.08 (Figure 1E, left, mean ±SD, n = 13) and a response peak that was approximately in phase *re* stimulus position (2.08° ±26.90°; Figure 1E, right, mean ±SD, n = 13). Statistical comparison of eye movements between one-eared tadpoles and controls revealed a significant reduction of the response gain (Figure 1E, left, p = 0.0338; Mann-Whitney U-test). In addition, the pronounced phase-lead of the peak responses relative to stimulus position in darkness was significantly delayed in one-eared tadpoles with respect to controls (Figure 1E, right, $p < 0.0001$; Mann-Whitney U-test). Accordingly, these data demonstrate that one-eared tadpoles are able to execute a horizontal aVOR in darkness

despite the lack of bilateral mirror-symmetric endorgans and indicate that the remaining intact inner ear is sufficient to produce gaze-stabilizing extraocular motor commands, even though with reduced efficacy. The phase-relationship of the responses in one-eared animals suggests a considerable temporal delay in the processing of signals from the right, singular, inner ear, likely through longer-latency, multisynaptic pathways.

Directional contributions of singular ears during horizontal aVOR

Head rotation is normally encoded by direction-specific strengthening/attenuation of vestibular nerve afferent signals (Paulin and Hoffman, 2019). In one-eared tadpoles, which maintain the ability to encode oscillatory motion in darkness (Figure 1), a single semicircular canal was found to be sufficient for eliciting a bidirectional horizontal aVOR. However, to separately investigate the directional contributions of a singular ear to leftward *versus* rightward head movements, eye motion amplitudes were evaluated over the first half-cycle of stimulation bouts during platform rotation exclusively to the left or to the right (Figure 2A). Eye movements during these half-cycle periods would therefore derive only from a unidirectional motion away from the singular ear (contraversive) or toward this intact ear (ipsiversive). In two-eared unmanipulated controls, eye movements evoked by unidirectional motion in the dark towards the left (Figure 2B, left; blue traces) or the right (Figure 2B, right; blue traces) were predictably opposite and statistically no different in response strength to stimulus direction within individual animals with mean amplitudes of 5.96° ±1.44° and 5.93° ±1.63°, respectively (Figure 2C, left, mean ±SD, $p > 0.9999$; Wilcoxon signed-rank test, $n = 4$ pairs). Eye movements in one-eared tadpoles evoked by leftward, contraversive, motion in the dark surprisingly were rather variable but astonishingly also robust and in opposition to head movements (Figure 2B, left; orange traces). Rightward ipsiversive motion, i.e., towards the side of the intact, singular ear, evoked responses that were even more variable between different animals, both in direction and magnitude (Figure 2B, right; orange traces). In addition, these eye movements were generally smaller than those driven by contraversive motion with mean amplitudes of 1.43° ±2.05° and 3.82° ±1.88°, respectively (Figure 2C, right, mean ±SD, $p = 0.0420$, Wilcoxon signed-rank test, $n = 11$ pairs). Surprisingly, despite the inner ear being intact on the right side, aVOR responses elicited by a rightward ipsiversive motion in one-eared tadpoles were severely impaired, at least in a number of animals compared to controls (Figure 2D, ipsi, $p = 0.0002$; Mann-Whitney *U*-test). Such a significant impairment

was also found for contraversive motion-driven eye movements toward the side lacking an ear (Figure 2D, contra, p = 0.0136; Mann-Whitney U-test), although this outcome was expected given the lack of conventional sensitivity of vestibular afferent activity for motion toward the impaired inner ear (see e.g., Soupiadou et al 2020). Thus, these sets of data indicate that one-eared tadpoles developed bidirectional vestibular detection and signal processing capacities that allow activating compensatory eye movements during rotation towards the side lacking an ear. However, this directional contribution obviously occurs at the expense of the performance of the aVOR towards the intact side, which becomes compromised during this process (Figure 2D).

Visuo-vestibular plasticity and influence on gaze-stabilizing reflexes

Motion-related sensory signals are known to participate in plasticity processes aiding recovery of acute vestibular loss (reviewed recently in Smith, 2022). In aquatic organisms, visual scene motion is a significant contributor in neuronal computations of self-motion behaviors (Roeser and Baier, 2003), particularly through optokinetic reflex (OKR) circuits which operate synergistically with aVOR signals (Souipadou et al., 2020). To investigate the extent that visual image motion assists vestibular-evoked eye movements in one-eared animals, tadpoles were subjected to horizontal sinusoidal rotation of the platform in the presence of a world-stationary illuminated black and white-striped visual pattern (light; Figure 3A). This experimental approach caused a synergistic activation of a horizontal aVOR and an OKR. Eye movements evoked in un-manipulated control tadpoles under this condition were oppositely directed (Figure 3B) with gain magnitudes of 0.22 ± 0.08 (Figure 3C, mean ±SD, n = 13) and were timed with stimulus position with relatively small phase leads of -18.74° ± 17.97° *re* head position (Figure 3F, mean ±SD, n = 13). When compared to similarly evoked movements in darkness (dark; Figure 1, Figure 3B, dotted blue line) gain magnitudes were found to be no different to eye movements evoked in light (Figure 3C, p = 0.6355; Wilcoxon signed-rank test, n = 13 pairs). In contrast, quantification of phase relationships revealed that eye movements evoked in light were considerably more in phase with stimulus head position (Figure 3F, p = 0.0002; Wilcoxon signed-rank test, n = 13 pairs). Such a relationship between aVOR responses in the presence of a world-stationary visual scene and aVOR in darkness in two-eared control animals complies with the expected impact of concurrent visual motion signals on gaze-stabilizing VOR behaviors, where visual image motion serves as ongoing feed-

back to adjust the VOR dynamically with only minor influences on response magnitude (see Straka and Dieringer, 2004). In one-eared tadpoles, vestibular-evoked eye movements in light were stimulus-timed and oppositely directed with gain and phase magnitudes of 0.16 ± 0.08 and 4.58° ± 14.71°, respectively (Figure 3D, G, mean ±SD, *n* = 13). Similar to un-manipulated controls, gain magnitudes did not differ statistically between light and dark conditions (Figure 3D, *p* = 0.1272; Wilcoxon signed-rank test, *n* = 13 pairs). However, in contrast, vestibular-evoked eye movements in one-eared animals in light did not exhibit a phase shift relative to head position as observed in control animals (Figure 3G, *p* = 0.3396; Wilcoxon signed-rank test, *n* = 13). This suggests the lack of a behaviorally observable influence of visual image motion on aVOR circuits in these animals.

Comparison of the performance of stimulus-evoked eye motion in one-eared animals and unmanipulated controls in the presence of an illuminated visual pattern revealed smaller overall gain values as well as significantly more in phase responses for one-eared animals (Figure 3E, H, *p* = 0.0441; Mann-Whitney *U*-test and *p* = 0.0020; Mann-Whitney *U*-test, respectively). This is consistent with differences observed in darkness (Figure 1E) and indicates that an influence of visual scene motion on temporal adjustments of the VOR does not occur in one-eared animals. Furthermore, these animals continue to perform statistically less robust than controls even in the presence of a visual scene.

To rule out that the optokinetic circuit itself was not disrupted as a result of the embryonic loss of one ear, separate activation by sinusoidal motion of a vertically-striped black and white pattern at different frequencies (0.1, 0.2, 0.5 Hz, peak positional excursion of ±10°) while the head/body remained stationary was performed (Figure S3A, C). This exclusive visual scene motion provoked syndirectional eye movements with respect to the stimulus direction (Figure S3B, D) with and a high level of conjugacy and comparable gain values between the two eyes (Figure S2G-L). Accordingly, the motion of the two eyes was again averaged prior to further processing. Thus, in control two-eared animals, averaged responses over single motion cycles at three different frequencies had average gains of 0.22 ±0.10, 0.11 ±0.07 and 0.05 ±0.03, respectively (mean ±SD; Figure S3E). Comparison indicated that the response gain was statistically different between all tested frequencies, with higher visual motion frequencies evoking considerably smaller eye motion responses as expected for visual image motion processing bandwidths (Figure S3E; Friedman nonparametric test for matched

pairs, $p < 0.0001$). Near similar differences were observed for phase *re* visual stimulus position relationships, with 0.5 Hz being considerably phase-lagged *re* stimulus (58.09° ±27.29°, mean ±SD) compared to the mostly in-phase responses at lower frequencies (Friedman nonparametric test for matched pairs, Dunn's multiple comparisons test; 0.1 Hz, $p < 0.0001$; 0.2 Hz, $p = 0.0181$; Figure S3G). In one-eared tadpoles, visual motion stimulation elicited eye movements with comparable magnitudes and phase relationships, with response gains of 0.27 ±0.17, 0.15 ±0.10 and 0.05 ±0.03 (mean ±SD) for stimulus frequencies of 0.1, 0.2 and 0.5 Hz, respectively (Figure S3E). Across this frequency range, eye movements at a frequency of 0.5 Hz were considerably weaker relative to 0.1 and 0.2 Hz (Friedman nonparametric test for matched pairs, Dunn's multiple comparisons test, $p < 0.0001$ and $p = 0.0239$, respectively). A similar relationship was found for phase characteristics of peak responses, where responses evoked at 0.5 Hz were substantially phase-lagged relative to lower frequencies (Figure S3G; 59.47° ±26.89°, mean ±SD; Friedman nonparametric test for matched pairs, Dunn's multiple comparisons test, $p < 0.0001$ and $p = 0.0429$, respectively). Irrespective of within group differences, comparison between one- and two-eared animals revealed only very few differences in response characteristics of gain and phase (Figure S3F, H; 0.2 Hz phase comparison, $p = 0.0355$, Mann-Whitney *U*-test). Comparatively, these data demonstrate that the visuo-motor ability is overall neither impaired nor greatly enhanced in one-eared tadpoles and follows response characteristics similar to unmanipulated controls. Given the lack of additional visual image motion-mediated modulation of the aVOR in these animals (Figure 3), this collectively suggests that the vestibular circuitry and performance in one-eared tadpoles derives exclusively from sensory inputs from the remaining inner ear with little influence from visuo-motor centers.

Physiological dynamics of one-ear-driven aVOR

In order to evaluate the presence of a modulated resting discharge in extraocular motor nerves that accompany aVOR eye movements, multi-unit extracellular recordings were performed. Modulated discharge dynamics have been previously shown to be immediately abolished after acute vestibular lesions in contralesional extraocular motor nerves in *Xenopus* tadpoles at mid-larval stages (Lambert et al., 2013; Branoner and Straka, 2018) and remained absent thereafter (Lambert et al., 2013). Motion of the eyes during horizontal aVOR, which is driven by the coordinated efforts of lateral recti (LR) muscles, is controlled by the firing

dynamics of bilateral abducens nerves which innervate each LR muscle. The discharge activity of these abducens nerves, herein referred to anatomically as left (Le) and right (Ri) abducens, irrespective of control or one-eared animal (Figure 4A), was therefore profiled during horizontal sinusoidal head rotation in darkness (0.5 Hz, positional excursion ±10°, peak velocity ±31.4°/s; Figure 4A).

In control two-eared animals (Figure 4A, blue traces), modulation of left and right abducens nerves occurred during sinusoidal rotation in darkness in approximate phase-opposition with respect to the same-sided directional head motion velocity (see shaded gray bars). These features were consistent with the push-pull functional dynamics of extraocular motor nerves during an aVOR (Straka and Dieringer, 2004). As a most remarkable feature, and in stark contrast to the condition after an acute vestibular lesion in mid-larval stage *Xenopus* tadpoles (Lambert et al., 2013), all recorded abducens nerves on both sides in one-eared animals expressed a distinct and modifiable resting discharge (Figure 4A, orange traces). However, the dynamic characteristics of this resting discharge were much less consistent across one-eared animals compared to controls. While left and right abducens nerves in control animals modulated generally in phase with their opposite directional head motion velocity (Figure 4B and 4C, upper panels), this effect appeared to be obscured in right abducens nerves of one-eared animals (Figure 4B and 4C, lower panels). Discharge modulation of these nerves were found to exhibit a considerable heterogeneity, with some nerves modulating with profiles that were entirely inconsistent with typical right abducens nerves of control animals. Quantification of phase relationships with respect to leftward head motion velocity (Figure 4D-E) was in agreement with such qualitative observations. Indeed, abducens nerves in controls were found to exhibit temporal-activity patterns consistent with those expected for their anatomical identity (Figure 4D), with no temporal overlap of the activity in their bilateral abducens counterparts (see blue hashed bars in Figure 4D). Directional phase analysis *re* leftward velocity revealed mean phase vectors of 143.92° ±13.52° (r = 0.973) and 329.86° ±23.48° (r = 0.919) for left and right abducens, respectively. These activity metrics are demonstrative of preferred directional firing, which indicates spatially separate tuning properties present in these nerves (Figure 4E; $p < 0.0001$ and $p = 0.000067$, Rayleigh's Uniformity Test for left and right abducens, respectively; $p < 0.001$, Moore's Paired Test). In contrast, left and right abducens nerves in one-eared animals showed

a large spread in temporal distribution of activity during rotation (Figure 4C-D), with mean directional vectors for the left and right abducens nerves of 152.77° ±21.24° (r = 0.934) and 282.16° ±102.02° (r = 0.205), respectively (Figure 4E). In particular, right abducens nerves appeared to modulate in some cases even during rightward peak velocity (Figure 4C-D) and failed to exhibit a preferred directional sensitivity (p = 0.614, Rayleigh's Uniformity Test). Conversely, left abducens nerves from one-eared animals largely exhibited an appropriate temporal pattern of discharge modulation and grouped in a preferred direction ($p < 0.001$, Rayleigh's Uniformity Test). These results suggest a clear lack of entirely separate spatial tuning between both nerves ($p > 0.05$, Moore's Paired Test). The mean angular directional preferences for left abducens nerves between controls and one-eared animals were found to be no different (p = 0.365, Watson-Williams F-test), as well as for comparison of right abducens nerves (p = 0.241, Watson-Williams F-test), suggesting that in some animals appropriate tuning properties are present, despite the heterogeneity introduced by individual animals.

Amplitude-dependent features, such as the depth of modulation, which estimates the magnitude of change of discharge within a single head motion cycle, were found to be not statistically different between anatomical left and right nerves within controls and manipulated animals (Figure S4A-B; p = 0.1563, $p > 0.9999$; Wilcoxon signed-rank test, n = 6 pairs of controls and n = 5 pairs of one-eared animals, respectively). Such features are characteristic of a spatially appropriate push-pull aVOR organization (Straka and Dieringer, 2004). In addition, the spontaneous activity, corresponding to discharge rates during periods of no head motion, were similarly invariant between left and right nerves in both animal groups (Figure S4C-D; p = 0.5625, p = 0.6250; Wilcoxon signed-rank test, n = 6 pairs of controls and n = 5 pairs of one-eared animals, respectively), suggesting the presence of a homeostatic plasticity during the ontogenetic establishment of the circuitry that apparently aims at symmetric driving forces. Comparison of discharge rates during the application of rotational stimuli relative to spontaneous resting activity rates (modulation index) revealed expected response profiles in control nerves (Figure S4E). Left and right abducens nerves appeared to modulate around their spontaneous firing rate, with frequencies modulating below and above their resting rate, corresponding to stimulus-evoked periods of discharge facilitation and disfacilitation (Figure S4E, blue heat maps). Modulation around resting activity was

observed less often in one-eared animals, in both left and right nerves, suggesting that at least in some cases these nerves in one-eared animals suffer from a lack of appropriate facilitation/disfacilitation dynamics based on the activity pattern from the singular ear (Figure S4E, orange heat maps). Between control and one-eared animals, the modulation depths in both nerves were significantly less robust (Figure S4F-G; p = 0.0463, p = 0.0011; Mann-Whitney U-test for left and right abducens nerves, respectively), while resting rates were found to be no different (Figure S4F-G; p = 0.3823, p = 0.1876; Mann-Whitney U-test for left and right abducens, respectively). Beyond differences in modulation depth, these physiological profiles suggest a striking dissimilarity in bilateral abducens nerve activity during the aVOR for animals which have developed with only a singular ear. Motor transformations from such singular ears appear to follow temporal dynamics of comparable extent as would be expected in unmanipulated control animals for anatomically defined left abducens nerves. This is not too surprising given the major driving force of abducens motor nerve activity from the contralateral ear, which is the residual singular ear in one-eared animals. In contrast, right abducens nerves exhibit a prominent temporal heterogeneity. The disparity between the two nerves, which in control conditions does not exist, is indicative of potentially equally heterogenic mechanisms used to permit modulatory activity that is necessary to yoke the eyes.

Discussion

Unilateral extirpation of the embryonic otic placode generated tadpoles that developed with a singular ear. These one-eared tadpoles exhibited a considerable degree of developmental plasticity, observable during execution of the horizontal vestibulo-ocular reflex. Eye movements, though weaker compared to two-eared controls, demonstrated successful execution of sensorimotor transformations despite the lack of bilateral mirror-symmetric vestibular endorgans. Achievement of this capacity occurs through neuronal computations of inputs from the singular inner ear in hindbrain vestibular centers. Once in the hindbrain, input from the single ear is sufficient to drive bilateral directed gaze stabilizing reflexes (Figure 5). The developing central nervous system is therefore capable of establishing directionally sensitive sensorimotor processing capabilities from self-motion information originating from a single set of vestibular endorgans. The mechanisms driving this capacity

likely derive from individualized strategies of circuit plasticity during development which are largely independent of visual-motion contributions.

Developmental plasticity in unilateral sensory deprived vestibulo-ocular circuits

Surgical excision of the otic placode at very early stages in *Xenopus laevis* generated embryos which experienced the complete absence of one inner ear and were thus challenged with detecting self-motion stimuli with only one set of endorgans. Downstream of such challenges in sensory detection, integration of vectorially different inputs through peripheral pathways was continued, despite the fact that these pathways typically receive bilateral motion vectors (Glasauer and Knorr, 2020). Unilateral ablation techniques such as this have previously been demonstrated as a suitable approach to assess the anatomical effects of sensory deprivation on hindbrain targets in *Xenopus* (Fritzsch, 1990; Elliott et al., 2015a, 2015b), chick (Levi-Montalcini, 1949; Peusner and Morest, 1977), and salamanders (Goodman and Model, 1988). Such studies were pivotal in identifying the effects on central vestibular circuit development, however, detailed profiling of the behavioral impact and electrophysiological execution of sensorimotor transformations from the remaining singular inner ear by vestibular-ocular and visuo-motor centers is so far unexplored. Ear extirpation in *Xenopus* at later embryonic periods during which the inner ear is well into its development examined resulting behavioral consequences (Rayer et al., 1983; Rayer and Horn, 1986), although exploration was mostly limited to vestibular stimulation in darkness during static head positions without the presence of OKR feedback and to our knowledge has not been profiled on an electrophysiological level. Related embryonic manipulations such as surgical rotation (Lilian et al., 2019; Elliott et al., 2015b) or addition of supernumerary ears (Elliott et al., 2015a; Gordy et al., 2018), profiled functional achievements to a successful degree, though central computations retain inputs of variable degrees and spatio-temporal composition from both sides (Lilian et al., 2019; Elliott et al., 2015a,b).

Beyond different surgical techniques, non-invasive methods have been used to profile vestibular sensory loss, particularly from selective deficiencies in microgravity (Horn, 2003), inner ear genetic manipulations with permanent effects (Kopecky et al., 2012; Macova et al., 2019) or those of a more transitory nature, such as the generation of Zebrafish with temporary utricular deprivation (Roberts et al., 2017; Ehrlich and Schoppik, 2019). Such

manipulations, however, were either not specific to one side (Kopecky et al., 2012), lack uniformity of deprivation across all sensory epithelia (Roberts et al., 2017), or present with defects in various sensorimotor areas (Patten et al., 2012). Functional consequences of these conditions would therefore derive from motion information of both sides, albeit with varying degrees of asymmetric signaling. In contrast, one-eared animals in the current study receive self-motion information solely through one inner ear, which lacks its bilateral mirror-symmetric compliment, but normally develops all other sensorimotor systems, with minimal detrimental effects on adjacent placode-derived sensory organs (Elliott et al., 2010). The overall retention of vestibulo-motor responses in the presence of a singular ear (Figure 1) demonstrates the capacity of one-eared animals to execute adequate spatio-temporal VOR transformations. Execution of gaze stabilizing vestibular reflexes in darkness, and thus without visually derived motion-signaling, demonstrate that these animals have generated sufficient plastic vestibular alterations to transform directionally specific inputs from the singular ear. Such plastic capabilities have not been observed in previous behavioral assessments of one-eared *Xenopus* tadpoles (Zarei et al., 2017), where Mauthner-cell mediated swimming startle responses were of appropriate measure, although directionally biased with respect to inputs from the singular ear (Zarei et al., 2017). The latter finding is not entirely surprising, given the physiological basis of Mauthner cell-mediated startle behaviors (Korn and Faber, 2005), where no morpho-physiological modifications within the singular ear can obviously encode bidirectional stimuli. In contrast, in the current study, lateralized horizontal rotation is detectable by the singular horizontal semicircular canal and was shown to derive from the structurally guided facilitation/disfacilitation dynamics of semicircular canal afferent signals (Figure 2).

Particularly surprising was the unexpected inequality in eye motion amplitudes during contraversive *versus* ipsiversive (with respect to the single ear) rotation, which favored more robust responses during disfacilitation of the singular right ear. Acute lesion of a single stato-acoustic nerve in *Xenopus* tadpoles showed a physiologically more expected effect where rotation toward the lesion side elicited very poor eye movements, a feature consistent with the sudden loss of a predominant directional sensitivity (Soupiadou et al., 2020), which is likely due to the resulting absence of the driving force supplying relevant extraocular motoneurons (Branoner and Straka, 2018). Here, despite the obvious bidirectional sensitivity

of the singular inner ear, such asymmetric motor output highlights individualized differential strengths in computation within brainstem processing regions. This suggests that plasticity mechanisms are not goal-directed at consistently aiming for production of suitable motor commands that equalize sensitivity vectors (Dieringer, 2003). Instead, behavioral responses during head oscillation-driven facilitation and disfacilitation of singular ears seems to provide sufficient dynamics for the production of spatio-temporally appropriate aVOR responses beyond differences in directional vectors. In animals with an acute loss of inputs from one inner ear, the residual oscillatory motion-driven aVOR is much less robust and generally rather asymmetric with a predominance of responses during rotations toward the intact side (Soupiadou et al., 2020). This is likely related to the fact that the effects of such an acute lesion were assessed in post-embryonic animals with a well-established and functionally mature vestibular system. In contrast, one-eared animals in this study were generated prior to the development of otic neurosensory and central vestibular elements. By comparison, here, plasticity mediated generation of vestibular behaviors is thus challenged during development of the vestibular system and reports on the extent to which bilateral peripheral input is required or dispensable during this ontogenetic period. Lesions in tadpoles, which is at variance with the otic extirpation in embryos in the current study, present with permanent morphological detriments, which are retained even into post-metamorphic adult stages (Lambert et al., 2013), highlighting that such perturbations in *Xenopus* tadpoles occurs after a period where relevant circuitries have already developed and thus reveal the emerging consequences after a unilateral loss of vestibular sensory inputs.

In the visual system, early reversible monocular deprivation in the cat leads to an increased responsiveness to signals from the remaining eye in cortical areas, with a concomitant expense of target sensitivity to inputs from the shunted eye (Wiesel and Hubel, 1963). The data presented here suggest the opposite, with a dampening in motion vector sensitivity in the excitatory on-direction of the singular ear. However, the marginal redundancy in visual input originating from individual eyes during visual motion detection, even among lateral- and frontal-eyed animals which present with markedly strong directional asymmetries (Masseck and Hoffmann, 2009; Wagner et al., 2022) does not exist for vestibular signal encoding and processing, where mirror-symmetric endorgans encode directional domains that are almost mutually exclusive. Therefore, that the remaining inner ear

maintains and potentially increases the ability to peripherally distinguish directional vectors (Figure 2) suggests that one-eared tadpoles have individually activated developmental strategies that ultimately provide preservation or extension of bidirectional sensitives. Two-eared mediated bilateral modulation of motion-related neuronal activity is known to depend on spontaneous afferent discharge levels, which provide a larger range for bidirectional motion encoding at higher resting rates and a more directionally restricted sensitivity at low or very low afferent firing rates as usually present in amphibian species (Blanks and Precht, 1976; Honrubia et al., 1981, 1989). Here, a generalized strategy to generate bidirectional sensitivity from singular inner ears might involve the establishment of higher resting discharge rates in vestibular afferent fibers beyond the usually low firing rates to allow encoding of head motion only in the on- but not in the off-direction (Figure 5C). Developmentally established higher resting rates of vestibular afferents innervating the singular ear would thus extend the dynamic range for the motion encoding by increasing the degree for a firing rate disfacilitation during contraversive head movements.

One-eared *Xenopus* tadpoles subjected to drop-swim assays showed deficits in postural stabilization (Elliott et al., 2015b), which suggests an inability to correct for directionally asymmetric vestibular inputs. However, the extent to which this reflects a limitation in processing bandwidth required for integrating otolith and semicircular canal inputs, or is merely a developmental restriction, given that tadpoles were assessed relatively shortly after the ear removal, remained untested (Elliott et al., 2015b). Developmental progression of similarly manipulated tadpoles to the physiological stages assayed here has been done previously but was limited to tract tracing observations alone (Fritzsch et al., 1990). The capability of one-eared animals in this study to execute a spatially appropriate aVOR provides a unique perspective on the developmental strategies for adaptive plasticity, highlighting the extent to which directional sensitivities may develop despite lacking structures for their detection. These results expand upon the observed persistency of appropriate vestibular processing despite embryonic deficiencies in peripheral inputs. Indeed, delayed bilateral otolith formation in Zebrafish demonstrated a similar autonomy for nascent posture-stabilizing circuits (Roberts et al., 2017). The extent of developmental plasticity observed in the current study compliments with previous experimental models in the visual system of amphibians (e.g., Constantine-Paton and Law, 1978; Ruthazer et al., 2003;

Blackiston et al., 2017) and teleosts (e.g., Ramdya and Engert, 2008), which served to highlight the remarkable degree of flexibility during development of sensory systems. A potential mechanism in the case of one-eared tadpoles might include altered resting discharge rates as well as a shift in the push-pull organization of inhibitory and excitatory vestibulo-ocular connections beyond the typical three-neuronal connections. Such mechanisms could generate a spectrum of individually specific encoding capacities for bilateral extraocular motor commands through alterations in the degree of excitation or disinhibition (see below).

Mechanisms of developmental vestibular plasticity

Firing activity of extraocular motor nerves represent the terminal site of VOR sensorimotor transformations originating from inner ear peripheral inputs (Gensberger et al., 2016). Extracellular discharge dynamics of these motoneurons, particularly those of the abducens nerve, have previously been used to profile downstream circuit computations after an acute vestibular loss in *Xenopus* (Lambert et al., 2013; Branoner and Straka, 2018), and various species of *ranid* frogs (e.g., Rohregger and Dieringer, 2003), as well as following embryonically guided introduction of additional vestibular inputs (Gordy et al., 2018). Here, profiling abducens nerve dynamics in one-eared animals reported on a considerable range of developmental plasticity measures. Despite the absence of one inner ear, a sustained and robust spontaneous resting rate of the extraocular motor nerve was observed. The presence of such robust rates contrasts with animals following an acute unilateral vestibular loss where an elimination of resting activity in extraocular motor nuclei contralateral to the lesioned ear was reliably demonstrated (Branoner and Straka, 2018; Lambert et al., 2013). Given that motoneurons of the right abducens nerve in one-eared tadpoles exhibit such prominent resting rates despite lacking a contralateral left inner ear, which under control conditions provides the excitatory drive (Straka and Dieringer, 1993), suggests the presence of homeostatic mechanisms which likely aim at establishing symmetric driving forces during ontogeny. Following an acute lesion of one stato-acoustic nerve at the tadpole stage (e.g., Lambert et al., 2013), such a loss is likely driven and permanently maintained by the weighted inputs on abducens motor targets from second-order vestibular neurons which suddenly lack excitatory inputs from the lesioned side while maintaining continued ipsilateral inhibition from the remaining ear. In the current study, the development of a suitable driving force could likely be generated by both a decrease in inhibitory inputs to the right abducens nucleus as

well as by an indirect excitatory input from the remaining inner ear (Figure 5A). Unilateral labyrinth-ectomized *ranid* frogs appear to rely heavily on the former compensatory strategy, though were also rather heterogeneous in the efficacy of their responses (Agosti et al., 1986).

In the current one-eared animals, the impaired ability of right abducens nerves to modulate around their respective resting rates in some animals suggests a degree of inadequacy in disinhibition and might lend support to this notion. Indirect excitatory contributions might be the result of midline crossing commissural pathways in the hindbrain (Figure 5A; Straka, 2020), particularly of excitatory fibers which innervate horizontal semicircular canal second-order vestibular neurons (Holler and Straka, 2001) and assist the generation of symmetric resting rates, as might be the case for the acute loss in *ranid* frogs (Agosti et al., 1986). The relative synaptic weights of such excitatory connections, their second-order targets, and the distributions relative to inhibitory commissural fibers is thus of great interest to investigate. The longer response latency in one-eared aVOR eye movements of the current study tends to support such a claim, given the delay to reach peak eye motion velocity relative to control conditions and could be due to additional synaptic relays during sensorimotor transformation (Figures 1, 2; see Figure 5 for a summary). The presence of additional synaptic sites likely supplements the traditional three-neuronal reflex circuit typical for aVOR processing and thus offers a potential mechanistic site for assisting appropriate eye movements during head rotations in the absence of the former. If indeed such crossed synaptic additions are utilized and have become a dominant pathway in these animals requires further investigation into frequency sensitivities. This would be of particular interest to explore due to possible resultant behavioral constraints given that VOR responses are considerably sensitive to high frequency head movements. As a result, response delays might compromise appropriate eye movements during high frequencies, whereas low frequency head movements could likely cope with such synaptic strategies. Commissural pathway-mediated generation of such symmetry would be opposite to that observed in cats, where a loss of crossed vestibular commissural inhibition causes an increase in the resting discharge of contralesional second-order vestibular neurons, which, however, decreases over time (Yagi and Markham, 1984). In chicks, an increase in excitatory inputs on the lesioned side was found only in animals which had not been classified as being able to behaviorally compensate for an acute unilateral vestibular loss (Shao et al., 2012). The similar resting rates between bilateral

abducens nerves in embryonically manipulated *Xenopus* tadpoles approximate a considerable extent of symmetric activity in their upstream vestibular nuclei. These animals, though lacking behavioral and physiological robustness at control levels, have seemingly developed such a symmetry, which permits appropriate motor output and highlights the general need of symmetric activity levels in vestibular nuclei, as has been proposed in several experimental models (Lambert and Straka, 2012).

Motion evoked discharge rates in the abducens nerves of one-eared tadpoles were cyclic with respect to the stimulus. Despite differences in the ability to modulate around their respective resting rates, abducens activity profiles clearly demonstrated a general capability to execute sensorimotor transformations originating from inputs from the singular inner ear. However, the notable heterogeneity in the response phase of individual nerves indicates a range of temporal relationships. This is particularly evident for right abducens nerves, where peak firing rates temporally extended even in some cases to periods with inappropriate motion direction. In these abducens motoneuron populations, the lack of direct excitatory input from the operated side, despite disinhibitory contributions from the remaining ear, might seem to be a detriment that was sometimes developmentally uncompensated for, particularly given that all left abducens nerve responses appeared appropriate in phase (with excitatory inputs from the residual singular inner ear). However, the behavioral data suggests against this, particularly given the activation of considerably strong eye movements during sinusoidal and unilateral motion toward the operated side. Therefore, right abducens motoneurons with directionally inappropriate phase metrics might be supplemented with temporally complimenting, though phase shifted, discharge rates in medial rectus-innervating oculomotor motoneurons, which would provide suitable antagonistic yoking (Figure 5B) required for the aVOR (Horn and Straka, 2021). Post-lesional plasticity in *ranid* frogs has so far demonstrated a considerable variability in the spatial tuning of the abducens nerve activity during linear and angular motion-evoked VOR, which was demonstrated to be behaviorally detrimental but likely beneficial for the survival of deafferented central vestibular neurons, illustrating the lack of a robust singular principle for recovery (Goto et al., 2001; Rohregger and Dieringer, 2003). In tadpoles of the current study, the ability to execute spatially meaningful aVOR behaviors suggests that inappropriate tuning of abducens nerve activity might only play a minor role. This variability in response timing indicates either an absence of

a unifying goal-directed neuronal strategy or a permissive mechanistic framework for amelioration following vestibular loss similar to the previously reported spatial plasticity of the VOR (for review see Dieringer, 2003). Precise tuning characteristics of central vestibular neurons would be beneficial to further explore, such as in recent approaches quantifying tuning and convergence properties in Zebrafish (Liu et al., 2020).

Motion-sensitive sensory modality integration is prominent in brainstem gaze and posture processing centers (Angelaki and Cullen, 2008), and plasticity-based reorganization following vestibular loss is typically supplemented by these modalities (Curthoys, 2000). In tadpoles of the current study, concurrent optokinetic flow appeared to not supplement aVOR responses neither in amplitude nor in temporal attributes. These animals have therefore developed a vestibular processing regime without relying on augmented synergistic visual motion signals, which suggests the location of plasticity as being possibly exclusive to vestibular circuit elements alone. A wealth of studies has reached similar or contrasting conclusions, which highlights broad species differences in the apparent extent of modality substitution following vestibular deprivation (for review see e.g., Dieringer, 1995; Darlington and Smith, 2000). The current study is thus the first instance of unilateral embryonic vestibular deprivation demonstrating the impact on the performance of vestibulo-ocular reflexes that align with independence from visually mediated substitution. Cerebellar contributions to developmental maturation of vestibular evoked posture-stabilization (Ehrlich and Schoppik, 2019), as well as homeostatic mechanisms following prolonged rotation (Dietrich and Straka, 2016) implicate the possibility of the cerebellum as being involved in plasticity strategies here as well, though experimental validation is still pending. Ontogenetic development of brainstem vestibular circuits might be highly plastic and can be exploited to drive functionally appropriate motor outputs despite lacking peripheral sensors. Considerations to such plasticity extents would be beneficial for targeted therapeutics, such as those aimed at using transplantation approaches to replace vestibular deficits (Elliott et al., 2022), and might aid in the holistic understanding of adaptability in vestibular development and processing.

Limitations of Study

Electrophysiological data from abducens nerves were acquired by extracellular multi-unit recordings with separately crafted electrode capillaries of different diameters to fit individual nerves across animals. Electrode capillary sizes determine the capacity to detect specific units and therefore can obscure a comprehensive assessment of the entire population discharge dynamics by reducing the resolution to specific sets of individual motoneurons. Additionally, removal of the otic placode, though clearly demonstrated, is an experimental physical manipulation and could present with unintended side-effects as a byproduct of surgical intervention. Genetic ablation of the otic placode could potentially serve to substantiate the absence of such effects in these developing embryos, although this might also introduce other detrimental consequences for the experimental outcome. *Xenopus* tadpoles in this study are head-fixed during behavioral trials. Head fixation restricts the ability of behaviorally substituting strategies during horizontal rotation, such as saccadic head movements common in anurans, and could therefore impart a bias in the efficacy of observed gaze-stabilization strategies.

Acknowledgements

The authors thank Michael Forsthofer for his insightful and constructive comments on earlier versions of this manuscript as well as Dr. François Lambert, Gabriel Barrios, Michael Forsthofer, and Prof. Dr.-Ing. Stefan Glasauer for guidance with the analysis and scripts. Gratitude is also due to the LMU Biocenter Animal Facility veterinarian staff for their assistance in rearing experimental animals. Confocal microscopy was performed in the "Center for Advanced Light Microscopy" (CALM) facilities of the LMU Munich. This research was supported by the Deutsche Forschungsgemeinschaft (German Science Foundation; CRC 870, RTG 2175, STR 478/3-1).

Author Contributions

Conceptualization, C.G. and H.S.; Methodology, C.G. and H.S.; Software, C.G.; Validation, C.G.; Formal Analysis, C.G.; Investigation, C.G.; Resources, H.S.; Data Curation, C.G and H.S.; Writing – Original Draft, C.G. and H.S.; Writing – Review and Editing, C.G. and H.S.; Visualization, C.G.; Supervision, H.S.; Project Administration, H.S.; Funding Acquisition, H.S.

Declaration of Interests

The authors declare no competing interests.

Main Figure Titles and Legends

Figure 1. Vestibulo-ocular reflex performance in one-eared *Xenopus laevis* tadpoles. (A) Schematic depicting the experimental procedure and developmental timeline following unilateral embryonic removal of the otic placode (stages 25-27; lateral view) followed by rearing of the one-eared embryos to tadpole stages (stage 46-57; dorsal view); note the lack of the left inner ear (orange *) and corresponding neurosensory and accessory otic structures, illustrated by images from the left (Extirpated side) and right side (Unmanipulated side) of a stage 46 larva, with whole-mount antibody stainings against neurons (acetylated tubulin, green) and hair cells (myosin-VI, red) in the otic region. **(B)** Schematic of a semi-intact preparation used for functional profiling of control and one-eared tadpoles during horizontal sinusoidal rotation coupled with live motion-tracking of both eyes. **(C)** Representative example of oppositely-directed, compensatory eye oscillations (lower traces) during five cycles of horizontal sinusoidal head rotation (±10°, peak velocity ±31.4°/s) at 0.5 Hz (upper trace) in an unmanipulated control (blue) and a one-eared (orange) tadpole. Responses are averages of both eyes, respectively. (**D**) Averaged responses over a single horizontal rotation cycle of controls (*n* = 13, individual gray traces; from 6-40 cycles) and one-eared animals (*n* = 13, individual gray traces; from 12-66 cycles); blue and orange traces represent the population mean response over one motion cycle (black trace) for the respective group of animals (**D**); averaged responses were used to individually calculate the gain (left in **E**) and phase value *re* stimulus position (right in **E**). Significance levels are indicated by asterisks: * $p \leq 0.05$, **** $p \leq 0.0001$ (Mann-Whitney *U*-test). R, rostral; C, caudal; V, ventral; D, dorsal; M, medial; op, otic placode; ov, optic vesicle; cg, cement gland; oe, olfactory epithelium. Immunohistochemical stainings in **A** were counterstained with the nuclear marker DAPI. Scale bars in **A** are 100 µm. Data in **E** are represented as mean ± SD. See also Figures S1 and S2.

Figure 2. Directional sensitivities of singular ears during horizontal aVOR. (A) Schematic depicting unidirectional horizontal angular rotation of control and one-eared animals; rotations were performed either toward (ipsiversive, ipsi) or away from the residual singular ear (contraversive, contra) without oscillation between the two directions. **(B)** Eye movements of individual control (*n* = 9; thin blue traces) and one-eared (*n* = 13; thin orange traces) animals during unidirectional rotation, averaged over 1-6 half-cycles, respectively,

that were obtained from the onset of sinusoidal stimulus events shown in Figure 1D; thick blue and orange traces represent respective population means. **(C, D)** Comparison of peak response amplitudes during contraversive and ipsiversive positional excursions within **(C)** controls (blue) and one-eared animals (orange), respectively, and for the two directions between controls and one-eared animals **(D)**. Data points in **C** reflect all animals which had a VOR half-cycle response; lines connecting data points indicate animals that had a response in both directions which was used for paired statistical comparison. Dotted lines in **C** and **D** represent the reversal lines of eye motion direction; note that peak amplitudes during ipsiversive rotations were inverted to facilitate a comparison between the responses for the two stimulus directions; significance levels are indicated by asterisks: * $p \leq 0.05$ (Wilcoxon signed-rank test) *** $p \leq 0.001$ (Mann-Whitney *U*-test). Data in **D** are represented as mean ± SD.

Figure 3. Visuo-vestibular reflex plasticity. (A) Schematic depicting the experimental condition that consisted of a horizontal sinusoidal head rotation in the presence of a world-stationary, illuminated black and white-striped visual pattern (Light). **(B)** Averaged responses over a single head motion cycle in light (gray traces from 6-77 cycles, respectively) and population means (solid-colored traces) in controls (n = 13) and one-eared animals (n = 13); dotted blue and orange traces depict population means obtained from head rotations in darkness (Dark) illustrated in Figure 1D; black sine waves indicate the stimulus position. (**C-H**) Gain **(C-E)** and phase *re* stimulus position **(F-H)** calculated from averaged responses over a single motion cycle in Dark and Light conditions of controls **(C, F)** and one-eared animals **(D, G)**; respective values for the light condition in the two experimental groups are compared in **E, F**. Significance levels are indicated by asterisks: * $p \leq 0.05$, ** $p \leq 0.01$, *** $p \leq 0.001$ (Wilcoxon signed-rank test in **F**, Mann-Whitney *U*-test in **E, H**). Horizontal dotted lines in **F-H** at 0° indicate phase alignment with the stimulus. Data in **E, H** are represented as mean ± SD. See also Figures S3 and S2.

Figure 4. Discharge dynamics of abducens motoneurons. (A) Recording sites of abducens motor nerves during sinusoidal head rotation (±10° positional excursion, peak velocity of

±31.4°/s, 0.5 Hz) in darkness (upper panel); multi-unit recordings of left (Le) and right (Ri) abducens nerves (lower panel) during head rotation, corresponding to peak leftward (lower peaks) and rightward (upper peaks) velocities (Vel) of ±31.4°/s (black sinusoidal velocity trace) in two-eared control (blue) and one-eared (orange) animals; shaded regions indicate periods of leftward head motion velocity. **(B)** Heat maps visualizing peri-stimulus time histograms of normalized discharge rates over a single cycle (from 12-28 and 14-54 cycles in *n* = 10 and *n* = 15 controls and one-eared animals, respectively) during directionally specific head motion velocity (gray sinusoidal traces); horizontal heat map rows represent individual animals. **(C)** Modulation depth as a function of phase *re* peak leftward stimulus velocity for left and right abducens nerves obtained from **B**, depicting the timing of the peak discharge within the cycle; closed and open circles indicate left and right abducens nerves, respectively; note the discrete clustering of left and right abducens nerve activity in controls (upper, blue) compared to one-eared animals (lower, orange). **(D)** Frequency distribution of response phases for right and left abducens nerves, obtained from the data depicted in **C**; bar amplitudes denote the total number of nerves *per* temporal allocation; hashed bars indicate the number of right abducens nerves within the total number *per* temporal allocation. **(E)** Polar plots depicting phase deviations *re* peak leftward velocity (gray vertical line indicates phase of peak leftward velocity during stimulus motion) from **C-D** represented across 360°; arrows indicate the calculated mean vector for pooled left (filled arrowhead) and right (shaded arrowhead) abducens nerve discharge profiles in controls (upper) and one-eared (lower) animals; values next to vector arrows are respective metrics of mean angular direction and vector length (μ, r). See also Figure S4.

Figure 5. Putative plasticity mechanisms in embryonically generated one-eared tadpoles. Schematic depicting the speculated horizontal aVOR circuitry during a leftward heard turn in a one-eared animal and proposed plasticity mechanisms (orange boxes, orange cells and axons). Leftward head rotation (black arrow) elicits oppositely directed horizontal eye movements (blue arrows) through muscle contractions of the lateral and medial recti (LR, MR, blue) driven from off-direction hair cell and afferent activity modulation of the singular horizontal semicircular canal (HC, blue). Disfacilitation (gray colored cells and axons) of second-order vestibular target neurons (2°VN) and HC afferent fibers (1°HC) produces eye

movements which are delayed relative to control conditions, potentially due to **(A)** augmented crossed excitatory (green, +) or inhibitory (magenta, -) commissural gating of contralateral 2°VN target neuronal activity (orange line). Upstream of driving force computations, temporally inappropriate firing dynamics of abducens (VI) motoneurons are potentially offset **(B)** by the activity of antagonistic muscles, i.e., the ipsilateral MR muscle. Increased levels of afferent discharge rates **(C**; see inset**)** may contribute to the encoding ability for off-directional head movements. III, oculomotor nerve; VI-INT, abducens internuclear neurons. Blue, eye motion direction and corresponding horizontal endorgan; green, excitatory connections; magenta, inhibitory connections; gray, disfacilitation; orange, proposed sites and mechanisms of plasticity in one-eared animals.

STAR Methods

RESOURCE AVAILABILITY

Lead Contact

Further information and requests for resources and reagents should be directed to and will be fulfilled by the lead contact, Dr. Hans Straka (straka@lmu.de).

Materials availability

This study did not generate new unique reagents.

Data and code availability

- All data reported in this paper will be shared by the lead contact upon request.
- All original code has been deposited at Mendeley Data and is publicly available as of the date of publication. DOIs are listed in the key resources table.
- Any additional information required to reanalyze the data reported in this paper is available from the lead contact upon request.

EXPERIMENTAL MODEL AND SUBJECT DETAILS

Xenopus laevis

Experiments were conducted on wild-type *Xenopus laevis* embryos and larvae of either sex at developmental stages 25-27, 46, and 53-57 (Nieuwkoop and Faber, 1994). Embryos were obtained through induced ovulation by injection of human chorionic gonadotropin, followed by *in vitro* fertilization with sperm suspension in 1 x Modified Barth's Saline (MBS, diluted from 10 x stock; 880 mM NaCl, 10 mM KCl, 100 mM HEPES, 25 mM $NaHCO_3$, pH 7.6) or manual collection after natural mating. Embryos from either fertilization method were de-jellied with 2% cysteine and incubated in 0.1 x Marc's Modified Ringer's Solution (MMR, diluted from 10 x stock; 1 M NaCl, 18 mM KCl, 20 mM $CaCl_2$, 10 mM $MgCl_2$, 150 mM HEPES, pH 7.6-7.8) until animals reached stage 46, when tadpoles were transferred and housed jointly in standing tanks of de-chlorinated water of appropriate volume (McNamara et al., 2018), maintained at 17-19°C under a 12 hour/12 hour light/dark cycle, and fed daily with a powdered Spirulina (Algova, Germany) suspension in tank water. One-eared experimental tadpoles were housed in the same environmentally controlled room and exposed to same aqueous medium as control siblings. After reaching stage 53-57, tadpoles

were used for behavioral and/or physiological assessment in accordance with the "Principles of animal care" publication No. 86–23, revised 1985, of the National Institutes of Health and were carried out in accordance with the ARRIVE guidelines and regulations. Permission for the experiments was granted by the legally responsible governmental body of Upper Bavaria (Regierung von Oberbayern) under the license codes ROB-55.2-1-54-2532-14-2016, ROB-55.2.2532.Vet_03-17-24 and ROB-55.2.2532.Vet_02-19-146. In addition, all experiments were performed in accordance with the relevant guidelines and regulations of the Ludwig-Maximilians-University Munich.

METHOD DETAILS

Inner Ear Extirpation

Extirpations of the inner ear anlage (the otic placode) were performed in 1.0 x MMR at a room temperature of 22°C on stage 25-27 embryos. Embryos were anesthetized with 0.02% Benzocaine (Sigma-Aldrich, E1501; Elliott and Fritzsch, 2010) prior to the surgical manipulations. All surgical interventions were performed with fine tungsten needles (0.125 mm, Fine Science Tools, 10130-05). Access to the developing inner ear following visual identification of the target area was made by peeling back the dorsolateral ectoderm-derived layer overlying the developing otic placode. Placodes were subsequently identified by visual inspection and were surgically excised from the surrounding tissue (Video S1). Removals were done unilaterally, with the contralateral side left unmanipulated. Care was taken to minimize the ablation and disturbance of adjacent non-otic tissue such as to exclusively remove the developing ear. After the surgery, embryos were maintained for 30 minutes in 1.0 x MMR to permit healing of the exposed tissue before being returned to 0.1 x MMR and reared until reaching the desired stages for the different types of experiments (see below). A representative video of ear extirpation was captured on a SteREO Discovery.V20 stereo microscope with a Axiocam 305 color camera (Carl Zeiss Microscopy GmbH) taken at 8 fps and exported at 15 fps using ZEN software 3.4.91 (Carl Zeiss Microscopy GmbH).

Experimental preparations

All experiments were performed on semi-intact *in vitro* preparations generated from tadpoles that had been subjected to a unilateral embryonic inner ear extirpation or from untreated control animals and were obtained following a protocol described previously (Knorr

et al., 2021; specified in detail by Özugur et al., 2022). Tadpoles were first anesthetized in 0.05% 3-aminobenzoic acid ethyl ester methanesulfonate (MS-222; Pharmaq Ltd. UK) at a room temperature of 22°C for 3-5 min and were then transferred into ice cold frog Ringer solution (75 mM NaCl, 25 mM $NaHCO_3$, 2 mM $CaCl_2$, 2 mM KCl, 0.1 mM $MgCl_2$, and 11 mM glucose, pH 7.4). An *in vitro* preparation was generated by decapitation, removal of the lower jaw, and evisceration. The skin covering the dorsal part of the head including the otic capsule(s) was removed, the cartilaginous skull opened and the choroid plexus detached to allow access of the Ringer solution to the brainstem through the open fourth ventricle. Such *in vitro* preparations maintain fully functional sensory organs (e.g., ears and eyes) as well as all central nervous circuits, and contain intact peripheral motor nerves and effector organs (e.g., extraocular muscles; see Straka and Simmers, 2012). Following surgical procedures, animals were allowed to recover for 2 hours at 17°C.

Visuo-vestibular motion stimulation

Vestibular sensory stimulation was provided by a six-axis motion stimulator (PI H-840, Physik Instrumente, Karlsruhe, Germany) mounted onto a breadboard table (TMC Ametek). Semi-intact tadpole preparations were mechanically secured with insect pins in the center of a Sylgard-lined chamber (Ø 5 cm) and continuously superfused with oxygenated (Carbogen: 95% O_2, 5% CO_2) Ringer solution to maintain a constant temperature of 17.5 ± 1.0°C. For behavioral experiments, horizontal sinusoidal motion stimuli were generated by a custom written software in C++ (Soupiadou et al., 2020) and delivered to the control unit of the motion stimulator. Stimulation paradigms consisted for each animal as follows: bouts of sinusoidal vestibular stimulation were provided through oscillating horizontal rotation performed at 0.5 Hz with a peak velocity of ±31.4°/s for 15 consecutive cycles, followed by an inter-stimulus period of at least 60 seconds. Each animal was provided with the horizontal rotational stimuli first in darkness and then in light, with the light condition corresponding to motion in the presence of a world-stationary visual scene consisting of black and white stripes used for optokinetic stimulation described below. In both darkness and light, stimulation bouts were initiated with motion beginning either in the leftward or rightward directions prior to oscillation at 0.5 Hz (2 second period) between both directions, with leftward initiating bouts occurring first in the order of presented stimulus paradigms before those starting rightward. In all bouts, the first half cycle (1.0 second) of each bout were classified as

unidirectional stimulation for subsequent analyses. Optokinetic stimuli were generated by three digital light processing video projectors (Aiptek V60). Visual patterns were projected onto a cylindrical screen (Ø 8 cm, height 5 cm) positioned around the center of the motion platform, providing a 275° visual field with a refresh rate of 60 Hz. Patterns consisted of equally spaced vertically oriented black and white stripes of 16°/16° spatial size. Optokinetic stimuli were presented at three frequencies, initiating in the following order: 0.1, 0.2 and 0.5 Hz, and occurred in 3 repetitions of 15 consecutive cycles per frequency, interrupted by a stationary period of at least 15 seconds. Vestibular stimulation paradigms for electrophysiological recordings of extraocular motor nerve discharge were performed similarly with consistent sinusoidal parameters, however stimulation was performed only in darkness, and consisted of at least two stimulation bouts of 5-15 cycles each (at 0.5 Hz with a peak velocity of ±31.4°/s as indicated above). Vestibular and optokinetic stimulus profiles were set to be sampled into Spike2 signal recording software (Cambridge Electronic Design, UK) at a rate of 50 Hz.

Eye Motion Tracking

Eye movements, in response to head motion (vestibular) and exclusive visual image motion (optokinetic) stimulation, were recorded by a digital camera (Grasshopper Mono, Point Grey Research Inc., Canada) fitted with a high-pass infrared filter lens and appropriate zoom objective (Optem Zoom 70XL, Qioptiq Photonics GmbH & Co. KG, Germany; M25 × 0.75 + 0.25). The camera was mounted onto the motion simulator platform and centered directly above the head. Video sequences were recorded with a frame capture rate of 30 Hz using the FlyCap2 software (v2.3.2.14.) under illumination with an infrared light source. Positional changes of both eyes over time were quantitatively assessed (Beck et al., 2004; Soupiadou et al., 2020) by fitting an ellipse to each eye independently and computing the deviation of the major axis of each ellipse from the longitudinal image axis in each video frame. Behavioral data were captured and digitized at 30 Hz by a CED 1401 A/D interface and associated Spike2 program (Cambridge Electronic Design Ltd., United Kingdom).

Electrophysiological recordings of extraocular motor nerves

Extracellular multi-unit spike discharge was recorded from the severed ends of the *lateral rectus* (LR) motor nerves close to the innervation site of their respective bilateral eye muscles with glass suction electrodes. Electrodes were made from glass capillaries (Science

Products, GB100-10) with a horizontal puller (P-87, Sutter Instruments Co., USA) and were individually broken to fit to the size of each nerve. Multi-unit spike activity was recorded (EXT 10-2F; npi electronic GmbH, Germany) and digitized at 20 kHz by the CED 1401 A/D interface in Spike2.

Immunohistochemistry

Young tadpoles at stage 46 were anesthetized in 0.5% MS-222 and fixed by immersion in 4% paraformaldehyde (PFA) in phosphate-buffered saline (PBS) for at least 3 hours at 4°C. Following, tadpoles were dissected by removal of the lower jaws and viscera, decapitated at the head/tail junction, and freed from the skin overlying the dorsal head. Subsequently, samples were dehydrated in 70% ethanol for a period of 1 - 12 hours, followed by washing 3 x in 0.1x PBS before immersion for 1 hour at a room temperature of 22°C in 5% normal goat serum with 0.1% Triton X100 to block the immunoreactive epitopes. Samples were then incubated overnight at 36°C with primary antibodies against the hair cell marker Myosin VI (1:400; Proteus Biosciences, 25-6791) and the neuronal marker acetylated-tubulin (1:800; Sigma-Aldrich, T7451). Afterwards, washing and blocking reactions were repeated as above, prior to incubation for 1 hour at room temperature with species-specific secondary antibodies (1:500; Alexa Goat anti-Mouse IgG2b, A-21141; Alexa Goat anti-Rabbit IgG, A32733) and DAPI (Thermo Fisher Scientific; 62248; 1:1000) for 1 hour at room temperature. Following a series of washes (6x) in 0.1x PBS, animals were mounted on microscope slides, coverslipped with Aqua Polymount (Polyscience, 18606) and subsequently imaged on a Leica SP5-2 confocal microscope.

QUANTIFICATION AND STATSTICAL ANALYSIS

Data Analysis

Data analysis of eye motion and extraocular motoneuron spike discharge recordings were conducted post-hoc in Python 3 following export from the Spike2 acquisition software into MATLAB (The Mathworks, Inc.) data files. Tadpoles selected for functional assays were excluded from behavioral and electrophysiological testing if they presented with developmental defects, exhibited aberrant motor behaviors, or did not respond to stimulation paradigms. Post-hoc exclusion was met in behavioral experiments if eye motion data presented with spontaneous nystagmus movements in the absence of visual/vestibular

motion stimulation. Post-hoc exclusion was met in electrophysiological experiments if discharge responses were masked by excessive noise levels. Eye positions for both eyes were re-sampled at 200 Hz and low-pass filtered with a cut-off frequency of 4 Hz (Butterworth; 2nd order). Following, the responses of both eyes were combined, owing to the similar response levels between the left and right eyes in both controls and one-eared animals for vestibular and visual motion stimulation (Figure S2). Individual sinusoidal stimulus cycles, which were determined to contain episodes of stimulus-unrelated eye twitches, corresponding to fast-phases or other spontaneously occurring eye movements, were manually identified and removed from subsequent analysis (Beck et al., 2004). Responses evoked by individual sine waves were averaged across multiple cycles within each animal. The general lack of visuo-vestibular motion stimulus-driven resetting fast phases in *Xenopus* tadpoles at the tested stimulus settings facilitated the calculation of response gains as: the ratio of peak-to-peak eye position to peak-to-peak stimulus position, and corresponding phase metrics as: temporal delay between peak stimulus position and peak eye position calculated as an angular fraction of the motion cycle. Peak amplitudes during unidirectional stimulation were calculated during the first half cycle (1 second) initiating a stimulation bout, corresponding to the peak eye motion response across this period.

Extraocular motor discharge data was filtered with a Butterworth bandpass filter with lower and upper limits of 200 and 600 Hz, respectively, to reduce noise generated by the platform motion. Discharge rates were calculated from spike counts over time following a manual amplitude and spike interval-dependent threshold selection, which was determined for each individual nerve in each animal. Spike counts during each stimulus cycle were used to produce a peri-stimulus time histogram (PSTH; bin size 0.05 seconds) over a single cycle. For PSTH generation, stimulus cycles were selected from sinusoidal bouts with respect to peak directional velocity contralateral to each nerve to better identify the temporal dynamics. Spike rates were then calculated by first dividing spike counts within each histogram bin by the number of cycles and then by bin size. Responses which contained episodes of stimulus-unrelated eye twitches were excluded manually. For visualization of PSTHs in heat maps, responses were either normalized to their respective peak discharge rate per individual animal or as raw rates as indicated. Resting nerve discharge rates were calculated from the average of 20 seconds of spontaneous activity during periods where the head remained

stationery either prior to and/or between stimulus bouts. Discharge rates over a single motion cycle were used to calculate parameters of modulation depth and phase. These values correspond respectively to the difference between the highest and lowest firing rate during a head motion cycle in the former, which quantitatively reports on the extent of sensorimotor transmission onto motoneurons, and the angular fraction of the difference between peak discharge rate and peak stimulus directional velocity in the latter. This latter calculation was also done with respect to opposite velocity motion for each nerve by shifting the angular location of peak firing rate forward by 180° along a 360° scale prior to determining the angular difference as above. Owing to unequal sampling rates in stimulus motion position, stimulus velocity metrics were acquired by re-sampling a single positional cycle to 20 kHz and fitting to a sine wave prior to differentiation.

Statistics

Statistical differences between independent (two-eared control *versus* one-eared animals) data sets were assessed using the Mann-Whitney *U*-test for unpaired nonparametric data, and the Wilcoxon matched-pairs signed-rank test for paired (within experimental groups) nonparametric data in Prism (GraphPad Software 8.4.3, Inc, USA). Nonparametric tests were used owing to the generally small sample size. To aid comparisons of paired data, graphs were visualized with connecting lines between data points with corresponding paired values. Data points shown without a connecting line reflect animals which did not have a corresponding paired measurement. Gain and phase comparisons for tadpoles across multiple frequencies were performed with the nonparametric Friedman test followed by a Dunn's multiple comparisons test. Conjugate movements of both eyes were approximated by plotting pooled average cycle responses of the left and right eye against each other followed by calculation of r^2 and slope values from linear regressions. Circular statistics for electrophysiological data was calculated in Oriana (Version 4.02; Kovach Computing Services) as shown previously (Bacqué-Cazenave et al., 2018). Pooled phase values *re* peak leftward velocity (see above) taken from left and right abducens nerves from individual animals were used to calculate a mean vector, defined by an angular direction in degrees (μ, ± circular standard deviation) and a corresponding length metric approximating clustering strength around the mean (r). Assessment of uniform distribution, indicative of no preferred direction, was calculated by Rayleigh's Uniformity Test (p). Significance of difference between mean

angular directions from pooled left and right abducens nerves in each animal group was tested with Moore's Paired Test. Differences between mean angular directions in control and one-eared animals was assessed with pairwise Watson-Williams F-test. A significance threshold of 0.05 was used for all analyses. Population data is reported as mean ± standard deviation (SD) unless otherwise stated. Statistical tests used and their details can also be found in the relevant figure legends and/or corresponding result sections. n-values used in statistical tests represent number of animals.

1023 **Video S1. Embryonic extirpation of the otic placode, Related to Figure 1.** Representative
1024 procedure of a unilateral removal of the inner ear anlage in a stage 26 *Xenopus laevis* embryo.

1025

References

Agosti, R., Dieringer, N., and Precht, W. (1986). Partial restitution of lesion-induced deficits in the horizontal vestibulo-ocular reflex performance measured from the bilateral abducens motor output in frogs. Exp. Brain Res. 61, 291-302. doi: 10.1007/BF00239519

Angelaki, D. E., and Cullen, K. E. (2008). Vestibular system: the many facets of a multimodal sense. Annu. Rev. Neurosci. 31, 125-150. doi:10.1146/annurev.neuro.31.060407.125555.

Bacqué-Cazenave, J., Courtand, G., Beraneck, M., Lambert, F. M., and Combes, D. (2018). Temporal relationship of ocular and tail segmental movements underlying locomotor-induced gaze stabilization during undulatory swimming in larval *Xenopus*. Front. Neural Circuits. 12, 95. doi:10.3389/fncir.2018.00095.

Beck, J. C., Gilland, E., Tank, D. W., and Baker, R. (2004). Quantifying the ontogeny of optokinetic and vestibuloocular behaviors in Zebrafish, Medaka, and Goldfish. J. Neurophysiol. 92, 3546-3561. doi:10.1152/jn.00311.2004.

Blackiston, D. J., Vien, K., and Levin, M. (2017). Serotonergic stimulation induces nerve growth and promotes visual learning via posterior eye grafts in a vertebrate model of induced sensory plasticity. NPJ Regen. 8, 1-11. doi:10.1038/s41536-017-0012-5.

Blanks, R. H., and Precht, W. (1976). Functional characterization of primary vestibular afferents in the frog. Exp. Brain Res. 25, 369-390. doi:10.1007/BF00241728.

Branoner, F., and Straka, H. (2018). Semicircular canal influences on the developmental tuning of the translational vestibulo-ocular reflex. Front. Neurol. 9, 404. doi: 10.3389/fneur.2018.00404

Chagnaud, B. P., Engelmann, J., Fritzsch, B., Glover, J. C., and Straka, H. (2017). Sensing external and self-motion with hair cells: a comparison of the lateral line and vestibular systems from a developmental and evolutionary perspective. Brain Behav. Evol. 90, 98-116. doi:10.1159/000456646.

Constantine-Paton, M., and Law, M. I. (1978). Eye-specific termination bands in tecta of three-eyed frogs. Science 202, 639-641. doi:10.1126/science.309179.

1055 Curthoys, I. S. (2000). Vestibular compensation and substitution. Curr. Opin. Neurol. 13, 27-
1056 30. doi:10.1097/00019052-200002000-00006.

1057 Darlington, C. L., and Smith, P. F. (2000). Molecular mechanisms of recovery from vestibular
1058 damage in mammals: recent advances. Progr. Neurobiol. 62, 313-325. doi:
1059 10.1016/S0301-0082(00)00002-2.

1060 Dieringer, N. (1995). 'Vestibular compensation': neural plasticity and its relations to functional
1061 recovery after labyrinthine lesions in frogs and other vertebrates. Prog. Neurobiol. 46,
1062 97–129. doi:10.1016/0301-0082(95)80009-W.

1063 Dieringer, N. (2003). Activity-related postlesional vestibular reorganization. Ann. N Y Acad.
1064 Sci. 1004, 50-60.

1065 Dieterich M., and Brandt T. (2015). The bilateral central vestibular system: its pathways,
1066 functions, and disorders. Ann. N Y Acad. Sci. 1343, 10-26. doi:10.1111/nyas.12585.

1067 Dietrich, H., and Straka, H. (2016). Prolonged vestibular stimulation induces homeostatic
1068 plasticity of the vestibulo-ocular reflex in larval Xenopus laevis. Eur. J. Neurosci. 44,
1069 1787-1796. doi:10.1111/ejn.13269.

1070 Dutia, M. B. (2010). Mechanisms of vestibular compensation: recent advances. Curr. Opin.
1071 Otolaryngol. Head Neck Surg., 18, 420-424. doi: 10.1097/MOO.0b013e32833de71f.

1072 Ehrlich, D. E., and Schoppik, D. (2019). A primal role for the vestibular sense in the
1073 development of coordinated locomotion. Elife 8, e45839. doi:10.7554/eLife.45839.

1074 Elliott, K. L., and Fritzsch, B. (2010). Transplantation of *Xenopus laevis* ears reveals the ability
1075 to form afferent and efferent connections with the spinal cord. Int. J. Dev. Biol. 54,
1076 1443-1451. doi:10.1387/ijdb.103061ke.

1077 Elliott, K. L., Fritzsch, B., Yamoah, E. N., and Zine, A. (2022). Age-Related Hearing Loss: Sensory
1078 and Neural Etiology and Their Interdependence. Frontiers in aging neuroscience, 14.
1079 doi:10.3389/fnagi.2022.814528

1080 Elliott, K. L., Houston, D. W., DeCook, R., and Fritzsch, B. (2015a). Ear manipulations reveal a
1081 critical period for survival and dendritic development at the single-cell level in
1082 Mauthner neurons. Dev. Neurobiol. 75, 1339-1351. doi:10.1002/dneu.22287.

1083 Elliott, K. L., Houston, D. W., and Fritzsch, B. (2015b). Sensory afferent segregation in three-
1084 eared frogs resemble the dominance columns observed in three-eyed frogs. Sci. Rep.
1085 5, 1-7. doi:10.1038/srep08338.

1086 Fetter, M. (2016). Acute unilateral loss of vestibular function. Handb. Clin. Neurol. 137, 219-
1087 229. doi:10.1016/b978-0-444-63437-5.00015-7.

1088 Fritzsch, B. (1990). Experimental reorganization in the alar plate of the clawed toad, *Xenopus*
1089 *laevis*. I. Quantitative and qualitative effects of embryonic otocyst extirpation. Dev.
1090 Brain Res. 51, 113-122. doi:10.1016/0165-3806(90)90263-X.

1091 Fritzsch, B., and Straka, H. (2014). Evolution of vertebrate mechanosensory hair cells and inner
1092 ears: toward identifying stimuli that select mutation driven altered morphologies. J.
1093 Comp. Physiol. A 200, 5-18. doi:10.1007/s00359-013-0865-z.

1094 Gensberger, K. D., Kaufmann, A. K., Dietrich, H., Branoner, F., Banchi, R., Chagnaud, B. P., and
1095 Straka, H. (2016). Galvanic vestibular stimulation: cellular substrates and response
1096 patterns of neurons in the vestibulo-ocular network. J. Neurosci. 36, 9097-9110.
1097 doi:10.1523/JNEUROSCI.4239-15.2016.

1098 Glasauer, S., and Knorr, A. G. (2020). Physical nature of vestibular stimuli. In The Senses: A
1099 Comprehensive Reference, Vol. 6, B. Fritzsch and H. Straka, eds (Elsevier), pp. 6-11.
1100 doi:10.1016/B978-0-12-809324-5.23909-6.

1101 Goodman, L. A., and Model, P. G. (1988). Superinnervation enhances the dendritic branching
1102 pattern of the Mauthner cell in the developing axolotl. J. Neurosci. 8, 776-791.
1103 doi:10.1523/JNEUROSCI.08-03-00776.1988.

1104 Gordy, C., Straka, H., Houston, D. W., Fritzsch, B., and Elliott, K. L. (2018). Transplantation of
1105 ears provides insights into inner ear afferent pathfinding properties. Dev. Neurobiol.
1106 78, 1064-1080. doi:10.1002/dneu.22629.

1107 Goto, F., Straka, H., and Dieringer, N. (2001). Postlesional vestibular reorganization in frogs:
1108 evidence for a basic reaction pattern after nerve injury. J. Neurophysiol. 85, 2643-
1109 2646. doi:10.1152/jn.2001.85.6.2643.

1110 Holler, S., and Straka, H. (2001). Plane-specific brainstem commissural inhibition in frog
1111 second-order semicircular canal neurons. Exp. Brain Res. 137, 190-196. doi:
1112 10.1007/s002210000670.

1113 Horn, A. K., and Straka, H. (2021). Functional organization of extraocular motoneurons and
1114 eye muscles. Annu. Rev. Vis. Sci. 7, 793-825. doi:10.1146/annurev-vision-100119-
1115 125043.

1116 Horn, E. R. (2003). The development of gravity sensory systems during periods of altered
1117 gravity dependent sensory input. Adv. Space Biol. Med. 9, 133-171.
1118 doi:10.1016/s1569-2574(03)09006-3.

1119 Honrubia, V., Hoffman, L. F., Sitko, S., and Schwartz, I. R. (1989). Anatomic and physiological
1120 correlates in bullfrog vestibular nerve. J. Neurophysiol. 61, 688-701.
1121 doi:10.1152/jn.1989.61.4.688.

1122 Honrubia, V., Sitko, S., Kimm, J., Betts, W., and Schwartz, I. (1981). Physiological and
1123 anatomical characteristics of primary vestibular afferent neurons in the bullfrog. Int.
1124 J. Neurosci. 15, 197-206. doi:10.3109/00207458108985857.

1125 Knorr, A. G., Gravot, C. M., Glasauer, S., and Straka, H. (2021). Image motion with color
1126 contrast suffices to elicit an optokinetic reflex in *Xenopus laevis* tadpoles. Sci. Rep. 11,
1127 1-12. doi:10.1038/s41598-021-87835-2.

1128 Kopecky, B., Decook, R., and Fritzsch, B. (2012). Mutational ataxia resulting from abnormal
1129 vestibular acquisition and processing is partially compensated for. Behav. Neurosci.
1130 126, 301-313. doi:10.1037/a0026896.

1131 Korn, H., and Faber, D. S. (2005). The Mauthner cell half a century later: a neurobiological
1132 model for decision-making? Neuron 47, 13-28. doi:10.1016/j.neuron.2005.05.019.

1133 Lambert, F. M., Beck, J. C., Baker, R., and Straka, H. (2008). Semicircular canal size determines
1134 the developmental onset of angular vestibuloocular reflexes in larval *Xenopus*. J.
1135 Neurosci. 28, 8086-8095. doi:10.1523/JNEUROSCI.1288-08.2008.

1136 Lambert, F. M., Malinvaud, D., Gratacap, M., Straka, H., and Vidal, P.-P. (2013). Restricted
1137 neural plasticity in vestibulospinal pathways after unilateral labyrinthectomy as the

origin for scoliotic deformations. J. Neurosci. 33, 6845-6856. doi:10.1523/jneurosci.4842-12.2013.

Lambert, F., and Straka, H. (2012). The frog vestibular system as a model for lesion-induced plasticity: basic neural principles and implications for posture control. Front. Neurol. 3, 42. doi:10.3389/fneur.2012.00042.

Levi-Montalcini, R. (1949). The development of the acoustico-vestibular centres in the chick embryo in the absence of the afferent root fibers and of descending fiber tracts. J. Comp. Neurol. 91, 209-241. doi:10.1002/cne.900910204.

Lilian, S. J., Seal, H. E., Popratiloff, A., Hirsch, J. C., and Peusner, K. D. (2019). A new model for congenital vestibular disorders. J. Assoc. Res. Otolaryngol. 20, 133-149. doi:10.1007/s10162-018-00705-z.

Liu, Z., Kimura, Y., Higashijima, S.-i., Hildebrand, D. G. C., Morgan, J. L., and Bagnall, M. W. (2020). Central vestibular tuning arises from patterned convergence of otolith afferents. Neuron 108, 748-762. doi:10.1016/j.neuron.2020.08.019.

Llinás, R., and Walton, K. (1979). Vestibular compensation: a distributed property of the central nervous system. In Integration in the Nervous System, H. Asanuma and V. J. Wilson, eds (Igaku Shoin), pp. 145–166.

Macova, I., Pysanenko, K., Chumak, T., Dvorakova, M., Bohuslavova, R., Syka, J., Fritzsch, B., and Pavlinkova, G. (2019). Neurod1 is essential for the primary tonotopic organization and related auditory information processing in the midbrain. J. Neurosci. 39, 984-1004. doi:10.1523/JNEUROSCI.2557-18.2018.

Malinvaud, D., Vassias, I., Reichenberger, I., Rössert, C., and Straka, H. (2010). Functional organization of vestibular commissural connections in frog. J. Neurosci. 30, 3310-3325. doi:10.1523/JNEUROSCI.5318-09.2010.

Markham, C. H., Yagi, T., and Curthoys, I. S. (1977). The contribution of the contralateral labyrinth to second order vestibular neuronal activity in the cat. Brain Res. 138, 99-109. doi: 10.1016/0006-8993(77)90786-7.

Masseck, O. A., and Hoffmann, K. P. (2009). Comparative neurobiology of the optokinetic reflex. Ann. N Y Acad. Sci. 1164, 430-439. doi:10.1111/j.1749-6632.2009.03854.x.

McNamara, S., Wlizla, M., and Horb, M. E. (2018). Husbandry, general care, and transportation of *Xenopus laevis* and *Xenopus tropicalis*. Meth. Mol. Biol. 1865, 1-17. doi:10.1007/978-1-4939-8784-9_1.

Nieuwkoop, P.D., and Faber, J. (1994). Normal Table of Xenopus laevis (Daudin): A Systematical and Chronological Survey of the Development from the Fertilized Egg Till the End of Metamorphosis. (Garland Publisher).

Özugur, S., Chávez, M.N., Sanchez-Gonzalez, R., Kunz, L., Nickelsen, J., Straka, H. (2022). Transcardial injection and vascular distribution of microalgae in Xenopus laevis as means to supply the brain with photosynthetic oxygen. STAR Protoc. 3, 1-20. doi: 10.1016/j.xpro.2022.101250.

Patten, S. A., Jacobs-McDaniels, N. L., Zaouter, C., Drapeau, P., Albertson, R. C., and Moldovan, F. (2012). Role of Chd7 in zebrafish: a model for CHARGE syndrome. PLoS One, 7, e31650. doi:10.1371/journal.pone.0031650.

Paulin, M.G., and Hoffman, L.F. (2019). Models of vestibular semicircular canal afferent neuron firing activity. J. Neurophysiol. 122, 2548-2567. 10.1152/jn.00087.2019. doi:10.1152/jn.00087.2019.

Peusner, K. D., and Morest, D. K. (1977). Neurogenesis in the nucleus vestibularis tangentialis of the chick embryo in the absence of the primary afferent fibers. Neuroscience 2, 253-270. doi:10.1016/0306-4522(77)90092-6.

Ramdya, P., and Engert, F. (2008). Emergence of binocular functional properties in a monocular neural circuit. Nat. Neurosci. 11, 1083-1090. doi:10.1038/nn.2166.

Rayer, B., Cagol, E., and Horn, E. (1983). Compensation of vestibular-induced deficits in relation to the development of the southern clawed toad, *Xenopus laevis Daudin*. J. Comp. Physiol. A 151, 487-498. doi:10.1007/BF00605466.

Rayer, B., and Horn, E. (1986). The development of the static vestibulo-ocular reflex in the southern clawed toad, *Xenopus laevis*. J. Comp. Physiol. A 159, 887-895. doi: 10.1007/BF00603742.

1194 Roberts, R., Elsner, J., and Bagnall, M. W. (2017). Delayed otolith development does not
1195 impair vestibular circuit formation in zebrafish. J. Assoc. Res. Otolaryngol. 18, 415-425.
1196 doi:10.1007/s10162-017-0617-9.

1197 Roeser, T., and Baier, H. (2003). Visuomotor behaviors in larval zebrafish after GFP-guided
1198 laser ablation of the optic tectum. J. Neurosci. 23, 3726-3734. doi:
1199 10.1523/jneurosci.23-09-03726.2003.

1200 Rohregger, M., and Dieringer, N. (2003). Postlesional vestibular reorganization improves the
1201 gain but impairs the spatial tuning of the maculo-ocular reflex in frogs. J.
1202 Neurophysiol., 90, 3736-3749. doi:10.1152/jn.00561.2003.

1203 Ruthazer, E. S., Akerman, C. J., and Cline, H. T. (2003). Control of axon branch dynamics by
1204 correlated activity in vivo. Science 301, 66-70. doi:10.1126/science.1082545.

1205 Shao, M., Hirsch, J. C., and Peusner, K. D. (2012). Plasticity of spontaneous excitatory and
1206 inhibitory synaptic activity in morphologically defined vestibular nuclei neurons during
1207 early vestibular compensation. J. Neurophysiol. 107, 29-41. doi:
1208 10.1152/jn.00406.2011.

1209 Smith, P.F. (2022). Hearing loss versus vestibular loss as contributors to cognitive dysfunction.
1210 J. Neurol. 269, 87-99. doi:10.1007/s00415-020-10343-2.

1211 Soupiadou, P., Gordy, C., Forsthofer, M., Sanchez-Gonzalez, R., and Straka, H. (2020). Acute
1212 consequences of a unilateral VIIIth nerve transection on vestibulo-ocular and
1213 optokinetic reflexes in *Xenopus laevis* tadpoles. J. Neurol. 267 (Suppl 1): S62-S75.
1214 doi:10.1007/s00415-020-10205-x.

1215 Straka, H. (2020). Functional organization of vestibular commissural pathways. in The Senses:
1216 A Comprehensive Reference, Vol. 6, B. Fritzsch and H. Straka, eds (Elsevier), pp. 371–
1217 388. doi:10.1016/b978-0-12-809324-5.23907-2.

1218 Straka, H., and Dieringer, N. (1993). Electrophysiological and pharmacological
1219 characterization of vestibular inputs to identified frog abducens motoneurons and
1220 internuclear neurons in vitro. Eur. J. Neurosci. 5, 251-260. doi: 10.1111/j.1460-
1221 9568.1993.tb00491.x.

1222 Straka, H., and Dieringer, N. (2004). Basic organization principles of the VOR: lessons from
1223 frogs. Prog. Neurobiol. 73, 259-309. doi:10.1016/j.pneurobio.2004.05.003.

1224 Straka, H., and Gordy, C. (2020). The Vestibular system: The "LeathermanTM" among sensory
1225 systems. In The Senses: A Comprehensive Reference, Vol. 6, B. Fritzsch and H. Straka,
1226 eds (Elsevier), pp. 708–720. doi:10.1016/b978-0-12-809324-5.24179-5.

1227 Straka, H., and Simmers, J. (2012). Xenopus laevis: An ideal experimental model for studying
1228 the developmental dynamics of neural network assembly and sensory-motor
1229 computations. Dev. Neurobiol., 72, 649-663. doi: 10.1002/dneu.20965.

1230 Straka, H., Vibert, N., Vidal, P. P., Moore, L. E., and Dutia, M. B. (2005). Intrinsic membrane
1231 properties of vertebrate vestibular neurons: function, development and plasticity.
1232 Progr. Neurobiol., 76, 349-392. doi:10.1016/j.pneurobio.2005.10.002.

1233 Strupp, M., and Brandt, T. (2013). Peripheral vestibular disorders. Curr. Opin. Neurol. 26, 81-
1234 89. doi:10.1097/WCO.0b013e32835c5fd4.

1235 Szentágothai, J. (1950). The elementary vestibulo-ocular reflex arc. J. Neurophysiol., 13, 395-
1236 407. doi: 10.1152/jn.1950.13.6.395.

1237 Vidal, P. P., Waele, C. D., Vibert, N., and Mühlethaler, M. (1998). Vestibular compensation
1238 revisited. Otolaryngol. Head Neck Surg. 119, 34-42. doi: 10.1016/S0194-
1239 5998(98)70171-8.

1240 Wagner, H., Pappe, I., and Nalbach, H. O. (2022). Optocollic responses in adult barn owls (Tyto
1241 furcata). J. Comp. Physiol. A 208, 239-251. doi:10.1007/s00359-021-01524-z.

1242 Wiesel, T. N., and Hubel, D. H. (1963). Single-cell responses in striate cortex of kittens deprived
1243 of vision in one eye. J. Neurophysiol. 26, 1003-1017. doi: 10.1152/jn.1963.26.6.1003.

1244 Yagi, T., and Markham, C. H. (1984). Neural correlates of compensation after
1245 hemilabyrinthectomy. Exp. Neurol. 84, 98-108. doi:10.1016/0014-4886(84)90008-6.

1246 Zarei, K., Elliott, K. L., Zarei, S., Fritzsch, B., and Buchholz, J. H. (2017). A method for detailed
1247 movement pattern analysis of tadpole startle response. J. Exp. Anal. Behav. 108, 113-
1248 124. doi: https://doi.org/10.1002/jeab.263.

1249 Zhao, X., Jones, S.M., Yamoah, E.N., and Lundberg, Y.W. (2008). Otoconin-90 deletion leads
1250 to imbalance but normal hearing: A comparison with other otoconia mutants.
1251 Neuroscience 153, 289-299. doi:10.1016/j.neuroscience.2008.01.055.

1252

HIGHLIGHTS

- *Xenopus laevis* embryos with an extirpated otic placode develop with one inner ear
- One-eared tadpoles can execute horizontal gaze-stabilizing eye movements
- Off-direction evoked vestibular-ocular responses are present and remarkably robust
- Developmental plasticity of gaze stabilization is unaided by visuo-motor signaling

KEY RESOURCES TABLE

REAGENT or RESOURCE	SOURCE	IDENTIFIER
Antibodies		
Myosin VI antibody	Proteus Biosciences	Cat#25-6791
Acetylated-tubulin antibody	Sigma-Aldrich	Cat#T7451
Goat anti-Mouse IgG2b Secondary Antibody, Alexa Fluor™ 488	Invitrogen	Cat#A-21141
Goat anti-Rabbit IgG Secondary Antibody, Alexa Fluor™ Plus 647	Invitrogen	Cat#A32733
Chemicals, Peptides, and Recombinant Proteins		
DAPI	Thermo Scientific	Cat#62248
Aqua-Poly/Mount	Polysciences	Cat#18606
3-aminobenzoic acid ethyl estermethanesulfonate (MS-222)	Pharmaq Ltd. UK	N/A
NaCl	Carl Roth, Germany	Cat#3957.3
KCl	Carl Roth, Germany	Cat#P017.1
$NaHCO_3$	Carl Roth, Germany	Cat#8551.1
HEPES	Carl Roth, Germany	Cat#9105.4
$CaCl_2$	Carl Roth, Germany	Cat#A119.1
$MgCl_2$	Carl Roth, Germany	Cat#2189.1
Glucose monohydrate	Carl Roth, Germany	Cat#6780.1
Benzocaine	Sigma-Aldrich	Cat#E1501
L-Cysteine	Sigma-Aldrich	Cat#168149
Paraformaldehyde	Carl Roth, Germany	Cat# 0335.3
Deposited Data		
Original analysis code	This paper	Gordy, Clayton; Straka, Hans (2022), "Gordy and Straka [ISCIENCE-D-22-02377R1]", Mendeley Data, V1, doi: 10.17632/wb3xfw75zz.1
Experimental Models: Organisms/Strains		
Model organism: *Xenopus laevis*	Institutional breeding facility, Faculty of Biology, Ludwig-Maximilians-UniversityMunich	N/A
Software and Algorithms		
Figure assembly: Affinity Designer 1.10.5.1342	Serif	N/A
ZEN Imaging software (blue edition) 3.4.91	Carl Zeiss Microscopy GmbH	N/A

Data acquisition: Spike 2 version 7.04	Cambridge Electric Design Limited (CED), UK	N/A
Data analysis: Python 3.7.6	Anaconda Inc. (https://www.anaconda.com/products/distribution)	N/A
Data visualization and statistics: GraphPad Prism 8.4.3	Graphpad Software, LLC, Inc, USA	N/A
Circular statistics: Oriana 4.02	Kovach Computing Services	N/A
Leica Application Suite X	Leica Microsystems CMS GmbH	N/A
Other		
Tungsten Needles for ear extirpation	Fine Science Tools	Cat#10130-05
H-840 6-Axis Hexapod	Physik Instrumente GmbH & Co. KG	Cat#PI H-840
A/D Interface CED 1401	Cambridge Electric Design Limited (CED), UK	Micro3

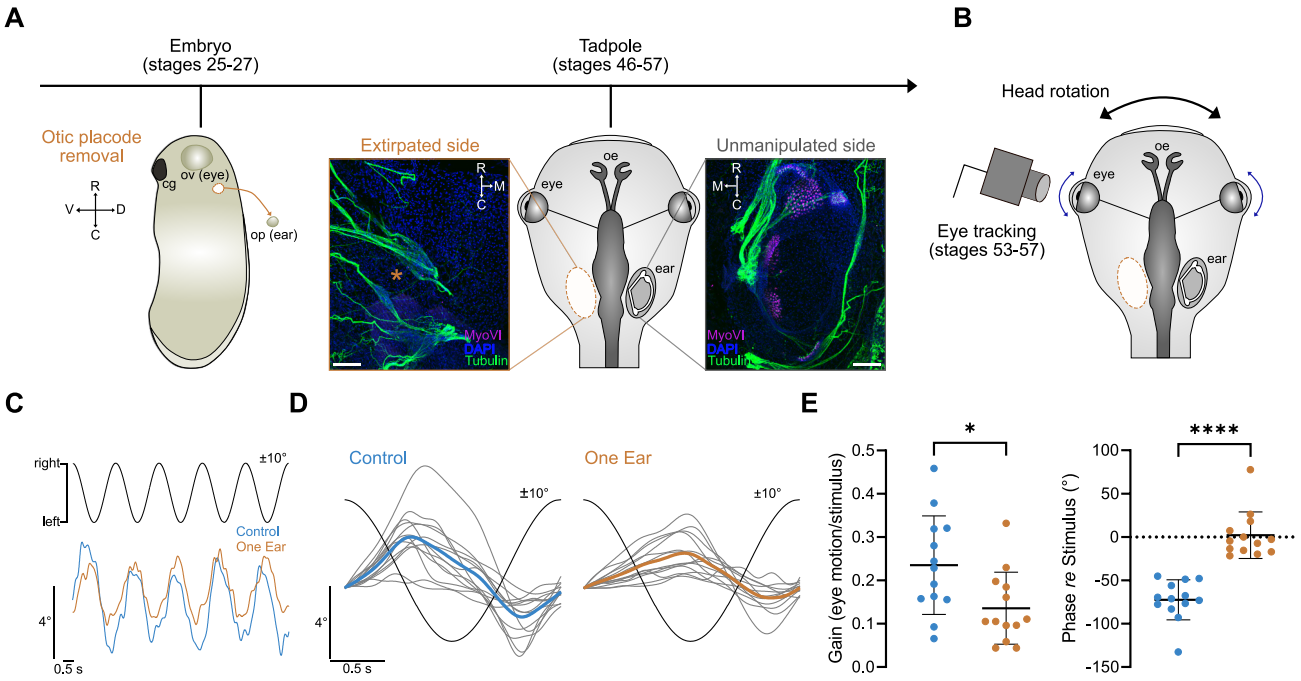

Figure 1. Vestibulo-ocular reflex performance in one-eared *Xenopus laevis* tadpoles. (A) Schematic depicting the experimental procedure and developmental timeline following unilateral embryonic removal of the otic placode (stages 25-27; lateral view) followed by rearing of the one-eared embryos to tadpole stages (stage 46-57; dorsal view); note the lack of the left inner ear (orange *) and corresponding neurosensory and accessory otic structures, illustrated by images from the left (Extirpated side) and right side (Unmanipulated side) of a stage 46 larva, with whole-mount antibody stainings against neurons (acetylated tubulin, green) and hair cells (myosin-VI, red) in the otic region. **(B)** Schematic of a semi-intact preparation used for functional profiling of control and one-eared tadpoles during horizontal sinusoidal rotation coupled with live motion-tracking of both eyes. **(C)** Representative example of oppositely-directed, compensatory eye oscillations (lower traces) during five cycles of horizontal sinusoidal head rotation (±10°, peak velocity ±31.4°/s) at 0.5 Hz (upper trace) in an unmanipulated control (blue) and a one-eared (orange) tadpole. Responses are averages of both eyes, respectively. (**D**) Averaged responses over a single horizontal rotation cycle of controls (n = 13, individual gray traces; from 6-40 cycles) and one-eared animals (n = 13, individual gray traces; from 12-66 cycles); blue and orange traces represent the population mean response over one motion cycle (black trace) for the respective group of animals (**D**); averaged responses were used to individually calculate the gain (left in **E**) and phase value *re* stimulus position (right in **E**). Significance levels are indicated by asterisks: * $p \leq 0.05$, **** $p \leq 0.0001$ (Mann-Whitney *U*-test). R, rostral; C, caudal; V, ventral; D, dorsal; M, medial; op, otic placode; ov, optic vesicle; cg, cement gland; oe, olfactory epithelium. Immunohistochemical stainings in **A** were counterstained with the nuclear marker DAPI. Scale bars in **A** are 100 µm. Data in **E** are represented as mean ± SD. See also Figures S1 and S2.

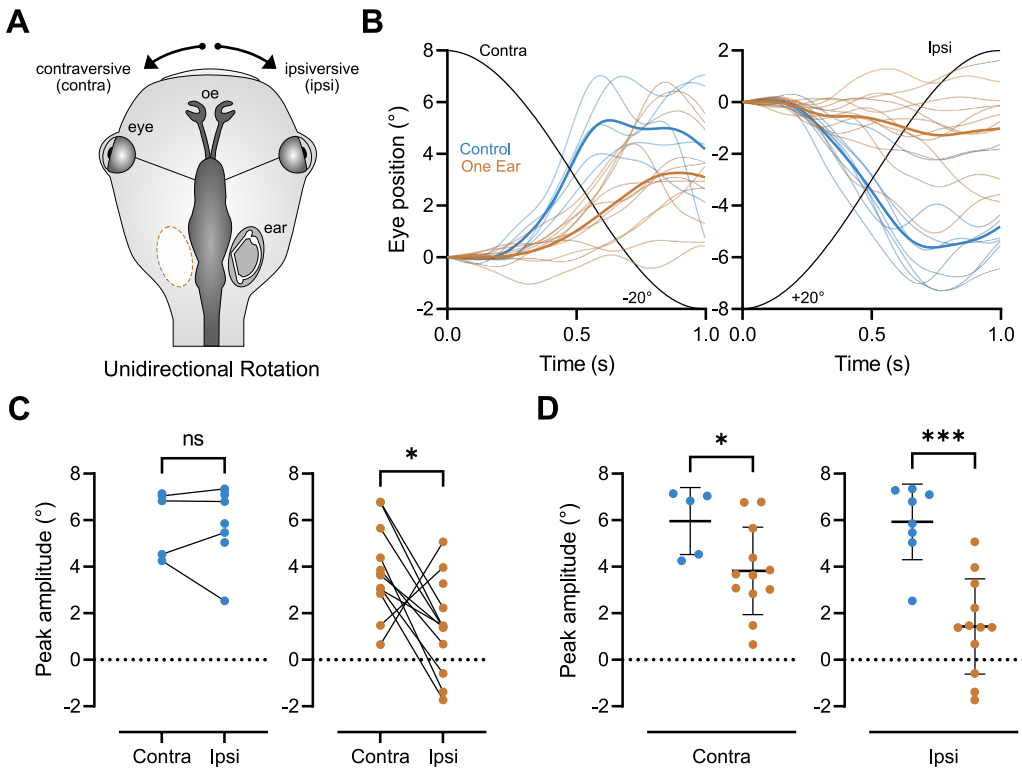

Figure 2. Directional sensitivities of singular ears during horizontal aVOR. (A) Schematic depicting unidirectional horizontal angular rotation of control and one-eared animals; rotations were performed either toward (ipsiversive, ipsi) or away from the residual singular ear (contraversive, contra) without oscillation between the two directions. **(B)** Eye movements of individual control (n = 9; thin blue traces) and one-eared (n = 13; thin orange traces) animals during unidirectional rotation, averaged over 1-6 half-cycles, respectively, that were obtained from the onset of sinusoidal stimulus events shown in Figure 1D; thick blue and orange traces represent respective population means. **(C, D)** Comparison of peak response amplitudes during contraversive and ipsiversive positional excursions within **(C)** controls (blue) and one-eared animals (orange), respectively, and for the two directions between controls and one-eared animals **(D)**. Data points in **C** reflect all animals which had a VOR half-cycle response; lines connecting data points indicate animals that had a response in both directions which was used for paired statistical comparison. Dotted lines in **C** and **D** represent the reversal lines of eye motion direction; note that peak amplitudes during ipsiversive rotations were inverted to facilitate a comparison between the responses for the two stimulus directions; significance levels are indicated by asterisks: * $p \leq 0.05$ (Wilcoxon signed-rank test) *** $p \leq 0.001$ (Mann-Whitney U-test). Data in **D** are represented as mean ± SD.

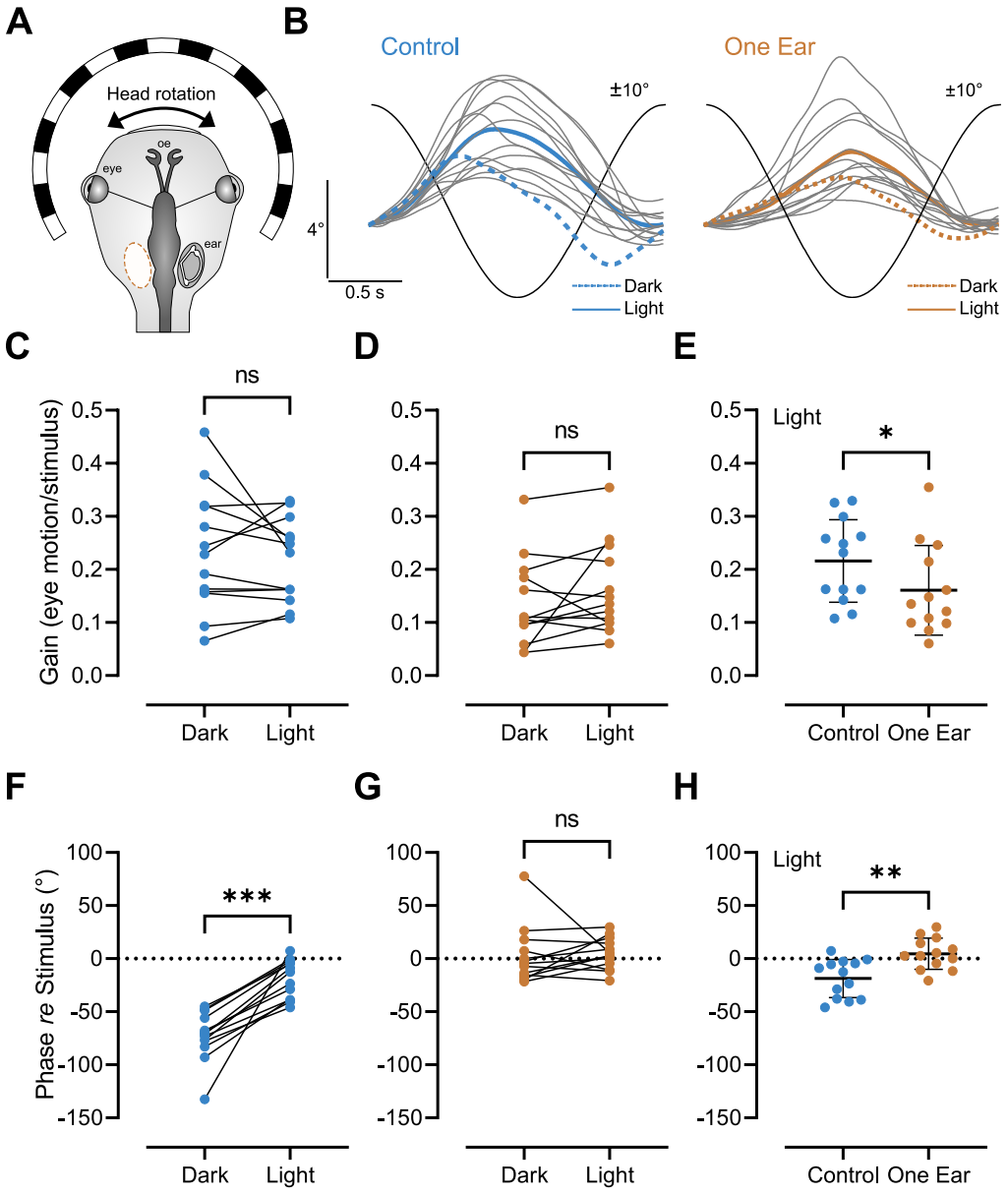

Figure 3. Visuo-vestibular reflex plasticity. (A) Schematic depicting the experimental condition that consisted of a horizontal sinusoidal head rotation in the presence of a world-stationary, illuminated black and white-striped visual pattern (Light). **(B)** Averaged responses over a single head motion cycle in light (gray traces from 6-77 cycles, respectively) and population means (solid-colored traces) in controls (n = 13) and one-eared animals (n = 13); dotted blue and orange traces depict population means obtained from head rotations in darkness (Dark) illustrated in Figure 1D; black sine waves indicate the stimulus position. (**C-H**) Gain **(C-E)** and phase *re* stimulus position **(F-H)** calculated from averaged responses over a single motion cycle in Dark and Light conditions of controls **(C, F)** and one-eared animals **(D, G)**; respective values for the light condition in the two experimental groups are compared in **E, F**. Significance levels are indicated by asterisks: * $p \leq 0.05$, ** $p \leq 0.01$, *** $p \leq 0.001$ (Wilcoxon signed-rank test in **F**, Mann-Whitney U-test in **E, H**). Horizontal dotted lines in **F-H** at 0° indicate phase alignment with the stimulus. Data in **E, H** are represented as mean ± SD. See also Figures S3 and S2.

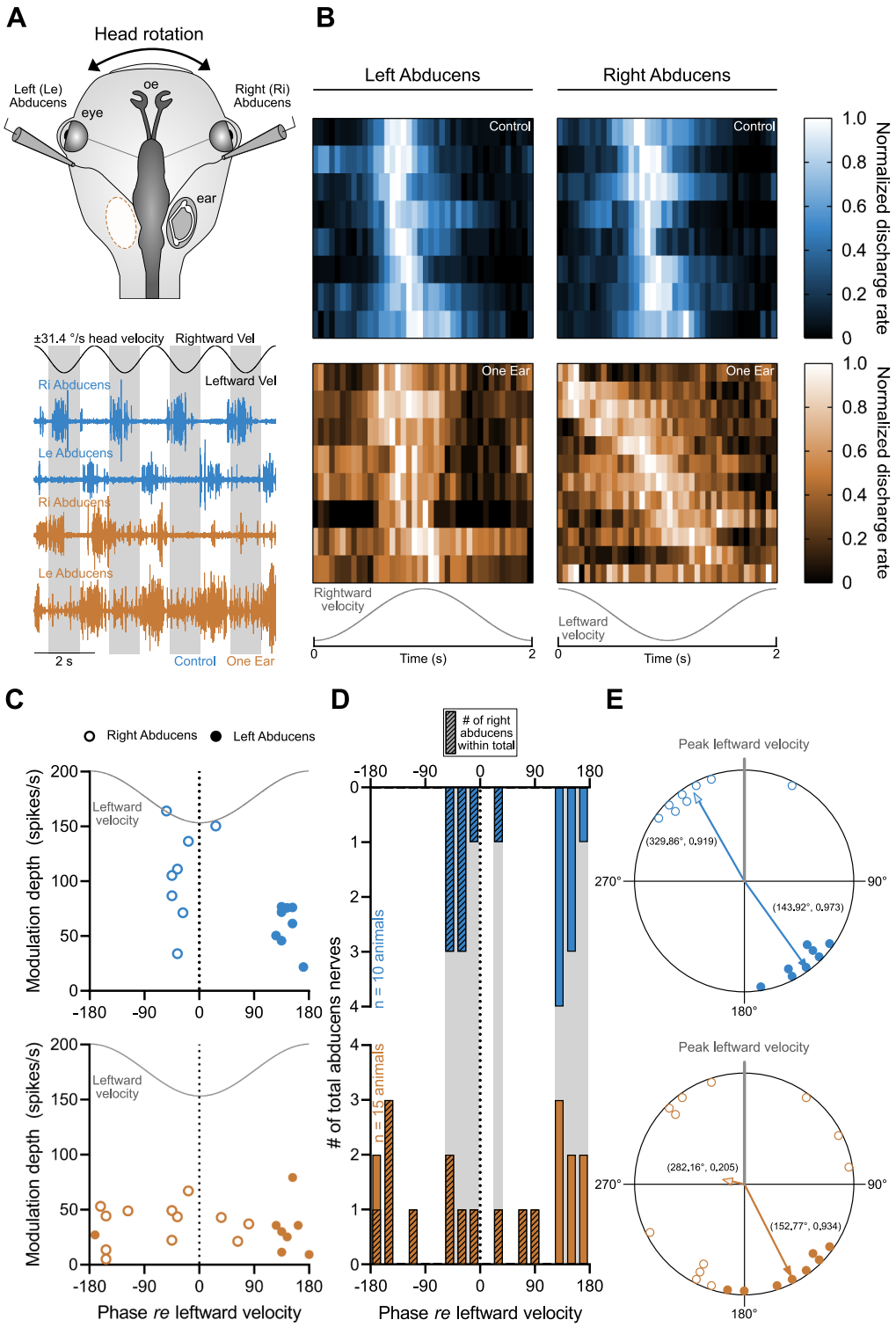

Figure 4. Discharge dynamics of abducens motoneurons. (A) Recording sites of abducens motor nerves during sinusoidal head rotation (±10° positional excursion, peak velocity of ±31.4°/s, 0.5 Hz) in darkness (upper panel); multi-unit recordings of left (Le) and right (Ri) abducens nerves (lower panel) during head rotation, corresponding to peak leftward (lower peaks) and rightward (upper peaks) velocities (Vel) of ±31.4°/s (black sinusoidal velocity trace) in two-eared control (blue) and one-eared (orange) animals; shaded regions indicate periods of leftward head motion velocity. **(B)** Heat maps visualizing peri-stimulus time histograms of normalized discharge rates over a single cycle (from 12-28 and 14-54 cycles in *n* = 10 and *n* = 15 controls and one-eared animals, respectively) during directionally specific head motion velocity (gray sinusoidal traces); horizontal heat map rows represent individual animals. **(C)** Modulation depth as a function of phase *re* peak leftward stimulus velocity for left and right abducens nerves obtained from **B**, depicting the timing of the peak discharge within the cycle; closed and open circles indicate left and right abducens nerves, respectively; note the discrete clustering of left and right abducens nerve activity in controls (upper, blue) compared to one-eared animals (lower, orange). **(D)** Frequency distribution of response phases for right and left abducens nerves, obtained from the data depicted in **C**; bar amplitudes denote the total number of nerves *per* temporal allocation; hashed bars indicate the number of right abducens nerves within the total number *per* temporal allocation. **(E)** Polar plots depicting phase deviations *re* peak leftward velocity (gray vertical line indicates phase of peak leftward velocity during stimulus motion) from **C-D** represented across 360°; arrows indicate the calculated mean vector for pooled left (filled arrowhead) and right (shaded arrowhead) abducens nerve discharge profiles in controls (upper) and one-eared (lower) animals; values next to vector arrows are respective metrics of mean angular direction and vector length (*μ, r*). See also Figure S4.

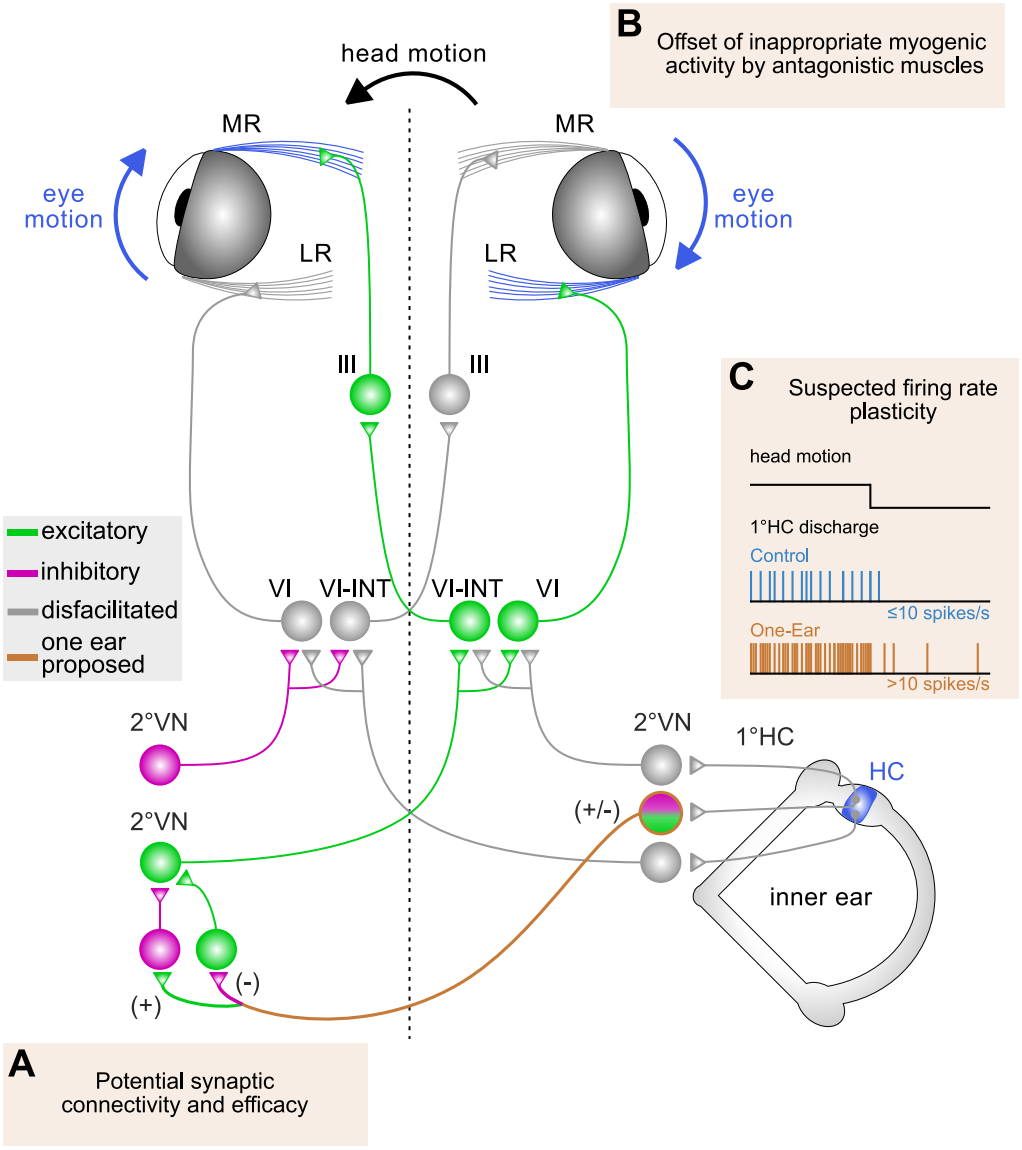

Figure 5. Putative plasticity mechanisms in embryonically generated one-eared tadpoles. Schematic depicting the speculated horizontal aVOR circuitry during a leftward heard turn in a one-eared animal and proposed plasticity mechanisms (orange boxes, orange cells and axons). Leftward head rotation (black arrow) elicits oppositely directed horizontal eye movements (blue arrows) through muscle contractions of the lateral and medial recti (LR, MR, blue) driven from off-direction hair cell and afferent activity modulation of the singular horizontal semicircular canal (HC, blue). Disfacilitation (gray colored cells and axons) of second-order vestibular target neurons (2°VN) and HC afferent fibers (1°HC) produces eye movements which are delayed relative to control conditions, potentially due to **(A)** augmented crossed excitatory (green, +) or inhibitory (magenta, -) commissural gating of contralateral 2°VN target neuronal activity (orange line). Upstream of driving force computations, temporally inappropriate firing dynamics of abducens (VI) motoneurons are potentially offset **(B)** by the activity of antagonistic muscles, i.e., the ipsilateral MR muscle. Increased levels of afferent discharge rates **(C**; see inset**)** may contribute to the encoding ability for off-directional head movements. III, oculomotor nerve; VI-INT, abducens internuclear neurons. Blue, eye motion direction and corresponding horizontal endorgan; green, excitatory connections; magenta, inhibitory connections; gray, disfacilitation; orange, proposed sites and mechanisms of plasticity in one-eared animals.

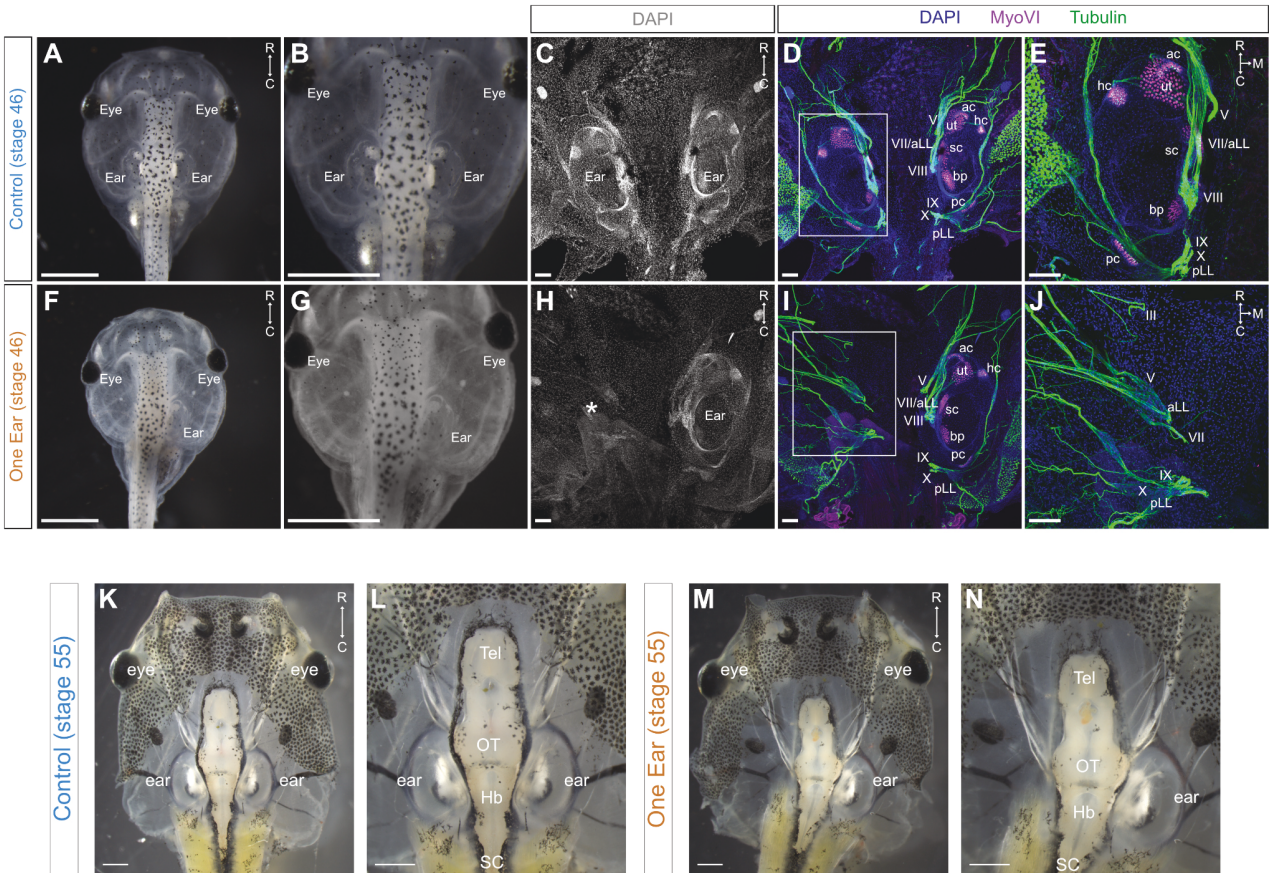

Figure S1. Phenotype validation of one-eared tadpoles, Related to Figure 1. (A-J) Representative unmanipulated control **(A-B)** and left-side otic placode-extirpated **(F-G)** stage 46 tadpoles, specifically depicting the two bilateral and the one unilateral inner ear(s), respectively; whole-mount immunohistochemical labeling of control **(C-E)** and one-eared **(H-J)** tadpoles stained for the nuclear marker DAPI (gray; **C, H**) revealed the structure of the inner ears **(C, H** right**)** and the cranial otic region in the absence of an ear **(**white * in **H)**; neuronal marker, acetylated tubulin (green), and hair cell/muscle marker, myosin-VI (red), identifies **(D-E**, **I-J**) hair cell clusters and corresponding VIIIth nerve innervations, indicative of inner ear endorgans **(E)**, which are entirely absent from the corresponding region on the left side of one-eared animals **(J)**; **C** and **H** are single color channels of **D, I**, respectively; white boxes in **D, I** approximate the region of higher magnification shown in **E, J**. **(K-N)** Representative stage 55 control **(K-L)** and one-eared **(M-N)** animals depicting the absence of an otic capsule and inner ear endorgans on the left side; **L** and **N** are higher magnifications of images in **K**, **M**; Scale bars are 1 mm in **A-B** and **F-G**, 100 µm in **C-E** and **H-J** and 2 mm in **K-N**. R, rostral; C, caudal; M, medial; ac, hc, pc, anterior, posterior, horizontal semicircular canal cristae; ut, sc, utricular, saccular macula; bp, basilar papilla; aLL, pLL, anterior, posterior lateral line nerve; III, oculomotor nerve; V, trigeminal nerve; VII, `facial´ nerve; VIII; stato-acoustic nerve; IX, glossopharyngeal nerve; X, vagus nerve; Tel, telencephalon; OT, optic tectum; Hb, hindbrain; SC, spinal cord.

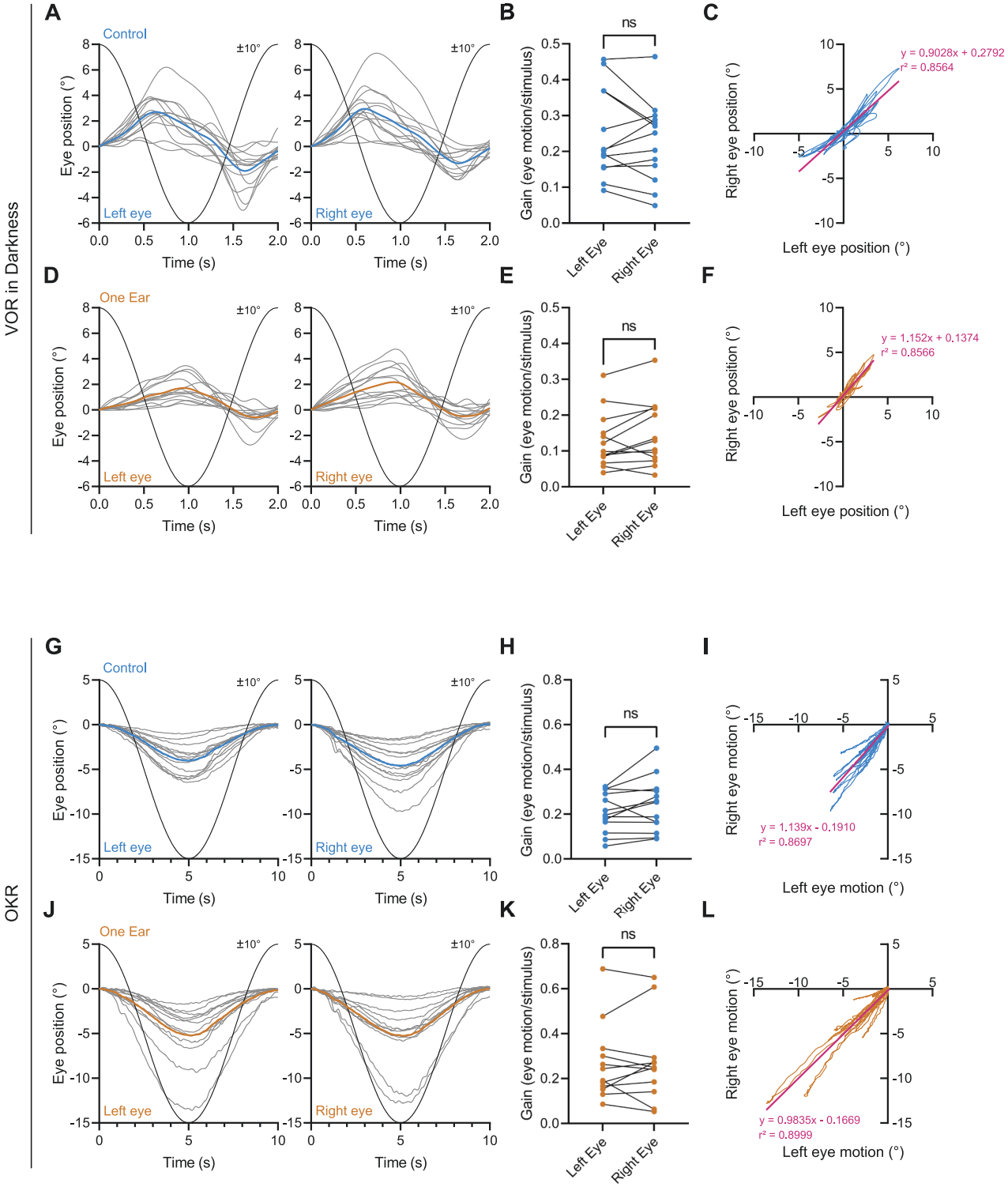

Figure S2. Conjugate eye movements during horizontal aVOR and OKR, Related to Figure 1. (A, D) Averaged responses over a single cycle of horizontal angular rotation in darkness (Darkness; ±10°, peak velocity ±31.4°/s, 0.5 Hz) for left and right eyes in controls (**A**; *n* = 13, gray traces; from 6-40 cycles) and animals which embryonically had their left ear removed (**D**; one-eared animals; *n* = 13, gray traces; from 12-66 cycles); blue and orange traces depict the population mean response over one motion cycle (black trace); **(B, E)** Gain comparisons between left and right eyes for controls **(B)** and one-eared animals **(E)**. **(C, F)** Conjugation correlation plots of pooled average cycle responses from data in **A, D** for controls (**C**) and one-eared animals (**F**), respectively. **(G, J)** Averaged responses during sinusoidal motion of vertically-stiped black and white pattern (OKR; ±10°, peak velocity ±6.28°/s, 0.1 Hz) with corresponding gain calculations **(H, K)** and conjugation correlation plots **(I, L)**; averaged OKR responses (gray traces in **G, J**) from 21-45 cycles in *n* = 13 and *n* = 12 controls and one-eared animals, respectively. Non-Significance designations indicated by *ns* (Wilcoxon signed-rank test in **B, E, H, K**). Best-fit line in **C, F, I, L** and computed equation from linear regressions are depicted in magenta, respectively.

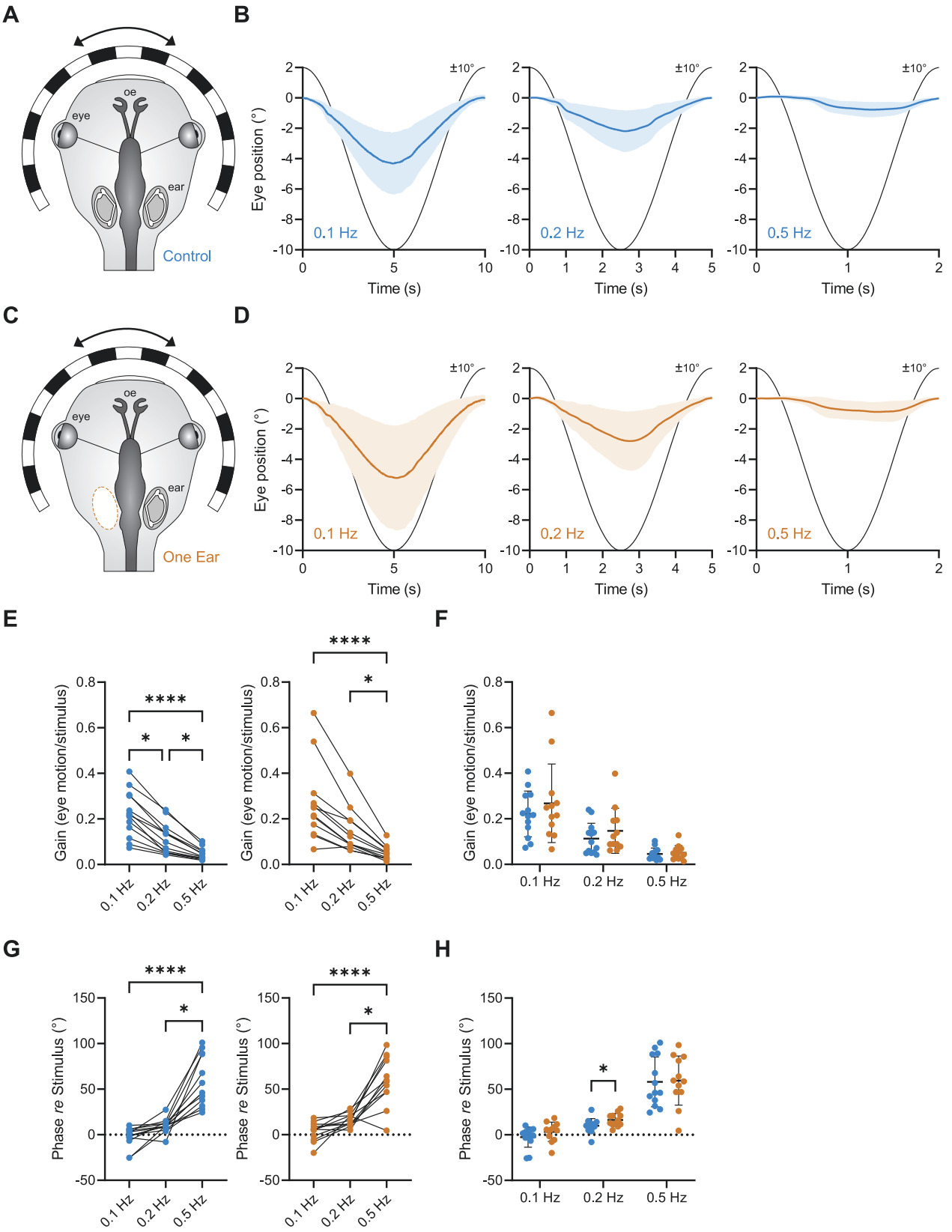

Figure S3. Optokinetic reflex performance in one-eared tadpoles, Related to Figure 3. (A, C) Schemes of the experimental approach depicting sinusoidal horizontal rotation of a patterned black- and white-striped visual scene (±10° movement excursion) while the head is maintained stationary in controls (**A**) and one-eared animals (**C**). **(B, D)** Averaged responses over a single cycle of visual image motion at 0.1 Hz (left, peak velocity: 6.28°/s), 0.2 Hz (middle, peak velocity: 12.57°/s) and 0.5 Hz (right, peak velocity: 31.4°/s) for controls (**B**; *n* = 13, calculated from 21-45 cycles) and one-eared animals (**D**; *n* = 12, calculated from 26-45 cycles). Blue- and orange-colored lines and shading indicate population means ±SD. Solid black lines indicate the visual scene motion stimulus; individually calculated gain **(E-F)** and phase *re* visual stimulus position **(G-H)** for all three stimulus frequencies of each experimental group (**E, G**; left, control; right, one-eared animals) and comparison between experimental groups (**F, H**). Significance levels are indicated by asterisks: * $p \leq 0.05$, *** $p \leq 0.001$, **** $p \leq 0.0001$ (Friedman nonparametric test for matched pairs with Dunn's multiple comparison test in **E, G**, Mann-Whitney *U*-test in **F, H**). Horizontal dotted lines in **G-H** at 0° indicate phase alignment of the stimulus. Data in F, H are represented as mean ± SD.

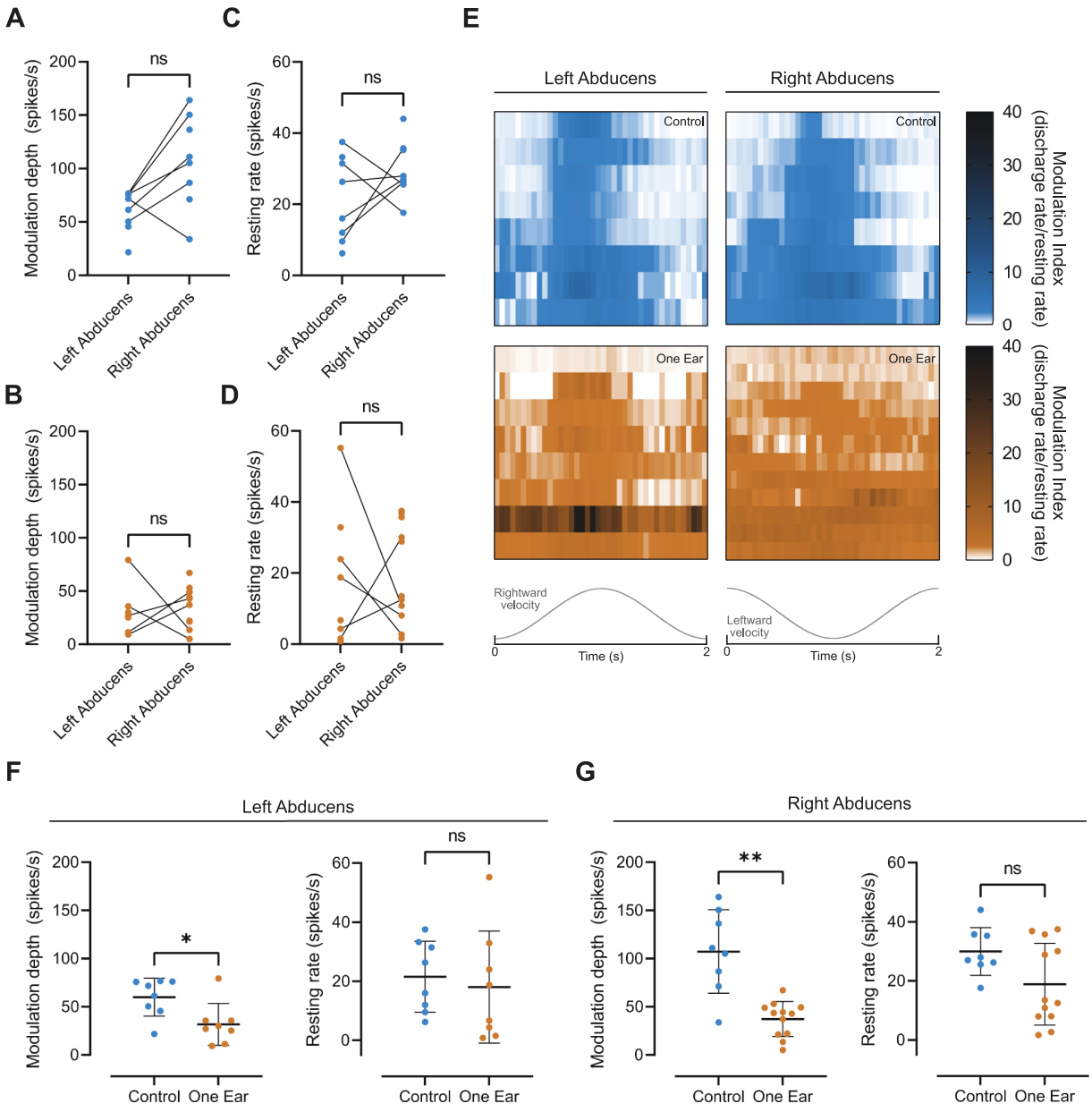

Figure S4. Multi-unit discharge dynamics in abducens motor nerves, Related to Figure 4. (A-D) Comparison of the discharge modulation depth (**A-B**) during sinusoidal head rotation in darkness (0.5 Hz, peak velocity: ±31.4°/s; see peri-stimulus time histograms in Figure 4) and spontaneous firing rate in the absence of head motion (stationary) in darkness (**C-D**) of the left and right abducens motor nerve in controls (**A, C**) and one-eared animals (**B, D**). Data points in (**A-D**) reflect each animal with recorded discharge activity in abducens nerves; lines connecting data points indicate animals which expressed a discharge activity for both their left and right abducens nerves, which was used for paired statistical comparison. **(E)** Heat maps of peri-stimulus time histograms depicting the individual activity modulation index (discharge rate/resting rate) during rotation for individual controls (blue) and one-eared (orange) animals (from 12-28 and 14-54 cycles in n = 10 and n = 15 controls and one-eared animals, respectively; see Figure 4); horizontal rows represent data from individual animals; comparisons of modulation depth and resting rate obtained from controls and one-eared animals for left **(F)** and right **(G)** abducens nerves. Significance levels are indicated by asterisks: * $p \leq 0.05$, ** $p \leq 0.01$ (Mann-Whitney U-test); *ns*, no significance (Wilcoxon signed-rank test in **A-D**; Mann-Whitney U-test in **F-G**). Data in F, G are represented as mean ± SD.

CHAPTER III:

CAUDAL TRANSPLANTATION OF EARS PROVIDES INSIGHTS INTO INNER EAR AFFERENT PATHFINDING PROPERTIES

Clayton Gordy[1, 2, 3], Hans Straka[2], Douglas W. Houston[1], Bernd Fritzsch[1] and Karen L. Elliott[1*]

[1]Department of Biology, University of Iowa, Iowa City, Iowa

[2]Department Biology II, Ludwig-Maximilians-University Munich, Planegg, Germany

[3]Graduate School of Systemic Neurosciences, Ludwig-Maximilians-University Munich, Planegg, Germany

*Correspondence: karen-elliott@uiowa.edu (K. L. E.)

Contribution of authors:

K.L.E. and B.F. conceived the goals and aims. C.G., B.F., and K.L.E designed paradigms and collected data for the embryonic, dye tracing, and immunohistochemical experiments. C.G. and H.S. designed paradigms and collected data for the electrophysiological studies. K.L.E designed paradigms and collected data for behavior testing. C.G. and K.L.E analyzed embryonic, dye tracing, and immunohistochemical data. K.L.E analyzed behavior data. C.G. and H.S. analyzed electrophysiological data. C.G., H.S., D.W.H., B.F. and K.L.E. interpreted all the data. C.G., K.L.E, and H.S. created the figures. C.G. wrote the original draft of the manuscript. All authors reviewed and edited the manuscript. Resources were provided by B.F., D.W.H, and H.S. Supervision provided by K.L.E, B.F. and H.S. Project administration provided by K.L.E. Funding acquired by K.L.E, B.F., and H.S.

My contributions to this publication in detail:

K.L.E., B.F., and I designed experimental paradigms and generated three-eared frogs and performed quantification of animals from this technique. I created Table 1. Along with K.L.E and B.F., I performed immunohistochemical and dye tracing experiments on three-eared animals and analyzed the data. With K.L.E and B.F., I created Figure 1, and Figure 2, Figure 3, Figure 6, and Figure 7. K.L.E performed 3D reconstruction of data panels in Figure 3B'' 3D'' and 2A. I generated three-eared animals for rearing and subsequent physiological testing. Along with H.S., I performed electrophysiological experiments,

relevant analysis, and along with H.S. created Figure 5. I wrote the initial version of the manuscript and edited all versions of it.

The following manuscript has been published in *Developmental Neurobiology*. Permission for reuse in this dissertation granted to C.G. by John Wiley and Sons under the Copyright Clearance Center RightsLink license number: 5333521139999.

For online access, please refer to the following: https://doi.org/10.1002/dneu.22629

Caudal Transplantation of Ears Provides Insights into Inner Ear Afferent Pathfinding Properties

Clayton Gordy[1,2,3], Hans Straka[2], Douglas W. Houston[1], Bernd Fritzsch[1], Karen L. Elliott[1],

[1] Department of Biology, University of Iowa, Iowa City, Iowa
[2] Department Biology II, Ludwig-Maximilians-University Munich, Planegg, Germany
[3] Graduate School of Systemic Neurosciences, Ludwig-Maximilians-University Munich, Planegg, Germany

Received 21 November 2018; revised 15 June 2018; accepted 3 July 2018

ABSTRACT: Numerous tissue transplantations have demonstrated that otocysts can develop into normal ears in any location in all vertebrates tested thus far, though the pattern of innervation of these transplanted ears has largely been understudied. Here, expanding on previous findings that transplanted ears demonstrate capability of local brainstem innervation and can also be innervated themselves by efferents, we show that inner ear afferents grow toward the spinal cord mostly along existing afferent and efferent fibers and preferentially enter the dorsal spinal cord. Once in the dorsal funiculus of the spinal cord, they can grow toward the hindbrain and can diverge into vestibular nuclei. Inner ear afferents can also project along lateral line afferents. Likewise, lateral line afferents can navigate along inner ear afferents to reach hair cells in the ear. In addition, transplanted ears near the heart show growth of inner ear afferents along epibranchial placode-derived vagus afferents. Our data indicate that inner ear afferents can navigate in foreign locations, likely devoid of any local ear-specific guidance cues, along existing nerves, possibly using the nerve-associated Schwann cells as substrate to grow along. However, within the spinal cord and hindbrain, inner ear afferents can navigate to vestibular targets, likely using gradients of diffusible factors that define the dorso-ventral axis to guide them. Finally, afferents of transplanted ears functionally connect to native hindbrain vestibular circuitry, indicated by eliciting a startle behavior response, and providing excitatory input to specific sets of extraocular motoneurons. © 2018 Wiley Periodicals, Inc. Develop Neurobiol 78: 1064–1080, 2018

Key words: **Xenopus laevis, ear, transplantation, afferent innervation**

INTRODUCTION

Afferents that develop from the inner ear establish precise connections between hair cells and central nuclei (Mao *et al.*, 2014; Fritzsch *et al.*, 2015; Goodrich, 2016). Within the central nervous system (CNS), these neurons terminate in anatomic and modality specific regions in the hindbrain: vestibular ganglion afferents reach vestibular nuclei and auditory afferents reach auditory nuclei (Maklad and Fritzsch, 2003; Fritzsch *et al.*, 2005a). To ensure the discrete processing of auditory and vestibular mechanical stimuli, growing afferents must correctly navigate within the CNS to reach selectively their target nuclei. The central navigational properties of developing inner ear afferents is incompletely understood (Maklad and Fritzsch, 2003), but can be partially derailed in mutants of certain transcription factors such as Neurod1 (Jahan *et*

Correspondence to: Karen L. Elliott (karen-elliott@uiowa.edu).
Contract grant sponsor: NIH R03; contract grant number: DC015333.
Contract grant sponsor: NASA Iowa Space Grant Consortium; contract grant number: NNX10AK63H.
Contract grant sponsor: German Science Foundation; contract grant number: CRC 870, RTG 2175.

Published online 15 September 2018 in Wiley Online Library (wileyonlinelibrary.com).
DOI 10.1002/dneu.22629

al., 2010) and several others (Goodrich, 2016). In addition, afferent projections are established in a spatiotemporal progressing manner (Fritzsch *et al*., 2005a; Zecca *et al*., 2015) likely using Wnt gradients to navigate (Fritzsch and Elliott, 2017; Yang *et al*., 2017) and can do so even if target nuclei are molecularly ablated (Elliott *et al*., 2017).

In contrast to the ear, the molecular basis of the retinotopic projection of the eye is better understood in terms of Eph and ephrin gradients (Kullander and Klein, 2002; Liu *et al*., 2016) to set up the chemoaffinity-mediated retinotopic map (Sperry, 1963). In addition, retinal afferents may be attracted to the midbrain as revealed by transplantation of a developing eye onto the spinal cord in *Xenopus laevis* embryos that showed fibers to reach the midbrain (Giorgi and Van der Loos, 1978). More recent work in transplanting an eye to the trunk demonstrated the ability of afferents to provide successful sensory input into the CNS, but did not reveal how afferent information reached the CNS (Blackiston *et al*., 2017). Collectively, this suggests the possibility of long range cues acting in retinal ganglion cell afferent pathfinding. Additional work on olfactory transplantations suggest that olfactory afferents can navigate and interact with any nearby part of the brain, including the hindbrain but not the spinal cord (Stout and Graziadei, 1980; Klein and Graziadei, 1983; Magrassi and Graziadei, 1985).

As with eyes (Giorgi and Van der Loos, 1978; Blackiston *et al*., 2017) and the olfactory system, transplantation of developing ears has long been used to demonstrate normal development in foreign positions (Yntema, 1955; Jacobson, 1963; Fritzsch *et al*., 1998a; Swanson *et al*., 1990). How ears compare to such transplantations with respect to homing to their targets has only been assessed for the hindbrain and midbrain: Transplantation of a third ear rostral to the native ear demonstrated afferent capability to enter the hindbrain and reach the vestibular nucleus (Elliott *et al*., 2015a; Elliott *et al*., 2015b) somewhat similar to retinal afferents ability to reach the midbrain in three eyed frogs (Constantine-Paton and Law, 1978) or eyes transplanted to the spinal cord (Giorgi and Van der Loos, 1978). In contrast, ear afferents reaching the midbrain could not navigate in any discernible patterns (Elliott *et al*., 2013), suggesting that hindbrain navigation is guided by molecular cues that are not present in the midbrain, clearly distinct from retinal afferents coming from the spinal cord or the midbrain to extend under certain circumstances to the hindbrain (Manns and Fritzsch, 1991).

Previous work transplanting an ear caudally to the trunk has shown that inner ear afferents can enter the spinal cord (Elliott and Fritzsch, 2010); however, it remains unclear if ear transplantations near the spinal cord can successfully integrate sensory information as has been shown for eyes (Blackiston *et al*., 2017). Given the above outlined ability of inner ear afferents to navigate to and within the hindbrain from altered entry positions, we investigate here if inner ear afferents transplanted to the trunk can reach the vestibular nucleus in the hindbrain either through the spinal cord or through fasciculation along other peripheral nerves. We assess this capability through transplantation of ears at different developmental time points to various caudal locations on the animal, specifically both along the spinal cord or near the heart. Our data reveal that inner ear afferents can navigate either on their own or along peripheral nerves to reach the spinal cord and, if they grow along existing central fibers to the hindbrain, can reach vestibular nuclei once they reach the hindbrain. Physiological and behavioral data support that transplanted ear afferents establish meaningful connections with brainstem neurons to guide escape responses and provide excitatory input to specific sets of extraocular motoneurons.

MATERIAL AND METHODS

Animals

Xenopus laevis embryos of either sex were obtained through induced ovulation by injection of human chorionic gonadotropin, followed with fertilization by sperm suspension in 0.3X Marc's Modified Ringer's Solution (MMR, diluted from 10X stock; 1M NaCl, 18mM KCl, 20 mM $CaCl_2$, 10 mM $MgCl_2$, 150 mM HEPES, pH 7.6–7.8). The jelly coat was removed with 2% cysteine in 0.1X MMR. Embryos were incubated in 0.1X MMR until having reached the desired stage for manipulation (see below), and until desired stages for tracing, behavior, and physiological experiments (described below) as described by Nieuwkoop and Faber (1994).

Ear Transplantations

All surgical manipulations were performed in 1.0X MMR at room temperature. Animals were anesthetized with 0.02% Benzocaine (Crook and Whiteman, 2006) prior to and during all manipulations. Otic placodes and otic vesicles from donor embryos were removed and transplanted to recipient hosts at stage 25–27 and 28–36, respectively. Removed placodes or

vesicles were grafted adjacent to the spinal cord in place of a removed somite on one side of the embryo. Additionally, otic vesicles from stage 32–36 donor embryos were transplanted to the ventral heart region, in the vicinity of the vagus nerve trajectory. Embryos were kept in 1.0X MMR after surgery for 15–30 min to allow healing. Animals were then transferred into 0.1X MMR. Animals to be used for behavioral and physiological assays were processed as below. Animals used only for immunohistochemistry and dye labeling were allowed to grow until stage 46, and subsequently anesthetized in 0.02% Benzocaine and fixed by immersion in either 4% paraformaldehyde (PFA), when used for immunohistochemistry or dextran tracing, or in 10% PFA when used for lipophilic dye tracing (see below). Successful development of the ear was confirmed at stage 46 based on the presence or absence of an ear in the region of transplantation and by the presence of otoconia. Ear development was further assessed using anti-Myo6 antibody to label hair cells and anti-tubulin antibody to label nerve fibers (see immunochemical analysis below). Only animals with fully formed transplanted ears, as indicated by otoconia in position above sensory epithelia, were used for further analysis.

C-start Startle Assay and Analysis

For startle response testing, donor ears were transplanted to the trunk at stage 25–27 as described above, but at a slightly more rostral position along the spinal cord. At stage 40–42, the native two ears were removed. For controls, both native ears were removed at stage 40 from animals that did not have an ear transplanted to the trunk. This time point of stage 40–42 was selected since nearly all Mauthner cells, the cells in the hindbrain that drive the c-start startle response from inner ear stimulation (Korn and Faber, 2005), survive with ear removal at stage 40 (Elliott *et al.*, 2015a). Animals were allowed to grow until stage 46. Tadpoles were placed individually in a 50 mm diameter Petri dish containing 0.1X MMR for the startle assay. Startle responses were elicited from dropping a 3.5 kg standardized object from a 12 cm height onto a sturdy lab bench, adjacent to the Petri dish containing the tadpole. Subsequent C-start startle response behavior was video recorded in slow-motion from a fixed distance directly above the Petri dish. Each of 13 control animals and 15 animals with transplanted ears were subjected to four trials and the presence or absence of a response, as well as the initial direction of the response, if present, was documented. Significance of direction of turn (Zarei *et al.*, 2017) was calculated using a Chi-Square analysis with Microsoft Excel. Following behavioral analysis, animals were anesthetized in 0.02% Benzocaine and fixed by immersion 10% PFA as described above and were then processed for lipophilic dye labeling.

Electrophysiology

Following ear transplantations at stage 28–29 (see above), *Xenopus laevis* tadpoles of either sex were obtained from the in-house animal breeding facility at the Biocenter-Martinsried at the Biomedical Center of the Ludwig-Maximilians-University Munich. Tadpoles were kept in tanks filled with 17–18°C non-chlorinated water at a 12/12 light/dark cycle. A total of 5 animals at developmental stages 54–57 were used for recordings of neuronal activity. Experiments were performed *in vitro* on isolated, semi-intact preparations and comply with the National Institute of Health publication entitled "Principles of animal care," No. 86-23, revised 1985. Permission for these experiments was granted by the governmental institution at the Regierung von Oberbayern/Government of Upper Bavaria (55.2-1-54-2532-14-2016; 55.2-1-54-2532.0-24-2017).

For all experiments, tadpoles were anesthetized in 0.05% 3-aminobenzoic acid ethyl ester (MS-222; Pharmaq Ltd., United Kingdom) in frog Ringer (75 mM NaCl, 25 mM NaHCO3, 2 mM CaCl2, 2 mM KCl, 0.5 mM MgCl2, and 11 mM glucose, pH 7.4) and decapitated ~10 segments below the transplanted ear. The skin above the head was removed, the skull and rostral vertebrae opened, and the forebrain disconnected. This surgical procedure preserved all inner ear organs, the CNS and the extraocular motor innervation and allowed natural and galvanic stimulation of vestibular endorgans and recording of extraocular motor responses (Gensberger *et al.*, 2016).

Extracellular multi-unit spike discharge from severed extraocular motor nerves was recorded with glass suction electrodes from the cut end of the extraocular motor nerves as described earlier (Lambert *et al.*, 2008). Glass microelectrodes were made with a horizontal puller (P-87, Sutter Instruments Co., USA) and were individually adjusted at the tip to fit the diameter of the respective target nerves. Extraocular motor nerve activity was recorded (EXT 10-2F; npi electronic GmbH, Germany), digitized at 10–20 kHz (CED 1401, Cambridge Electronic Design Ltd., United Kingdom), and stored on a computer for offline analysis. For the analysis, responses obtained during 20–120 repetitions of sinusoidal turntable

oscillations or sinusoidally modulated current stimuli (see below) were averaged to obtain the mean response ± standard error of the mean (SEM) over a single cycle.

Motion and Galvanic Vestibular Stimulation

The recording chamber with the semi-intact *Xenopus* preparations was mounted on a computer-controlled, motorized two-axis turntable (ACT-1002, Acutronic USA Inc., Switzerland) with the preparation centered in the horizontal and vertical rotation axes to provide optimal activation of semicircular canal organs (Gensberger *et al.*, 2016; Lambert *et al.*, 2008). Motion stimuli consisted of sinusoidal rotations across frequencies that ranged from 0.2 to 1 Hz (peak velocities: ±12–60°/s). Sinusoidally modulated galvanic currents were applied by stimulus electrodes that consisted of two Teflon-coated silver wires (diameter: 0.76 mm; AG 25-T, Science Products GmbH, Germany), placed on the outer surface of the native otic capsules or the transplanted third ear. The two stimulus electrodes were cut at the tip, chlorinated to minimize polarization, and separately attached to a micromanipulator, to enable precise positioning under visual guidance. For most experiments, electrodes were placed bilaterally in close proximity of the visible cupulae of a specific bilateral coplanar semicircular canal pair (e.g., left posterior and right anterior semicircular canal). To stimulate the third ear, one electrode was placed on the outer surface of the visible otic capsule and the second electrode at a distance of ~10 mm from the first in the Ringer solution of the recording chamber. Sine waves for the galvanic vestibular stimulation (GVS) were produced with a linear stimulus isolator (WPI A395, World Precision Instruments Inc., USA), triggered by the analog output from an analog/digital converter (CED 1401). The galvanic currents were applied to the two electrodes in phase-opposition (Gensberger *et al.*, 2016) and consisted of sinusoidally modulated currents at frequencies of 0.2–1 Hz and magnitudes of ±50–200 μA for GVS of the native semicircular canals and of ±200–500 μA for GVS of the third ear.

Lipophilic Dye Labeling

Axonal projections from transplanted ears were labeled using NeuroVue lipophilic dyes (Fritzsch *et al.*, 2016a). NeuroVue™ Maroon, NeuroVue™ Red, and NeuroVue™ Jade (Polysciences, Inc.) dye-soaked filter paper pieces were cut to fit and were placed inside transplanted ears. Care was taken to place the dye on regions of sensory epithelia as determined by location of otoconia. Dye placed in transplanted ears labels inner ear afferent axons through backfilling of dendritic processes, terminating on hair cells, into ganglion cell bodies. Dye was also placed into the spinal cord following transection, either rostral or caudal, to the adjacently transplanted ear to fill inner ear afferent axonal processes within the spinal cord as they project within it and into the hindbrain. To determine lateral line innervation of an ear transplanted adjacent to the spinal cord, dye was placed into the posterior lateral line ganglia caudal and adjacent to the native ear, filling lateral line afferents to neuromast (lateral line) organs along the trunk of the animal. In the same animals, dye was placed into the spinal cord to label afferents entering the CNS. Native ear afferent projections into the hindbrain were labeled with dye inserted into each native ear. Following dye insertions, animals were kept in 0.4% PFA and incubated at 60°C or 36°C to permit diffusion. Dye placed in the spinal cord or posterior lateral line ganglia were incubated at 60°C for 60 hr. Dye placed into transplanted ears near the spinal cord were incubated for 18 hr at 36° to determine the spinal cord entry point or for 60 hr at 60° to assess hindbrain innervation. Ears transplanted to the heart region were labeled with dye insertions either into the transplanted ear or into the vagus nerve directly and were incubated for 3 days at 60°. Native ear dye placements were incubated for 18 hr at 36°. Following diffusion, the brain and spinal cord was dissected out and the specimens were mounted in glycerol for imaging on a TCS SP5 Multi-photon confocal microscope using excitation emission settings specific for the different lipophilic dyes used (Tonniges *et al.*, 2010).

Dextran amine Labeling

Dextran amine dye injections into ears transplanted adjacent to the spinal cord were used to evaluate inner ear afferent projection in the CNS. Entry points of inner ear afferents into the spinal cord as well as their projections into the hindbrain were evaluated using Texas red, tetramethylrhodamine, Alexa Fluor 647, and Alexa Fluor 488 dye (Molecular Probes). A small incision was made into the transplanted ear of anesthetized animals (0.02% Benzocaine) and a recrystallized drop of the labeling dye on a tungsten needle was inserted (Fritzsch, 1993). Care was taken to fill the ear entirely with the dye. Animals were washed in 0.1X MMR three times in succession and kept in a dish containing 0.1X MMR for 2–3 hr. Afterwards, the embryos were reanesthetized in 0.02% Benzocaine

Table 1 Success of Transplantations

Location of transplantation	Development with otoconia	Development without otoconia	No ear development
Adjacent to Spinal Cord Early[a] (117)	98	11	8
Adjacent to Spinal Cord Late[b] (45)	36	1	8
Adjacent to Heart (25)	21	0	4

[a]Early is defined as transplantations occurring during stages 25–27.

[b]Late is defined as transplantations occurring during stages 28–36.

and fixed in 4.0% PFA. After fixation, the brain and spinal cord was dissected out and the specimens were mounted in glycerol for imaging on a TCS SP5 Multi-photon confocal microscope using appropriate excitation/emission filter settings. Dextran amine tracing served to verify lipophilic dye tracing as it is not known to diffuse transcellularly.

Immunohistochemistry

To determine presence of sensory epithelia in transplanted ears, as well as local innervation of the ear and its surroundings, PFA fixed stage 46 animals were dissected to remove the lower jaw and skin and were dehydrated in 70% ethanol overnight. Animals were washed in 1X PBS three times for 10 min each before being blocked in 5.0% normal goat serum (NGS) with 0.1% Triton-X 100 for 1 hr. Following a brief wash in 1X PBS, primary antibodies against neuronal marker acetylated tubulin (1:800, Cell Signaling Technology) and against hair cell marker Myosin VI (1:400, Proteus Biosciences) were incubated with the embryos overnight at 36°C. Animals were washed thrice for 10 min and blocked in 5.0% NGS + 0.1% Triton X 100 for 1 hr prior to incubation with species-specific secondary antibodies (1:500, Alexa) along with nuclei marker Hoechst 33342 (Invitrogen) overnight. Animals were washed in 1X PBS six times for 15 min each and mounted in glycerol for imaging on a TCS SP5 Multi-photon confocal microscope. In animals where neuromast organs and lateral line afferents were of interest, the skin was kept on during the procedures listed above.

Three-Dimensional Reconstructions

Three-dimensional reconstructions were made from confocal images as previously described (Kopecky *et al*., 2012). Briefly, ears transplanted to the trunk that were immunostained for tubulin and MyoVI as described above were mounted with the trunk lateral side up on a microscope slide in glycerol. In addition, brains from animals in which the transplanted and native ears or the spinal cord and native ears were labeled with lipophilic dye as described above were removed, hemisected along the midline and mounted lateral side up on a slide in glycerol. Confocal z-series images were taken using a Leica TCS SP5 confocal microscope. Z-series stacks were loaded into Amira software (Version 5.4) for manual segmentation, as previously described (Kopecky *et al*., 2012). Fibers were individually traced and reconstructed as previously described for dendrites (Elliott *et al*., 2015a)

RESULTS

Success and Development of Transplantations

Success of transplantations was assessed based on the presence and degree of development of an ear with otoconia at the place of transplantation (Table 1, Fig. 1A-C). While most transplants were successful in that they developed ears with otoconia, in some instances ears developed without otoconia or formed otoconia-free vesicles (Table 1), consistent with data from similar placements adjacent to the spinal cord to assess the ability of spinal motor neurons to become efferents to inner ear hair cells (Elliott and Fritzsch, 2010). Similar rates of success were found for ears transplanted adjacent to the spinal cord and ventrally near the heart; 83 and 84 percent of animals had transplanted ears with otoconia, respectively (Table 1, Fig. 1). Only ears that contained otoconia were used for further analysis as presence of otoconia always coincides with hair cell formation (Elliott and Fritzsch, 2010). Transplanted ears containing otoconia were examined for degree of development by immunostaining with antibodies against MyoVI and acetylated tubulin, markers for

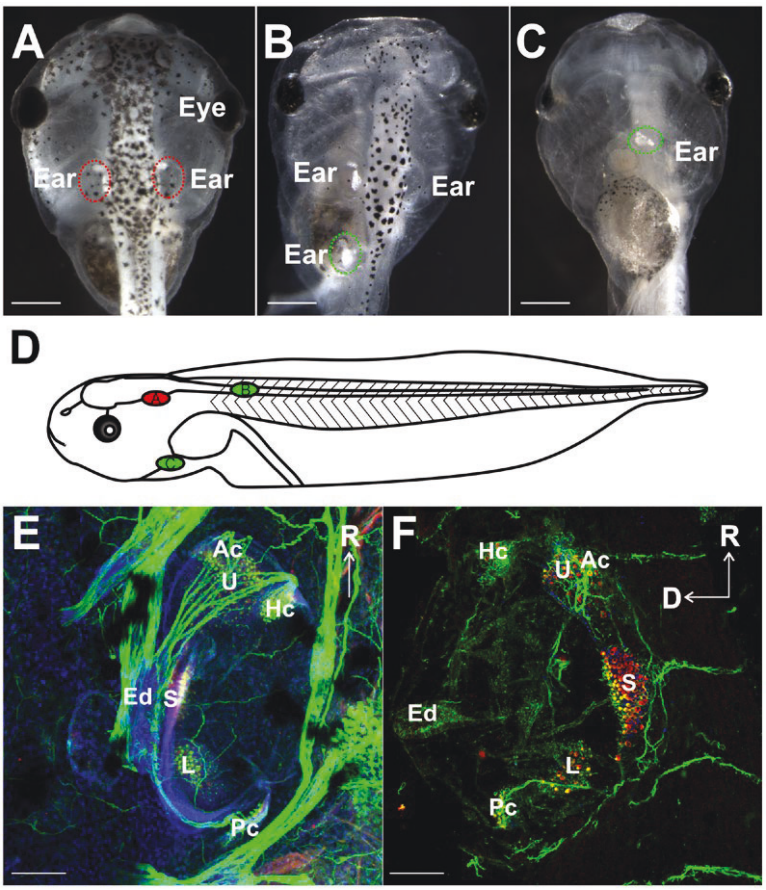

Figure 1 Evaluation of ear transplantations (A–D) Stage 46 *X. laevis* embryos showing positions of native ears and transplanted ears (circled). (A) Control animal. (B) Embryo with a third ear transplanted adjacent to the spinal cord. (C) Ventral view of embryo with a third ear transplanted next to the heart. (D) Schematic diagram representing a lateral view of stage 46 *X. laevis* demonstrating the positions of the native ear (red, A) and the two different transplantations (green, B,C). (E) Control ear and (F) a transplanted ear labeled with antibodies against MyoVI (red) and tubulin (green) demonstrating the presence of hair cells in six distinct epithelia along with Hoechst nuclei counterstain (blue) (Utricle, U; Saccule, S; Lagena, L; Anterior canal, Ac; Horizontal canal, Hc; Posterior canal, Pc) and neurons, respectively. Endolymphatic duct is labeled Ed. Scale bars in A–C are 0.5 mm and 100 μm in E–F Rostral, R; Dorsal, D. [Colour figure can be viewed at wileyonlinelibrary.com]

hair cells and neurons, respectively. Positive MyoVI staining revealed the presence of hair cells in transplanted ears (Fig. 1F). Hair cells were found to be in discrete clusters within the ear, indicating distinct vestibular end-organ sensory epithelia formation consistent with near normal ear development. Additionally, tubulin identified neurons and their processes associating with sensory epithelia in the transplanted ears (Fig. 1F). These results indicate that ears transplanted in this study are capable of developing hair cells and neurons, similar to those present in native ears and consistent with past work (Harrison, 1935; Yntema, 1955; Fritzsch *et al.*, 1998a).

Entry and Projection of Afferents in Ears Transplanted to the Spinal Cord

Since ear afferent connections with the spinal cord in identical transplants have been observed previously by retrograde labeling of ganglion cells from dye injection into the spinal cord (Elliott and Fritzsch, 2010), as well as in this study (Fig. 2A,E–F), afferent axon projections into the spinal cord were traced from the ear using lipophilic or dextran amine dyes (Fritzsch, 1993; Fritzsch *et al.*, 2005b). We aimed to determine if inner ear afferents from an ear transplanted adjacent to the spinal cord enter and project dorsally in

the spinal cord as native afferent fibers do in the hindbrain.

Following labeling of afferent projections from the ear, the brain and spinal cord were dissected from the embryo and the entry point along the dorsal-ventral (D-V) axis of the spinal cord was determined (Fig. 2B–D). In assigning the D-V plane of entry, confocal scanning of the spinal cord along the entire D-V plane was used to define a midline position, where the middle of the z-series stack was considered neither dorsal nor ventral, while labeled afferents observed above or below this midline were considered to be dorsal and ventral entering, respectively (Fig. 2D). The majority of cases (14/20; 70%) had projections with a dorsal entry point, whereas five animals showed a ventral entry point and one animal had afferents enter at the midline (Fig. 2D′).

Plane of fiber projection within the spinal cord was assessed in a similar manner and was defined by the D-V plane where fibers were observed to project once inside the spinal cord. Regardless of entry point, all 20 animals examined had afferents projecting dorsally within the spinal cord (Fig. 2D′). Additionally, these projections extended both rostral and caudal from the entry site. These results suggest that similar cues guide inner ear afferents in the hindbrain and spinal cord, consistent with known molecular conservation of dorso-ventral patterning in these areas of the CNS (Fritzsch *et al*., 2006; Fritzsch and Elliott, 2017).

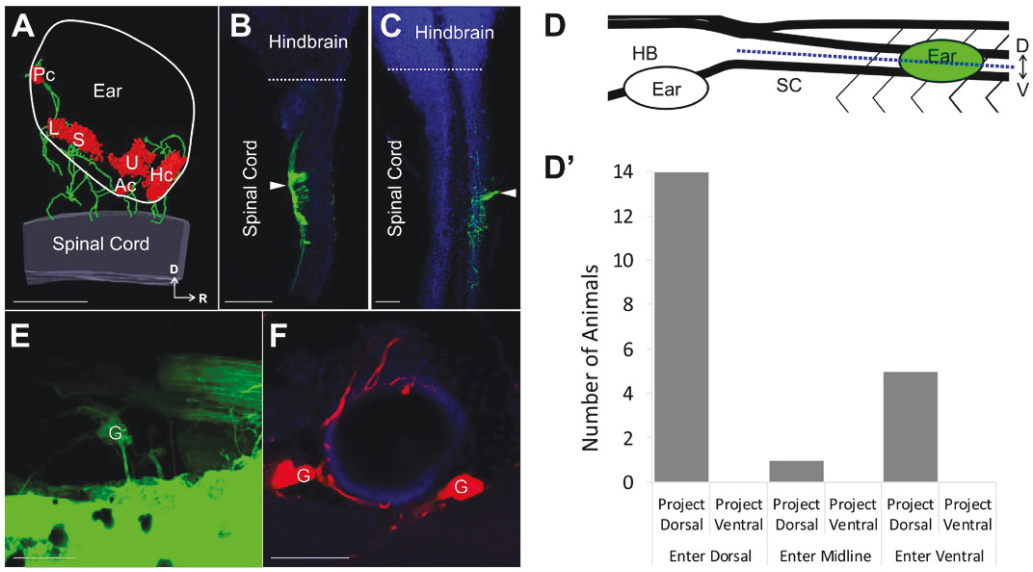

Figure 2 Ear afferent innervation of the spinal cord (A) 3D reconstruction of an ear transplanted adjacent to the spinal cord labeled with antibodies against Tubulin (green) and MyoVI (red) displaying neurons and hair cells, respectively. (B–C) Single optical sections of an *X. laevis* brain and spinal cord (blue, autofluorescence) in the dorsal (B) and ventral (C) plane following injection of dye (green) into an adjacently transplanted ear shows afferents entering the spinal cord dorsally and ventrally, respectively. White arrowhead indicates the entry point of inner ear afferent projections. (D) Lateral view schematic diagram showing the position of the transplanted ear and the defined midline position (blue dotted line) along the dorsal-ventral axis of the spinal cord used to assign entry and projection planes of labeled afferents in B–C. (D′) Analysis of entry point and plane of projection for animals with ears transplanted adjacent to the spinal cord. Serial optical sections were analyzed for entry point of labeled fibers (dorsal, midline, ventral) and for plane of projection (dorsal, ventral). $n = 20$. (E) Backfilling of inner ear ganglion cells in an ear adjacent to the spinal cord from dye injection into the spinal cord rostral to the transplanted ear. (F) Backfilling (red) of inner ear ganglia and peripheral afferent processes on hair cells in an ear adjacent to the spinal cord from dye injection into the spinal cord. Hoechst nuclei counterstained in blue. Spinal Cord, SC; Hindbrain, HB; Dorsal, D; Ventral, V; Rostral, R; Ganglion cells, G; Utricle, U; Saccule, S; Lagena, L; Anterior canal, Ac; Horizontal canal, Hc; Posterior canal, Pc. Scale bars are 100 μm. [Colour figure can be viewed at wileyonlinelibrary.com]

Ears Transplanted Adjacent to the Spinal Cord Project to the Hindbrain

Since ear afferent projections into the spinal cord appear to project dorsally regardless of entry point (Fig. 2), we next sought to identify if the afferent fibers projected into the hindbrain, and once within, if connections are established with the dorsally located vestibular nucleus, extending beyond past research showing such projections after ear transplantations adjacent to the hindbrain itself or adjacent to cranial nerves projecting to the hindbrain (Elliott *et al.*, 2013; Elliott *et al.*, 2015b). In control animals, dye injection into the spinal cord (Fig. 3A) labels all ascending spinal tracts as well as trigeminal (V) nucleus afferents in the hindbrain (Fig. 3A′–B, green), as there exists a continuity between the hindbrain located descending tracts of V and ascending spinals (Maklad and Fritzsch, 2003). In animals with an ear transplanted next to the spinal cord, dye injection into the transplanted ear (Fig. 3C) also label dorsal ascending spinal tracts, as well as trigeminal tracts in the hindbrain (Fig. 3C′–D), suggesting that afferents from the transplanted ear fasciculate with ascending spinal tracts to enter the hindbrain and further continue along centrally located trigeminal tracts (Fig. 3C′–D).

To determine whether these afferents from transplanted ears terminated in the dorsally located vestibular nucleus, dye was implanted into the native ears to label the vestibular nucleus (Fig. 3, red), providing a reference point with which to assess if transplanted inner ear afferents reroute from the more ventrally located trigeminal tracts they project with upon entering the hindbrain. In these transplanted ear animals, fibers apparently rerouted from the trigeminal tracts and into the vestibular nucleus upon reaching the hindbrain (Fig. 3C′–D″). Given the well-defined positions of sensory tracts and nuclei along the alar plate (Fritzsch *et al.*, 2005a), closer examination showed that all 8 animals had fibers approaching and/or projecting directly into the vestibular nucleus. In contrast, in 8 control animals, no fibers from the spinal labeled tracts and hindbrain trigeminal tracts display any rerouting into the vestibular nucleus (Fig.

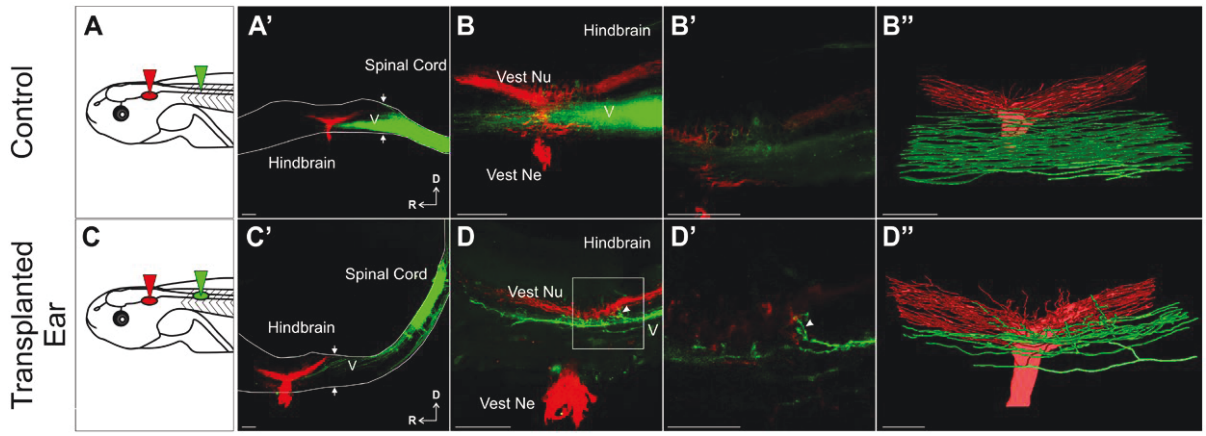

Figure 3 Afferent innervation of the hindbrain by ears transplanted adjacent to the spinal cord (A) Schematic of dye placement for control animals. (A′) Control hemisection of the brain and spinal cord showing ascending spinal fibers (green) enter the hindbrain and fill the descending tract of trigeminal nucleus (V, unlabeled). Native ear projections (red) into the vestibular nucleus in the hindbrain are labeled. Note the lack of overlap between the trigeminal nucleus and vestibular nucleus at higher magnification of A′ (B) and of B, shown as a single optical section (B′). (B″) 3D reconstruction of entire stack in B. (C) Schematic of dye placement for animals with ears transplanted adjacent to the spinal cord. (C′) Hemisection showing ascending spinal tracts and spinal cord transplanted ear afferent fibers projecting into the hindbrain (green) along the descending tract of V (unlabeled). (D) Higher magnification of C′ showing inner ear afferents projecting into the vestibular nucleus from the trigeminal nucleus (arrowhead). (D′) Higher magnification of box in D showing projections into the vestibular nucleus (arrowhead) in a single optical section. (D″) 3D reconstruction of entire stack in D. 8 experimental animals were analyzed. Arrows denote the hindbrain/spinal cord boundary. Scale bars are 100 μm in A′, B, B″, C′, C″, D and 50 μm in B′, D′. Vest Ne vestibular nerve, Vest Nu vestibular nucleus, D dorsal, R rostral. [Colour figure can be viewed at wileyonlinelibrary.com]

3A′–B″). Collectively these data show that inner ear afferents that enter the hindbrain from the spinal cord are capable of projecting to the vestibular nucleus, suggesting vestibular afferents are being navigationally instructed through yet unknown molecular cues once entering the hindbrain.

Transplanted Ears Make Functional Connections With The Hindbrain

To determine whether the inner ear afferents that reach the vestibular nucleus are making functional connections, behavioral and functional assays were conducted. To test for functional connections between the inner ear afferents of the transplanted ear and a second-order neuron in the vestibular nucleus of the hindbrain, the Mauthner cell (Korn and Faber, 2005), we utilized a C-start startle assay (Zarei *et al.*, 2017). We tested 13 control animals in which both native ears were removed, thus lacking any inner ear input, and 15 animals in which both native ears were removed but had an ear transplanted adjacent to the spinal cord. Native ear removals were performed between stages 40–42 to ensure survivability of the Mauthner cells (Elliott *et al.*, 2015a). Attempts to elicit a C-start startle response in the thirteen control animals lacking all ears were unsuccessful (Fig. 4A). In contrast, in animals with an ear transplanted to the spinal cord and the native ears removed, eliciting a C-start startle response was successful in five of fifteen animals (Fig. 4A). Of these five animals, one animal responded in all four trials, one responded in two of four trials, and three animals responded in one of four trials. Of these nine trials that had responses, eight resulted in turns away from the transplanted ear and only one toward (Fig. 4A′). This was significantly different from an

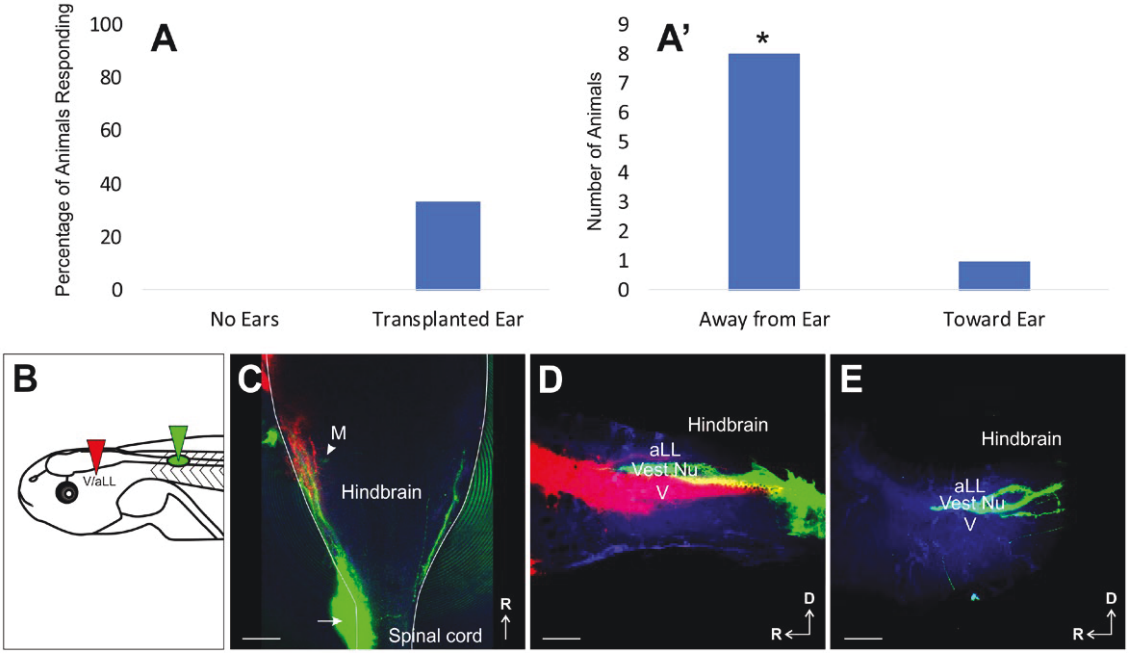

Figure 4 C-Start Startle Response by Transplanted Ears. (A) Percentage of animals that displayed a C-start startle response following stimulation in control animals with no ears and in animals in which the only ear was the transplanted ear adjacent to the spinal cord. (A′) Direction in each trial with a positive response observed in A from animals in which the only ear was the transplanted ear adjacent to the spinal cord. *$P < 0.05$, Chi-Square analysis. (B) Schematic of dye placement. (C) Whole-mount of a hindbrain from an animal that had a response in all four trials, three were in the direction away from the transplanted ear and one in the direction toward the transplanted ear. Arrow designates entry point of transplanted inner ear afferents. M, Mauthner cell. (D) Lateral view of ipsilateral hemisected hindbrain showing projections of transplanted ear afferents (green) in between anterior lateral line (aLL) and trigeminal (V) afferent central projections (red). (E) Lateral view of contralateral hemisected hindbrain showing projections of a transplanted ear afferents (green) in between the region where the anterior lateral line (aLL) and trigeminal (V) nuclei are located. Autofluorescence is in blue. Scale bars are 100 μm. [Colour figure can be viewed at wileyonlinelibrary.com]

expected absence of directional bias ($P < 0.05$). Given that wild type animals with both native ears turn in either direction with equal probability and those with one ear removed turn away from the remaining ear nearly every time (Zarei *et al.*, 2017), our data suggest that the ears transplanted adjacent to the spinal cord can develop functional connections within the vestibular nucleus that direct the movement of the tadpole away from the incoming stimulus from that ear. Furthermore, lipophilic dye tracing (Fig. 4B) of transplanted ears in these animals revealed inner ear afferents navigating to the vestibular nucleus in those animals that responded. In fact, the animal that responded in all four trials was the only one that had robust innervation of the ipsilateral vestibular nucleus and to a lesser degree, the contralateral vestibular nucleus (Fig. 4C–4E). This may explain why this animal had three turns away from the transplanted ear and one turn toward the transplanted ear. In addition, the Mauthner cell could be transcellularly labeled through the transplanted ear afferents (Fig. 4C), further supporting physical and functional contacts of these afferents with second-order neurons in the vestibular nucleus.

Further validation of functionally adequate synaptic wiring was examined by testing the connectivity of the transplanted ear with the vestibulo-ocular reflex (VOR) circuitry. Semi-intact *in vitro* preparations (Straka and Simmers, 2012) of animals at stage 53–57 ($n = 5$) with a transplanted third ear were employed to test the performance of the VOR during natural motion (Lambert *et al.*, 2008) and GVS of native and ectopic inner ears (Gensberger *et al.*, 2016). After disconnection from the target eye muscle, multi-unit spike discharge of various extraocular motor nerves ($n = 15$), such as the inferior rectus (IR) nerve were recorded (Fig. 5A,B). The multi-unit discharge of all recorded extraocular motor nerves (mean resting rate ± SE: 28.7 ± 3.8 spikes/s; $n = 15$) was cyclically modulated during spatially specific sinusoidal rotation (1 Hz and ± 2° position oscillation; Fig. 5A). The multi-unit firing rate of the IR nerve for example (Fig. 5C) oscillated during sinusoidal turntable motion along a plane formed by the ipsilateral anterior (iAC) and contralateral posterior semicircular canal (cPC). In this case, the discharge modulation was due to a robust excitatory component from the cPC (peak discharge: 60–90 spikes/s; Fig. 5D). A comparable discharge modulation was obtained by sinusoidal GVS (1 Hz and ± 200 μA) of the same native bilateral semicircular canal pair, i.e., the iAC and cPC (Fig. 5E,F). The peak discharge occurred during galvanic depolarization of the cPC (Fig. 5F), complied with the prediction from the phase relationship of the spike firing during motion stimulation (Fig. 5D), and outlined the connectivity of the underlying VOR circuitry between the bilateral inner ear and the IR eye muscle (Straka *et al.*, 2014).

Given that motion stimulation activates vestibular endorgans in native ears as well as the ectopic ear, we applied sinusoidal GVS exclusively to the transplanted ear (Fig. 5A) to evaluate if the transplanted ear is functionally connected to the native VOR circuitry. In 10 out of 15 extraocular motor nerves recorded in 5 animals, sinusoidal GVS of the transplanted ear provoked a modulation of the spontaneous multi-unit discharge as exemplified for the contralateral IR nerve (Fig. 5G,H). The discharge modulation was robust across most trials (Fig. 5G) with a mean peak discharge (± SE) of 23.3 ± 4.2 spikes/s ($n = 10$). At variance with sinusoidal GVS of the native inner ears, the modulation consisted exclusively of an excitatory component as indicated by the lack of a firing rate disfacilitation (blue line in Fig. 5H). Also, the current intensity necessary to evoke a modulated discharge was higher for the transplanted ear (± 300 μA) compared to the native ears (± 100 μA). Most importantly, however, the peak discharge coincided with the depolarization of the cPC epithelium (green dotted line in Fig. 5H), confirmed by trials with inversed current polarities. This clearly indicates that the transplanted ear functionally links with excitatory vestibulo-ocular projection neurons known to form connections with contralateral extraocular motoneurons as the major driving force for the semicircular canal-dependent VOR. The failure to induce a discharge modulation of ipsilateral extraocular motoneurons by galvanic stimulation of the ectopic inner ear (5 out of 15 extraocular motor nerves) clearly indicates that the transplanted ear is exclusively connected to excitatory VOR pathways.

Collectively, the results obtained from testing the connectivity that arises from the transplanted ear suggests that afferent projections to hindbrain neuronal targets are indeed functionally meaningful. Additional work will define rules and constraints for integrating spinal cord-derived vestibular inputs into synaptic computations performed in native neural networks.

Fasciculation with Peripheral Nerves

Following a placodal origin in close proximity to native ears, pLL primordia migrate caudally toward the trunk and are found along the dorsal fin at stage 40 (Nieuwkoop and Faber, 1994). Given the caudal placement of the transplanted ear adjacent to the spinal

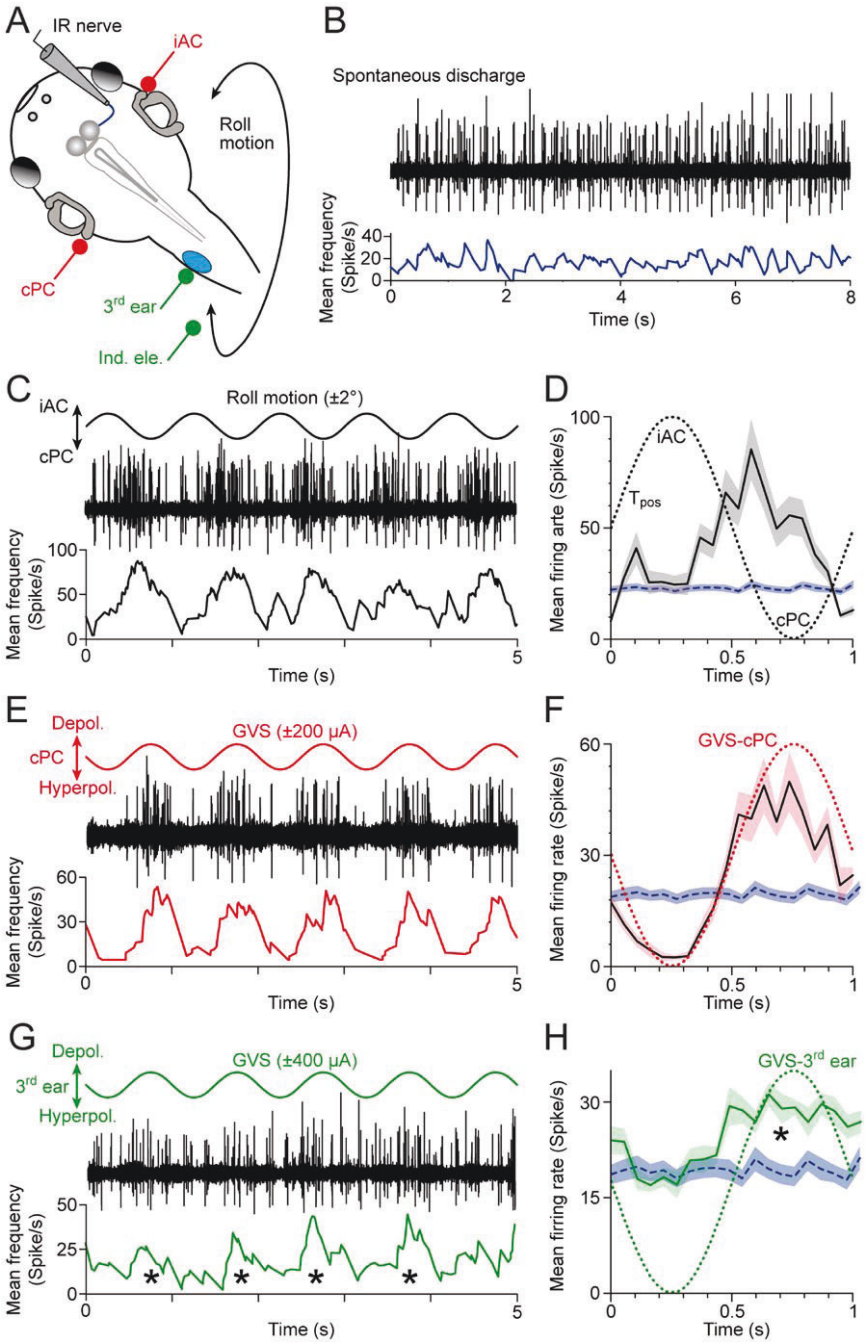

Figure 5 Multi-unit inferior rectus (IR) nerve discharge during activation of native bilateral semicircular canals and a transplanted third ear on the spinal cord. (A) Schematic of a semi-intact *Xenopus* preparation depicting the recording of the right IR nerve during roll motion (black curved double arrow), galvanic vestibular stimulation (GVS) of the contralateral posterior (cPC) and iAC semicircular canal epithelia (iAC; red electrodes) and of the transplanted third ear (green electrodes). (B) Episode of spontaneous IR nerve discharge (black trace) with an average resting rate of ~20 spikes/s (blue trace) in an isolated preparation obtained from a stage 55 tadpole. (C, E, G) Modulated multi-unit discharge (black traces) and mean firing rate (lower colored traces) of the same IR nerve during roll motion in the cPC-iAC plane (C), during GVS of the cPC-iAC (E) and during GVS of the third ear (G); sinusoids indicate the waveform (1 Hz) for natural and galvanic stimulation. (D, F, H) Modulated mean IR nerve firing rate over a single cycle (black traces) ± SEM (color-shaded areas) of the responses shown in C,E,G; the averages were obtained from 20-120 single cycles, respectively; the colored dotted sinusoids indicate the motion stimulus (D) and GVS of the cPC (F) and third ear (H), and the blue dashed line and horizontal band the mean ± SEM resting rate of the IR nerve. Note that the IR nerve increases firing during motion in direction of the cPC (D), galvanic depolarization of the cPC epithelium (F) and galvanic depolarization of the third ear (*in G, H). T_{pos}, position signal of the turntable. [Colour figure can be viewed at wileyonlinelibrary.com]

cord, we next sought to identify if there would be an interaction with neurosensory components of the posterior lateral line (pLL) system. Specifically, are inner ear afferents able to navigate along the lateral line nerve and could lateral line afferents innervate the transplanted ear (Fritzsch *et al.*, 1998b)? Dye was placed into the pLL ganglia itself and into the pLL nerve caudal to the transplanted ear (Fig. 6A). Afferents of the pLL were observed to innervate the skin above the transplanted ear as well as continue a caudal trajectory past the ear along the dorsal fin (Fig. 6B), unlike in native ears where the skin above the ear is devoid of lateral line (Elliott and Fritzsch, 2010). Furthermore, pLL afferents were found to innervate the transplanted ear (Fig. 6B, arrowheads), as no inner ear ganglia were detected with the lipophilic dye from

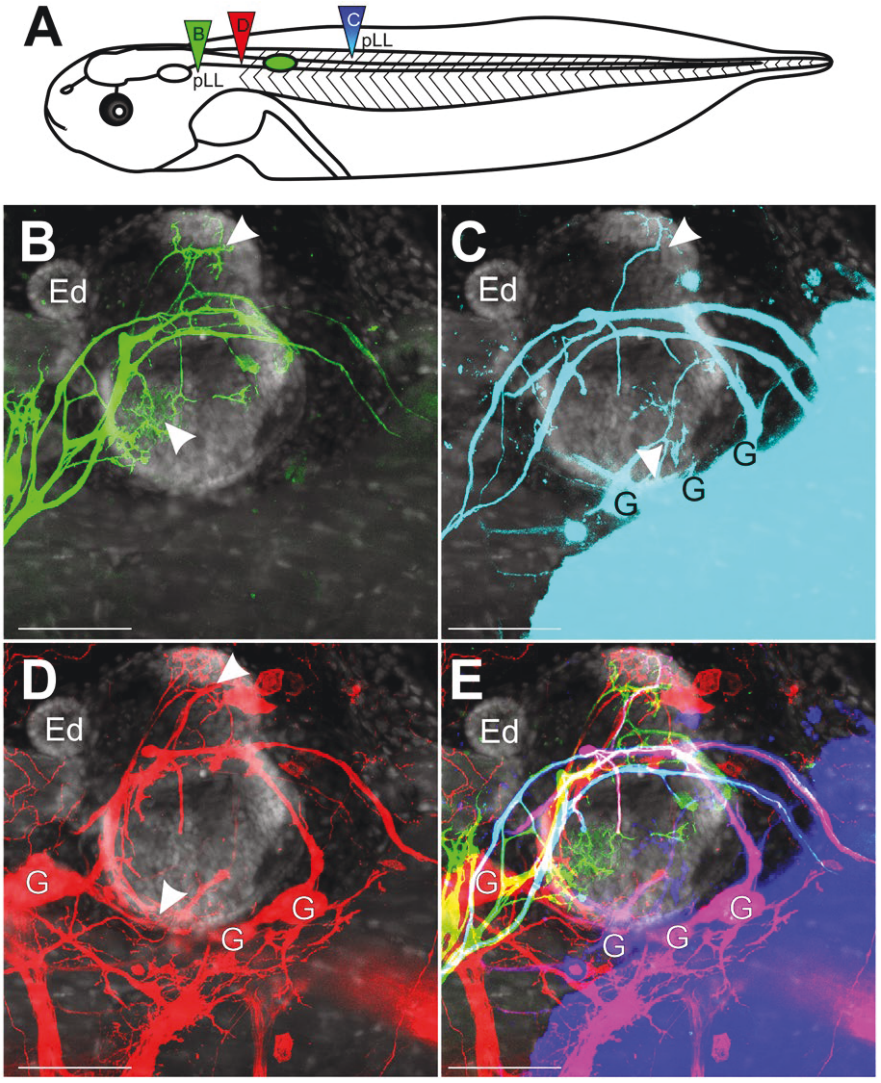

Figure 6 Inner Ear Afferent Fasciculation with Lateral Line. (A) Schematic of dye placement for the different transplants. (B) Lateral view of afferents of the pLL projecting over and into the ear (green, dye injection B in panel A). The ear was transplanted adjacent to the spinal cord at stage 32–36. No ganglia were labeled. (C) Lateral view of pLL and inner ear afferents from a caudal dye injection into caudal portion of the pLL nerve (cyan, dye injection C in panel A). G, ganglia. (D) Lateral view of inner ear afferents from a spinal cord injection rostral to the transplanted ear (red, dye injection D in panel A) G, ganglia. (E) Merge of B-D. Cyan of panel C has been replaced by blue. Panels B–E are counterstained for nuclei marker Hoechst (gray). Arrowheads indicate areas of innervation of the inner ear. Scale bars are 100 μm. Endolymphatic duct, Ed. [Colour figure can be viewed at wileyonlinelibrary.com]

this injection. Placement of dye caudal to the transplanted ear, in the pathway of a more caudal segment of the pLL nerve, labeled inner ear ganglion cells (Fig. 6C), suggesting fasciculation between inner ear and pLL afferents. Furthermore, this caudal injection revealed innervation of the transplanted ear (Fig. 6C, arrowheads), most likely by inner ear afferents given the labeling of ganglia, though additional contribution of lateral line afferents to the innervation cannot be ruled out. Injection of dye directly into the spinal cord (Fig. 6A) labeled many more afferents and associated ganglia (Fig. 6D) than was labeled with a caudal application to the pLL nerve (Fig. 6C), though some afferents were labeled with both spinal cord and caudal lateral line dye applications (Fig. 6E). These data suggest that afferents of the inner ear are capable of projecting with peripheral nerves but do so as undirected growth along existing peripheral nerves.

To further test the possibility of fasciculation with any peripheral nerve bundles, we transplanted the ear ventrally into the region of the developing heart (Figs. 1C–D, 7B–C). Dye injections into the transplanted ear (Fig. 7A) identified afferents of the inner ear projecting with the vagus nerve (Fig. 7B). Furthermore, placement of dye into the vagus nerve (Fig. 7A) labeled ganglion cells of the transplanted ear, as well as their associated peripheral processes into the ear (Fig. 7C). These results further suggest that afferents of the inner ear are capable of fasciculation with any nearby peripheral nerve and that this potentially may be occurring without instructive signaling from nearby CNS sources.

DISCUSSION

Past research has demonstrated that various cranial sensory organs can be transplanted and develop normally even if not associated with their specific area of the brain (Yntema, 1955; Jacobson, 1963; Swanson *et al.*, 1990). Evidence indicates that several of these transplanted sensory organs can establish contact with the brain. Importantly, transplanted eyes and ears can project and interact with native projections to form columns of fibers suggestive of a compromise between molecular cues and activity (Constantine-Paton

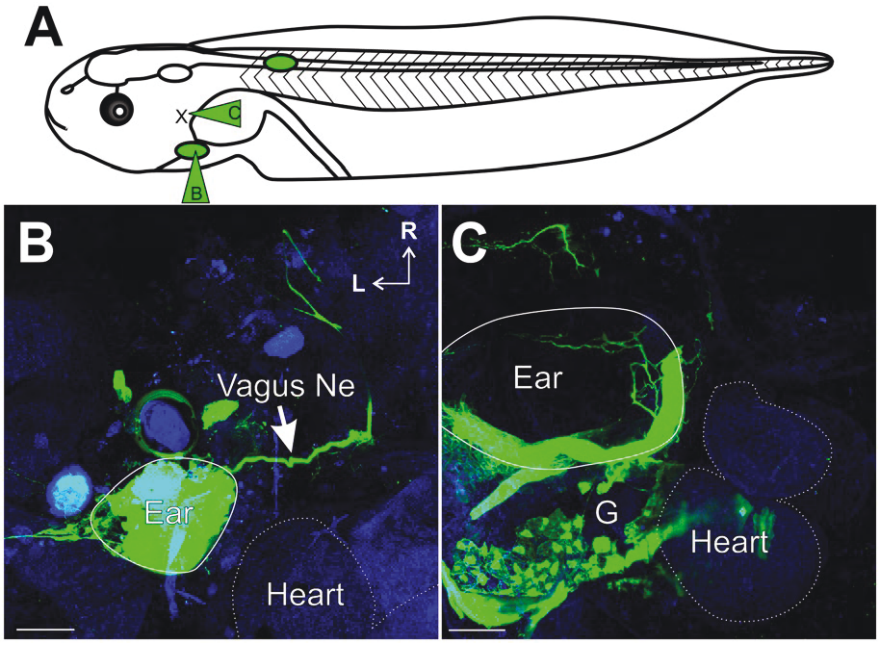

Figure 7 Inner Ear Afferent Fasciculation with the Vagus nerve. (A) Schematic of ear transplants showing dye placement for the ears transplanted adjacent to the heart. (B) Ventral view of an animal with an ear transplanted into the heart region showing ear afferents projecting with the vagus nerve (green, dye injection B in panel A; Vagus Ne, arrow). Heart is outlined with a dotted line as determined from autofluorescence background (blue). (C) Ventral view of an animal with an ear transplanted next to the heart. Labeling (green) from dye injection into the vagus nerve (dye injection C in panel A) showing innervation of the ear and labeling of inner ear ganglia. Autofluorescense background (blue). Scale bars are 100 μm. Rostral, R; Lateral, L. [Colour figure can be viewed at wileyonlinelibrary.com]

and Law, 1978; Elliott *et al.*, 2015b). Furthermore, retinal afferents may home to the midbrain from the spinal cord (Giorgi and Van der Loos, 1978) or may bring their information through unclear routes to the CNS (Blackiston *et al.*, 2017). The olfactory system seems to show no homing to a specific part of the brain but rather interacts with whatever brain area they reach (Stout and Graziadei, 1980; Morrison and Graziadei, 1983; Magrassi and Graziadei, 1985) possibly using the molecular guidance cues inherent to different olfactory receptors (Mombaerts *et al.*, 1996).

Transplanted ears have thus far only been analyzed regarding their homing behavior within the CNS if transplanted near the hindbrain or the midbrain. In the hindbrain, inner ear afferents navigate to reach the vestibular nuclei no matter their entry point and interact with native afferents (Elliott *et al.*, 2015b). In contrast, inner ear afferents project in a highly variable pattern into the midbrain, implying little to no guidance cues in this foreign territory (Elliott *et al.*, 2013). Our data provide clear evidence that the spinal cord allows inner ear afferents to navigate to a dorsal position comparable to the hindbrain (Figs. 2 and 3), strikingly unlike the midbrain. This distinction may be owing to a stronger effect of dorso-ventral patterning molecular cues in the hindbrain and spinal cord, including Shh, Wnt, and BMPs, whereas the midbrain may require additional signals from the isthmus that alter navigation (Fritzsch *et al.*, 2006; Hernandez-Miranda *et al.*, 2016; Lai *et al.*, 2016; Fritzsch and Elliott, 2017; Glover *et al.*, 2018). While inner ear afferents entering the spinal cord project along the dorsal funiculus both in caudal and rostral directions, afferents that reach the hindbrain can form collaterals that reach the vestibular nuclei, overlapping with native projections, much like inner ear afferents reaching the hindbrain when transplanted adjacent to the native ear (Elliott *et al.*, 2015b). This suggests that molecular cues in the hindbrain, possibly associated with the Wnt signaling pathway that drives dorsally directed cochlear collaterals (Yang *et al.*, 2017), drive inner ear afferent collaterals to expand outside the trigeminal afferent fascicles to reach the vestibular nuclei. This ability to navigate in an as of yet incompletely understood molecular gradient seems also to allow inner ear afferents to navigate dorsally in the spinal cord, even if they entered ventrally. Our data thus suggest that a shared molecular patterning system guides inner ear afferents in the hindbrain and spinal cord and that this system is absent in the midbrain, explaining the random afferent trajectories in the latter (Elliott *et al.*, 2013) and the targeted projections in the former [Fig. 3 and (Elliott *et al.*, 2015b)]. There is no strong evidence that these molecular cues act over long distances to attract spinal cord entering afferent fibers as suggested for transplanted eyes (Giorgi and Van der Loos, 1978). Rather, it appears that fasciculation along existing dorsal root fibers, equally sorted by possibly the same gradient (Lai *et al.*, 2016), may by chance guide some afferents within the reach of local cues in the hindbrain that can diverge them to reach vestibular nuclei.

Inner ear afferents either directly labeled through dye injection into the ear (Figs. 2 and 3) or filled from the spinal cord (Fig. 2) show mostly a directed growth toward the spinal cord. This could simply be so because other earlier routes taken by various fibers have been eliminated between our transplantation time and observation time. Whether this apparent targeted growth of inner ear afferents to the spinal cord is due to neurotropic attractive interactions (fibers are specifically attracted to the spinal cord or more generally to the CNS) or due to neurotrophic interactions (early fibers that reached areas without proper support were eliminated) requires additional work on various early stages after transplantation. However, our data suggest that inner ear afferents prefer to fasciculate with existing nerves (Fig. 3). This observation is particularly obvious in the case of the lateral line nerve fibers, where such afferents can innervate the transplanted ear (Fig. 6) presumably by being supported through hair cell released neurotrophins such as BDNF that appear to be common to all hair cells (Fritzsch *et al.*, 2016b; Hallböök *et al.*, 2006). Likewise, inner ear afferents that navigate along lateral line afferents to reach neuromasts could be supported by BDNF released from neuromast hair cells. For the lateral line/inner ear afferent interactions there is random, non-directed growth along each other which appears to be not corrected for. This follows from data suggesting that neurotrophic support via common molecules released from inner ear/lateral line hair cells rescues the random growth of inner ear afferents toward the tail-ward neuromasts (Fig. 6). Obviously, these inner ear afferents have no chance of ever reaching the hindbrain These data are consistent with previous preliminary reports on afferent growth to the spinal cord (Elliott and Fritzsch, 2010) or along lateral line nerves (Fritzsch *et al.*, 1998b; Fritzsch, 1999).

Epibranchial placode-derived neurons are unique in that they not only express the neurotrophin receptor TrkB but also express BDNF (Fritzsch *et al.*, 1997; Patel *et al.*, 2010). Inner ear afferents growing along the epibranchial placode-derived vagus afferents should thus fasciculate with that nerve. Our data of

ear transplantation near the heart show that inner ear afferents fasciculate along the vagus nerve without any apparent deviation, indicating that neurotrophic survival support combined with fasciculation along Schwann cells suffices for an apparently directed growth of inner ear afferents along the vagus nerve toward the brain.

As a result of the observed capability to reroute into the vestibular nuclei, afferents from the spinal cord transplanted ear make functional connections with vestibular brainstem circuitry (see Fig. 5G,H). The modulated discharge of the majority of extraocular motor nerves during GVS clearly indicates that afferents from the transplanted ear form non-selective, ubiquitous excitatory connections with second-order vestibular neurons. However, the supplemental ocular motor activation trough central vestibular neurons is obviously restricted to excitatory VOR neurons, since a discharge modulation is only observed in extraocular motoneurons that are located contralateral to the transplanted ear. This connectivity pattern complies with the crossed excitatory circuit component of the native VOR that forms the dominant part of the classical push-pull organization (Straka *et al.*, 2014). This interpretation also corroborates the responses of tadpoles subjected to the startle assay that revealed a biased turn away from the ear, indicating that stimulation of the transplanted ear facilitates an excitation of the Mauthner cell (Fig. 4).

The ubiquitous excitation of hindbrain vestibular neurons including the Mauthner cell is not too surprising but appears to challenge the functionality of the connections. While a general activation of central vestibular neurons by afferents from the transplanted ear might be detrimental for the spatial specificity of the VOR, it is more likely not, given the presence of concurrent powerful afferent inputs from the native ears. In fact, a comparable situation has been described in adult ranid frogs after a partial loss of the VIIIth nerve (Goto *et al.*, 2001; Rohregger and Dieringer, 2003). Part of the post-lesional vestibular reorganization included an expansion of excitatory connections from the remaining intact afferent fibers onto functionally "incorrect" central vestibular neurons that have lost their peripheral inputs. The formation of such inappropriate connections that ensure the survival of the deafferented neurons was compensated by remaining adequate connections that guaranteed the maintenance of spatially appropriate reflexes. Thus, together, our results indicate that the hindbrain exhibits a remarkable plasticity in response to integrating rerouted novel vestibular inputs from the spinal cord. Nonetheless, further work is required to identify proper conditions that increase the efficacy of innervation from ectopic ear placements and the connectivity with functionally appropriate circuit components (Blackiston *et al.*, 2017). Our data imply that vestibular (and possibly auditory) connections can be made from transplanted ears to guide respective modality-specific behaviors.

ACKNOWLEDGMENTS

This material is based upon work supported by the NASA Iowa Space Grant Consortium under Grant No. NNX10AK63H. KE is supported by an NIH R03 (DC015333). The authors acknowledge financial support by the Collaborative Research Center (CRC 870) and the Research Training Group (RTG 2175) of the German Science Foundation. The use of the Leica TCS SP5 multi-photon confocal microscope was made possible by a grant from the Roy. J. Carver Charitable Trust. The authors wish to thank K. Gensberger for technical help with initial electrophysiology experiments. We also thank the Office of the Vice President for Research (OVPR) of the University of Iowa for support. The authors have no conflicts of interest to declare.

REFERENCES

Blackiston, D.J., Vien, K. and Levin, M. (2017) Serotonergic stimulation induces nerve growth and promotes visual learning via posterior eye grafts in a vertebrate model of induced sensory plasticity. *NPJ Regenerative Medicine*, 2, 8.

Constantine-Paton, M. and Law, M.I. (1978) Eye-specific termination bands in tecta of three-eyed frogs. *Science*, 202(4368), 639–641.

Crook, A.C. and Whiteman, H.H. (2006) An evaluation of MS-222 and benzocaine as anesthetics for metamorphic and paedomorphic tiger salamanders (Ambystoma tigrinum nebulosum) *The American Midland Naturalist*, 155, 417–421.

Elliott, K.L. and Fritzsch, B. (2010) Transplantation of *Xenopus laevis* ears reveals the ability to form afferent and efferent connections with the spinal cord. *The International Journal of Developmental Biology*, 54(10), 1443–1451.

Elliott, K.L., Houston, D.W., DeCook, R. and Fritzsch, B. (2015a) Ear manipulations reveal a critical period for survival and dendritic development at the single-cell level in Mauthner neurons. *Developmental Neurobiology*, 75(10), 1339–1351.

Elliott, K.L., Houston, D.W. and Fritzsch, B. (2015b) Sensory afferent segregation in three-eared frogs resemble the dominance columns observed in three-eyed frogs. *Scientific reports*, 8, 8338.

Elliott, K.L., Houston, D.W. and Fritzsch, B. (2013) Transplantation of *Xenopus laevis* tissues to determine the ability of motor neurons to acquire a novel target. *PLoS One*, 8, e55541.

Elliott, K.L., Kersigo, J., Pan, N., Jahan, I. and Fritzsch, B. (2017) Spiral ganglion neuron projection development to the hindbrain in mice lacking peripheral and/or central target differentiation. *Frontiers in Neural Circuits*, 11, 25.

Fritzsch, B. (1993) Fast axonal diffusion of 3000 molecular weight dextran amines. *Journal of Neuroscience Methods*, 50, 95–103.

Fritzsch B. (1999) Hearing in Two Worlds: Theoretical and Actual Adaptive Changes of the Aquatic and Terrestrial Ear for Sound Reception. In: Fay R.R., Popper A.N. (eds) Comparative Hearing: Fish and Amphibians. Springer Handbook of Auditory Research, vol 11. Springer, New York, NY

Fritzsch, B. (1999) Hearing in two worlds: theoretical and actual adaptive changes of the aquatic and terrestrial ear for sound reception In Comparative hearing: fish and amphibians. New York: Springer, pp. 15–42.

Fritzsch, B., Barald, K.F. and Lomax, M.I. (1998a) Early embryology of the vertebrate ear. In Development of the auditory system. New York: Springer, pp. 80–145.

Fritzsch, B., Barbacid, M. and Silos-Santiago, I. (1998b) Nerve dependency of developing and mature sensory receptor cells. *Annals of the New York Academy of Sciences*, 855, 14–27.

Fritzsch, B., Duncan, J.S., Kersigo, J., Gray, B. and Elliott, K.L. (2016a) Neuroanatomical tracing techniques in the ear: history, state of the art, and future developments. In B. Sokolowski (Ed.), Auditory and vestibular research: methods and protocols. New York: Springer, pp. 221–246.

Fritzsch, B. and Elliott, K.L. (2017) Gene, cell, and organ multiplication drives inner ear evolution. *Developmental Biology*, 431, 3–15.

Fritzsch, B., Gregory, D. and Rosa-Molinar, E. (2005a) The development of the hindbrain afferent projections in the axolotl: evidence for timing as a specific mechanism of afferent fiber sorting. *Zoology (Jena)*, 108, 297–306.

Fritzsch, B., Kersigo, J., Yang, T., Jahan, I. and Pan, N. (2016b) Neurotrophic factor function during ear development: expression changes define critical phases for neuronal viability, In The primary auditory neurons of the mammalian cochlea. New York: Springer, pp. 49–84.

Fritzsch, B., Muirhead, K.A., Feng, F., Gray, B.D. and Ohlsson-Wilhelm, B.M. (2005b) Diffusion and imaging properties of three new lipophilic tracers, NeuroVue Maroon, NeuroVue Red and NeuroVue Green and their use for double and triple labeling of neuronal profile. *Brain research bulletin*, 66, 249–258.

Fritzsch, B., Pan, N., Jahan, I. and Elliott, K.L. (2015) Inner ear development: building a spiral ganglion and an organ of corti out of unspecified ectoderm. *Cell and Tissue Research*, 361, 7–24.

Fritzsch, B., Pauley, S., Feng, F., Matei, V. and Nichols, D., 2006. The molecular and developmental basis of the evolution of the vertebrate auditory system. *International Journal of Comparative Psychology* 19.

Fritzsch, B., Sarai, P., Barbacid, M. and Silos-Santiago, I. (1997) Mice with a targeted disruption of the neurotrophin receptor trkB lose their gustatory ganglion cells early but do develop taste buds. *International Journal of Developmental Neuroscience*, 15, 563–576.

Gensberger, K.D., Kaufmann, A.K., Dietrich, H., Branoner, F., Banchi, R., Chagnaud, B.P., *et al*. (2016) Galvanic vestibular stimulation: cellular substrates and response patterns of neurons in the vestibulo-ocular network. *The Journal of Neuroscience*, 36(35), 9097–9110.

Giorgi, P. and Van der Loos, H. (1978) Axons from eyes grafted in Xenopus can grow into the spinal cord and reach the optic tectum. *Nature*, 275(5682), 746–748.

Glover, J.C., Elliott, K.L., Erives, A., Chizhikov, V.V. and Fritzsch, B. (2018) Wilhelm His' lasting insights into hindbrain and cranial ganglia development and evolution. *Developmental Biology*.

Goodrich, L.V. (2016) Early development of the spiral ganglion. In A. Dabdoub, B. Fritzsch, A.N. Popper and R.R. Fay (Eds.), The Primary Auditory Neurons of the Mammalian Cochlea. New York: Springer. pp. 11–48.

Goto, F., Straka, H. and Dieringer, N. (2001) Postlesional vestibular reorganization in frogs: evidence for a basic reaction pattern after nerve injury. *Journal of Neurophysiology*, 85, 2643–2646.

Hallböök, F., Wilson, K., Thorndyke, M. and Olinski, R.P. (2006) Formation and evolution of the chordate neurotrophin and Trk receptor genes. *Brain, Behavior and Evolution*, 68, 133–144.

Harrison, R.G., 1935. The Croonian lecture: on the origin and development of the nervous system studied by the methods of experimental embryology. *Proceedings of the Royal Society of London. Series B, Biological Sciences*, 118(808), 155–196.

Hernandez-Miranda, L.R., Müller, T. and Birchmeier, C. (2016) The dorsal spinal cord and hindbrain: from developmental mechanisms to functional circuits. *Developmental biology*.

Jacobson, A.G. (1963) The determination and positioning of the nose, lens and ear. I. Interactions within the ectoderm, and between the ectoderm and underlying tissues. *Journal of Experimental Zoology Part A: Ecological Genetics and Physiology*, 154, 273–283.

Jahan, I., Kersigo, J., Pan, N. and Fritzsch, B. (2010) Neurod1 regulates survival and formation of connections in mouse ear and brain. *Cell and Tissue Research*, 341, 95–110.

Klein, S. and Graziadei, P. (1983) The differentiation of the olfactory placode in *Xenopus laevis*: a light and electron

microscope study. *Journal of Comparative Neurology*, 217, 17–30.

Kopecky, B.J., Duncan, J.S., Elliott, K.L. and Fritzsch, B. (2012) Three-dimensional reconstructions from optical sections of thick mouse inner ears using confocal microscopy. *Journal of Microscopy*, 248, 292–298.

Korn, H. and Faber, D.S. (2005) The Mauthner cell half a century later: a neurobiological model for decision-making? *Neuron*, 47, 13–28.

Kullander, K. and Klein, R. (2002) Mechanisms and functions of eph and ephrin signalling. *Nature Reviews Molecular Cell Biology*, 3, 475–486.

Lai, H.C., Seal, R.P. and Johnson, J.E. (2016) Making sense out of spinal cord somatosensory development. *Development*, 143(19), 3434–3448.

Lambert, F.M., Beck, J.C., Baker, R. and Straka, H. (2008) Semicircular canal size determines the developmental onset of angular vestibuloocular reflexes in larval Xenopus. *The Journal of Neuroscience: The official Journal of the Society for Neuroscience*, 28(32), 8086–8095.

Liu, Z., Hamodi, A.S. and Pratt, K.G. (2016) Early development and function of the Xenopus tadpole retinotectal circuit. *Current Opinion in Neurobiology*, 41, 17–23.

Magrassi, L. and Graziadei, P. (1985) Interaction of the transplanted olfactory placode with the optic stalk and the diencephalon in *Xenopus laevis* embryos. *Neuroscience*, 15, 903–921.

Maklad, A. and Fritzsch, B. (2003) Development of vestibular afferent projections into the hindbrain and their central targets. *Brain Research Bulletin*, 60, 497–510.

Manns, M. and Fritzsch, B. (1991) The eye in the brain: retinoic acid effects morphogenesis of the eye and pathway selection of axons but not the differentiation of the retina in *Xenopus laevis*. *Neuroscience letters*, 127, 150–154.

Mao, Y., Reiprich, S., Wegner, M. and Fritzsch, B. (2014) Targeted deletion of Sox10 by Wnt1-cre defects neuronal migration and projection in the mouse inner ear. *PLoS ONE*, 9, e94580.

Mombaerts, P., Wang, F., Dulac, C., Chao, S.K., Nemes, A., Mendelsohn, M., *et al*. (1996) Visualizing an olfactory sensory map. *Cell*, 87, 675–686.

Morrison, E.E. and Graziadei, P.P. (1983) Transplants of olfactory mucosa in the rat brain I. A light microscopic study of transplant organization. *Brain Research*, 279, 241–245.

Nieuwkoop, P. and Faber, J. (1994) Normal table of *Xenopus Laevis* (Daudin): a systematical and chronological survey of the development from the fertilized egg till the end of metamorphosis. New York: Garland Publishing.

Patel, A.V., Huang, T. and Krimm, R.F. (2010) Lingual and palatal gustatory afferents each depend on both BDNF and NT-4, but the dependence is greater for lingual than palatal afferents. *Journal of Comparative Neurology*, 518(16), 3290–3301.

Rohregger, M. and Dieringer, N. (2003) Postlesional vestibular reorganization improves the gain but impairs the spatial tuning of the maculo-ocular reflex in frogs. *Journal of Neurophysiology*, 90, 3736–3749.

Sperry, R.W. (1963) Chemoaffinity in the orderly growth of nerve fiber patterns and connections. *Proceedings of the National Academy of Sciences*, 50, 703–710.

Stout, R. and Graziadei, P. (1980) Influence of the olfactory placode on the development of the brain in *Xenopus laevis* (Daudin): I. Axonal growth and connections of the transplanted olfactory placode. *Neuroscience*, 5(12), 2175–2186.

Straka, H., Fritzsch, B. and Glover, J.C. (2014) Connecting ears to eye muscles: evolution of a 'simple' reflex arc. *Brain, Behavior and Evolution*, 83, 162–175.

Straka, H. and Simmers, J. (2012) *Xenopus laevis*: an ideal experimental model for studying the developmental dynamics of neural network assembly and sensory-motor computations. *Developmental Neurobiology*, 72, 649–663.

Swanson, G.J., Howard, M. and Lewis, J. (1990) Epithelial autonomy in the development of the inner ear of a bird embryo. *Developmental biology*, 137, 243–257.

Tonniges, J., Hansen, M., Duncan, J., Bassett, M., Fritzsch, B., Gray, B., *et al*. (2010) Photo-and bio-physical characterization of novel violet and near-infrared lipophilic fluorophores for neuronal tracing. *Journal of microscopy*, 239, 117–134.

Yang, T., Kersigo, J., Wu, S., Fritzsch, B. and Bassuk, A.G. (2017) Prickle1 regulates neurite outgrowth of apical spiral ganglion neurons but not hair cell polarity in the murine cochlea. *PLoS ONE*, 12, e0183773.

Yntema, C. (1955) Ear and nose. *Analysis of Development*, 415–428.

Zarei, K., Elliott, K.L., Zarei, S., Fritzsch, B. and Buchholz, J.H.J. (2017) A method for detailed movement pattern analysis of tadpole startle response. *Journal of the Experimental Analysis of Behavior*, 108, 113–124.

Zecca, A., Dyballa, S., Voltes, A., Bradley, R. and Pujades, C. (2015) The order and place of neuronal differentiation establish the topography of sensory projections and the entry points within the hindbrain. *Journal of Neuroscience*, 35(19), 7475–7486.

CHAPTER IV:

IMPACT OF 4-AMINOPYRIDINE ON VESTIBULO-OCULAR REFLEX PERFORMANCE

Marliawaty I Gusti Bagus[1 2**], **Clayton Gordy**[1 2**], Rosario Sanchez-Gonzalez[1], Michael Strupp[3], Hans Straka[1*]

[1]Department Biology II, Ludwig-Maximilians-University Munich, Großhaderner Str. 2, 82152 Planegg, Germany

[2]Graduate School of Systemic Neurosciences, Ludwig-Maximilians-University Munich, Großhaderner Str. 2, 82152 Planegg, Germany

[3]Department of Neurology and German Center for Vertigo and Balance Disorders (DSGZ), Ludwig-Maximilians-University, Campus Großhadern, Marchioninistr. 15, 81377 Munich, Germany

**Contributed equally to this work *Correspondence: straka@lmu.de (H.S.)

Contribution of authors:

H.S. conceived the goals and aims. M.I.G.B. and C.G. designed paradigms and collected data for electrophysiological experiments. M.I.G.B., C.G., and R.S.G designed paradigms and collected data for immunohistochemistry experiments. M.I.G.B, C.G., and H.S. analyzed data for electrophysiological experiments. R.S.G and C.G. analyzed data for immunohistochemistry experiments. M.I.G.B, C.G., and H.S. interpreted electrophysiological data. All authors interpreted immunohistochemistry data. M.I.G.B, C.G., and H.S. created electrophysiological figures. R.S.G and C.G. created the immunohistochemistry figure panels. M.I.G.B, C.G., and H.S. wrote the original draft of the manuscript. All authors reviewed and edited the manuscript. Resources, supervision, project administration, and funding acquired by H.S.

My contributions to this publication in detail:

M.I.G.B. and I designed paradigms and collected electrophysiological data on animals prior to and during 4-AP application. H.S., M.I.G.B., and I collaboratively analyzed the electrophysiological data and contributed to the creation of Figures 1 and 2. M.I.G.B., R.S.G, and I performed and collected data from immunohistochemical staining experiments. R.S.G and I analyzed immunohistochemical data

and created Figure 3 panels a-c. H.S. and M.I.G.B. and I contributed to the first draft of the paper and all authors edited all versions of the manuscript.

The following manuscript has been published in the *Journal of Neurology*. Reproduced with permission from Springer Nature. Permission for reuse in this dissertation granted to C.G. by Springer Nature under the Copyright Clearance Center RightsLink license number: 5333530078712.

For online access, please refer to the following: https://doi.org/10.1007/s00415-019-09452-4

Journal of Neurology (2019) 266 (Suppl 1):S93–S100
https://doi.org/10.1007/s00415-019-09452-4

ORIGINAL COMMUNICATION

Impact of 4-aminopyridine on vestibulo–ocular reflex performance

Marliawaty I Gusti Bagus[1,2] · Clayton Gordy[1,2] · Rosario Sanchez-Gonzalez[1] · Michael Strupp[3] · Hans Straka[1]

Received: 6 May 2019 / Revised: 25 June 2019 / Accepted: 26 June 2019 / Published online: 3 July 2019

Abstract

Vestibulo–ocular reflexes (VOR) are mediated by frequency-tuned pathways that separately transform the different dynamic and static aspects of head motion/position-related sensory signals into extraocular motor commands. Voltage-dependent potassium conductances such as those formed by Kv1.1 are important for the ability of VOR circuit elements to encode highly transient motion components. Here we describe the impact of the Kv1.1 channel blocker 4-aminopyridine (4-AP) on spontaneous and motion-evoked discharge of superior oblique motoneurons. Spike activity was recorded from the motor nerve in isolated preparations of *Xenopus laevis* tadpoles. Under static conditions, bath application of 1–10 µM 4-AP increased the spontaneous firing rate and provoked repetitive bursts of spikes. During motion stimulation 4-AP also augmented and delayed the peak firing rate suggesting that this drug affects the magnitude and timing of vestibular-evoked eye movements. The exclusive Kv1.1 expression in thick vestibular afferent fibers in larval *Xenopus* at this developmental stage suggests that the altered extraocular motor output in the presence of 4-AP mainly derives from a firing rate increase of irregular firing vestibular afferents that propagates along the VOR circuitry. Clinically and pharmacologically, the observed 4-AP-mediated increase of peripheral vestibular input under resting and dynamic conditions can contribute to the observed therapeutic effects of 4-AP in downbeat and upbeat nystagmus as well as episodic ataxia type 2, by an indirect increase of cerebellar Purkinje cell discharge.

Keywords Vestibulo–ocular reflex · Semicircular canal · Extraocular motoneurons · Potassium channels

Introduction

The vestibulo–ocular reflex (VOR) is the dominating contributor to gaze stabilization during head/body motion (VOR) [1]. This reflex depends on the transformation of vestibular sensory signals into spatio-temporally adequate extraocular motor commands [2]. The neuronal pathway between inner ear hair cells and extraocular muscle fibers consists of frequency-tuned, parallel information channels [3]. The dynamic diversity of the respective cellular elements correlates with the necessity to encode and mediate signals over a wide range of head motion frequencies and acceleration profiles [4, 5]. Accordingly, the three-neuronal VOR pathway is composed of functional subgroups of cells with distinct intrinsic properties and response dynamics at each hierarchical level [3]. The dynamically different cell types form neuronal filters that are ideally suited for the encoding of particular temporal aspects of head/body movements, respectively [6].

Filter properties of vestibular neurons derive from specific sets of ion channels [7–9]. The highly transient firing

Marliawaty I Gusti Bagus and Clayton Gordy contributed equally to this work.

This manuscript is part of a supplement sponsored by the German Federal Ministry of Education and Research within the funding initiative for integrated research and treatment centers.

✉ Hans Straka
straka@lmu.de

[1] Department Biology II, Ludwig-Maximilians-University Munich, Großhaderner Str. 2, 82152 Planegg, Germany

[2] Graduate School of Systemic Neurosciences, Ludwig-Maximilians-University Munich, Großhaderner Str. 2, 82152 Planegg, Germany

[3] Department of Neurology and German Center for Vertigo and Balance Disorders (DSGZ), Ludwig-Maximilians-University, Campus Großhadern, Marchioninistr. 15, 81377 Munich, Germany

dynamics of neuronal elements that comprise phasic VOR pathway components are caused by voltage-dependent potassium channels of the Kv1.1 type [9]. These channels are abundant in a particular subgroup of first- [8] and second-order vestibular neurons [6, 10]. Blocking Kv1.1 channels with low concentrations of 4-aminopyridine (4-AP) diminishes the transient response dynamics and assigns to these neurons more low-pass filter-like properties [6].

Clinically, 4-AP has been proven as potent therapeutic agent for symptoms associated with vestibular and cerebellar disorders, such as downbeat nystagmus [11–13], episodic ataxia type 2 [14, 15] and upbeat nystagmus [16]. The improvement of the clinical symptoms presumably derives from discharge regularization of vestibular/cerebellar circuit elements [17], potentially in combination with a general increase in firing rate. In upbeat nystagmus, 4-AP evidently acts by restoring visuo-ocular function to suppress the nystagmus [16]. Finally, in a single case with severe head-shaking nystagmus due to neurovascular compression, aminopyridine reduced the symptoms by likely improving action potential propagation including spike conduction along the vestibular nerve [18].

To decipher the neuronal substrates and reveal alterations of VOR performance at the cellular and circuit level following 4-AP administration, we used semi-intact preparations of *Xenopus laevis* tadpoles. The effect of the drug on discharge rate and dynamics of superior oblique (SO) motoneurons was tested at rest and during head/body motion. This allowed estimating the contribution of Kv1.1 channels to the transformation of vestibular sensory signals into extraocular motor commands.

Material and methods

Animals and experimental preparation

Xenopus laevis tadpoles of either sex ($n = 21$) at developmental stages 51–53 [19] were obtained from the in house animal breeding facility at the Biocenter-Martinsried of the Ludwig-Maximilians-University Munich. Tadpoles were maintained in tanks with non-chlorinated water (17–18 °C) at a 12/12 light/dark cycle. Experiments were performed in vitro on semi-intact preparations and comply with the "Principles of animal care", publication No. 86-23, revised 1985 of the National Institute of Health. Permission for these experiments was granted by the Regierung von Oberbayern (ROB-55.2-2532.Vet_03-17-24).

Tadpoles were anesthetized in 0.05% 3-aminobenzoic acid ethyl ester methanesulfonate (MS-222; Pharmaq Ltd. UK) in ice-cold frog Ringer solution (75 mM NaCl, 25 mM $NaHCO_3$, 2 mM $CaCl_2$, 2 mM KCl, 0.1 mM $MgCl_2$, and 11 mM glucose, pH 7.4) and decapitated at the level of the upper spinal cord. The skin was removed, the skull opened from dorsal and the forebrain disconnected [20]. The remaining central nervous system, vestibular sensory periphery with afferent connections, and extraocular motoneuronal projections were functionally preserved. This allowed a natural activation of the VOR on a 6d-motion stimulator (PI H-840, Physik Instrumente, Karlsruhe, Germany). Extraocular motor units were recorded from the trochlear nerve after disconnection from the SO target muscle at the innervation site (Fig. 1a). For all experiments, preparations were placed in a Sylgard-lined recording chamber that was continuously superfused with oxygenated (Carbogen: 95% O_2, 5% CO_2) Ringer solution at a constant temperature of 17.0 ± 0.1 °C.

Electrophysiology and pharmacology

The recording chamber with the preparation affixed to the Sylgard floor was mounted in the center of the rotation axes of the 6d-motion stimulator [21]. Spontaneous and motion-evoked multi-unit spike discharge of the SO nerve was recorded extracellularly (EXT 10-2F; npi electronics; Tamm, Germany) with glass suction electrodes, digitized at 20 kHz (CED 1401, Cambridge Electronic Design, UK) and stored on computer for offline analysis. Suction electrodes were made from borosilicate glass (Science Products, Hofheim, Germany), pulled on a P-87 Brown/Flaming electrode puller. A modulation of SO nerve activity was elicited by sinusoidal rotations (1 Hz; ± 12.5°/s peak velocity) in a plane formed by the ipsilateral posterior (iPC) and contralateral anterior vertical semicircular canal (cAC) pair (Fig. 1a) [22]. The role of Kv1.1 channels in the generation of extraocular motor commands was evaluated by bath application of 4-AP (1–10 µM; Sigma) dissolved in frog Ringer solution.

Data analysis

Peri-stimulus time histograms (PSTHs) of average SO nerve firing patterns over a single head motion cycle were obtained from raw data using Spike2 (Cambridge Electronic Design, UK) scripts. Average responses were calculated from 15 cycles. The phase relation of motion-induced discharge with respect to the table position was obtained by comparing the timing of peak neuronal spike activity with the timing of the maximal table deflection. The PSTHs were further processed and analyzed statistically using Microcal Origin 6.0G (OriginLab Corp., USA). PSTHs were normalized and averaged (± SEM; standard error of the mean) for comparison. Statistical differences were calculated with the Wilcoxon signed-rank test (paired parameters; Prism, Graphpad Software, Inc, USA).

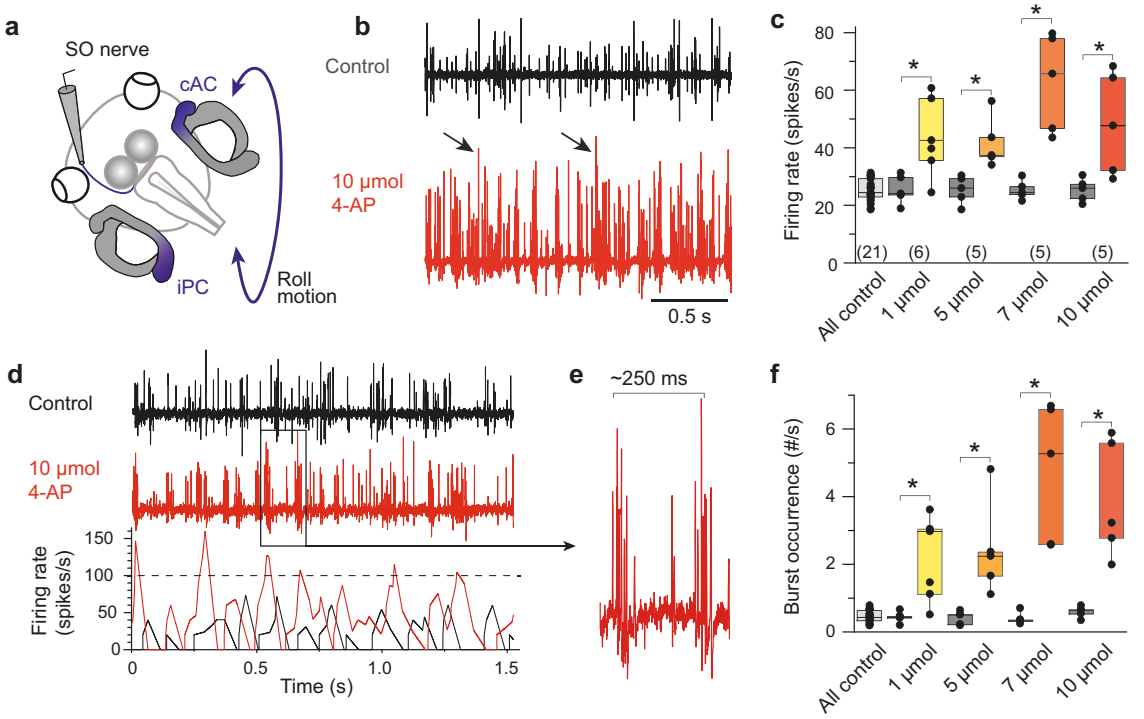

Fig. 1 Impact of 4-aminopyridine (4-AP) on spontaneous discharge of the superior oblique (SO) motor nerve. **a** Schematic of a semi-intact *Xenopus* preparation depicting multi-unit SO nerve recordings and the direction of applied roll motion. **b**, **c** Episode of spontaneous SO nerve discharge before (control, black in **b**) and during bath application of 10 µmol 4-AP (red in **b**); box plot in **c** depicts multi-unit SO nerve resting rates in the absence (gray bars) and presence of 1, 5, 7 and 10 µM 4-AP (colored bars). **d**–**f** Episodes of spontaneous SO nerve discharge (top and middle trace in **d**) and corresponding firing rates (bottom plot in **d**) before (control, black) and during bath application of 10 µmol 4-AP (red); two 4-AP-related bursts are depicted at higher temporal resolution in **e**; box plot in **f** depicts the number of spike bursts (#/s) with interspike frequencies > 100 Hz (sampled in periods of > 60 s, dashed line in bottom trace in **d**) in the absence (gray bars) and the presence of 1, 5, 7 and 10 µM 4-AP (colored bars). Numbers in brackets in **c** indicate the number of preparations and also apply to **f**; $*p < 0.05$ (Wilcoxon signed-rank test) indicates the significance of difference

Tissue processing and immunohistochemistry

Tadpoles ($n = 3$) were deeply anesthetized in 0.05% MS-222 in ice-cold frog Ringer solution. Following decapitation, the dorsal portion of the head and rostral spinal cord was fixed by immersion in 4% paraformaldehyde (PFA) in phosphate-buffered saline (PBS) for 3 h at 4 °C. After washing three times with PBS, the tissue was embedded in 3% agarose, cryoprotected in 30% sucrose in PBS, and cut at a thickness of 20 µm on a cryostat (Leica). To detect Kv1.1 channel, anti-Kv1.1 (APC-009, 1:200, Alomone Labs) primary antibody and subclass-specific secondary antibody labeled with Alexa488 (A-11008, 1:1000, Thermo Fisher) was used. Nuclear staining was performed with 4′6-diamidino-2-phenylindoledihydrochloride (DAPI) (Sigma) to identify cell bodies. All sections were embedded in Aqua Polymount (Polyscience). Images were acquired and analyzed with an Olympus Fluoview confocal microscope with FV10-ASW 2.1 software.

Results

Spontaneous and motion-evoked discharge of SO motor units

The motoneuronal discharge at rest and during roll motion was obtained in vitro by recording multi-unit spike activity of the trochlear nerve after disconnection from its SO target muscle (Fig. 1a). The magnitude of the discharge was variable between different recordings and depended on the number of electrically accessible units within the suction electrode. In the absence of passive head/body motion (black trace in Fig. 1b) the average resting rate was ~ 25 spikes/s (25.3 ± 0.8 spikes/s; mean ± SEM; $n = 21$; light gray bar in Fig. 1c). Natural stimulation of vestibular endorgans was performed by sinusoidal roll motion (1 Hz; ± 12.5°/s peak velocity) in a plane formed by the iPC and cAC pair (dark blue shading in Fig. 1a). This motion caused a robust, phase-timed modulation of the multi-unit spike discharge (black

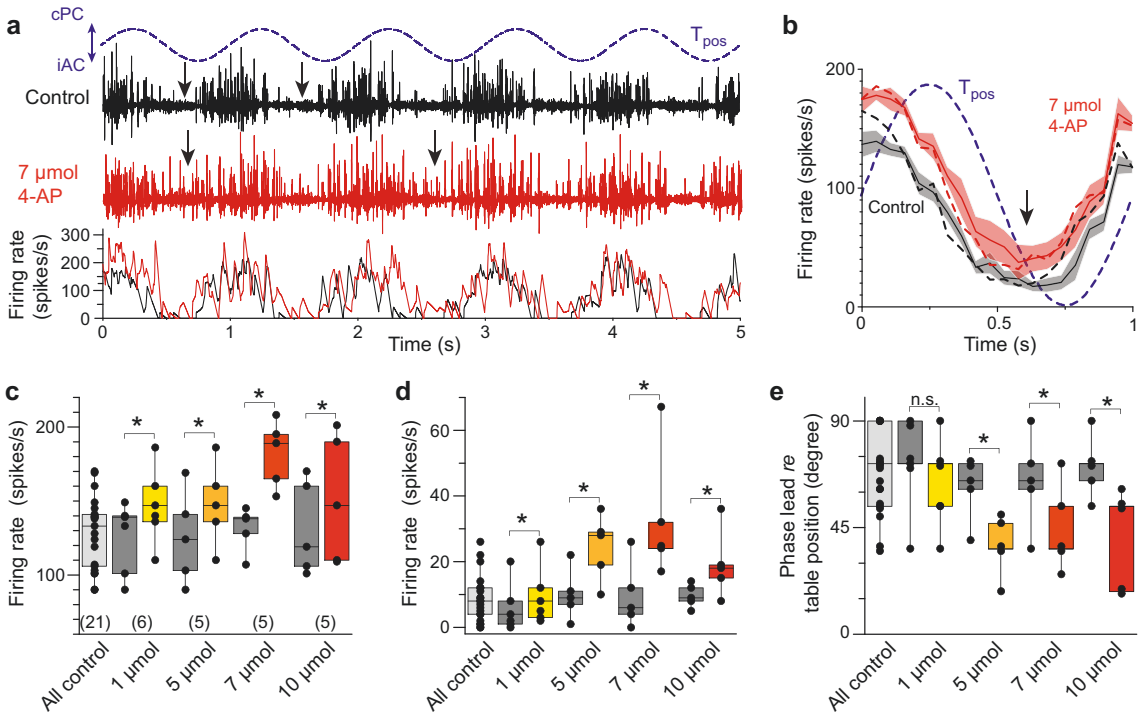

Fig. 2 Impact of 4-aminopyridine (4-AP) on motion-evoked discharge of the superior oblique (SO) motor nerve. **a** SO nerve discharge (top and middle trace) during sinusoidal roll motion (blue sine wave; 1 Hz, ± 12.5°/s peak velocity) and corresponding firing rates (bottom plot) before (control, black) and during bath application of 7 µmol 4-AP (red). **b** Average firing rate modulation over a single cycle (dashed blue sine wave) of roll motion before (control, gray and black curves) and during bath application of 7 µM 4-AP (red and pink curves); solid curves and light shaded areas represent the mean firing rate ± SEM ($n = 5$ preparations); dashed gray and pink curves indicate the average discharge modulation of the typical example shown in **a**. **c**–**e** Box plots depicting peak discharge (**c**), minimal firing rate (**d**; see arrows in **a**, **b**) and phase relation of the response re table position (**e**) during sinusoidal rotation in the absence (gray bars) and presence of 1, 5, 7 and 10 µM 4-AP (colored bars). Numbers in brackets in **c** indicate the number of preparations and also apply to **d**, **e**; $*p < 0.05$ (Wilcoxon signed-rank test) indicates the significance of difference; *n.s.* not significant, T_{pos} table position

trace in Fig. 2a). Firing increased during roll motion in the direction of the iPC with an average peak discharge rate of ~ 130 spikes/s (130.2 ± 5.1 spikes/s; mean ± SEM; $n = 21$) and a phase-lag of ~ 20° re table velocity (21.8° ± 3.9°; mean ± SEM; $n = 21$). This phase relation complies with previously established values and suggests both semicircular canal and otolith hair cells as the origin of the extraocular motor responses [23]. During motion in the direction of the cAC, the spike firing often ceased at the maximal roll position (black trace in Fig. 2b) with an average minimal firing rate of ~ 9 spikes/s (red arrow in Fig. 2b; 8.6 ± 1.6 spikes/s; mean ± SEM; $n = 21$).

Bath application of 4-AP caused an increase of the multi-unit resting discharge (red traces in Fig. 1b, d), which was found to be statistically significant ($p < 0.05$; Wilcoxon signed-rank test) across all concentrations relative to the discharge rate prior to 4-AP application (Fig. 1c). The effect of 4-AP was reversible and usually lasted > 1–2 h but was not further investigated here. The augmentation of the firing rate was accompanied by a recruitment of additional motor units with very large amplitudes (arrow heads in Fig. 1b), which were absent under control conditions. Although spike shape analysis was impossible to perform due to high firing rates of the multi-unit discharge, close inspection of the spikes clearly confirmed a separate class based on spike amplitude, which only appeared after 4-AP application. These neurons likely coincide with the previously reported subgroup of large, high-dynamic extraocular motoneurons with very low resting rates in *Xenopus* tadpoles [20]. In addition, 4-AP altered the irregular spontaneous discharge into a pattern that consisted of short, repetitive bursts of spikes (Fig. 1d, e). These bursts contained few spikes with interspike frequencies well above 100 Hz (see black curve at bottom of Fig. 1d) and, when sampled over a period of > 60 s, were relatively rare under control conditions (gray bars in Fig. 1f). The occurrence of these bursts increased considerably after bath application of 4-AP in a dose-dependent manner (colored bars in Fig. 1f) with an average inter-burst interval of 200–250 ms (Fig. 1e) at 4-AP concentrations > 7 µM. The slight decrease of firing rate increase and burst occurrence for 4-AP concentrations > 7 µM potentially derives from a sustained depolarization of the membrane potential beyond

spike threshold and a consequent dropout of action potentials in some neurons along the VOR pathway.

The robust, phase-timed modulation of the multi-unit discharge during sinusoidal roll motion stimulation persisted in the presence of 4-AP (red trace in Fig. 2a, b). However, the peak discharge increased at all concentrations of 4-AP compared to control conditions (colored bars in Fig. 2c). In addition, the burst-like firing in the presence of 4-AP was also maintained during motion stimulation, causing a rather noisy PSTH after averaging the discharge over single motion cycles (Fig. 2a, b). During roll motion in the direction of the cAC, the spike discharge did not cease, as often seen prior to drug application, but usually continued firing (arrows in Fig. 2a, b). Calculation of the respective averages over single cycles revealed a significant increase of the minimal discharge (arrow in Fig. 2b and colored bars in Fig. 2d) from ~ 9 spikes/s under control conditions to ~ 30 spikes/s in the presence of 7 µM 4-AP (32.8 ± 8.9 spikes/s; mean ± SEM; $n = 5$). In addition to the generally elevated firing rates, the motion-evoked responses altered the phase re velocity from ~ 20° in controls to > 45° in the presence of 4-AP (colored bars in Fig. 2e).

Immunohistochemistry of Kv1.1 in vestibular pathways

The substrate for 4-AP is a voltage-dependent potassium conductance generated by the Kv1.1 channel. Immunohistochemical labeling with a Kv1.1 antibody successfully identified populations of vestibular afferent fibers and their associated cell bodies in the ganglion of Scarpa (Fig. 3a). Ganglion cells were found to be non-uniformly labeled, with only a specific subset of cells with particularly large somata being Kv1.1-immuno-positive (Fig. 3a, see arrowhead). Processes of Kv1.1-immuno-positive vestibular ganglion cells were observed to project peripherally and centrally. Peripheral processes appeared to project into the vestibular sensory epithelia within the inner ear (VE in Fig. 3a), while centrally projecting processes extended with the VIIIth nerve into the dorsal part of the hindbrain (Fig. 3b, c). These latter central projections terminated in topographically identified vestibular regions and likely connect with central vestibular targets, confirming the contribution of Kv1.1-expressing afferent fibers to vestibulo–motor transformations (Fig. 3d).

Discussion

The three major findings of this study were as follows: first, systemically applied 4-AP increased the spontaneous discharge of SO motoneurons and caused repetitious bursts of spikes under static conditions; second, during sinusoidal head motion, the peak firing rate was augmented; third, the overall higher firing rates and phase-shifted cyclic extraocular motor output in the presence of 4-AP likely derive from blocked Kv1.1 channels in thick vestibular nerve afferents. Our findings suggest propagation of the pharmacologically altered afferent firing rate properties throughout the VOR network.

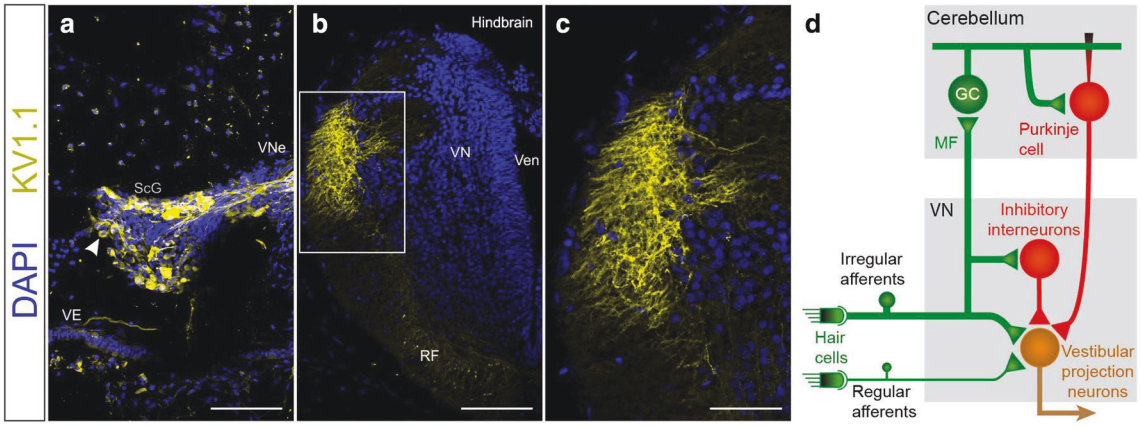

Fig. 3 Kv1.1-immuno-histochemistry and outline of central vestibular and cerebellar circuits. **a**–**c** Coronal sections through a *Xenopus laevis* hindbrain labeled with an antibody against Kv1.1 (yellow) and counterstained with DAPI (blue); cell bodies of Scarpa's Ganglion (ScG, arrowhead) and associated proximal and distal central processes of Kv1.1-positive cells (**a**) outlining projections to the vestibular sensory epithelia (VE) and fasciculation within the vestibular nerve (VNe); distal projections of Kv1.1-positive afferent fibers in the dorsal region of the hindbrain at a lower (**b**) and higher (**c**, panel box in **b**) magnification. **d** Schematic of central vestibular and cerebellar circuits; axon collaterals of irregular vestibular afferents activate local vestibular interneurons (red) and as mossy fibers (MF) activate granule cells (GC) and consequently cerebellar Purkinje cells, which in turn mediate an inhibition (red) onto a directly activated (green) central vestibular projection neurons (light brown). *RF* reticular formation, *Ven* fourth ventricle, *VN* vestibular nuclei. Scale bars are 100 µm in **a**, **b** and 50 µm in **c**

Neuronal site of 4-AP action

The restriction of Kv1.1 immuno-positivity within the three-neuronal VOR pathway to large caliber vestibular nerve afferents in *Xenopus* tadpoles suggests that SO nerve firing rate alterations in the presence of 4-AP derive exclusively from a pharmacological block of voltage-dependent potassium conductances in these afferent fibers. The obvious lack of Kv1.1 immuno-labeled central vestibular neurons in tadpoles is at variance with the presence of large-celled Kv1.1 immuno-positive phasic second-order vestibular neurons in adult frogs [10]. This difference is likely related to different requirements for the detection of swimming-related motion dynamics of larval and adult frogs, and as such an eco-physiological adaptation of the membrane properties of central vestibular neurons [24]. The lack of Kv1.1 channels in vestibular neurons of tadpoles complies with the more tonic membrane properties of these neurons in larvae compared to those of adult frogs. Despite the absence of central Kv1.1 immuno-positive VOR neurons in tadpoles, the impact of 4-AP on a subset of vestibular afferents has a sufficiently profound impact on the spontaneous and motion-evoked extraocular motor spike discharge (Figs. 1, 2). This confirms the dominating role of afferent inputs for sensory-motor transformations of vestibular signals [25].

Increased SO nerve resting rates

Extraocular motor discharge depends on the integrity of vestibular sensory inputs, and thus on the firing rate of semicircular canal and otolith afferent nerve fibers as indicated by imbalanced SO motoneuronal spike discharge after unilateral transection of the VIIIth nerve [25]. Moreover, the localization of Kv1.1 channels in thick vestibular afferents suggests that the augmented SO spike discharge in the presence of 4-AP derives exclusively from a firing rate increase of the latter fibers. This complies with the observation that bath application of similar concentrations of 4-AP in larval *Xenopus* causes an increase and regularization of the spontaneous firing rate as well as an augmentation and phase shift of motion-evoked responses exclusively in thick, irregular but not in thinner regular firing vestibular afferent fibers [26], compatible with their Kv1.1 immuno-positivity (Fig. 3a, b). Thus, based on the organization of VOR circuits as frequency-tuned channels and the exclusive Kv1.1 immuno-labeling of thick vestibular afferents, the 4-AP-provoked phase shift of cyclic extraocular motor responses directly derives from a block of the transient response behavior and consequent temporal extension of the spike firing of phasic, irregularly firing afferents [26]. This afferent firing rate alteration propagates through central vestibular neurons onto extraocular motoneurons where corresponding changes were encountered (Figs. 1, 2). A firing rate increase and regularization of Purkinje cell spike discharge was also observed in mutant mice with episodic ataxia type 2 following 4-AP application [27]. This latter finding, however, does not exclude that the observed effect is only indirect and due to the alteration of the discharge pattern of irregular vestibular afferents that as mossy fibers represent a major source of synaptic input to the cerebellum (Fig. 3d). Interestingly, however, the 4-AP-induced discharge regularization of irregular firing vestibular afferents is not mirrored by extraocular motoneurons. Rather, the occurrence of repetitious spike bursts suggests additional synaptic modifications of the regularized vestibular afferent input along the VOR circuitry.

4-AP-induced extraocular motor spike bursts

A likely synaptic substrate for generating repetitive spike bursts following application of 4-AP is a cyclic truncation of the excitation of central vestibular neurons by an inhibition that derives from local vestibular side loops [28] and cerebellar Purkinje cells (Fig. 3d) [29]. Both circuits are activated by irregular vestibular afferent fibers [9, 28], which in the presence of the Kv1.1 channel blocker increase the synaptic drive of these networks but also facilitate the feed-forward synaptic inhibition. These inhibitory side loops are capable of truncating the direct monosynaptic excitation that is mediated from irregular afferents onto central vestibular neurons (Fig. 3d). This creates more or less rhythmic spike bursts that are interrupted by variably sized and timed inhibition. Thus, while 4-AP regularizes the discharge of irregular firing vestibular afferents and that of directly connected postsynaptic elements, additional inhibitory circuits shape the firing pattern to generate oscillating spike bursts.

Clinical implications

The observed changes by the Kv1.1 blocker 4-AP in *Xenopus* tadpoles predict that 4-AP-induced increased vestibular afferent discharge—as the main driving force for all vestibular circuits—can contribute to the improvement of symptoms in patients treated with 4-AP for various diseases, such as downbeat and upbeat nystagmus or episodic ataxia type 2. This assumption is further supported by the fact that irregular firing vestibular afferents in amphibians and mammals have similar conductances [8, 26] and central connectivity [29]. However, 4-AP-related improvements of gaze and posture deficits in patients might be dominated by drug effects at multiple sites including central vestibular [9] and cerebellar neurons [27], potentially explaining the range of ameliorated behaviors and response patterns. The 4-AP sensitivity of multiple central areas is in fact supported by the abundance of Kv1.1 immuno-positive neurons in cerebellar and vestibular circuits in mice [30]. Nonetheless,

the current results suggest that part of the reported 4-AP-induced improvements of clinical symptoms might also derive from a firing rate increase of vestibular nerve afferents, which so far has been underestimated as a potential target for this drug and the origin of improved symptoms. A contribution of afferent fibers is supported by the fact that the morpho-physiological organization of the peripheral and central vestibular system is highly conserved across vertebrates [2] including the presence of Kv1.1 channels in vestibular afferents of rodents [8], primates and humans (Mayadali and Horn, personal communication).

A large fraction of firing rate regularization of vestibular and cerebellar neurons in mammals [17] as well as the improved vestibular reflexes in patients [31] in the presence of 4-AP thus potentially depends on a firing rate increase in vestibular afferents. This can augment the direct effects of 4-AP on cerebellar Purkinje cells whose resting discharge rate and excitability are also increased by 4-AP at the same concentrations as used in the current and an earlier study [32]. In addition, in an animal model of episodic ataxia type 2, the tottering mouse, 4-AP reduced the irregularity of spontaneous firing of cerebellar Purkinje cells. In conclusion, the 4-AP-induced increase of peripheral vestibular input under static and dynamic conditions in the current study might explain at least in part the therapeutic effects of 4-AP in downbeat nystagmus and cerebellar ataxia. Given the robust increase and regularization of the firing rate in irregular/phasic vestibular afferents, it is possible that 4-AP might also have beneficial effects for peripheral vestibular disorders through a partial or complete rescue of spontaneous afferent activity.

Acknowledgements The authors acknowledge financial support from the German Science Foundation (CRC 870; STR 478/3-1; RTG 2175) and the German Federal Ministry of Education and Research under the Grant code 01 EO 0901.

Compliance with ethical standards

Conflicts of interest The authors declare no competing financial interests.

Ethical standards All studies have been approved by the appropriate ethics committee (ROB-55.2-2532.Vet_03-17-24) and have therefore been performed in accordance with the ethical standards laid down in the 1964 Declaration of Helsinki and its later amendments.

References

1. Angelaki DE, Cullen KE (2008) Vestibular system: the many facets of a multimodal sense. Annu Rev Neurosci 31:125–150
2. Straka H, Fritzsch B, Glover JC (2014) Connecting ears to eye muscles: evolution of a 'simple' reflex arc. Brain Behav Evol 83:162–175
3. Straka H, Lambert FM, Pfanzelt S, Beraneck M (2009) Vestibulo–ocular signal transformation in frequency-tuned channels. Ann NY Acad Sci 1164:37–44
4. Carriot J, Jamali M, Chacron MJ, Cullen KE (2014) Statistics of the vestibular input experienced during natural self-motion: implications for neural processing. J Neurosci 34:8347–8357
5. Hänzi S, Straka H (2017) Developmental changes in head movement kinematics during swimming in *Xenopus laevis* tadpoles. J Exp Biol 220:227–236
6. Beraneck M, Straka H (2011) Vestibular signal processing by separate sets of neuronal filters. J Vestib Res 21:5–19
7. Goldberg JM (2000) Afferent diversity and the organization of central vestibular pathways. Exp Brain Res 130:277–297
8. Eatock RA, Songer JE (2011) Vestibular hair cells and afferents: two channels for head motion signals. Annu Rev Neurosci 34:501–534
9. Straka H, Vibert N, Vidal PP, Moore LE, Dutia MB (2005) Intrinsic membrane properties of vertebrate vestibular neurons: function, development and plasticity. Prog Neurobiol 76:349–392
10. Beraneck M, Pfanzelt S, Vassias I, Rohregger M, Vibert N, Vidal PP, Moore LE, Straka H (2007) Differential intrinsic response dynamics determine synaptic signal processing in frog vestibular neurons. J Neurosci 27:4283–4296
11. Strupp M, Schüler O, Krafczyk S, Jahn K, Schautzer F, Büttner U, Brandt T (2003) Treatment of downbeat nystagmus with 3,4-diaminopyridine: a placebo-controlled study. Neurology 61:165–170
12. Claassen J, Spiegel R, Kalla R, Faldon M, Kennard C, Danchaivijitr C, Bardins S, Rettinger N, Schneider E, Brandt T, Jahn K, Teufel J, Strupp M, Bronstein A (2013) A randomised double-blind, cross-over trial of 4-aminopyridine for downbeat nystagmus—effects on slowphase eye velocity, postural stability, locomotion and symptoms. J Neurol Neurosurg Psychiatry 84:1392–1399
13. Strupp M, Teufel J, Zwergal A, Schniepp R, Khodakhah K, Feil K (2017) Aminopyridines for the treatment of neurologic disorders. Neurol Clin Pract 7:65–76
14. Strupp M, Kalla R, Dichgans M, Freilinger T, Glasauer S, Brandt T (2004) Treatment of episodic ataxia type 2 with the potassium channel blocker 4-aminopyridine. Neurology 62:1623–1625
15. Strupp M, Kalla R, Claassen J, Adrion C, Mansmann U, Klopstock T, Freilinger T, Neugebauer H, Spiegel R, Dichgans M, Lehmann-Horn F, Jurkat-Rott K, Brandt T, Jen JC, Jahn K (2011) A randomized trial of 4-aminopyridine in EA2 and related familial episodic ataxias. Neurology 77:269–275
16. Glasauer S, Kalla R, Büttner U, Strupp M, Brandt T (2005) 4-Aminopyridine restores visual ocular motor function in upbeat nystagmus. J Neurol Neurosurg Psychiatry 76:451–453
17. Glasauer S, Rössert C, Strupp M (2011) The role of regularity and synchrony of cerebellar Purkinje cells for pathological nystagmus. Ann N Y Acad Sci 1233:162–167
18. Strupp M, Querner V, Eggert T, Straube A, Brandt T (2003) 3,4-Diaminopyridine improves head-shaking nystagmus caused by neurovascular cross-compression. Ann N Y Acad Sci 1004:506–510
19. Nieuwkoop PD, Faber J (1994) Normal table of *Xenopus laevis* (Daudin): a systematical and chronological survey of the development from the fertilized egg till the end of metamorphosis. Garland Publishing, New York
20. Dietrich H, Glasauer S, Straka H (2017) Functional organization of vestibulo–ocular responses in abducens motoneurons. J Neurosci 37:4032–4045
21. Soupiadou P, Branoner F, Straka H (2018) Pharmacological profile of vestibular inhibitory inputs to superior oblique motoneurons. J Neurol 265(Suppl 1):S18–S25

22. Branoner F, Straka H (2015) Semicircular canal-dependent developmental tuning of translational vestibulo–ocular reflexes in *Xenopus laevis*. Dev Neurobiol 75:1051–1067
23. Lambert FM, Beck JC, Baker R, Straka H (2008) Semicircular canal size determines the developmental onset of angular vestibuloocular reflexes in larval *Xenopus*. J Neurosci 28:8086–8096
24. Beraneck M, Lambert FM, Straka H (2008) Membrane properties of central vestibular neurons in larval *Xenopus*: eco-physiological adaptations to locomotor strategy. Soc Neurosci Abstr 34(169):12
25. Branoner F, Straka H (2018) Semicircular canal influences on the developmental tuning of the translational vestibulo–ocular reflex. Front Neurol 9:404
26. Gensberger KD, Wühr M, Hoffman LF, Paulin MG, Straka H (2017) Spike time regularity of horizontal canal afferent fibers as decisive factor for motion encoding in *Xenopus laevis* tadpoles. Soc Neurosci Abstr 43(225):11
27. Alviña K, Khodakhah K (2010) The therapeutic mode of action of 4-aminopyridine in cerebellar ataxia. J Neurosci 30:7258–7268
28. Straka H, Dieringer N (2000) Convergence pattern of uncrossed excitatory and inhibitory semicircular canal-specific inputs onto second-order vestibular neurons of frogs. Exp Brain Res 135:462–473
29. Straka H, Dieringer N (2004) Basic organization principles of the VOR: lessons from frogs. Prog Neurobiol 73:259–309
30. Wang H, Kunkel DD, Schwartzkroin PA, Tempel BL (1994) Localization of Kv1.1 and Kv1.2, two K channel proteins, to synaptic terminals, somata, and dendrites in the mouse brain. J Neurosci 14:4588–4599
31. Kalla R, Teufel J, Feil K, Muth C, Strupp M (2016) Update on the pharmacotherapy of cerebellar and central vestibular disorders. J Neurol 263(Suppl 1):S24–S29
32. Etzion Y, Grossman Y (2001) Highly 4-aminopyridine sensitive delayed rectifier current modulates the excitability of guinea pig cerebellar Purkinje cells. Exp Brain Res 139:419–425

CHAPTER V:

DISCUSSION AND FUTURE DIRECTIONS

This dissertation aimed at exploring neuronal plasticity in sensorimotor brainstem vestibular networks. In the chapters above I have presented empirical data which have expanded on our erstwhile knowledge of the events and principles which occur during adaptive reorganization of the vestibular system. I primarily utilized the vestibular-ocular reflex as a model system to approximate these events both during nascent development and in a case of acute signaling disruption on mature circuits. As a main result of this work, the vestibular system reliably demonstrated a considerable plasticity in sensorimotor processing. The major findings across these three studies converges to the following important two points: 1) *despite conditions which challenge stereotyped sensory encoding, execution of VOR responses was a consistent functional outcome*. This outcome likely arises from a variable suite of mechanisms which 2) *converge on establishing and maintaining homeostatic activity levels which can modulate along a dynamic range*. However, preservation of the ability to execute a VOR following such sensory challenges does not imply that consistent spatiotemporal perfection will exist in these transformations. Indeed, the results here demonstrate a spectrum of success with respect to VOR production. Nonetheless, that VOR transformations are present in any case is a striking representation of the efficacy with which this system can reorganize in order to produce environmentally relevant computations.

While the individual discussion sections in the proceeding chapters provide experiment-specific considerations with focus on specific biological questions, here I will provide a more holistic discussion of the main findings presented above. In the following pages I will make emphasis on the observed permissive functional bandwidths across the three different manipulations. In addition, I discuss the limitations of establishing such bandwidths, as well as speculate as to the potential causative mechanisms contributing to these observed results by highlighting specific functional and anatomical evidence. Finally, I will present some considerations on potential broad-scale implications of these results and state possible directions for future vestibular research.

Maintenance of dynamic processing bandwidths

Detection of the sensory world permits organisms to respond to their surroundings. Environments can be complex, and evolution has optimized the central and peripheral nervous systems to detect many of the complex features of these environments (Linford et al., 2011). Through these detection measures, intricate motor commands can be consistently generated which drive necessary animal behaviors (Linford et al., 2011). However, sensorimotor structures are not perfectly suited to respond with immediate perfection to all manner of possible stimuli complexities. Balancing the need to maintain stereotyped processing measures while also maintaining a degree of flexibility is the purview of neuronal plasticity. Thus, adaptive reorganization in neuronal networks makes use of existing structures and processes (Pascual-Leone et al., 2005). The discussion of these events in light of the results presented here will therefore be examined in the context of general functional principles of the vestibular system.

A hallmark feature of vestibular sensory encoding is in establishing a baseline level of symmetric and balanced bilateral activity which can be cyclically modulated. Such activity levels and dynamic modulations are apparent at the level of afferent fibers, central vestibular neurons, and extraocular motoneurons (Fetter, 2007; Beraneck and Idoux, 2012; Branoner and Straka, 2018; Paulin and Hoffman, 2019), and are ultimately driven by afferents themselves (Fetter, 2007). Acute unilateral loss of vestibular input is sufficient to evoke an imbalance in activity levels throughout the elements of the entire VOR circuit (Dieringer and Precht, 1977; Ris et al., 1997; Lambert et al., 2013) even in higher order centers beyond VOR pathways (Zwergal et al., 2016). Following, resulting sensory imbalances are interpreted by the CNS as a consistent detection of self-motion (Fetter, 2016) which is in mismatch with information from other sensory modalities. In a similar fashion to the amelioration events which follow such an acute loss, the data presented in all three manipulation studies in this dissertation suggest a similar response course which aimed at establishing dynamic ranges of activity modulation. *Xenopus* tadpoles in chapter II (Gordy and Straka, 2022) developed with only a single ear. Without bilateral afferent fibers, a progressive yet severe imbalance of activity onto vestibular projection neurons would have likely occurred during normal development. Tadpoles from chapter III (Gordy et al., 2018) likewise developed with an imbalance, albeit the supernumerary spinal-cord originating ear would have created a graded difference between the two sides, as evident from the mostly ipsilateral projections (chapter III, Figure 3-4). An equalization of this imbalance is the inferred developmental outcome across these manipulations, largely given that the recorded extraocular motor nerves presented with sustained base level firing rates (chapter III, Figure 5; chapter II, Figure 4, S4). Indeed, resting rates in these animals are rather comparable to control spontaneous discharge

rates from animals in chapter II and IV of this dissertation (compare Figures S4, 1, and 5 from chapters II, IV and III, respectively). In the case of one-eared animals, such levels were even indistinguishable from controls (chapter II, Figure S4). Immediate unilateral vestibular loss in *Xenopus* presents with a complete absence of contralateral extraocular firing discharge (Lambert et al., 2013; Branoner and Straka, 2018) with resulting behavioral and morphological consequences (Lambert et al., 2013; Soupiadou et al., 2020). That the former result was not observed in these animals can most parsimoniously be explained by an equalization of activity levels on both sides. This is consistent with previous observations following unilateral acute lesion that demonstrated equalization in bilateral activity levels in the vestibular nuclei (Vibert et al., 1999; Paterson et al., 2005) that has been demonstrated in a variety of species such as frog (Dieringer and Precht, 1977), guinea pigs (Ris et al., 1995; Ris et al., 1997), and rat (Hamann and Lannou, 1988). Examination of afferent discharge levels and recording or functional imaging of vestibular neurons would be of benefit to experimentally verify such a condition and uncover possible time course and localization metrics.

Homogenization of activity levels by itself, however, is rather useless for dynamic vestibular processing. Transient motion-related modulation of symmetric levels is a critical feature for VOR transformations (see above, Fetter, 2007). In fact, the push-pull arrangement for VOR processing is contingent on these dynamics and in the absence of modifiable activity levels the generation of appropriate motor transformations would be impaired. Indeed, assumed full loss of vestibular input on both sides has been reported to drive near-absent or fully-absent VOR function with mitigating compensatory catch-up saccades, at least in patients (Strupp et al., 2017). While one- and three-eared tadpoles generated a symmetric resting activity state, they also exhibited the ability to modulate around their homeostatic levels to some degree. One-eared tadpoles were found to do this remarkably well when profiled at the abducens motoneuron level (chapter II, Figure 4, S4), which resulted in behaviorally relevant movements of the eyes (chapter II, Figure 1-3) and demonstrated period discharge modulations which extended below and above their resting rates. Following vestibular nerve lesions in ranid frogs, abducens nerve discharge modulations were present but only cyclic below resting activity (Rohregger and Dieringer, 2002). Comparison between the later findings and one-eared tadpoles here, which developed with only a singular ear and with prominent bilateral homogeneity, might suggest that activity equalizations are a prerequisite for robust VOR, and/or are followed by other adaptive modifications. While left (opposite to the singular ear) abducens nerve discharge dynamics here were far more spatio-temporally appropriate than right (same side as the singular ear) abducens nerve counterparts, the later were likely influenced by their differentially tuned responses (chapter II, Figure 4). Three-eared frogs were capable of this as well, with considerable modulatory ability during rotation and thus concomitant activation of all three inner ears. The

comparable response level during galvanic evoked stimulation of only the two native ears indicated that additional input did not negatively influence VOR transformations (chapter III, Figure 5D, F), which suggests that the maintenance of a dynamic processing range is ensured despite additional and asymmetric input. An argument could be made that the transplanted ear adjacent to the spinal cord might not be sufficiently developed and thus not be co-activated during natural stimuli. By extension, VOR transformations would occur consistently through canonical pathways with little contribution from the third ear. While inner ear structural characterizations (Bever and Fekete, 2002; Bever et al., 2003) would help shed light on the possibility of such a claim, particularly for the semi-circular canal dimensions (Calabrese and Hullar, 2006), the selective stimulation of the third ear helps reduce ambiguity to some extent. Galvanic activation of this ear produced excitatory drives above resting rates (chapter III, Figure 5G-H) though it lacked sensory relay through inhibitory ipsilateral circuits. That the third ear can integrate its input faithfully suggests some degree of co-activation is possible, particularly given that activity is speculated to help consolidate the initially broad innervation of afferents into the vestibular nuclei (Straka et al., 1997; Straka et al., 2002; Straka et al., 2014) and these afferents appear to connect only with crossed excitatory pathways. With respect to the lack of inhibitory circuit contributions, a potential explanation to this observation may be a lack of anatomical connections entirely, or alternatively that excitatory drives on these neurons are simply too weak to be effective. If the exclusive crossed-excitatory circuit connections are the default state for transplanted additional input remains to be tested, though it likely is not the case if given a full complement of afferent fibers. That only a qualitatively small number of fibers reached the nuclei relative to native ears here (chapter III, Figure 3-4), as compared to third ears transplanted in the otic region (Elliott et al., 2015b), indicates that only a partial contribution of the third ear occurred in this study. If the introduction of additional afferent fibers would permit inhibitory pathway responses would be a valid future assessment.

While one- and three-eared animals offer a unique perspective on imbalanced input between bilateral sides, chapter IV generated an experimental condition where a signaling change was executed uniformly. In these animals, dynamic processing bandwidths were challenged by the elevation of resting discharge rates of afferent fibers (chapter IV, Figure 1, 2). The regularization of phasic sensory neuron responses into more sustained, tonic, firing was the driving force of this elevation (chapter IV, Figure 1) and was inferred to continue through the entire VOR circuit by recordings of the superior oblique motor nerve. A “simple” elevation of resting activity in VOR circuits would not require any plasticity-based homogenization, as is occurring following sudden loss (e.g., Beraneck et al., 2003), as differences between bilateral activity levels remain consistent during pharmacological bath application. However, the increasing of base level activity has the potential to

enforce an upper saturation limit of VOR elements. Despite pushing VOR bandwidths closer toward an extreme upper limit however, 4-AP exposed tadpoles were able to successfully execute VOR transformations (chapter IV, Figure 2). Though these responses were in general more elevated in overall discharge rate across the cycle and delayed relative to controls, modulation was clearly present. Importantly, a cyclic high frequency bursting was noted during periods absent of stimulation. This bursting phenotype, which as mentioned previously is speculated to be the result of co-opting feedback inhibitory side loops either locally within the vestibular nuclei (Straka and Dieringer, 1996) or though the cerebellum (Boyden et al., 2004), likely contributes to the ability to appropriately execute VOR responses. Regardless of the mechanisms involved (which will be discussed below) the overall ability of these tadpoles to modulate extraocular activity despite elevated base firing levels suggests that if processing bandwidths become too uniform or restrictive, alternate methods can assist in helping generate rhythmic activity levels. Therefore, in these animals, the general strategy appears to be recruitment of feedback loops imposed on sustained activity levels rather than reducing activity levels downward. An obvious caveat to this interpretation is the fact that our functional assessments were conducted on a relatively short time scale which restricts the resolution of plasticity measures to the window examined. Timing is an important factor for VOR adaptation and plasticity (Titley et al., 2007), particularly in the case of long-term consolidation in vestibular nuclei (Kassardjian et al., 2005). Changes of vestibular neuron intrinsic membrane properties (e.g., Him and Dutia, 2001) would likely only make contributions during longer time scales. Additionally, the 4-AP induced elevation could perhaps not be as influential to narrowing permissive bandwidths as expected given that these animals were exposed up to only 10 micromolar concentrations. Future studies would benefit from examinations during longer time periods.

In summary, the key findings of these experiments can be inferred to follow the already established observations that plasticity amelioration of atypical sensory conditions consist of equalizing asymmetric activity levels and/or ensuring that functional bandwidths remain (Dieringer and Precht, 1977; Ris et al., 1997; Vibert et al., 1999; Dutia, 2010). These findings, particularly chapter II and III, add new perspectives to vestibular compensation which has previously been overwhelmingly focused on unilateral loss in mature fully formed circuits beyond select studies examined in the embryo (e.g., Rayer et al., 1983; Rayer and Horn, 1986). That developmental imbalances are likely regulated in a similar manner gives merit to the concept that sudden adaptive plasticity mechanisms recapitulate those which occur during development (Tien and Kerschensteiner, 2018). Such processes are not perfect, however. Dynamic symptoms following acute sensory imbalance hardly ever recover fully (Curthoys, 2000) or can occur unexpectedly following certain conditions (Hamann et al., 1998). The data presented here are not quite of a similar inclination. Transformations often demonstrated a

general inability to reach control levels properly, but nonetheless were executable (chapters II, III, IV). However, such detriments may not be particularly relevant during behavior, as other substituting mechanisms may assist where the VOR fails (Dieringer, 1998; Vibert et al., 1999, see also the discussion of chapter II). The following section will explore this concept in more detail.

Multi-level reorganization

Attempts to equalize activity imbalances and maintain dynamic bandwidths require suitable neuronal and behavioral mechanisms. The veritable suite of possible mechanisms during vestibular compensation, and thus plasticity in this system, can range across systemic levels (see introductory chapter; also, Dutia, 2010). While such methods are very likely to be shared to some extent across the manipulations presented here, they nonetheless will be considered separately, largely due to the disparity in the individual manipulations themselves.

One-eared animals demonstrated a remarkable VOR execution ability during off-direction rotation of the singular ear, which came at the expense of on-direction activity (chapter II, Figure 2). Bidirectional sensitivity is present in mechanosensory hair cells (Hudspeth, 1985). Despite this sensitivity however, it is important to note that unmanipulated individual inner ears facilitate VOR circuit components during on-direction rotation only. That the singular ear in these animals can contribute to excitatory and inhibitory VOR computations during off-direction rotation suggests that a considerable level of reorganization occurred during development. The location of such reorganization could occur at many sites rather than a singular location/mechanism (chapter II, Figure 5). Given the substantial temporal delay of VOR eye movements and frequent instances of improperly tuned ipsilateral (with respect to the singular ear) abducens motoneurons, the prevailing hypothesis is that crossed commissural connections play a significant role. Whether disfacilitation of the singular ear provokes an increase in activity through inhibitory or excitatory commissural fibers is a necessary next set of experiments. While both could be possible (Dieringer and Precht, 1977; Ris et al., 1995), it is compelling to suspect that excitatory commissural signaling would be more prevalent, as this would also assist in equalizing any activity balances between the two sides at rest. However, it is probably the case that equal contributions are utilized. Efferent regulation of hair cell-afferent synapses is potentially a source as well, as unilateral labyrinthectomy does not appear to change afferent response characteristics but rather drives an increase in the number of irregular firing fibers (Sadeghi et al., 2007). Distinguishing afferent population metrics is readily accessible in *Xenopus* and would be of interest here (Gensberger et al., 2016). This later conversion would be ideal to reduce the tonic

commissural inhibition if indeed present. Modifications of the intrinsic membrane properties of vestibular neurons on one or both sides presumably occur in these animals (Him and Dutia, 2001; Beraneck et al., 2003), particularly given that extensive time during development has been permitted to allow such deep-rooted modifications (Vibert et al., 1999; Beraneck and Idoux, 2012). A shift of central vestibular neurons to having more phasic responses would be an ideal condition, particularly considering such a condition would assist in reducing tonic inhibition to vestibular targets on the extirpated side. Adaptive elevation of resting discharge rates of afferent fibers in these animals is another hypothesized site of reorganization. Increased resting rates would likely provide a broader bandwidth during off-direction rotation. Amphibians, including *Xenopus*, normally operate with afferent resting rates of less than 10 Hz (Blanks and Precht, 1976; Gensberger et al., 2016) compared to other organisms such as primates and birds who present with around 100 Hz (Anastasio et al., 1985; Goldberg, 2000). A developmental increase in resting activity to rates closer to primates and birds might offer more of a dynamic range during off-direction motion and permit more spatiotemporally relevant sensory encoding.

Animals which developed with a third ear on their spinal cord (chapter III) presumably use similar mechanisms to equalize activity imbalances as mentioned above. Prior to this however, the transplanted ear must have been able to extend afferent axons onto vestibular projection neurons as fibers were readily observed in the vestibular nucleus (chapter III, Figure 3) and functional excitation was shown (chapter III, Figure 5). Challenged with atypical entry into the CNS, afferent fibers fasciculated on spinal projecting nerves and routed themselves rostrally to reach the vestibular nuclei. Accomplishment of this pathfinding ability makes use of the intrinsic ability of afferent fibers to fasciculate on pioneer axons into the hindbrain (Hidalgo and Brand, 1977; Zecca et al., 2015; Bhat and Hutter, 2016). However, this process is not perfect, nor goal directed to reach the hindbrain. Some fasciculation was observed with lateral line afferents both caudally and rostrally (chapter III, Figure 6). Ventrally transplanted inner ears, those which developed next to the heart, fasciculated with the vagus nerve (chapter III, Figure 7), and ears transplanted in place of the eye were shown to follow other cranial nerves such as the trigeminal nerve (Elliott et al., 2013). If chance fasciculation into the spinal cord was permitted, entry was followed by use of conserved navigation cues established by common patterning of longitudinal columns in the hindbrain and spinal cord to reach the vestibular nuclei (Hernandez-Miranda et al., 2017; Elliott and Fritzsch, 2018). That inner ear afferents can travel along existing fibers in a manner consistent with normal pioneer entry (Zecca et al., 2015) is an indicator that an intrinsic flexibility permits the travel with a variety of nerves outside those of otic origin. Once in the hindbrain, as mentioned above, connections were made to central vestibular neurons with crossed excitatory projections. If connections to ipsilaterally projecting inhibitory

neurons are absent entirely, are simply silent (Sethuramanujam et al., 2017), or merely lack a sufficient depolarizing ability given that afferents only opportunistically enter the brain, is currently unknown. However, activity-based refinement of central connections (Kirkby et al., 2013) could assist in the process of any of these outcomes, as suggested by the sensitivity of sensory afferents to patterned input in a variety of systems (Constantine-Paton and Law, 1978; Elliott et al., 2015b). The data from chapter III collectively align with the concept of goal directed measures following vestibular adaptive measures being absent (Dieringer, 1995). Rather, intrinsic mechanisms are simply executed and if they occur in sufficient time and space, can permit functional ability. In transplantation studies of the optic anlage in *Xenopus*, RGC axons from eyes which developed on the trunk did not appear to extend consistently beyond diverse ramification within the local spinal cord (Giorgi and van der Loos, 1978; Blackiston and Levin, 2013; Blackiston et al., 2017). However, visual input could be integrated and influence sensorimotor control considerably despite the absence of direct axonal connections in the tectum (Blackiston and Levin, 2013; Blackiston et al., 2017). The disparity between these two systems is difficult to reconcile, yet nonetheless highlights the impressive ability to incorporate atypical sensory information.

The cerebellum is the primary influencer of vestibular motor learning (Miles and Lisberger, 1981) and is therefore a pivotal contributor to plasticity mechanisms (Boyden et al., 2004). The assumption that cerebellar signaling assisted in the functional acquisition of VOR transformations in one-eared and three-eared frogs would not be unfounded. Indeed, both experimental groups are near-congenital in their sensory manipulations and therefore would have experienced much of their post-embryonic life with influence from the cerebellum. A provocative consideration would be that cerebellar feedback mechanisms assisted in establishing dynamic VOR processing which might be stored in the nuclei itself (Shuto et al., 2006). Certainly, the cerebellum would continue to exert its adaptive control over VOR processes, particularly during prolonged sensory stimulations and assist in maintaining homeostatic response levels (Dietrich and Straka, 2016). Understanding the exact nature of the cerebellar influence in these animals would require ablations or inactivation (e.g., Markov et al., 2021) followed by functional assays as described here. In particular, cerebellar inactivation or genetic ablation early in development compared to an acute ablation would assist in determining the location of dynamic VOR influences if present. In mice lacking proper cerebellar feedback, compensation processes are heavily impaired (Faulstich et al., 2006; Beraneck et al., 2008). Interestingly, these mice revealed an even stronger impairment during ipsilesional directed head motion whereas some degree of non-cerebellar compensation was able to assist in recovering contralesional evoked responses (Beraneck et al., 2008). In contrast to the findings here, the embryonically generated one-eared animals here had considerably stronger VOR during ipsilesionally

directed head movements (chapter II, Figure 2), indicating a possible role for the cerebellum in assisting this acquisition during development. Cerebellar contributions to VOR plasticity are also speculated in the results in chapter IV. Administration of 4-AP is typically used to treat patients with cerebellar and vestibular disorders by improving motor symptoms (Strupp et al., 2004). In the course of symptom management, an increase of VOR gain was observed (Kalla et al., 2004), suggesting a considerable modulatory ability in VOR adaptation. Although the mechanism of this process is still unclear (Alviña and Khodakhah, 2010), activity modifications are believed to occur by regularizing Purkinje cell firing and increasing action potential time courses (Alviña and Khodakhah, 2010). 4-AP application in a set of non-pathologic mice, however, did not demonstrate a considerable effect on VOR eye movements, leaving the relative influence of this drug on VOR plasticity up to interpretation (Stahl and Thumser, 2013). The results of chapter IV suggest a considerable effect of 4-AP on non-pathological animals. This does not strictly report a causation with respect to the cerebellum, given that Kv1.1 channels were not expressly observed outside of afferents in these larval *Xenopus*. Nonetheless, cerebellar contributions are inferred based on the general elevation of input from afferent regularization (chapter IV, Figure 1) which could drive feed-forward inhibition from cerebellar-vestibular inhibitory pathways (Blazquez et al, 2004; Boyden et al., 2004). As mentioned previously, proper characterization of the necessity of the cerebellum would be prudent to disassociate local vestibular inhibitory contributions over cerebellar derived influences. Further, assessment at different developmental stages would be beneficial given that adult grass frogs express Kv1.1 in central vestibular neurons (Beraneck et al., 2007). Regardless of the source of phasic bursting in extraocular discharge, the general bursting principle could be important in facilitation of dynamic VOR responses. However, the delay in peak extraocular VOR discharge could potentially arise from the influence of these inhibitory side loops as well. The difference between VOR ability in control mice (Stahl and Thumser, 2013) and here (chapter IV) should be viewed carefully however, as extraocular discharge is not behavior and eye movements may not precisely be impaired despite discharge delays or peak rate differences. Regardless of the mechanism or extent of influence, short term changes in vestibular circuits seem to provoke neuronal reactions that aim at providing cyclic discharges within VOR circuits. If this is necessary for execution of VOR behaviors in these conditions remains to be assessed.

Absence of vestibular signaling can be compensated to some degree by sensory inputs from other self-motion modalities (Darlington and Smith, 2000; Sadeghi et al., 2012). Here, sensory substation through optic flow was only profiled in one-eared animals (chapter II) and reported a surprising lack of compensatory influence during VOR processing. Specifically, visuo-vestibular interaction did not supplement VOR performance and OKR ability was generally unimpaired in these

animals (chapter II, Figure 3, S3). This lack of influence is shared with *Xenopus* following unilateral lesion of the statoacoustic nerve (Soupiadou et al., 2020). Interestingly, the delayed deterioration in OKR and continued reduction in VOR in the later study is surprising only by comparison to the consistent VOR impairment here, whereas the OKR was rather robust. It therefore seems that the secondary effects following sudden vestibular loss in *Xenopus* (Soupiadou et al., 2020) on visuo-motor centers was compensated for in these embryonic one-eared animals. Disruptions in vestibular signaling can drive changes in relative weights of visual cues for establishing postural control (Lacour et al., 1997). Heightened sensitivity to visual flow in vestibular neurons following unilateral vestibular loss has been demonstrated to this effect (e.g., in the cat; Zennou-Azogui et al., 1994). The absence of such a reliance in the animals here was a surprising result. However, a complete independence from visual feedback may not be entirely the case. Given that one-eared animals here were reared in typical light/dark circadian periods, visual input consolidation into the vestibular nuclei from visuo-cerebellar pathways cannot be ruled out. Organisms reared in darkness, and thus without visual feedback, show poor performance parameters in VOR ability but can nonetheless execute them (Collewijn, 1977, Harris and Cynader, 1981), which highlights the dispensability of visual input for initial development of VOR processing (Berthoz et al., 1975; Curthoys, 1979). Experimental visuo-vestibular mismatch conditions reduce VOR (França de Barros et al., 2020). Congenitally blind patients, however, seem to not be able to execute VOR at all (Kömpf and Piper, 1987). Valid future experiments would be rearing the animals here in complete darkness to see the true extent of visual input influence or necessity during development of one-eared animals. Substitution through proprioception or efference copy signaling likewise have not been examined but would be beneficial, although the former may not contribute substantially given its inability to correct for static postural deficits in permanently aquatic *Xenopus* (Lambert et al., 2009) compared to grass frogs (Dieringer, 1995). Behavioral substitutions, such as saccades in primates (Curthoys, 2000; Schubert and Zee, 2010) or saccade-like movements of the head in anurans (Dieringer, 1988) might have also limited the resolution of the results here. Since all VOR assessments were performed on head-fixed tadpoles, these contributions could not be examined, but such behavioral strategies could certainly contribute to performance metrics in some fashion. A final point to be made here is that VOR stimulation paradigms were restricted to 0.5-1 Hz. However, higher frequency stimulations show progressive decrease in VOR gain across compensated organisms (Gilchrist, 1998). Determination of frequency bandwidths would also be of interest to further disentangle dynamic processing measures.

Conclusions and future directions: “Lessons from frogs, part II”

As aptly stated in the comprehensive volume of Straka and Dieringer (2004), neurobiological knowledge can originate from many sources. The results from this dissertation have expanded on our current understanding of the extents and limitations of neuronal reorganization in the vestibular system. Neurobiological research on frogs, particularly *Xenopus laevis*, has extensive roots in neuroscience (Pratt and Khakalin, 2013; Bestman et al., 2015), including in the vestibular system (Straka and Dieringer, 2004; Straka and Simmers, 2012) and neuronal plasticity (Lambert and Straka, 2012; Lee-Liu et al., 2017). For *Xenopus* afficionados, a wealth of excellent information on using this model organism for scientific research can be found in book: Xenopus*: From Basic Biology to Disease Models in the Genomic Era* (2022). This dissertation has used *Xenopus laevis* to further our knowledge on plasticity of the vestibular system and the results here find applicability toward other vertebrate species. Understanding how the brain can adapt to the environment is a critical venture, as organisms are confronted with considerably complex environments and must respond appropriately. Yet the nervous system is equally complex, and thus reconciling the biological considerations of adaptive reorganization is an extensive endeavor. Nonetheless, the work here faithfully reports on the remarkable extent with which vestibular networks can respond to induced changes. This work contributes to existing scopes of literature which have focused on how sensory input influences the development of the brain (e.g., Peusner and Morest, 1977; Elliott et al., 2015a; Roberts et al., 2017) as well as adaptive responses following injury and disease (e.g., Dieringer, 1995; Dutia, 2010; Cassel et al., 2018).

Embryonic reduction or addition of sensory input demonstrated the potential to be compensated for, particularly to extents that permitted behaviorally relevant computations. Such changes during development likely manifest along several systemic levels and can be related to those which occur following injury or disease. Manipulations of sensory input on mature circuits likewise demonstrated the ability to evoke sensorimotor transformations and offer some perspective into the responsive capabilities that can be found in adult organisms. In the proceeding paragraphs several experimental directions have been proposed to further explore the biological results here. In addition to adding depth to these topics, future work should most certainly consider comparative aspects of developmental plasticity to that which occur in mature organisms. Exploiting such comparisons has practical use. Given the high prevalence of vestibular disorders in patients (Strupp et al., 2020), which can range from congenital (Abadie et al., 2000; Peusner et al., 2021) to sudden onset (Zwergal et al., 2020), research along these lines can aid in therapeutic measures, particularly in aging populations who suffer often from balance disorders (Agrawal et al., 2020). Such considerations have been suggested previously following functional assessments of embryonic plasticity extents (Elliott and Fritzsch, 2018; Lilian et al., 2019; Elliott et al., 2022) which has even been explored in other systems

such as the visual system (Blackiston et al., 2017). Developmental aspects aside, taking advantage of intrinsic flexibility in vestibular neuronal pathways has its own measure of therapeutic advantages such as in aiding motion sickness amelioration (Idoux et al., 2018; Heffernan et al., 2021). Beyond medical use, industrial innovations will most certainly benefit from biological knowledge of flexibility in vestibular and self-motion networks. Leveraging such knowledge can lead to further insights in, e.g., augmented, or virtual reality technologies and advancements (Knorr et al., 2018; Nürnberger et al., 2021), as well as on topics relevant to vestibular processing during space travel and exposure to microgravity (Hupfeld et al., 2022). To summarize, vestibular networks are incredibly plastic and understanding the events which govern and are executed during neuronal adaptations has many interesting practical uses which can be discovered from basic biological research.

REFERENCES

Abadie, V., Wiener-Vacher, S., Morisseau-Durand, M.P., Poree, C., Amiel, J., Amanou, L., Peigne, C., Lyonnet, S., and Manac'h, Y. (2000). Vestibular anomalies in CHARGE syndrome: investigations on and consequences for postural development. Eur J Pediatr *159*, 569-574.

Agrawal, Y., Merfeld, D.M., Horak, F.B., Redfern, M.S., Manor, B., Westlake, K.P., Holstein, G.R., Smith, P.F., Bhatt, T., Bohnen, N.I.*, et al.* (2020). Aging, Vestibular Function, and Balance: Proceedings of a National Institute on Aging/National Institute on Deafness and Other Communication Disorders Workshop. J Gerontol A Biol Sci Med Sci *75*, 2471-2480.

Alagramam, K.N., Stahl, J.S., Jones, S.M., Pawlowski, K.S., and Wright, C.G. (2005). Characterization of vestibular dysfunction in the mouse model for Usher syndrome 1F. J Assoc Res Otolaryngol *6*, 106-118.

Almasoudi, S.H., and Schlosser, G. (2021). Otic Neurogenesis in Xenopus laevis: Proliferation, Differentiation, and the Role of Eya1. Front Neuroanat *15*, 722374.

Alvina, K., and Khodakhah, K. (2010). The therapeutic mode of action of 4-aminopyridine in cerebellar ataxia. J Neurosci *30*, 7258-7268.

Anastasio, T.J., Correia, M.J., and Perachio, A.A. (1985). Spontaneous and driven responses of semicircular canal primary afferents in the unanesthetized pigeon. J Neurophysiol *54*, 335-347.

Angelaki, D.E. (2014). How Optic Flow and Inertial Cues Improve Motion Perception. Cold Spring Harb Symp Quant Biol *79*, 141-148.

Angelaki, D.E., and Cullen, K.E. (2008). Vestibular system: the many facets of a multimodal sense. Annu Rev Neurosci *31*, 125-150.

Angelaki, D.E., and Hess, B.J. (1996). Organizational principles of otolith- and semicircular canal-ocular reflexes in rhesus monkeys. Ann N Y Acad Sci *781*, 332-347.

Angelaki, D.E., and Hess, B.J. (2005). Self-motion-induced eye movements: effects on visual acuity and navigation. Nat Rev Neurosci *6*, 966-976.

Appler, J.M., and Goodrich, L.V. (2011). Connecting the ear to the brain: Molecular mechanisms of auditory circuit assembly. Prog Neurobiol *93*, 488-508.

Bagnall, M.W., and Schoppik, D. (2018). Development of vestibular behaviors in zebrafish. Curr Opin Neurobiol *53*, 83-89.

Baker, R., and Highstein, S.M. (1975). Physiological identification of interneurons and motoneurons in the abducens nucleus. Brain Res *91*, 292-298.

Baker, R., Precht, W., and Berthoz, A. (1973). Synaptic connections to trochlear motoneurons determined by individual vestibular nerve branch stimulation in the cat. Brain Res *64*, 402-406.

Barlow, H.B., and Hill, R.M. (1963). Selective sensitivity to direction of movement in ganglion cells of the rabbit retina. Science *139*, 412-414.

Barmack, N.H., Baughman, R.W., Errico, P., and Shojaku, H. (1993). Vestibular primary afferent projection to the cerebellum of the rabbit. J Comp Neurol *327*, 521-534.

Beck, J.C., Gilland, E., Tank, D.W., and Baker, R. (2004). Quantifying the ontogeny of optokinetic and vestibuloocular behaviors in zebrafish, medaka, and goldfish. J Neurophysiol *92*, 3546-3561.

Beisel, K.W., Wang-Lundberg, Y., Maklad, A., and Fritzsch, B. (2005). Development and evolution of the vestibular sensory apparatus of the mammalian ear. J Vestib Res *15*, 225-241.

Bell, D., Streit, A., Gorospe, I., Varela-Nieto, I., Alsina, B., and Giraldez, F. (2008). Spatial and temporal segregation of auditory and vestibular neurons in the otic placode. Dev Biol *322*, 109-120.

Beraneck, M., Hachemaoui, M., Idoux, E., Ris, L., Uno, A., Godaux, E., Vidal, P.P., Moore, L.E., and Vibert, N. (2003). Long-term plasticity of ipsilesional medial vestibular nucleus neurons after unilateral labyrinthectomy. J Neurophysiol *90*, 184-203.

Beraneck, M., and Idoux, E. (2012). Reconsidering the role of neuronal intrinsic properties and neuromodulation in vestibular homeostasis. Front Neurol *3*, 25.

Beraneck, M., and Lambert, F.M. (2020). Differential Organization of Intrinsic Membrane Properties of Central Vestibular Neurons and Interaction With Network Properties. In The Senses: A Comprehensive Reference, Vol 6, Fritzsch, B., Straka, H., eds (Elsevier), pp. 273-289.

Beraneck, M., McKee, J.L., Aleisa, M., and Cullen, K.E. (2008). Asymmetric recovery in cerebellar-deficient mice following unilateral labyrinthectomy. J Neurophysiol *100*, 945-958.

Beraneck, M., Pfanzelt, S., Vassias, I., Rohregger, M., Vibert, N., Vidal, P.P., Moore, L.E., and Straka, H. (2007). Differential intrinsic response dynamics determine synaptic signal processing in frog vestibular neurons. J Neurosci *27*, 4283-4296.

Beraneck, M., and Straka, H. (2011). Vestibular signal processing by separate sets of neuronal filters. J Vestib Res *21*, 5-19.

Bermingham, N.A., Hassan, B.A., Price, S.D., Vollrath, M.A., Ben-Arie, N., Eatock, R.A., Bellen, H.J., Lysakowski, A., and Zoghbi, H.Y. (1999). Math1: an essential gene for the generation of inner ear hair cells. Science *284*, 1837-1841.

Berthoz, A., Jeannerod, M., Vital-Durand, F., and Oliveras, J.L. (1975). Development of vestibulo-ocular responses in visually deprived kittens. Exp Brain Res *23*, 425-442.

Bestman, J.E., Huang, L.C., Lee-Osbourne, J., Cheung, P., and Cline, H.T. (2015). An in vivo screen to identify candidate neurogenic genes in the developing Xenopus visual system. Dev Biol *408*, 269-291.

Bever, M.M., and Fekete, D.M. (2002). Atlas of the developing inner ear in zebrafish. Dev Dyn *223*, 536-543.

Bever, M.M., Jean, Y.Y., and Fekete, D.M. (2003). Three-dimensional morphology of inner ear development in Xenopus laevis. Dev Dyn *227*, 422-430.

Bhagavatula, P.S., Claudianos, C., Ibbotson, M.R., and Srinivasan, M.V. (2011). Optic flow cues guide flight in birds. Curr Biol *21*, 1794-1799.

Bhat, J.M., and Hutter, H. (2016). Pioneer Axon Navigation Is Controlled by AEX-3, a Guanine Nucleotide Exchange Factor for RAB-3 in Caenorhabditis elegans. Genetics *203*, 1235-1247.

Bianco, I.H., Ma, L.H., Schoppik, D., Robson, D.N., Orger, M.B., Beck, J.C., Li, J.M., Schier, A.F., Engert, F., and Baker, R. (2012). The tangential nucleus controls a gravito-inertial vestibulo-ocular reflex. Curr Biol *22*, 1285-1295.

Birinyi, A., Straka, H., Matesz, C., and Dieringer, N. (2001). Location of dye-coupled second order and of efferent vestibular neurons labeled from individual semicircular canal or otolith organs in the frog. Brain Res *921*, 44-59.

Bjorke, B., Shoja-Taheri, F., Kim, M., Robinson, G.E., Fontelonga, T., Kim, K.T., Song, M.R., and Mastick, G.S. (2016). Contralateral migration of oculomotor neurons is regulated by Slit/Robo signaling. Neural Dev *11*, 18.

Blackiston, D.J., and Levin, M. (2013). Ectopic eyes outside the head in Xenopus tadpoles provide sensory data for light-mediated learning. J Exp Biol *216*, 1031-1040.

Blackiston, D.J., Vien, K., and Levin, M. (2017). Serotonergic stimulation induces nerve growth and promotes visual learning via posterior eye grafts in a vertebrate model of induced sensory plasticity. NPJ Regen Med *2*, 8.

Blanks, R.H., Estes, M.S., and Markham, C.H. (1975). Physiologic characteristics of vestibular first-order canal neurons in the cat. II. Response to constant angular acceleration. J Neurophysiol *38*, 1250-1268.

Blanks, R.H., and Precht, W. (1976). Functional characterization of primary vestibular afferents in the frog. Exp Brain Res *25*, 369-390.

Blazquez, P.M., Hirata, Y., and Highstein, S.M. (2004). The vestibulo-ocular reflex as a model system for motor learning: what is the role of the cerebellum? Cerebellum *3*, 188-192.

Bok, J., Dolson, D.K., Hill, P., Ruther, U., Epstein, D.J., and Wu, D.K. (2007). Opposing gradients of Gli repressor and activators mediate Shh signaling along the dorsoventral axis of the inner ear. Development *134*, 1713-1722.

Borst, A. (2007). Correlation versus gradient type motion detectors: the pros and cons. Philos Trans R Soc Lond B Biol Sci *362*, 369-374.

Boyden, E.S., Katoh, A., and Raymond, J.L. (2004). Cerebellum-dependent learning: the role of multiple plasticity mechanisms. Annu Rev Neurosci *27*, 581-609.

Branoner, F., Chagnaud, B.P., and Straka, H. (2016). Ontogenetic Development of Vestibulo-Ocular Reflexes in Amphibians. Front Neural Circuits *10*, 91.

Branoner, F., and Straka, H. (2015). Semicircular canal-dependent developmental tuning of translational vestibulo-ocular reflexes in Xenopus laevis. Dev Neurobiol *75*, 1051-1067.

Branoner, F., and Straka, H. (2018). Semicircular Canal Influences on the Developmental Tuning of the Translational Vestibulo-Ocular Reflex. Front Neurol *9*, 404.

Brecha, N., and Karten, H.J. (1979). Accessory optic projections upon oculomotor nuclei and vestibulocerebellum. Science *203*, 913-916.

Brecha, N., Karten, H.J., and Hunt, S.P. (1980). Projections of the nucleus of the basal optic root in the pigeon: an autoradiographic and horseradish peroxidase study. J Comp Neurol *189*, 615-670.

Brichta, A.M., and Goldberg, J.M. (1998). The papilla neglecta of turtles: a detector of head rotations with unique sensory coding properties. J Neurosci *18*, 4314-4324.

Briggman, K.L., Helmstaedter, M., and Denk, W. (2011). Wiring specificity in the direction-selectivity circuit of the retina. Nature *471*, 183-188.

Brooks, J.X., and Cullen, K.E. (2014). Early vestibular processing does not discriminate active from passive self-motion if there is a discrepancy between predicted and actual proprioceptive feedback. J Neurophysiol *111*, 2465-2478.

Broussard, D.M., and Kassardjian, C.D. (2004). Learning in a simple motor system. Learn Mem *11*, 127-136.

Brown, R., and Groves, A.K. (2020). Hear, Hear for Notch: Control of Cell Fates in the Inner Ear by Notch Signaling. Biomolecules *10*.

Bryant, J.P., Chandrashekhar, V., Cappadona, A.J., Lookian, P.P., Chandrashekhar, V., Donahue, D.R., Munasinghe, J.B., Kim, H.J., Vortmeyer, A.O., Heiss, J.D*., et al.* (2021). Multimodal Atlas of the Murine Inner Ear: From Embryo to Adult. Front Neurol *12*, 699674.

Burgess, H.A., and Granato, M. (2007). Sensorimotor gating in larval zebrafish. J Neurosci *27*, 4984-4994.

Burns, J.C., and Stone, J.S. (2017). Development and regeneration of vestibular hair cells in mammals. Semin Cell Dev Biol *65*, 96-105.

Busch, C., Borst, A., and Mauss, A.S. (2018). Bi-directional Control of Walking Behavior by Horizontal Optic Flow Sensors. Curr Biol *28*, 4037-4045 e4035.

Büttner-Ennever, J.A. (1992). Patterns of connectivity in the vestibular nuclei. Ann N Y Acad Sci *656*, 363-378.

Büttner-Ennever, J.A. (1999). A review of otolith pathways to brainstem and cerebellum. Ann N Y Acad Sci *871*, 51-64.

Büttner-Ennever, J.A. (2006). The extraocular motor nuclei: organization and functional neuroanatomy. Prog Brain Res *151,* 95-125.

Calabrese, D.R., and Hullar, T.E. (2006). Planar relationships of the semicircular canals in two strains of mice. J Assoc Res Otolaryngol *7*, 151-159.

Cang, J., Savier, E., Barchini, J., and Liu, X. (2018). Visual Function, Organization, and Development of the Mouse Superior Colliculus. Annu Rev Vis Sci *4*, 239-262.

Carriot, J., Jamali, M., Cullen, K.E., and Chacron, M.J. (2017). Envelope statistics of self-motion signals experienced by human subjects during everyday activities: Implications for vestibular processing. PLoS One *12*, e0178664.

Cassel, R., Wiener-Vacher, S., El Ahmadi, A., Tighilet, B., and Chabbert, C. (2018). Reduced Balance Restoration Capacities Following Unilateral Vestibular Insult in Elderly Mice. Front Neurol *9*, 462.

Chagnaud, B.P., Banchi, R., Simmers, J., and Straka, H. (2015). Spinal corollary discharge modulates motion sensing during vertebrate locomotion. Nat Commun *6*, 7982.

Chagnaud, B.P., Engelmann, J., Fritzsch, B., Glover, J.C., and Straka, H. (2017). Sensing External and Self-Motion with Hair Cells: A Comparison of the Lateral Line and Vestibular Systems from a Developmental and Evolutionary Perspective. Brain Behav Evol *90*, 98-116.

Chang, W., Brigande, J.V., Fekete, D.M., and Wu, D.K. (2004). The development of semicircular canals in the inner ear: role of FGFs in sensory cristae. Development *131*, 4201-4211.

Chen, C.C., Bockisch, C.J., Olasagasti, I., Weber, K.P., Straumann, D., and Huang, M.Y. (2014). Positive or negative feedback of optokinetic signals: degree of the misrouted optic flow determines system dynamics of human ocular motor behavior. Invest Ophthalmol Vis Sci *55*, 2297-2306.

Chen, H., Bagri, A., Zupicich, J.A., Zou, Y., Stoeckli, E., Pleasure, S.J., Lowenstein, D.H., Skarnes, W.C., Chédotal, A., and Tessier-Lavigne, M. (2000). Neuropilin-2 regulates the development of selective cranial and sensory nerves and hippocampal mossy fiber projections. Neuron *25*, 43-56.

Chen, H., Epstein, J., and Stern, E. (2010). Neural plasticity after acquired brain injury: evidence from functional neuroimaging. PM & R *2*, S306-312.

Chen, Y., Takano-Maruyama, M., Fritzsch, B., and Gaufo, G.O. (2012). Hoxb1 controls anteroposterior identity of vestibular projection neurons. PLoS One *7*, e34762.

Chilton, J.K., and Guthrie, S. (2017). Axons get ahead: Insights into axon guidance and congenital cranial dysinnervation disorders. Dev Neurobiol *77*, 861-875.

Chow, D.M., Theobald, J.C., and Frye, M.A. (2011). An olfactory circuit increases the fidelity of visual behavior. J Neurosci *31*, 15035-15047.

Clark, C., Austen, O., Poparic, I., and Guthrie, S. (2013). alpha2-Chimaerin regulates a key axon guidance transition during development of the oculomotor projection. J Neurosci *33*, 16540-16551.

Clendaniel, R.A., and Mays, L.E. (1994). Characteristics of antidromically identified oculomotor internuclear neurons during vergence and versional eye movements. J Neurophysiol *71*, 1111-1127.

Cline, H.T., and Constantine-Paton, M. (1989). NMDA receptor antagonists disrupt the retinotectal topographic map. Neuron *3*, 413-426.

Clopath, C., Badura, A., De Zeeuw, C.I., and Brunel, N. (2014). A cerebellar learning model of vestibulo-ocular reflex adaptation in wild-type and mutant mice. J Neurosci *34*, 7203-7215.

Cochran, S.L., Dieringer, N., and Precht, W. (1984). Basic optokinetic-ocular reflex pathways in the frog. J Neurosci *4*, 43-57.

Collewijn, H. (1977). Optokinetic and vestibulo-ocular reflexes in dark-reared rabbits. Exp Brain Res *27*, 287-300.

Collewijn, H. (1989). The vestibulo-ocular reflex: an outdated concept? Prog Brain Res *80,* 197-209.

Collewijn, H., and Grootendorst, A.F. (1979). Adaptation of Optokinetic and Vestibulo-Ocular Reflexes to Modified Visual Input in the Rabbit. Prog Brain Res *50,* 771-781.

Collewijn, H., and Smeets, J.B. (2000). Early components of the human vestibulo-ocular response to head rotation: latency and gain. J Neurophysiol *84*, 376-389.

Collins, W.E., and Updegraff, B.P. (1966). A comparison of nystagmus habituation in the cat and the dog. Acta Otolaryngol *62*, 19-26.

Constantine-Paton, M., and Law, M.I. (1978). Eye-specific termination bands in tecta of three-eyed frogs. Science *202*, 639-641.

Contini, D., Holstein, G.R., and Art, J.J. (2022). Simultaneous Dual Recordings From Vestibular Hair Cells and Their Calyx Afferents Demonstrate Multiple Modes of Transmission at These Specialized Endings. Front Neurol *13*, 891536.

Cramer, S.C., Sur, M., Dobkin, B.H., O'Brien, C., Sanger, T.D., Trojanowski, J.Q., Rumsey, J.M., Hicks, R., Cameron, J., Chen, D*., et al.* (2011). Harnessing neuroplasticity for clinical applications. Brain *134*, 1591-1609.

Crampton, W.G.R. (2019). Electroreception, electrogenesis and electric signal evolution. J Fish Biol *95*, 92-134.

Cullen, K.E., and Zobeiri, O.A. (2021). Proprioception and the predictive sensing of active self-motion. Curr Opin Physiol *20*, 29-38.

Curthoys, I.S. (1979). The vestibulo-ocular reflex in newborn rats. Acta Otolaryngol *87*, 484-489.

Curthoys, I.S. (1981). Scarpa's ganglion in the rat and guinea pig. Acta Otolaryngol *92*, 107-113.

Curthoys, I.S. (2000). Vestibular compensation and substitution. Curr Opin Neurol *13*, 27-30.

Curthoys, I.S. (2020). The Anatomical and Physiological Basis of Clinical Tests of Otolith Function. A Tribute to Yoshio Uchino. Front Neurol *11*, 566895.

Curthoys, I.S., Smith, P.F., and Darlington, C.L. (1988). Postural compensation in the guinea pig following unilateral labyrinthectomy. Prog Brain Res *36,* 357-384.

Darlington, C.L., and Smith, P.F. (2000). Molecular mechanisms of recovery from vestibular damage in mammals: recent advances. Prog Neurobiol *62*, 313-325.

Daudet, N., and Lewis, J. (2005). Two contrasting roles for Notch activity in chick inner ear development: specification of prosensory patches and lateral inhibition of hair-cell differentiation. Development *132*, 541-551.

De Zeeuw, C.I., and Yeo, C.H. (2005). Time and tide in cerebellar memory formation. Curr Opin Neurobiol *15*, 667-674.

Deans, M.R. (2021). Conserved and Divergent Principles of Planar Polarity Revealed by Hair Cell Development and Function. Front Neurosci *15*, 742391.

Deans, M.R., Antic, D., Suyama, K., Scott, M.P., Axelrod, J.D., and Goodrich, L.V. (2007). Asymmetric distribution of prickle-like 2 reveals an early underlying polarization of vestibular sensory epithelia in the inner ear. J Neurosci *27*, 3139-3147.

Delhaye, B.P., Long, K.H., and Bensmaia, S.J. (2018). Neural Basis of Touch and Proprioception in Primate Cortex. Comp Physiol *8*, 1575-1602.

Devaud, J.M., Acebes, A., and Ferrús, A. (2001). Odor exposure causes central adaptation and morphological changes in selected olfactory glomeruli in Drosophila. J Neurosci *21*, 6274-6282.

Diaz, C., and Glover, J.C. (2022). The Vestibular Column in the Mouse: A Rhombomeric Perspective. Front Neuroanat *15*, 806815.

Diaz, C., and Puelles, L. (2019). Segmental Analysis of the Vestibular Nerve and the Efferents of the Vestibular Complex. Anat Rec (Hoboken) *302*, 472-484.

Dichgans, J., and Brandt, T. (1978). Visual-Vestibular Interaction: Effects on Self-Motion Perception and Postural Control. In Perception, R. Held, H.W. Leibowitz, and H.-L. Teuber, eds. (Berlin, Heidelberg: Springer Berlin Heidelberg), pp. 755-804.

Dickman, J.D., Angelaki, D.E., and Correia, M.J. (1991). Response properties of gerbil otolith afferents to small angle pitch and roll tilts. Brain Res *556*, 303-310.

Dieringer, N. (1988). Immediate saccadic substitution for deficits in dynamic vestibular reflexes of frogs with selective peripheral lesions. Prog Brain Res *76,* 403-409.

Dieringer, N. (1995). 'Vestibular compensation': neural plasticity and its relations to functional recovery after labyrinthine lesions in frogs and other vertebrates. Prog Neurobiol *46*, 97-129.

Dieringer, N. (2003). Activity-Related Postlesional Vestibular Reorganization. Ann N Y Acad Sci *1004*, 50-60.

Dieringer, N., and Precht, W. (1977). Modification of synaptic input following unilateral labyrinthectomy. Nature *269*, 431-433.

Dieringer, N., and Precht, W. (1979). Mechanisms of compensation for vestibular deficits in the frog. I. Modification of the excitatory commissural system. Exp Brain Res *36*, 311-328.

Dietrich, H., Glasauer, S., and Straka, H. (2017). Functional Organization of Vestibulo-Ocular Responses in Abducens Motoneurons. J Neurosci *37*, 4032-4045.

Dietrich, H., and Straka, H. (2016). Prolonged vestibular stimulation induces homeostatic plasticity of the vestibulo-ocular reflex in larval Xenopus laevis. Eur J Neurosci *44*, 1787-1796.

Dow, E.R., and Anastasio, T.J. (1998). Analysis and neural network modeling of the nonlinear correlates of habituation in the vestibulo-ocular reflex. J Comput Neurosci *5*, 171-190.

du Lac, S., Raymond, J.L., Sejnowski, T.J., and Lisberger, S.G. (1995). Learning and memory in the vestibulo-ocular reflex. Annu Rev Neurosci *18*, 409-441.

Duncan, J.S., Fritzsch, B., Houston, D.W., Ketchum, E.M., Kersigo, J., Deans, M.R., and Elliott, K.L. (2019). Topologically correct central projections of tetrapod inner ear afferents require Fzd3. Sci Rep *9*, 10298.

Duncan, J.S., Stoller, M.L., Francl, A.F., Tissir, F., Devenport, D., and Deans, M.R. (2017). Celsr1 coordinates the planar polarity of vestibular hair cells during inner ear development. Dev Biol *423*, 126-137.

Dutia, M.B. (2010). Mechanisms of vestibular compensation: recent advances. Curr Opin Otolaryngol Head Neck Surg *18*, 420-424.

Dutia, M.B., and Johnston, A.R. (1998). Development of action potentials and apamin-sensitive after-potentials in mouse vestibular nucleus neurones. Exp Brain Res *118*, 148-154.

Eatock, R.A., and Songer, J.E. (2011). Vestibular hair cells and afferents: two channels for head motion signals. Annu Rev Neurosci *34*, 501-534.

Eatock, R.A., Xue, J., and Kalluri, R. (2008). Ion channels in mammalian vestibular afferents may set regularity of firing. J Exp Biol *211*, 1764-1774.

Ehrlich, D.E., and Schoppik, D. (2019). A primal role for the vestibular sense in the development of coordinated locomotion. eLife *8,* e45839*.*

Ekdale, E.G. (2013). Comparative Anatomy of the Bony Labyrinth (Inner Ear) of Placental Mammals. PLoS One *8*, e66624.

Elliott, K.L., and Fritzsch, B. (2010). Transplantation of Xenopus laevis ears reveals the ability to form afferent and efferent connections with the spinal cord. Int J Dev Biol *54*, 1443-1451.

Elliott, K.L., and Fritzsch, B. (2018). Ear transplantations reveal conservation of inner ear afferent pathfinding cues. Sci Rep *8*, 13819.

Elliott, K.L., Fritzsch, B., Yamoah, E.N., and Zine, A. (2022). Age-Related Hearing Loss: Sensory and Neural Etiology and Their Interdependence. Front Aging Neurosci *14*, 814528.

Elliott, K.L., and Gordy, C. (2020). Evolution and Plasticity of Inner Ear Vestibular Neurosensory Development. In The Senses: A Comprehensive Reference, Vol 6, Fritzsch, B., Straka, H., eds (Elsevier), pp. 145-161.

Elliott, K.L., Houston, D.W., DeCook, R., and Fritzsch, B. (2015a). Ear manipulations reveal a critical period for survival and dendritic development at the single-cell level in Mauthner neurons. Dev Neurobiol *75*, 1339-1351.

Elliott, K.L., Houston, D.W., and Fritzsch, B. (2015b). Sensory afferent segregation in three-eared frogs resemble the dominance columns observed in three-eyed frogs. Sci Rep *5*, 8338.

Elliott, K.L., Houston, D.W., and Fritzsch, B. (2013). Transplantation of Xenopus laevis tissues to determine the ability of motor neurons to acquire a novel target. PLoS One *8*, e55541.

Elliott, K.L., Kersigo, J., Pan, N., Jahan, I., and Fritzsch, B. (2017). Spiral Ganglion Neuron Projection Development to the Hindbrain in Mice Lacking Peripheral and/or Central Target Differentiation. Front Neural Circuits *11*, 25.

Fainsod, A., and Moody, S.A. (2022). Xenopus: From Basic Biology to Disease Models in the Genomic Era (Taylor & Francis).

Faulstich, M., van Alphen, A.M., Luo, C., du Lac, S., and De Zeeuw, C.I. (2006). Oculomotor plasticity during vestibular compensation does not depend on cerebellar LTD. J Neurophysiol *96*, 1187-1195.

Fekete, D.M., and Campero, A.M. (2007). Axon guidance in the inner ear. Int J Dev Biol *51*, 549-556.

Fekete, D.M., and Wu, D.K. (2002). Revisiting cell fate specification in the inner ear. Curr Opin Neurobiol *12*, 35-42.

Fetter, M. (2007). Vestibulo-ocular reflex. Dev Ophthalmol *40*, 35-51.

Fetter, M. (2016). Acute unilateral loss of vestibular function. Handb Clin Neurol *137*, 219-229.

França de Barros, F., Schenberg, L., Tagliabue, M., and Beraneck, M. (2020). Long term visuo-vestibular mismatch in freely behaving mice differentially affects gaze stabilizing reflexes. Sci Rep *10*, 20018.

Fredericks, C.A., Giolli, R.A., Blanks, R.H., and Sadun, A.A. (1988). The human accessory optic system. Brain Res *454*, 116-122.

Freter, S., Muta, Y., Mak, S.S., Rinkwitz, S., and Ladher, R.K. (2008). Progressive restriction of otic fate: the role of FGF and Wnt in resolving inner ear potential. Development *135*, 3415-3424.

Fritzsch, B. (1990). Experimental reorganization in the alar plate of the clawed toad, Xenopus laevis. I. Quantitative and qualitative effects of embryonic otocyst extirpation. Brain Res Dev Brain Res *51*, 113-122.

Fritzsch, B. (1998). Evolution of the vestibulo-ocular system. Otolaryngol Head Neck Surg *119*, 182-192.

Fritzsch, B. (2003). Development of inner ear afferent connections: forming primary neurons and connecting them to the developing sensory epithelia. Brain Res Bull *60*, 423-433.

Fritzsch, B., and Beisel, K.W. (2001). Evolution and development of the vertebrate ear. Brain Res Bull *55*, 711-721.

Fritzsch, B., Beisel, K.W., Jones, K., Farinas, I., Maklad, A., Lee, J., and Reichardt, L.F. (2002). Development and evolution of inner ear sensory epithelia and their innervation. J Neurobiol *53*, 143-156.

Fritzsch, B., Eberl, D.F., and Beisel, K.W. (2010). The role of bHLH genes in ear development and evolution: revisiting a 10-year-old hypothesis. Cell Mol Life Sci *67*, 3089-3099.

Fritzsch, B., and Elliott, K.L. (2017a). Evolution and Development of the Inner Ear Efferent System: Transforming a Motor Neuron Population to Connect to the Most Unusual Motor Protein via Ancient Nicotinic Receptors. Font Cell Neurosci *11,* 114.

Fritzsch, B., and Elliott, K.L. (2017b). Gene, cell, and organ multiplication drives inner ear evolution. Dev Biol *431*, 3-15.

Fritzsch, B., Elliott, K.L., Yamoah, E.N. (2022). Neurosensory development of the four brainstem-projecting sensory systems and their integration in the telencephalon. Front Neural Circuits *16,* 913480.

Fritzsch, B., Gregory, D., and Rosa-Molinar, E. (2005). The development of the hindbrain afferent projections in the axolotl: evidence for timing as a specific mechanism of afferent fiber sorting. Zoology (Jena) *108*, 297-306.

Fritzsch, B., Pan, N., Jahan, I., Duncan, J.S., Kopecky, B.J., Elliott, K.L., Kersigo, J., and Yang, T. (2013). Evolution and development of the tetrapod auditory system: an organ of Corti-centric perspective. Evol Dev *15*, 63-79.

Fritzsch, B., Pan, N., Jahan, I., and Elliott, K.L. (2015). Inner ear development: building a spiral ganglion and an organ of Corti out of unspecified ectoderm. Cell Tissue Res *361*, 7-24.

Fritzsch, B., Pauley, S., Feng, F., Matei, V., and Nichols, D. (2006). The molecular and developmental basis of the evolution of the vertebrate auditory system. Int J Comp Psychol *19,* 1-25.

Fritzsch, B., Sonntag, R., Dubuc, R., Ohta, Y., and Grillner, S. (1990). Organization of the six motor nuclei innervating the ocular muscles in lamprey. J Comp Neurol *294*, 491-506.

Fritzsch, B., and Straka, H. (2014). Evolution of vertebrate mechanosensory hair cells and inner ears: toward identifying stimuli that select mutation driven altered morphologies. J Comp Physiol A Neuroethol Sens Neural Behav Physiol *200*, 5-18.

Gensberger, K.D., Kaufmann, A.K., Dietrich, H., Branoner, F., Banchi, R., Chagnaud, B.P., and Straka, H. (2016). Galvanic Vestibular Stimulation: Cellular Substrates and Response Patterns of Neurons in the Vestibulo-Ocular Network. J Neurosci *36*, 9097-9110.

Gilchrist, D.P., Curthoys, I.S., Cartwright, A.D., Burgess, A.M., Topple, A.N., and Halmagyi, M. (1998). High acceleration impulsive rotations reveal severe long-term deficits of the horizontal vestibulo-ocular reflex in the guinea pig. Exp Brain Res *123*, 242-254.

Gilland, E., and Baker, R. (2005). Evolutionary patterns of cranial nerve efferent nuclei in vertebrates. Brain Behav Evol *66*, 234-254.

Giolli, R.A., Blanks, R.H., and Lui, F. (2006). The accessory optic system: basic organization with an update on connectivity, neurochemistry, and function. Prog Brain Res *151*, 407-440.

Giorgi, P.P., and Van der Loos, H. (1978). Axons from eyes grafted in Xenopus can grow into the spinal cord and reach the optic tectum. Nature *275*, 746-748.

Gittis, A.H., and du Lac, S. (2006). Intrinsic and synaptic plasticity in the vestibular system. Curr Opin Neurobiol *16*, 385-390.

Glasauer, S., and Knorr, A.G. (2020). Physical Nature of Vestibular Stimuli. In The Senses: A Comprehensive Reference, Vol 6, Fritzsch, B., Straka, H., eds (Elsevier), pp. 6-11.

Glasauer, S., and Straka, H. (2022). Low Gain Values of the Vestibulo-Ocular Reflex Can Optimize Retinal Image Slip. Front Neurol *13*, 897293.

Glover, J.C. (1996). Development of second-order vestibular projections in the chicken embryo. Ann N Y Acad Sci *781*, 13-20.

Glover, J.C. (2000). Neuroepithelial 'compartments' and the specification of vestibular projections. Prog Brain Res *124*, 3-21.

Glover, J.C. (2003). The development of vestibulo-ocular circuitry in the chicken embryo. J Physiol Paris *97*, 17-25.

Glover, J.C. (2020). Development and Evolution of Vestibulo-Ocular Reflex Circuitry. In The Senses: A Comprehensive Reference, Vol 6, Fritzsch, B., Straka, H., eds (Elsevier), pp. 309-325.

Goldberg, J.M. (2000). Afferent diversity and the organization of central vestibular pathways. Exp Brain Res *130*, 277-297.

Goldberg, J.M., and Cullen, K.E. (2011). Vestibular control of the head: possible functions of the vestibulocollic reflex. Exp Brain Res *210*, 331-345.

Golovin, R.M., and Broadie, K. (2016). Developmental experience-dependent plasticity in the first synapse of the Drosophila olfactory circuit. J Neurophysiol *116*, 2730-2738.

Gopen, Q., Lopez, I., Ishiyama, G., Baloh, R.W., and Ishiyama, A. (2003). Unbiased stereologic type I and type II hair cell counts in human utricular macula. Laryngoscope *113*, 1132-1138.

Gordy, C., Straka, H., Houston, D.W., Fritzsch, B., and Elliott, K.L. (2018). Transplantation of Ears Provides Insights into Inner Ear Afferent Pathfinding Properties. Dev Neurobiol *78*, 1064-1080.

Gordy, C., Straka, H. (2022). Developmental eye motion plasticity after unilateral embryonic ear removal in *Xenopus laevis*. iScience. doi: 10.1016/j.isci.2022.105165.

Goto, F., Straka, H., and Dieringer, N. (2000). Expansion of afferent vestibular signals after the section of one of the vestibular nerve branches. J Neurophysiol *84*, 581-584.

Goto, F., Straka, H., and Dieringer, N. (2001). Postlesional vestibular reorganization in frogs: evidence for a basic reaction pattern after nerve injury. J Neurophysiol *85*, 2643-2646.

Gracheva, E.O., Ingolia, N.T., Kelly, Y.M., Cordero-Morales, J.F., Hollopeter, G., Chesler, A.T., Sanchez, E.E., Perez, J.C., Weissman, J.S., and Julius, D. (2010). Molecular basis of infrared detection by snakes. Nature *464*, 1006-1011.

Graf, W., and Baker, R. (1985a). The vestibuloocular reflex of the adult flatfish. I. Oculomotor organization. J Neurophysiol *54*, 887-899.

Graf, W., and Baker, R. (1985b). The vestibuloocular reflex of the adult flatfish. II. Vestibulooculomotor connectivity. J Neurophysiol *54*, 900-916.

Graf, W., and Brunken, W.J. (1984). Elasmobranch oculomotor organization: anatomical and theoretical aspects of the phylogenetic development of vestibulo-oculomotor connectivity. J Comp Neurol *227*, 569-581.

Graf, W., Gilland, E., McFarlane, M., Knott, L., and Baker, R. (2002). Central pathways mediating oculomotor reflexes in an elasmobranch, Scyliorhinus canicula. Biol Bull *203*, 236-238.

Graf, W., Spencer, R., Baker, H., and Baker, R. (1997). Excitatory and inhibitory vestibular pathways to the extraocular motor nuclei in goldfish. J Neurophysiol *77*, 2765-2779.

Graf, W., Spencer, R., Baker, H., and Baker, R. (2001). Vestibuloocular reflex of the adult flatfish. III. A species-specific reciprocal pattern of excitation and inhibition. J Neurophysiol *86*, 1376-1388.

Grassi, S., Dieni, C., Frondaroli, A., and Pettorossi, V.E. (2004). Influence of visual experience on developmental shift from long-term depression to long-term potentiation in the rat medial vestibular nuclei. J Physiol *560*, 767-777.

Gravot, C.M., Knorr, A.G., Glasauer, S., and Straka, H. (2017). It's not all black and white: visual scene parameters influence optokinetic reflex performance in Xenopus laevis tadpoles. J Exp Biol *220*, 4213-4224.

Greaney, M.R., Privorotskiy, A.E., D'Elia, K.P., and Schoppik, D. (2016). Extraocular motoneuron pools develop along a dorsoventral axis in zebrafish, Danio rerio. J Comp Neurol *525*, 65-78.

Groves, A.K., and Fekete, D.M. (2012). Shaping sound in space: the regulation of inner ear patterning. Development *139*, 245-257.

Gruberg, E.R., and Grasse, K.L. (1984). Basal optic complex in the frog (Rana pipiens): a physiological and HRP study. J Neurophysiol *51*, 998-1010.

Gutierrez-Castellanos, N., Winkelman, B.H., Tolosa-Rodriguez, L., De Gruijl, J.R., and De Zeeuw, C.I. (2013). Impact of aging on long-term ocular reflex adaptation. Neurobiol Aging *34*, 2784-2792.

Haddon, C., and Lewis, J. (1996). Early ear development in the embryo of the zebrafish, Danio rerio. J Comp Neurol *365*, 113-128.

Haddon, C.M., and Lewis, J.H. (1991). Hyaluronan as a propellant for epithelial movement: the development of semicircular canals in the inner ear of Xenopus. Development *112*, 541-550.

Hamann, K.F., Reber, A., Hess, B.J., and Dieringer, N. (1998). Long-term deficits in otolith, canal and optokinetic ocular reflexes of pigmented rats after unilateral vestibular nerve section. Exp Brain Res *118*, 331-340.

Hamann, K.F., and Lannou, J. (1988). Dynamic characteristics of vestibular nuclear neurons responses to vestibular and optokinetic stimulation during vestibular compensation in the rat. Acta Otolaryngol Suppl *445*, 1-19.

Harris, L.R., and Cynader, M. (1981). The eye movements of the dark-reared cat. Exp Brain Res *44*, 41-56.

Heffernan, A., Abdelmalek, M., and Nunez, D.A. (2021). Virtual and augmented reality in the vestibular rehabilitation of peripheral vestibular disorders: systematic review and meta-analysis. Sci Rep *11*, 17843.

Hellmann, B., and Fritzsch, B. (1996). Neuroanatomical and histochemical evidence for the presence of common lateral line and inner ear efferents and of efferents to the basilar papilla in a frog, Xenopus laevis. Brain Behav Evol *47*, 185-194.

Helmer, D., Geurten, B.R., Dehnhardt, G., and Hanke, F.D. (2017). Saccadic Movement Strategy in Common Cuttlefish (Sepia officinalis). Front Physiol *7*, 660.

Hensch, T.K. (2004). Critical period regulation. Annu Rev Neurosci *27*, 549-579.

Hernandez-Miranda, L.R., Muller, T., and Birchmeier, C. (2017). The dorsal spinal cord and hindbrain: From developmental mechanisms to functional circuits. Dev Biol *432*, 34-42.

Hidalgo, A., and Brand, A.H. (1997). Targeted neuronal ablation: the role of pioneer neurons in guidance and fasciculation in the CNS of Drosophila. Development *124*, 3253-3262.

Higuchi, S., Sugahara, F., Pascual-Anaya, J., Takagi, W., Oisi, Y., and Kuratani, S. (2019). Inner ear development in cyclostomes and evolution of the vertebrate semicircular canals. Nature *565*, 347-350.

Him, A., and Dutia, M.B. (2001). Intrinsic excitability changes in vestibular nucleus neurons after unilateral deafferentation. Brain Res *908*, 58-66.

Hirata, Y., and Highstein, S.M. (2002). Plasticity of the vertical VOR: a system identification approach to localizing the adaptive sites. Ann N Y Acad Sci *978*, 480-495.

Hodos, W., and Butler, A.B. (1997). Evolution of Sensory Pathways in Vertebrates. Brain, Behavior and Evolution *50*, 189-197.

Holstege, G., and Collewijn, H. (1982). The efferent connections of the nucleus of the optic tract and the superior colliculus in the rabbit. J Comp Neurol *209*, 139-175.

Holstein, G.R., Friedrich, V.L., Jr., Martinelli, G.P., Ogorodnikov, D., Yakushin, S.B., and Cohen, B. (2012). Fos expression in neurons of the rat vestibulo-autonomic pathway activated by sinusoidal galvanic vestibular stimulation. Front Neurol *3*, 4.

Holstein, G.R., Rabbitt, R.D., Martinelli, G.P., Friedrich, V.L., Jr., Boyle, R.D., and Highstein, S.M. (2004). Convergence of excitatory and inhibitory hair cell transmitters shapes vestibular afferent responses. Proc Natl Acad Sci U S A *101*, 15766-15771.

Honrubia, V., Hoffman, L.F., Sitko, S., and Schwartz, I.R. (1989). Anatomic and physiological correlates in bullfrog vestibular nerve. J Neurophysiol *61*, 688-701.

Horn, A.K.E. (2020). Neuroanatomy of Central Vestibular Connections. In The Senses: A Comprehensive Reference, Vol 6, Fritzsch, B., Straka, H., eds (Elsevier), pp. 21-37.

Horn, A.K.E., and Straka, H. (2021). Functional Organization of Extraocular Motoneurons and Eye Muscles. Annu Rev Vis Sci *7*, 793-825.

Horn, E., Lang, H.G., and Rayer, B. (1986). The development of the static vestibulo-ocular reflex in the southern clawed toad, Xenopus laevis. I. Intact animals. J Comp Physiol A *159*, 869-878.

Horn, E.R. (2014). Development of Vestibular Systems in Altered Gravity. In Development of Auditory and Vestibular Systems, Romand, R., Varela-Nieto, I., eds (Academic Press), pp. 489-533.

Hubel, D.H., and Wiesel, T.N. (1970). The period of susceptibility to the physiological effects of unilateral eye closure in kittens. J Physiol *206*, 419-436.

Hudspeth, A.J. (1985). The cellular basis of hearing: the biophysics of hair cells. Science *230*, 745-752.

Hudspeth, A.J. (1989). How the ear's works work. Nature *341*, 397-404.

Hudspeth, A.J. (1997). How hearing happens. Neuron *19*, 947-950.

Hullar, T.E. (2006). Semicircular canal geometry, afferent sensitivity, and animal behavior. Anat Rec A Discov Mol Cell Evol Biol *288*, 466-472.

Hupfeld, K.E., McGregor, H.R., Koppelmans, V., Beltran, N.E., Kofman, I.S., De Dios, Y.E., Riascos, R.F., Reuter-Lorenz, P.A., Wood, S.J., Bloomberg, J.J*., et al.* (2022). Brain and Behavioral Evidence for Reweighting of Vestibular Inputs with Long-Duration Spaceflight. Cereb Cortex *32*, 755-769.

I Gusti Bagus, M., Gordy, C., Sanchez-Gonzalez, R., Strupp, M., and Straka, H. (2019). Impact of 4-aminopyridine on vestibulo–ocular reflex performance. Journal of Neurology *266*, 93-100.

Idoux, E., Tagliabue, M., and Beraneck, M. (2018). No Gain No Pain: Relations Between Vestibulo-Ocular Reflexes and Motion Sickness in Mice. Front Neurol *9*, 918.

Isu, N., Graf, W., Sato, H., Kushiro, K., Zakir, M., Imagawa, M., and Uchino, Y. (2000). Sacculo-ocular reflex connectivity in cats. Exp Brain Res *131*, 262-268.

Ito, M. (1982). Cerebellar control of the vestibulo-ocular reflex--around the flocculus hypothesis. Annu Rev Neurosci *5*, 275-296.

Jahan, I., Kersigo, J., Pan, N., and Fritzsch, B. (2010). Neurod1 regulates survival and formation of connections in mouse ear and brain. Cell Tissue Res *341*, 95-110.

Jones, T.A., Jones, S.M., and Hoffman, L.F. (2008). Resting discharge patterns of macular primary afferents in otoconia-deficient mice. J Assoc Res Otolaryngol *9*, 490-505.

Kalla, R., Glasauer, S., Schautzer, F., Lehnen, N., Büttner, U., Strupp, M., and Brandt, T. (2004). 4-aminopyridine improves downbeat nystagmus, smooth pursuit, and VOR gain. Neurology *62*, 1228-1229.

Kalluri, R., Xue, J., and Eatock, R.A. (2010). Ion channels set spike timing regularity of mammalian vestibular afferent neurons. J Neurophysiol *104*, 2034-2051.

Kasahara, M., and Uchino, Y. (1974). Bilateral semicircular canal inputs to neurons in cat vestibular nuclei. Exp Brain Res *20*, 285-296.

Kassardjian, C.D., Tan, Y.F., Chung, J.Y., Heskin, R., Peterson, M.J., and Broussard, D.M. (2005). The site of a motor memory shifts with consolidation. J Neurosci *25*, 7979-7985.

Keshavarz, B., Hettinger, L.J., Vena, D., and Campos, J.L. (2014). Combined effects of auditory and visual cues on the perception of vection. Exp Brain Res *232*, 827-836.

Kha, C.X., Guerin, D.J., and Tseng, K.A. (2019). Using the Xenopus Developmental Eye Regrowth System to Distinguish the Role of Developmental Versus Regenerative Mechanisms. Front Physiol *10*, 502.

Kim, J., and Curthoys, I.S. (2004). Responses of primary vestibular neurons to galvanic vestibular stimulation (GVS) in the anaesthetised guinea pig. Brain Res Bull *64*, 265-271.

Kim, U.S., Mahroo, O.A., Mollon, J.D., and Yu-Wai-Man, P. (2021). Retinal Ganglion Cells-Diversity of Cell Types and Clinical Relevance. Front Neurol *12*, 661938.

Kirkby, L.A., Sack, G.S., Firl, A., and Feller, M.B. (2013). A role for correlated spontaneous activity in the assembly of neural circuits. Neuron *80*, 1129-1144.

Kist, A.M., and Portugues, R. (2019). Optomotor Swimming in Larval Zebrafish Is Driven by Global Whole-Field Visual Motion and Local Light-Dark Transitions. Cell Rep *29*, 659-670.

Knorr, A.G., Gravot, C.M., Gordy, C., Glasauer, S., and Straka, H. (2018). I spy with my little eye: a simple behavioral assay to test color sensitivity on digital displays. Biol Open *7*, bio035725.

Kolodkin, A.L., and Tessier-Lavigne, M. (2011). Mechanisms and molecules of neuronal wiring: a primer. Cold Spring Harb Perspect Biol *3*, a001727.

Kömpf, D., and Piper, H.F. (1987). Eye movements and vestibulo-ocular reflex in the blind. J Neurol *234*, 337-341.

Koundakjian, E.J., Appler, J.L., and Goodrich, L.V. (2007). Auditory neurons make stereotyped wiring decisions before maturation of their targets. J Neurosci *27*, 14078-14088.

Krumlauf, R., and Wilkinson, D.G. (2021). Segmentation and patterning of the vertebrate hindbrain. Development *148*, dev186460.

Kubo, F., Hablitzel, B., Dal Maschio, M., Driever, W., Baier, H., and Arrenberg, A.B. (2014). Functional architecture of an optic flow-responsive area that drives horizontal eye movements in zebrafish. Neuron *81*, 1344-1359.

Kugler, K., Greiter, W., Luksch, H., Firzlaff, U., and Wiegrebe, L. (2016). Echo-acoustic flow affects flight in bats. J Exp Biol *219*, 1793-1797.

Kugler, K., Luksch, H., Peremans, H., Vanderelst, D., Wiegrebe, L., and Firzlaff, U. (2019). Optic and echo-acoustic flow interact in bats. J Exp Biol *222*, jeb195404.

Kuruvilla, A., Sitko, S., Schwartz, I.R., and Honrubia, V. (1985). Central projections of primary vestibular fibers in the bullfrog: I. The vestibular nuclei. Laryngoscope *95*, 692-707.

Lacour, M. (2006). Restoration of vestibular function: basic aspects and practical advances for rehabilitation. Curr Med Res Opin *22*, 1651-1659.

Lacour, M., Barthelemy, J., Borel, L., Magnan, J., Xerri, C., Chays, A., and Ouaknine, M. (1997). Sensory strategies in human postural control before and after unilateral vestibular neurotomy. Exp Brain Res *115*, 300-310.

Lacour, M., and Tighilet, B. (2010). Plastic events in the vestibular nuclei during vestibular compensation: the brain orchestration of a "deafferentation" code. Restor Neurol Neurosci *28*, 19-35.

Lambert, F.M., Bacque-Cazenave, J., Le Seach, A., Arama, J., Courtand, G., Tagliabue, M., Eskiizmirliler, S., Straka, H., and Beraneck, M. (2020). Stabilization of Gaze during Early Xenopus Development by Swimming-Related Utricular Signals. Curr Biol *30*, 746-753.

Lambert, F.M., Beck, J.C., Baker, R., and Straka, H. (2008). Semicircular canal size determines the developmental onset of angular vestibuloocular reflexes in larval Xenopus. J Neurosci *28*, 8086-8095.

Lambert, F.M., Combes, D., Simmers, J., and Straka, H. (2012). Gaze stabilization by efference copy signaling without sensory feedback during vertebrate locomotion. Curr Biol *22*, 1649-1658.

Lambert, F.M., Malinvaud, D., Glaunes, J., Bergot, C., Straka, H., and Vidal, P.P. (2009). Vestibular asymmetry as the cause of idiopathic scoliosis: a possible answer from Xenopus. J Neurosci *29*, 12477-12483.

Lambert, F.M., Malinvaud, D., Gratacap, M., Straka, H., and Vidal, P.P. (2013). Restricted neural plasticity in vestibulospinal pathways after unilateral labyrinthectomy as the origin for scoliotic deformations. J Neurosci *33*, 6845-6856.

Lambert, F.M., and Straka, H. (2012). The frog vestibular system as a model for lesion-induced plasticity: basic neural principles and implications for posture control. Front Neurol *3*, 42.

Lance-Jones, C., Shah, V., Noden, D.M., and Sours, E. (2012). Intrinsic properties guide proximal abducens and oculomotor nerve outgrowth in avian embryos. Dev Neurobiol *72*, 167-185.

Land, M.F. (1999). Motion and vision: why animals move their eyes. J Comp Physiol A *185*, 341-352.

Land, M.F. (2015). Eye movements of vertebrates and their relation to eye form and function. J Comp Physiol A Neuroethol Sens Neural Behav Physiol *201*, 195-214.

Lappe, M., Bremmer, F., and van den Berg, A.V. (1999). Perception of self-motion from visual flow. Trends Cogn Sci *3*, 329-336.

Lasker, D.M., Han, G.C., Park, H.J., and Minor, L.B. (2008). Rotational responses of vestibular-nerve afferents innervating the semicircular canals in the C57BL/6 mouse. J Assoc Res Otolaryngol *9*, 334-348.

Lee-Liu, D., Mendez-Olivos, E.E., Munoz, R., and Larrain, J. (2017). The African clawed frog Xenopus laevis: A model organism to study regeneration of the central nervous system. Neurosci Lett *652*, 82-93.

Levi-Montalcini, R. (1949). The development to the acoustico-vestibular centers in the chick embryo in the absence of the afferent root fibers and of descending fiber tracts. J Comp Neurol *91*, 209-241, illust, incl 203 pl.

Lewis, E.R., and Li, C.W. (1975). Hair cell types and distributions in the otolithic and auditory organs of the bullfrog. Brain Res *83*, 35-50.

Li, A., Xue, J., and Peterson, E.H. (2008). Architecture of the mouse utricle: macular organization and hair bundle heights. J Neurophysiol *99*, 718-733.

Lilian, S.J., Seal, H.E., Popratiloff, A., Hirsch, J.C., and Peusner, K.D. (2019). A New Model for Congenital Vestibular Disorders. J Assoc Res Otolaryngol *20*, 133-149.

Linford, N.J., Kuo, T.H., Chan, T.P., and Pletcher, S.D. (2011). Sensory perception and aging in model systems: from the outside in. Annu Rev Cell Dev Biol *27*, 759-785.

Lisberger, S.G., Miles, F.A., and Zee, D.S. (1984). Signals used to compute errors in monkey vestibuloocular reflex: possible role of flocculus. J Neurophysiol *52*, 1140-1153.

Liu, Z., Hildebrand, D.G.C., Morgan, J.L., Jia, Y., Slimmon, N., and Bagnall, M.W. (2022). Organization of the gravity-sensing system in zebrafish. Nat Commun *13*, 5060.

Liu, Z., Kimura, Y., Higashijima, S.I., Hildebrand, D.G.C., Morgan, J.L., and Bagnall, M.W. (2020). Central Vestibular Tuning Arises from Patterned Convergence of Otolith Afferents. Neuron *108*, 748-762 e744.

Lunde, A., Okaty, B.W., Dymecki, S.M., and Glover, J.C. (2019). Molecular Profiling Defines Evolutionarily Conserved Transcription Factor Signatures of Major Vestibulospinal Neuron Groups. eNeuro *6*, e0475.

Lysakowski, A., and Goldberg, J.M. (2004). Morphophysiology of the Vestibular Periphery. In The Vestibular System, S.M. Highstein, R.R. Fay, and A.N. Popper, eds. (New York, NY: Springer New York), pp. 57-152.

Ma, Q., Anderson, D.J., and Fritzsch, B. (2000). Neurogenin 1 null mutant ears develop fewer, morphologically normal hair cells in smaller sensory epithelia devoid of innervation. J Assoc Res Otolaryngol *1*, 129-143.

Macdougall, H.G., and Curthoys, I.S. (2012). Plasticity during Vestibular Compensation: The Role of Saccades. Front Neurol *3*, 21.

Macova, I., Pysanenko, K., Chumak, T., Dvorakova, M., Bohuslavova, R., Syka, J., Fritzsch, B., and Pavlinkova, G. (2019). Neurod1 Is Essential for the Primary Tonotopic Organization and Related Auditory Information Processing in the Midbrain. J Neurosci *39*, 984-1004.

Maioli, C., and Precht, W. (1985). On the role of vestibulo-ocular reflex plasticity in recovery after unilateral peripheral vestibular lesions. Exp Brain Res *59*, 267-272.

Maklad, A., and Fritzsch, B. (1999). Incomplete segregation of endorgan-specific vestibular ganglion cells in mice and rats. J Vestib Res *9*, 387-399.

Maklad, A., and Fritzsch, B. (2002). The developmental segregation of posterior crista and saccular vestibular fibers in mice: a carbocyanine tracer study using confocal microscopy. Brain Res Dev Brain Res *135*, 1-17.

Maklad, A., and Fritzsch, B. (2003). Development of vestibular afferent projections into the hindbrain and their central targets. Brain Res Bull *60*, 497-510.

Maricich, S.M., Xia, A., Mathes, E.L., Wang, V.Y., Oghalai, J.S., Fritzsch, B., and Zoghbi, H.Y. (2009). Atoh1-lineal neurons are required for hearing and for the survival of neurons in the spiral ganglion and brainstem accessory auditory nuclei. J Neurosci *29*, 11123-11133.

Markl, H. (1974). The Perception of Gravity and of Angular Acceleration in Invertebrates. In Vestibular System Part 1: Basic Mechanisms, H.H. Kornhuber, ed. (Berlin, Heidelberg: Springer Berlin Heidelberg), pp. 17-74.

Markov, D.A., Petrucco, L., Kist, A.M., and Portugues, R. (2021). A cerebellar internal model calibrates a feedback controller involved in sensorimotor control. Nat Commun *12*, 6694.

Masseck, O.A., and Hoffmann, K.P. (2009a). Comparative neurobiology of the optokinetic reflex. Ann N Y Acad Sci *1164*, 430-439.

Masseck, O.A., and Hoffmann, K.P. (2009b). Question of reference frames: visual direction-selective neurons in the accessory optic system of goldfish. J Neurophysiol *102*, 2781-2789.

Matesz, C. (1990). Development of the abducens nuclei in the Xenopus laevis. Brain Res Dev Brain Res *51*, 179-184.

Mathews, M.A., Camp, A.J., and Murray, A.J. (2017). Reviewing the Role of the Efferent Vestibular System in Motor and Vestibular Circuits. Front Physiol *8*, 552.

Matsuda, K., and Kubo, F. (2021). Circuit Organization Underlying Optic Flow Processing in Zebrafish. Front Neural Circuits *15*, 709048.

McAssey, M., Dowsett, J., Kirsch, V., Brandt, T., and Dieterich, M. (2020). Different EEG brain activity in right and left handers during visually induced self-motion perception. J Neurol *267*, 79-90.

McElligott, J.G., Beeton, P., and Polk, J. (1998). Effect of cerebellar inactivation by lidocaine microdialysis on the vestibuloocular reflex in goldfish. J Neurophysiol *79*, 1286-1294.

McElvain, L.E., Bagnall, M.W., Sakatos, A., and du Lac, S. (2010). Bidirectional plasticity gated by hyperpolarization controls the gain of postsynaptic firing responses at central vestibular nerve synapses. Neuron *68*, 763-775.

McKenna, O.C., and Wallman, J. (1985). Accessory optic system and pretectum of birds: comparisons with those of other vertebrates. Brain Behav Evol *26*, 91-116.

Menzies, J.R., Porrill, J., Dutia, M., and Dean, P. (2010). Synaptic plasticity in medial vestibular nucleus neurons: comparison with computational requirements of VOR adaptation. PLoS One *5*, e13182.

Meredith, R.M., Dawitz, J., and Kramvis, I. (2012). Sensitive time-windows for susceptibility in neurodevelopmental disorders. Trends Neurosci *35*, 335-344.

Miles, F.A., and Lisberger, S.G. (1981). Plasticity in the vestibulo-ocular reflex: a new hypothesis. Annu Rev Neurosci *4*, 273-299.

Moravec, W.J., and Peterson, E.H. (2004). Differences between stereocilia numbers on type I and type II vestibular hair cells. J Neurophysiol *92*, 3153-3160.

Morsli, H., Choo, D., Ryan, A., Johnson, R., and Wu, D.K. (1998). Development of the mouse inner ear and origin of its sensory organs. J Neurosci *18*, 3327-3335.

Murphy, G.J., and Du Lac, S. (2001). Postnatal development of spike generation in rat medial vestibular nucleus neurons. J Neurophysiol *85*, 1899-1906.

Niedzielski, A.S., and Wenthold, R.J. (1995). Expression of AMPA, kainate, and NMDA receptor subunits in cochlear and vestibular ganglia. J Neurosci *15*, 2338-2353.

Nikolaou, N., Lowe, A.S., Walker, A.S., Abbas, F., Hunter, P.R., Thompson, I.D., and Meyer, M.P. (2012). Parametric functional maps of visual inputs to the tectum. Neuron *76*, 317-324.

Nurnberger, M., Klingner, C., Witte, O.W., and Brodoehl, S. (2021). Mismatch of Visual-Vestibular Information in Virtual Reality: Is Motion Sickness Part of the Brains Attempt to Reduce the Prediction Error? Front Hum Neurosci *15*, 757735.

Ohyama, T., Groves, A.K., and Martin, K. (2007). The first steps towards hearing: mechanisms of otic placode induction. Int J Dev Biol *51*, 463-472.

Ono, K., Keller, J., López Ramírez, O., González Garrido, A., Zobeiri, O.A., Chang, H.H.V., Vijayakumar, S., Ayiotis, A., Duester, G., Della Santina, C.C.*, et al.* (2020). Retinoic acid degradation shapes zonal development of vestibular organs and sensitivity to transient linear accelerations. Nat Commun *11*, 63.

Pantle, C., and Dieringer, N. (1998). Spatial transformation of semicircular canal signals into abducens motor signals. A comparison between grass frogs and water frogs. J Comp Physiol A *182*, 475-487.

Pascual-Leone, A., Amedi, A., Fregni, F., and Merabet, L.B. (2005). The plastic human brain cortex. Annu Rev Neurosci *28*, 377-401.

Pasqualetti, M., Diaz, C., Renaud, J.S., Rijli, F.M., and Glover, J.C. (2007). Fate-mapping the mammalian hindbrain: segmental origins of vestibular projection neurons assessed using rhombomere-specific Hoxa2 enhancer elements in the mouse embryo. J Neurosci *27*, 9670-9681.

Paterson, J.M., Menzies, J.R.W., Bergquist, F., and Dutia, M.B. (2005). Cellular Mechanisms of Vestibular Compensation. Neuroembryol Aging *3*, 183-193.

Paulin, M.G., and Hoffman, L.F. (2019). Models of vestibular semicircular canal afferent neuron firing activity. J Neurophysiol *122*, 2548-2567.

Peusner, K.D., Bell, N.M., Hirsch, J.C., Beraneck, M., and Popratiloff, A. (2021). Understanding the Pathophysiology of Congenital Vestibular Disorders: Current Challenges and Future Directions. Front Neurol *12*, 708395.

Peusner, K.D., and Morest, D.K. (1977). Neurogenesis in the nucleus vestibularis tangentialis of the chick embryo in the absence of the primary afferent fibers. Neuroscience *2*, 253-270.

Pfaff, C., Schultz, J.A., and Schellhorn, R. (2019). The vertebrate middle and inner ear: A short overview. J Morphol *280*, 1098-1105.

Pfanzelt, S., Rossert, C., Rohregger, M., Glasauer, S., Moore, L.E., and Straka, H. (2008). Differential dynamic processing of afferent signals in frog tonic and phasic second-order vestibular neurons. J Neurosci *28*, 10349-10362.

Platt, C., and Straka, H. (2020). Vestibular Endorgans in Vertebrates and Adequate Sensory Stimuli. In The Senses: A Comprehensive Reference, Vol 6, Fritzsch, B., Straka, H., eds (Elsevier), pp. 108-128.

Popper, A.N., Ramcharitar, J., and Campana, S.E. (2005). Why otoliths? Insights from inner ear physiology and fisheries biology. Marine and Freshwater Research *56,* 497-504.

Pratt, K.G., and Khakhalin, A.S. (2013). Modeling human neurodevelopmental disorders in the Xenopus tadpole: from mechanisms to therapeutic targets. Dis Model Mech *6*, 1057-1065.

Puzdrowski, R.L., and Leonard, R.B. (1994). Vestibulo-oculomotor connections in an elasmobranch fish, the Atlantic stingray, Dasyatis sabina. J Comp Neurol *339*, 587-597.

Quick, Q.A., and Serrano, E.E. (2005). Inner ear formation during the early larval development of Xenopus laevis. Dev Dyn *234*, 791-801.

Rayer, B., Cagol, E., and Horn, E. (1983). Compensation of vestibular-induced deficits in relation to the development of the Southern Clawed Toad, Xenopus laevis daudin. J Comp Physiol *151*, 487-498.

Rayer, B., and Horn, E. (1986). The development of the static vestibulo-ocular reflex in the southern clawed toad, Xenopus laevis. III. Chronic hemilabyrinthectomized tadpoles. J Comp Physiol A *159*, 887-895.

Raymond, J.L., and Lisberger, S.G. (1996). Behavioral analysis of signals that guide learned changes in the amplitude and dynamics of the vestibulo-ocular reflex. J Neurosci *16*, 7791-7802.

Raymond, J.L., and Lisberger, S.G. (2000). Hypotheses about the neural trigger for plasticity in the circuit for the vestibulo-ocular reflex. Prog Brain Res *124*, 235-246.

Ris, L., Capron, B., de Waele, C., Vidal, P.P., and Godaux, E. (1997). Dissociations between behavioural recovery and restoration of vestibular activity in the unilabyrinthectomized guinea-pig. J Physiol *500 (Pt 2)*, 509-522.

Ris, L., de Waele, C., Serafin, M., Vidal, P.P., and Godaux, E. (1995). Neuronal activity in the ipsilateral vestibular nucleus following unilateral labyrinthectomy in the alert guinea pig. J Neurophysiol *74*, 2087-2099.

Roberts, R., Elsner, J., and Bagnall, M.W. (2017). Delayed Otolith Development Does Not Impair Vestibular Circuit Formation in Zebrafish. J Assoc Res Otolaryngol *18*, 415-425.

Robinson, D.A. (1976). Adaptive gain control of vestibuloocular reflex by the cerebellum. J Neurophysiol *39*, 954-969.

Robinson, D.A. (1981). The use of control systems analysis in the neurophysiology of eye movements. Annu Rev Neurosci *4*, 463-503.

Rohregger, M., and Dieringer, N. (2002). Principles of linear and angular vestibuloocular reflex organization in the frog. J Neurophysiol *87*, 385-398.

Ross, R.J., and Smith, J.J.B. (1980). Detection of substrate vibrations by salamanders: Frequency sensitivity of the ear. Comp Biochem Physiol A: Physiol *65*, 167-172.

Rovainen, C.M. (1976). Vestibulo-ocular reflexes in the adult sea lamprey. J Comp Physiol *112*, 159-164.

Roy, J.E., and Cullen, K.E. (2001). Selective processing of vestibular reafference during self-generated head motion. J Neurosci *21*, 2131-2142.

Russell, S.A., and Bashaw, G.J. (2017). Axon guidance pathways and the control of gene expression. Dev Dyn *247*, 571-580.

Sadeghi, S.G., and Beraneck, M. (2020). Task-Specific Differentiation of Central Vestibular Neurons and Plasticity During Vestibular Compensation. In The Senses: A Comprehensive Reference, Vol 6, Fritzsch, B., Straka, H., eds (Elsevier), pp. 290-308.

Sadeghi, S.G., Minor, L.B., and Cullen, K.E. (2007). Response of vestibular-nerve afferents to active and passive rotations under normal conditions and after unilateral labyrinthectomy. J Neurophysiol *97*, 1503-1514.

Sadeghi, S.G., Minor, L.B., and Cullen, K.E. (2012). Neural correlates of sensory substitution in vestibular pathways following complete vestibular loss. J Neurosci *32*, 14685-14695.

Sasaki, M., Hiranuma, K., Isu, N., and Uchino, Y. (1991). Is there a three neuron arc in the cat utriculo-trochlear pathway? Exp Brain Res *86*, 421-425.

Sasaki, R., Angelaki, D.E., and DeAngelis, G.C. (2017). Dissociation of Self-Motion and Object Motion by Linear Population Decoding That Approximates Marginalization. J Neurosci *37*, 11204-11219.

Schlosser, G. (2006). Induction and specification of cranial placodes. Dev Biol *294*, 303-351.

Schlosser, G., and Northcutt, R.G. (2000). Development of neurogenic placodes in Xenopus laevis. J Comp Neurol *418*, 121-146.

Schneggenburger, R., Meyer, A.C., and Neher, E. (1999). Released fraction and total size of a pool of immediately available transmitter quanta at a calyx synapse. Neuron *23*, 399-409.

Schoppik, D., Bianco, I.H., Prober, D.A., Douglass, A.D., Robson, D.N., Li, J.M.B., Greenwood, J.S.F., Soucy, E., Engert, F., and Schier, A.F. (2017). Gaze-Stabilizing Central Vestibular Neurons Project Asymmetrically to Extraocular Motoneuron Pools. J Neurosci *37*, 11353-11365.

Schubert, M.C., and Zee, D.S. (2010). Saccade and vestibular ocular motor adaptation. Restor Neurol Neurosci *28*, 9-18.

Schweigart, G., Mergner, T., Evdokimidis, I., Morand, S., and Becker, W. (1997). Gaze stabilization by optokinetic reflex (OKR) and vestibulo-ocular reflex (VOR) during active head rotation in man. Vision Res *37*, 1643-1652.

Seiradake, E., Jones, E.Y., and Klein, R. (2016). Structural Perspectives on Axon Guidance. Annu Rev Cell Dev Biol *32*, 577-608.

Sethuramanujam, S., Yao, X., deRosenroll, G., Briggman, K.L., Field, G.D., and Awatramani, G.B. (2017). "Silent" NMDA Synapses Enhance Motion Sensitivity in a Mature Retinal Circuit. Neuron *96*, 1099-1111 e1093.

Sherman, A., and Dickinson, M.H. (2003). A comparison of visual and haltere-mediated equilibrium reflexes in the fruit fly Drosophila melanogaster. J Exp Biol *206*, 295-302.

Shutoh, F., Ohki, M., Kitazawa, H., Itohara, S., and Nagao, S. (2006). Memory trace of motor learning shifts transsynaptically from cerebellar cortex to nuclei for consolidation. Neuroscience *139*, 767-777.

Siddiqui, S.A., and Cramer, K.S. (2005). Differential expression of Eph receptors and ephrins in the cochlear ganglion and eighth cranial nerve of the chick embryo. J Comp Neurol *482*, 309-319.

Simpson, J.I., and Graf, W. (1981). Eye-muscle geometry and compensatory eye movements in lateral-eyed and frontal-eyed animals. Ann N Y Acad Sci *374*, 20-30.

Simpson, J.I., Leonard, C.S., and Soodak, R.E. (1988b). The accessory optic system of rabbit. II. Spatial organization of direction selectivity. J Neurophysiol *60*, 2055-2072.

Simpson, J.I., Leonard, C.S., and Soodak, R.E. (1988a). The accessory optic system. Analyzer of self-motion. Ann N Y Acad Sci *545*, 170-179.

Smith, P.F. (2018). Vestibular Functions and Parkinson's Disease. Front Neurol *9*, 1085.

Smith, P.F., and Curthoys, I.S. (1989). Mechanisms of recovery following unilateral labyrinthectomy: a review. Brain Res Brain Res Rev *14*, 155-180.

Soupiadou, P., Branoner, F., and Straka, H. (2018). Pharmacological profile of vestibular inhibitory inputs to superior oblique motoneurons. J Neurol *265*, 18-25.

Soupiadou, P., Gordy, C., Forsthofer, M., Sanchez-Gonzalez, R., and Straka, H. (2020). Acute consequences of a unilateral VIIIth nerve transection on vestibulo-ocular and optokinetic reflexes in Xenopus laevis tadpoles. J Neurol *267*, 62-75.

Spencer, R.F., and Porter, J.D. (2006). Biological organization of the extraocular muscles. Prog Brain Res *151,* 43-80.

Spencer, R.F., Wenthold, R.J., and Baker, R. (1989). Evidence for glycine as an inhibitory neurotransmitter of vestibular, reticular, and prepositus hypoglossi neurons that project to the cat abducens nucleus. J Neurosci *9*, 2718-2736.

Spoon, C., Moravec, W.J., Rowe, M.H., Grant, J.W., and Peterson, E.H. (2011). Steady-state stiffness of utricular hair cells depends on macular location and hair bundle structure. J Neurophysiol *106*, 2950-2963.

Stahl, J.S., and Thumser, Z.C. (2013). 4-aminopyridine does not enhance flocculus function in tottering, a mouse model of vestibulocerebellar dysfunction and ataxia. PLoS One *8*, e57895.

Stoner, Z.A., Ketchum, E.M., Sheltz-Kempf, S., Blinkiewicz, P.V., Elliott, K.L., and Duncan, J.S. (2022). Fzd3 Expression Within Inner Ear Afferent Neurons Is Necessary for Central Pathfinding. Front Neurosci *15*, 779871.

Storm, R., Cholewa-Waclaw, J., Reuter, K., Brohl, D., Sieber, M., Treier, M., Muller, T., and Birchmeier, C. (2009). The bHLH transcription factor Olig3 marks the dorsal neuroepithelium of the hindbrain and is essential for the development of brainstem nuclei. Development *136*, 295-305.

Straka, H., and Baker, R. (2013). Vestibular blueprint in early vertebrates. Front Neural Circuits *7*, 182.

Straka, H., Beraneck, M., Rohregger, M., Moore, L.E., Vidal, P.P., and Vibert, N. (2004). Second-order vestibular neurons form separate populations with different membrane and discharge properties. J Neurophysiol *92*, 845-861.

Straka, H., Biesdorf, S., and Dieringer, N. (1997). Canal-specific excitation and inhibition of frog second-order vestibular neurons. J Neurophysiol *78*, 1363-1372.

Straka, H., and Dieringer, N. (1991). Internuclear neurons in the ocular motor system of frogs. J Comp Neurol *312*, 537-548.

Straka, H., and Dieringer, N. (1993). Electrophysiological and pharmacological characterization of vestibular inputs to identified frog abducens motoneurons and internuclear neurons in vitro. Eur J Neurosci *5*, 251-260.

Straka, H., and Dieringer, N. (1996). Uncrossed disynaptic inhibition of second-order vestibular neurons and its interaction with monosynaptic excitation from vestibular nerve afferent fibers in the frog. J Neurophysiol *76*, 3087-3101.

Straka, H., and Dieringer, N. (2004). Basic organization principles of the VOR: lessons from frogs. Prog Neurobiol *73*, 259-309.

Straka, H., Fritzsch, B., and Glover, J.C. (2014). Connecting ears to eye muscles: evolution of a 'simple' reflex arc. Brain Behav Evol *83*, 162-175.

Straka, H., Holler, S., and Goto, F. (2002). Patterns of canal and otolith afferent input convergence in frog second-order vestibular neurons. J Neurophysiol *88*, 2287-2301.

Straka, H., Lambert, F.M., Pfanzelt, S., and Beraneck, M. (2009). Vestibulo-ocular signal transformation in frequency-tuned channels. Ann N Y Acad Sci *1164*, 37-44.

Straka, H., and Simmers, J. (2012). Xenopus laevis: an ideal experimental model for studying the developmental dynamics of neural network assembly and sensory-motor computations. Dev Neurobiol *72*, 649-663.

Straka, H., Simmers, J., and Chagnaud, B.P. (2018). A New Perspective on Predictive Motor Signaling. Curr Biol *28*, R232-R243.

Straka, H., Vibert, N., Vidal, P.P., Moore, L.E., and Dutia, M.B. (2005). Intrinsic membrane properties of vertebrate vestibular neurons: function, development and plasticity. Prog Neurobiol *76*, 349-392.

Straka, H., Zwergal, A., and Cullen, K.E. (2016). Vestibular animal models: contributions to understanding physiology and disease. J Neurol *263 Suppl 1*, S10-23.

Strupp, M., Dlugaiczyk, J., Ertl-Wagner, B.B., Rujescu, D., Westhofen, M., and Dieterich, M. (2020). Vestibular Disorders. Dtsch Arztebl Int *117*, 300-310.

Strupp, M., Kalla, R., Dichgans, M., Freilinger, T., Glasauer, S., and Brandt, T. (2004). Treatment of episodic ataxia type 2 with the potassium channel blocker 4-aminopyridine. Neurology *62*, 1623-1625.

Strupp, M., Kim, J. S., Murofushi, T., Straumann, D., Jen, J. C., Rosengren, S. M., Della Santina, C. C., and Kingma, H. (2017). Bilateral vestibulopathy: Diagnostic criteria Consensus document of the Classification Committee of the Bárány Society. J Vestib Res *27,* 177-189.

Szentagothai, J. (1950). The elementary vestibulo-ocular reflex arc. J Neurophysiol *13*, 395-407.

Tanahashi, S., Ashihara, K., and Ujike, H. (2015). Effects of auditory information on self-motion perception during simultaneous presentation of visual shearing motion. Front Psychol *6*, 749.

Tien, N.W., and Kerschensteiner, D. (2018). Homeostatic plasticity in neural development. Neural Dev *13*, 9.

Titley, H.K., Heskin-Sweezie, R., Chung, J.Y., Kassardjian, C.D., Razik, F., and Broussard, D.M. (2007). Rapid consolidation of motor memory in the vestibuloocular reflex. J Neurophysiol *98*, 3809-3812.

Tomas-Roca, L., Corral-San-Miguel, R., Aroca, P., Puelles, L., and Marin, F. (2016). Crypto-rhombomeres of the mouse medulla oblongata, defined by molecular and morphological features. Brain Struct Funct *221*, 815-838.

Torborg, C.L., and Feller, M.B. (2005). Spontaneous patterned retinal activity and the refinement of retinal projections. Prog Neurobiol *76*, 213-235.

Torres, M., and Giráldez, F. (1998). The development of the vertebrate inner ear. Mech Dev *71*, 5-21.

Tosches, M.A. (2017). Developmental and genetic mechanisms of neural circuit evolution. Dev Biol *431*, 16-25.

Uchino, Y., Ikegami, H., Sasaki, M., Endo, K., Imagawa, M., and Isu, N. (1994). Monosynaptic and disynaptic connections in the utriculo-ocular reflex arc of the cat. J Neurophysiol *71*, 950-958.

Uchino, Y., Sasaki, M., Sato, H., Imagawa, M., Suwa, H., and Isu, N. (1996). Utriculoocular reflex arc of the cat. J Neurophysiol *76*, 1896-1903.

Vibert, N., Bantikyan, A., Babalian, A., Serafin, M., Mühlethaler, M., and Vidal, P.P. (1999). Post-lesional plasticity in the central nervous system of the guinea-pig: a "top-down" adaptation process? Neuroscience *94*, 1-5.

Vibert, N., Beraneck, M., Bantikyan, A., and Vidal, P.P. (2000). Vestibular compensation modifies the sensitivity of vestibular neurones to inhibitory amino acids. Neuroreport *11*, 1921-1927.

Vidal, P.-P., Waele, C.D., Vibert, N., and Mühlethaler, M. (1998). Vestibular compensation revisited. Otolaryngology–Head and Neck Surgery *119*, 34-42.

von Bernhardi, R., Bernhardi, L.E., and Eugenin, J. (2017). What Is Neural Plasticity? Adv Exp Med Biol *1015*, 1-15.

Waespe, W., and Henn, V. (1977). Neuronal activity in the vestibular nuclei of the alert monkey during vestibular and optokinetic stimulation. Exp Brain Res *27*, 523-538.

Wagner, H., Pappe, I., Brill, S., and Nalbach, H.O. (2022). Development of the horizontal optocollic reflex in juvenile barn owls (Tyto furcata pratincola). J Comp Physiol A Neuroethol Sens Neural Behav Physiol *208*, 479-492.

Walls, G.L. (1962). The evolutionary history of eye movements. Vision Research *2*, 69-80.

Wan, G., Corfas, G., and Stone, J.S. (2013). Inner ear supporting cells: rethinking the silent majority. Semin Cell Dev Biol *24*, 448-459.

Wang, L., Zobeiri, O.A., Millar, J.L., Schubert, M.C., and Cullen, K.E. (2021). Head movement kinematics are altered during gaze stability exercises in vestibular schwannoma patients. Sci Rep *11*, 7139.

Wanner, S.J., and Miller, J.R. (2007). Regulation of otic vesicle and hair cell stereocilia morphogenesis by Ena/VASP-like (Evl) in Xenopus. J Cell Sci *120*, 2641-2651.

Whitfield, T.T., Riley, B.B., Chiang, M.Y., and Phillips, B. (2002). Development of the zebrafish inner ear. Dev Dyn *223*, 427-458.

Wibble, T., Pansell, T., Grillner, S., and Pérez-Fernández, J. (2022). Conserved subcortical processing in visuo-vestibular gaze control. Nat Commun *13*, 4699.

Wiesel, T.N., and Hubel, D.H. (1963). SINGLE-CELL RESPONSES IN STRIATE CORTEX OF KITTENS DEPRIVED OF VISION IN ONE EYE. J Neurophysiol *26*, 1003-1017.

Wiesel, T.N., and Hubel, D.H. (1965). Comparison of the effects of unilateral and bilateral eye closure on cortical unit responses in kittens. J Neurophysiol *28*, 1029-1040.

Wijesinghe, R., Protti, D.A., and Camp, A.J. (2015). Vestibular Interactions in the Thalamus. Front Neural Circuits *9*, 79.

Wu, D.K., and Kelley, M.W. (2012). Molecular mechanisms of inner ear development. Cold Spring Harb Perspect Biol *4*, a008409.

Yamanaka, T., Sasa, M., Amano, T., Miyahara, H., and Matsunaga, T. (1995). Role of glucocorticoid in vestibular compensation in relation to activation of vestibular nucleus neurons. Acta Otolaryngol Suppl *519*, 168-172.

Zdebik, A.A., Wangemann, P., and Jentsch, T.J. (2009). Potassium ion movement in the inner ear: insights from genetic disease and mouse models. Physiology (Bethesda) *24*, 307-316.

Zecca, A., Dyballa, S., Voltes, A., Bradley, R., and Pujades, C. (2015). The Order and Place of Neuronal Differentiation Establish the Topography of Sensory Projections and the Entry Points within the Hindbrain. J Neurosci *35*, 7475-7486.

Zennou-Azogui, Y., Xerri, C., and Harlay, F. (1994). Visual sensory substitution in vestibular compensation: neuronal substrates in the alert cat. Exp Brain Res *98*, 457-473.

Zhou, W., Weldon, P., Tang, B., and King, W.M. (2003). Rapid motor learning in the translational vestibulo-ocular reflex. J Neurosci *23*, 4288-4298.

Zwergal, A., Mohwald, K., Salazar Lopez, E., Hadzhikolev, H., Brandt, T., Jahn, K., and Dieterich, M. (2020). A Prospective Analysis of Lesion-Symptom Relationships in Acute Vestibular and Ocular Motor Stroke. Front Neurol *11*, 822.

Zwergal, A., Schlichtiger, J., Xiong, G., Beck, R., Gunther, L., Schniepp, R., Schoberl, F., Jahn, K., Brandt, T., Strupp, M., Bartenstein, P., Dieterich, M., Dutia, M.B., la Fougère, C. (2016). Sequential [(18)F]FDG microPET whole-brain imaging of central vestibular compensation: a model of deafferentation-induced brain plasticity. Brain Struct Funct *221*, 159-170.

PUBLICATIONS LIST

Gordy, C., Straka, H. (2022). Developmental eye motion plasticity after unilateral embryonic ear removal in *Xenopus laevis.* iScience. https://doi.org/10.1016/j.isci.2022.105165.

Gordy, C., Forsthofer, M., Soupiadou, P., Özugur, S., Straka, H. (2022). Functional neurobiology in Xenopus provides insights into health and disease. In: Moody, S., Fainsod, A. (Eds.), Xenopus, from basic biology to disease models in the genomic era. CRC Press. 277-288. https://doi.org/10.1201/9781003050230-22.

Gordy, C., Straka, H. (2021). Vestibular influence on vertebrate skeletal symmetry and body shape. (2021). Front. Syst. Neurosci. 15, 753207. https://doi.org/10.3389/fnsys.2021.753207.

Soupiadou, P., Gordy, C., Forsthofer, M., Sanchez-Gonzalez, R., Straka, H. (2020). Acute consequences of a unilateral VIIIth nerve transection on vestibulo-ocular and optokinetic reflexes in *Xenopus laevis* tadpoles. J. Neurol. 267, 62-65. https://doi.org/10.1007/s00415-020-10205-x.

Elliott, K.L., Gordy, C., 2020. Evolution and Plasticity of Inner Ear Vestibular Neurosensory Development. In: Fritzsch, B. (Ed.) and Straka, H. (Volume Editor), The Senses: A Comprehensive Reference, vol. 6. Elsevier, Academic Press. 145–161. https://doi.org/10.1016/B978-0-12-809324-5.24141-2.

Straka, H., Gordy, C., 2020. The Vestibular System: The "Leatherman™" Among Sensory Systems. In: Fritzsch, B. (Ed.) and Straka, H. (Volume Editor), The Senses: A Comprehensive Reference, vol. 6. Elsevier, Academic Press. 708–720. https://doi.org/10.1016/B978-0-12-809324-5.24179-5.

I Gusti Bagus, Marliawaty*, Gordy, C*, Sanchez-Gonzalez, R., Strupp, M., Straka, H. (2019). Impact of 4-aminopyridine on vestibulo-ocular reflex performance. J. Neurol. 266 (Suppl. 1), 93-100. https://doi.org/10.1007/s00415-019-09452-4.

Knorr, A. G., Gravot, C. M., Gordy, C., Glasauer, S., & Straka, H. (2018). I spy with my little eye: a simple behavioral assay to test color sensitivity on digital displays. Biol. Open. 7, bio035725. https://doi.org/10.1242/bio.035725.

Gordy, C., Straka, H., Houston, D. W., Fritzsch, B., & Elliott, K. L. (2018). Transplantation of Ears Provides Insights into Inner Ear Afferent Pathfinding Properties. Dev. Neurobiol. 78, 1064-1080. https://doi.org/10.1002/dneu.22629.

AFFIDAVIT

Eidesstattliche Versicherung/Affidavit

Hiermit versichere ich an Eides statt, dass ich die vorliegende Dissertation **Brainstem plasticity in vestibular motion-processing sensorimotor networks** selbstständig angefertigt habe, mich außer der angegebenen keiner weiteren Hilfsmittel bedient und alle Erkenntnisse, die aus dem Schrifttum ganz oder annähernd übernommen sind, als solche kenntlich gemacht und nach ihrer Herkunft unter Bezeichnung der Fundstelle einzeln nachgewiesen habe.

I hereby confirm that the dissertation **Brainstem plasticity in vestibular motion-processing sensorimotor networks** is the result of my own work and that I have only used sources or materials listed and specified in the dissertation.

_____ _____

München, 28.09.2022 Clayton Gordy

Munich, 28.09.2022 Unterschrift / signature

DECLARATION OF AUTHOR CONTRIBUTIONS

The following information details the authorship contributions for the data presented in this dissertation:

CHAPTER II:

Developmental eye motion plasticity after unilateral embryonic ear removal in *Xenopus laevis*

(Accepted for publication in *iScience*)

Contribution of authors:

C.G. and H.S. conceived the goals and aims. C.G. and H.S. designed methodological paradigms. C.G. collected data for all experiments. C.G. analyzed data for all experiments. C.G. and H.S. interpreted all data. C.G. created all the figures. C.G. wrote the original draft of the manuscript. C.G. and H.S. reviewed and edited the manuscript. Resources, supervision, project administration, and funding acquired by H.S.

My contributions to this publication in detail:

H.S. and I conceived the aims and experimental goals of this project. I designed the methodological paradigms with H.S. I performed all experiments and analyzed all data and created all the figures and supplemental material in this paper. I wrote the initial draft of this paper. H.S. and I edited all subsequent versions.

CHAPTER III:

Caudal Transplantation of Ears Provides Insights into Inner Ear Afferent Pathfinding Properties

(Published paper, *Developmental Neurobiology*, 2018)

Contribution of authors:

K.L.E. and B.F. conceived the goals and aims. C.G., B.F., and K.L.E designed paradigms and collected data for the embryonic, dye tracing, and immunohistochemical experiments. C.G. and H.S. designed paradigms and collected data for the electrophysiological studies. K.L.E designed paradigms and collected data for behavior testing. C.G. and K.L.E analyzed embryonic, dye tracing, and immunohistochemical data. K.L.E analyzed behavior data. C.G. and H.S. analyzed electrophysiological data. C.G., H.S., D.W.H., B.F. and K.L.E. interpreted all the data. C.G., K.L.E, and H.S. created the figures.

C.G. wrote the original draft of the manuscript. All authors reviewed and edited the manuscript. Resources were provided by B.F., D.W.H, and H.S. Supervision provided by K.L.E, B.F. and H.S. Project administration provided by K.L.E. Funding acquired by K.L.E, B.F., and H.S.

My contributions to this publication in detail:

K.L.E., B.F., and I designed experimental paradigms and generated three-eared frogs and performed quantification of animals from this technique. I created Table 1. Along with K.L.E and B.F., I performed immunohistochemical and dye tracing experiments on three-eared animals and analyzed the data. With K.L.E and B.F., I created Figure 1, and Figure 2, Figure 3, Figure 6, and Figure 7. K.L.E performed 3D reconstruction of data panels in Figure 3B'' 3D'' and 2A. I generated three-eared animals for rearing and subsequent physiological testing. Along with H.S., I performed electrophysiological experiments, relevant analysis, and along with H.S. created Figure 5. I wrote the initial version of the manuscript and edited all versions of it.

CHAPTER IV:

Impact of 4-aminopyridine on vestibulo–ocular reflex performance

(Published paper, *Journal of Neurology*, 2019)

Contribution of authors:

H.S. conceived the goals and aims. M.I.G.B. and C.G. designed paradigms and collected data for electrophysiological experiments. M.I.G.B., C.G., and R.S.G designed paradigms and collected data for immunohistochemistry experiments. M.I.G.B, C.G., and H.S. analyzed data for electrophysiological experiments. R.S.G and C.G. analyzed data for immunohistochemistry experiments. M.I.G.B, C.G., and H.S. interpreted electrophysiological data. All authors interpreted immunohistochemistry data. M.I.G.B, C.G., and H.S. created electrophysiological figures. R.S.G and C.G. created the immunohistochemistry figure panels. M.I.G.B, C.G., and H.S. wrote the original draft of the manuscript. All authors reviewed and edited the manuscript. Resources, supervision, project administration, and funding acquired by H.S.

My contributions to this publication in detail:

M.I.G.B. and I designed paradigms and collected electrophysiological data on animals prior to and during 4-AP application. H.S., M.I.G.B., and I collaboratively analyzed the electrophysiological data and contributed to the creation of Figures 1 and 2. M.I.G.B., R.S.G, and I performed and collected data from immunohistochemical staining experiments. R.S.G and I analyzed immunohistochemical data

and created Figure 3 panels a-c. H.S. and M.I.G.B. and I contributed to the first draft of the paper and all authors edited all versions of the manuscript.

I hereby confirm the accuracy of the above author contributions.

_____	_____
München, 28.09.2022	Clayton Gordy (doctoral student)
_____	_____
München, 28.09.2022	Prof. Dr. Hans Straka (supervisor)